Diversity and distribution of anuran blood parasites within the Vhembe Biosphere

J Du Buisson

orcid.org/0000-0002-6368-7917

Dissertation accepted in fulfilment of the requirements for the degree *Master of Science in Environmental Sciences* at the North-West University

Supervisor:	Dr EC Netherlands
Co-supervisor:	Prof LH du Preez

Graduation May 2023

27332322

ACKNOWLEDGEMENTS

I hear by thank the following:

- My supervisor, Dr. Edward Netherlands for all the support, patience, and guidance throughout the past two years;
- Co-supervisor, Prof Louis du Preez for being such a wonderful role model and inspiring me to be the best that I can be;
- Mom and dad, my number one supporters, thank you for always believing in me, through times that I didn't believe in myself, you were always there.

ABSTRACT

The Soutpansberg mountain range, the most northern mountain range in South Africa, forms part of the Vhembe Biosphere Reserve, a highly diverse region comprising at least three biomes and 23 different vegetation types. Furthermore, this area is known for its distinct biotypes, boasting a rich faunal and floral diversity. It is estimated that the Soutpansberg harbours at least 35 species of anurans. Additionally, anurans are known to host a variety of intra- and extracellular blood parasites, however, no data is currently available for the diversity and distribution of anurans and their blood parasites from within Soutpansberg mountain range. Thus, the aims of the present study were to document and compare the biodiversity and distribution of anurans and their associated blood parasites across the Soutpansberg mountain range. For monitoring anurans both active and passive sampling techniques were utilised. The mountain range was divided into three transects in which the species abundance and compositions was determined. Blood samples were collected, prepared, and screened for the presence of haemoparasites from 387 individual frogs. Molecular characterisation and phylogenetic analysis were conducted for positive samples. Overall, 89% (31/35) of expected anuran species were observed of which blood samples were collected from 11 families, 18 genera and 25 species of anuran. A total of 10% (38/387) of the anuran specimens were found infected within 20% (5/25) of the frog species observed. This includes trypanosomatids, haemogregarines, haemociccidians and filarial nematodes. *Trypanosoma* and *Hepatozoon* spp. accounted for the most infections, and *Neofoleyellides* and *Lankesterella*-like species with the least abundance. These results demonstrate a diverse parasite community across the Soutpansberg providing insight to understanding the diversity and distribution of South African anuran blood parasites.

Keywords: Amphibians, Haemoparasites, Soutpansberg, *Trypanosoma*, *Hepatozoon*, *Lankesterella,* Phylogenetic analysis.

TABLE OF CONTENTS

ACKNOWLEDGEMENTS ..... **I**

ABSTRACT ..... **II**

TABLE OF CONTENTS ..... **III**

LIST OF TABLES ..... **VII**

LIST OF FIGURES ..... **IX**

CHAPTER 1: **1**

GENERAL INTRODUCTION **1**

1.1 INTRODUCTION **1**

1.1.1 Research aims 2

1.1.2 Research objectives 2

1.1.3 Study design 2

CHAPTER 2: **3**

ANURAN DIVERSITY ACROSS THE SOUTPANSBERG MOUNTAIN RANGE **3**

2.1 GENERAL INTRODUCTION TO AMPHIBIANS **4**

2.1.1 South African amphibians 5

2.1.2 Limpopo: the Vhembe Biosphere reserve 5

2.1.3 Diversity within the Soutpansberg Mountain range 7

2.1.4 Amphibian diversity across the Soutpansberg Mountain range 11

2.2 RESEARCH METHODOLOGY 13

2.2.1 Locality and site selection 13

2.2.2 Sample collection 14

2.3 RESULTS 15

2.3.1 Amphibian diversity across the Soutpansberg mountain 15

2.3.2 Amphibian species distribution across the Soutpansberg 20

2.3.3 Description of the amphibian community from the mountain range 39

2.4 DISCUSSION 44

CHAPTER 3: 48

BLOOD PARASITE DIVERSITY WITHIN VHEMBE FROGS 48

3.1 INTRODUCTION 49

3.1.1 General introduction to blood parasites 49

3.1.2 Introduction to frog blood parasites 49

3.2 MATERIALS AND METHODS 52

3.2.1 Frog collection and blood sampling 52

3.2.2 Blood smear preparation and light microscopy screening 53

3.2.3 DNA extraction and PCR amplification 53

3.2.4 Phylogenetic analysis 56

3.2.5 Statistical analysis of parasite fauna 56

3.3 RESULTS 57

3.3.1 Overall prevalence and diversity of blood parasites 57

3.3.2 Frog blood parasites reported based on morphology 59

3.3.3 Statistical results 69

3.3.4 Phylogenetic analyses 72

3.4 DISCUSSION 77

CHAPTER 4: 80

MORPHOLOGICAL AND MOLECULAR DATA OF AN UNKNOWN HAEMOCOCCIDIAN PARASITIZING THE COMMON RIVER FROG, *AMIETIA DELALANDII*, FROM THE NORTHERN PARTS OF SOUTH AFRICA 80

4.1 INTRODUCTION 81

4.2 MATERIALS AND METHODS 84

4.2.1 Study area and sample collection 84

4.2.2 Sample processing and light microscopy screening 85

4.2.3 DNA extraction and PCR amplification 85

4.2.4 Phylogenetic analysis 86

4.3 RESULTS 87

4.3.1 Phylogenetic result analysis 91

4.4 DISCUSSION 96

CHAPTER 5: 98

INTERNAL TRANSCRIBED SPACER 1 (ITS-1) NUCLEOTIDE SEQUENCE VARIATION OF TWO *HEPATOZOON THEILERI* POPULATIONS IN SOUTH AFRICA 98

5.1 INTRODUCTION 99

5.2 MATERIALS AND METHODS 102

5.2.1 Sampling areas and frog collection 102

5.2.2 Blood sample collection, preparation and light microscopy 104

5.2.3 DNA extraction, PCR amplification and phylogenetic analysis 104

5.3 RESULTS 107

5.3.1. Phylogenetic analysis 107

5.3.2 Statistical analysis of haplotype network 109

5.4 DISCUSSION 112

CHAPTER 6: 114

SUMMATIVE DISCUSSION 114

REFERENCES 118

APPENDIX A 131

APPENDIX B 137

APPENDIX C 138

APPENDIX D 139

APPENDIX E 140

APPENDIX F 141

LIST OF TABLES

Table 2.1: Frog species likely to occur in the Vhembe Biosphere listed in alphabetical order with family (adapted from Du Preez and Carruthers, 2017). 9

Table 2.2: Frog species likely to occur on the Soutpansberg Mountain range listed in alphabetical order with family (adapted from Du Preez and Carruthers, 2017). 12

Table 2.3: All anuran species recorded calling from the Soutpansberg during the present study (adapted from Du Preez and Carruthers, 2017). 16

Table 2.4: All adult frog and tadpole species collected across the Soutpansberg Mountain range (adapted from Du Preez and Carruthers, 2017). 18

Table 2.5: Total number of adult frogs collected across the Soutpansberg Mountain Range throughout seven fieldtrips over three years. 19

Table 2.6: Total number of tadpoles across the Soutpansberg Mountain Range throughout six fieldtrips over two years. 20

Table 3.1: List of primer sets and PCR conditions of different genotypes for all parasite groups observed in the current study. 54

Table 3.2: Details on the phylogenetic analysis of the different parasite groups. 55

Table 3.3: Blood parasites prevalence (with 95% confidence intervals limits - CI) of amphibians from the Soutpansberg Mountain Range. The sample size of each frog species is indicated between the brackets. 58

Table 3.4: A list of the 22 morphologically distinct morphotypes of *Trypanosoma* spp. observed in the current study. Characteristics such as overall shape and size, presence of a free flagellum, shape and position of nucleus, posterior kinetoplast, intensity of granulated cytoplasm and an undulating membrane, was used to characterize these *Trypanosoma* morphotypes. 59

Table 3.5: Frog species infected with unknown non-protistan inclusions listed in alphabetical order with family. 67

Table 4.1: A summary of currently recognized anuran haemococcidian species. 83

Table 5.1: *Hepatozoon* species recorded from African amphibians. 100

Table 5.2: Sample collection sites where *Amietia delalandii* was collected at the Soutpansberg Mountain range, Limpopo. 103

Table 5.3: List of the ITS-1 sequences from amphibians used in the current study. Sequences generated from the same sample: 1_SPB6 and 3_SPB1; 1_P11, 2_P5 and 3_P1; 1_P14 and 3_P2; 2_SPB4 and 3_SPB3; 2_P6 and 3_P4. 106

Table A1: List of all 132 sample localities across the Soutpansberg mountain range. 131

Table B1: Full list of anuran species across the three transects from 2019 – 2021. 137

Table C1: Distribution of tadpoles collected across the three transects from 2020 – 2021. 138

Table D1: List of sequence data used to create the 18S-COI concatenated tree. 139

Table E1: Multiple alignment distance matrix percentage (%) comparison between *Hepatozoon theileri* samples generated in the current study. Alignment was checked and a distances matrix table was created within UGENE. 140

Table F1: Multiple alignment distance matrix nt substitution site comparison between *Hepatozoon theileri* samples generated in the current study. Alignment was checked and a distances matrix table was created within UGENE. 141

LIST OF FIGURES

Figure 2.1: Nature reserves and protected areas within the Vhembe Biosphere Reserve, Limpopo province. The Soutpansberg Mountain Range lies within the Vhembe Biosphere Reserve (shown with a black boarder). Fifty-four Nature Reserves, four Forest Nature Reserves, two Protected areas, two National Parks and one Heritage site resides within the Vhembe Biosphere Reserve. Only seven Nature Reserves and one Protected area, the Mphaphuli Protected Environment, falls within the Soutpansberg Mountain Range. 6

Figure 2.2: The various vegetation types within the Vhembe Biosphere Reserve, Limpopo province. The Limpopo province includes 53 vegetations types ranging from sandy bushvelds to mistbelt forests. Of these, 27 are within the Vhembe Biosphere Reserve. 7

Figure 2.3: The mosaic of vegetation types across the Soutpansberg Mountain Range including the sample localities used in the present study. Thirteen vegetation types forms part of the Soutpansberg Mountain Range. A total number of 131 localities were visited, shown as red diamonds with its assigned locality number. The black boarder shows the Vhembe Biosphere which separates the Blouberg mountains from the Soutpansberg Mountain Range, excluding it from the study area. 10

Figure 2.4: Sampling localities across the Soutpansberg Mountain Range across three transects. Transect 1 stretching for about 45 km from the most western mountain region. Transect 2 continues for about 35 km from the Sand River until just past the Nzhelele Nature Reserve. Transect 3 extending for 40 km from Albasini dam until Thohoyandou. 13

Figure 2.5: The distribution of capture localities of adult frog specimens. A total of 540 adult frogs, from 27 species, were collected at 78 sites within all three transects. 17

Figure 2.6: The distribution of tadpole collection localities. A total number of 509 tadpoles were collected at 38 sites comprising 24 species. Sampling occurred within all three transects. 17

Figure 2.7: Acoustic sampling localities across the mountain range. Acoustic recordings were successfully conducted at 56 localities with 20 species recorded. 17

Figure 2.8: Adult frog species recorded during the current study across the Soutpansberg. (A) *Amietia delalandii,* (B) *Arthroleptis stenodactylus,* (C) *Breviceps adspersus,* (D) *Breviceps s. taeniatus*, (E) *Cacosternum boettgeri,* (F) *Chiromantis xerampelina,* (G) *Hemisus marmoratus,* (H) *Hyperolius marmoratus,* (I) *Hyperolius pusillus,* (J) *Kassina senegalensis,* (K) *Phrynobatrachus mababiensis,* (L) *Phrynobatrachus natalensis,* (M) *Phrynomantis bifasciatus,* (N) *Poyntonophrynus fenoulheti,* and (O) *Ptychadena anchietae*. 22

Figure 2.8 continued: (P) *Ptychadena mossambica*, (Q) *Ptychadena uzungwensis*, (R) *Pyxicephalus edulis*, (S) *Schismaderma carens*, (T) *Sclerophrys garmani*, (U) *Sclerophrys gutturalis*, (V) *Sclerophrys pusilla*, (W) *Strongylopus fasciatus*, (X) *Strongylopus grayii*, (Y – BB) *Tomopterna* spp., (CC) *Xenopus laevis*, and (DD) *Xenopus muelleri*. 23

Figure 2.9: New site locality of *Arthroleptis stenodactylus* within the Luvuvhu catchment, Limpopo, South Africa. Six adult specimens were collected at this site. 24

Figure 2.10: (A) *Arthroleptis stenodactylus* species distribution range as currently reported by Du Preez and Carruthers (2017). (B) Arrow showing newly extended species distribution from the current study. 24

Figure 2.11: Site localities of *Breviceps adspersus* (yellow diamond) and *Breviceps s. taeniatus* (yellow circle) across the Soutpansberg. Both *Breviceps* species were collected at two sites each. 25

Figure 2.12: (A) *Breviceps s. taeniatus* species distribution range as currently reported by Du Preez and Carruthers (2017). (B) Arrow showing newly extended species distribution from the current study. The (*) asterisk indicates the distribution range of subspecies *Breviceps sylvestris sylvestris* that is not found on the mountain range. 26

Figure 2.13: Site locality *of Poyntonophrynus fenoulheti* across the Soutpansberg. A healthy population was found at one site locality within the Goro Game Reserve. 26

Figure 2.14: Site localities of *Schismaderma carens* across the Soutpansberg. Specimens were collected at 11 sites. 27

Figure 2.15: Site localities of *Sclerophrys gutturalis, S. garmani* and *S. pusilla* across the Soutpansberg. *Sclerophrys gutturalis* was collected at nine sites*, S. garmani* at two and *S. pusilla* at thee. 28

Figure 2.16: Site locality of *Hemisus marmoratus* across the Soutpansberg. Only a single specimen was collected at one site. 29

Figure 2.17: Site localities of *Hyperolius marmoratus* and *Hyp. pusillus* across the Soutpansberg. *Hyperolius marmoratus* was collected from three all transects. Only one specimen of *Hyp. pusillus* was collected. 30

Figure 2.18: Site localities of *Kassina senegalensis* across the Soutpansberg. Specimens were collected over a wide distribution range, spanning all three transects. 31

Figure 2.19: Site localities of *Phrynomantis bifasciatus* across the Soutpansberg. *Phrynomantis bifasciatus* was not present on the mountain, but, was collected in all three transects at seven sites. 32

Figure 2.20: Site localities of *Phrynobatrachus mababiensis* and *Phry. natalensis* across the Soutpansberg. *Phrynobatrachus mababiensis* was collected at five sites and *Phry. natalensi*s at one. 32

Figure 2.21: Site localities of *Ptychadena anchietae, Pt. mossambica* and *Pt. uzungwensis* across the Soutpansberg. *Ptychadena anchietae* was the most abundant, collected at 15 sites whereas *Pt. mossambica* and *Pt. uzungwensis* were collected at one site each. 33

Figure 2.22: (A) *Ptychadena uzungwensis* species distribution range as currently reported by Du Preez and Carruthers (2017). (B) Arrow showing newly extended species distribution from the current study. 34

Figure 2.23: Site localities of *Xenopus laevis* and *X. muelleri* across the Soutpansberg. *Xenopus laevis* was collected from all transects with *X. muelleri* only present in one transect. 34

Figure 2.24: Site localities of *Amietia delalandii* across the Soutpansberg. *Amietia delalandii* was the most abundant throughout the sampling trips and was distributed across all three transects. 35

Figure 2.25: Site localities of *Cacosternum boettgeri* across the Soutpansberg. Specimens were collected from three sites. 36

Figure 2.26: Site localities of *Pyxicephalus edulis* across the Soutpansberg. Specimens were collected mostly from the north-western area of the mountain range after heavy rains. 36

Figure 2.27: Site localities of *Strongylopus fasciatus* and *S. grayii* across the Soutpansberg. *Strongylopus fasciatus* was collected on both the southern and northern slopes areas whereas *S. grayii* was recorded from one elevated site on the southern slope. 37

Figure 2.28: Site localities of *Tomopterna* spp. across the Soutpansberg. Specimens were distributed throughout the entire mountain range. 38

Figure 2.29: Site localities of *Chiromantis xerampelina* across the Soutpansberg. *Chiromantis xerampelina* was not collected on the mountain but distributed across the flatter, arid, bushveld regions. 39

Figure 2.30: Sample size collected across 27 frog species throughout the Soutpansberg. The sample includes 540 adult frog specimens of 27 species across 78 sampling localities. 40

Figure 2.31: The rarefaction curves with 95% confidence intervals for the entire sample and separate transects. A monocoloured area around every curve marks the confidence intervals. 41

Figure 2.32: Each dot represents commonness indices of species for every frog species in the sample. Error bars represent bias-corrected and accelerated 95% confidence intervals computed with 1,000 bootstrap samples by row of the abundance matrix. Blue and pink indicate rare and common frog species, respectively. 42

Figure 2.33: Non-metric multidimensional scaling. The nMDS was built on Bray-Curtis dissimilarity matrix generated based on the abundance matrix. Each coloured dot represents a separate site. The colour indicates to which transect the site is assigned and the size of the coloured dot shows the number of frogs collected in this site. Centroids show which frog species are represented in separate dots, namely the closer a site dot is to the centroid of a particular species, the greater probability that this species is present in this site (coloured dot) and vice versa. 43

Figure 3.1: Sampling localities across the Soutpansberg Mountain range indicated by dots. Sites where no haemoparasites were detected indicated with an orange dot and in red where positive infections were detected. Multiple blood parasite species were observed within five frog species from 20 sample localities. The majority of the infections were located at the eastern sites. 57

Figure 3.2: *Trypanosoma* species observed in the peripheral blood of anurans from the Soutpansberg Mountain range. (A **–** G, J **–** O) *Trypanosoma* spp. infecting *Amietia delalandii*. (B, I) *Trypanosoma* spp. infecting *Ptychadena anchietae*. *Trypanosoma* sp. I will be excluded from the dataset, from now on, due to the infected frog being collected from Blouberg, which falls outside of the study area. (C, H) *Trypanosoma* spp. infecting *Hyperolius marmoratus*. (J) *Trypanosoma* sp. infecting *Sclerophrys pusilla*. Scale bar: 20 µm. 62

Figure 3.2 continued: *Trypanosoma* species observed in the peripheral blood of anurans from the Soutpansberg Mountain Range. (P **–** T) *Trypanosoma* spp. infecting *Amietia delalandii.* (U) *Trypanosoma* sp. infecting *Ptychadena anchietae*. (V) *Trypanosoma* sp. infecting *Sclerophrys pusilla*. Scale bar: 20 µm. 63

Figure 3.3: *Hepatozoon* spp. infecting three frog species across the Soutpansberg. (A **–** L) *Hepatozoon theileri* infecting *Amietia delalandii* (n = 15). (M) *Hepatozoon ixoxo* infecting *Ptychadena anchietae* (n = 1). (N **–** O) *Hepatozoon ixoxo* infecting a single *Sclerophrys gutturalis*. Scale bar is 20 µm. 64

Figure 3.4: *Lankesterella* sp. observed in a single *Amietia delalandii* at the Soutpansberg. Scale bar is 10 µm. 65

Figure 3.5: (A **–** E) *Neofoleyellides steyni* infecting four *Amietia delalandii* specimens across the Soutpansberg. Scale bar 20 µm. 66

Figure 3.6: Infections of uncertain status and non-protistan infecting 20 frog species across the Soutpansberg. Arrow indicated slightly purple stained borders of the larger circular inclusions. Arrowhead shows small purple inclusions. (M) All three forms observed within *Amietia delalandii*. Scale bar is 10 µm. 68

Figure 3.7: The overall infection prevalence for five frog species. The bars represent observed prevalence. The error bars show the Sterne confidence intervals. The colour of the bars reflects the sample size of frog species. 69

Figure 3.8: Number of infections by each parasite in five frog species. All *Trypanosoma* morphotypes are united in one group. 70

Figure 3.9: The average prevalence of species richness (number of parasite species per host individual) for five frog species. The error bars show the bootstrapped confidence intervals. The bars represent observed species richness. The colour of the bars meets the sample size of frog species. 71

Figure 3.10: Visualisation of species co-occurrence patterns in data set of five frog species. For each parasite species pair, the Spearman correlation coefficient was calculated and the significance level was estimated (the alpha value level was equal to 0.05). Only significant correlations are shown in the plot. 72

Figure 3.11: Bayesian inference (BI) phylogenetic tree based on 18S rDNA haemogregarine sequences. The phylogenetic analysis shows the positive identification of *Hepatozoon ixoxo* and *Hepatozoon theileri* isolates extracted from *Sclerophrys gutturalis* and *Amietia delalandii*, respectively. *Klossiella equi* was selected as the outgroup. General Time Reversible model (GTR + I + G) was used. The BI node support values (probability) above 0.50 is indicated. The scale bar represents 0.02 nucleotide substitutions per site. The legend indicates the host species group. 73

Figure 3.12: Bayesian inference (BI) phylogenetic tree based on 18S rDNA *Trypanosoma* spp. sequences. The phylogenetic analysis strongly supports the clustering of all anuran trypanosomes. *Trypanosoma borreli* was selected as an outgroup. The General Time Reversible model (GTR + I + G) was used with BI node support values above 0.50 indicated on the branch lengths. The scale bar represents 0.7 nucleotide substitutions per site. The legend indicates the host species group. 74

Figure 3.13: The BI phylogenetic tree based on 18S rDNA haemococcidian species sequences. The phylogenetic analysis shows a paraphyly in the *Lankesterella* genus. *Toxoplasma gondii* was selected as an outgroup. The General Time Reversible model (GTR + I + G) was used to generate the tree with the BI node support values above 0.50 displayed as the branch lengths. The scale bar represents 0.3 nucleotide substitutions per site. The legend indicates the host species group. 76

Figure 3.14: Bayesian Inference of 18S rRNA sequences of microfilariae, shows the relationship of *Neofoleyellides steyni* compared with anuran and reptile onchocercids. *Filaria latala* is chosen to root the tree. The Kimura 1980 model (K80 + I) was used to with the BI node support values above 0.50 displayed. The scale bar represents 0.03 nucleotide substitutions per site. The legend indicates the host species group. 76

Figure 4.1: Map of various sample localities across the Soutpansberg Mountain range, Limpopo, South Africa. Black pins indicate all sampling localities of Common River Frogs, *Amietia delalandii* and the orange pin indicates the locality of the infected *Amietia delalandii*. 84

Figure 4.2: *Lankesterella* sp. observed in the peripheral blood of (A) *Amietia delalandii* from Limpopo, South Africa. (B **–** D) Immature sporozoites. (E **–** L) Mature sporozoites with (E **–** F, H **–** I) purplish-pink stained spots at random and dark purple stained borders. (D **–** F) Arrow showing slightly enlarged PV. (F) Double infection of a single erythrocyte. (G) Cytoplasm or PV not stained, causing a white vacuole-like appearance. (G) Deformation of host cell shape. (C, H 90

– L) Arrowhead showing visible refractile bodies in immature and mature sporozoites. Scale bar: 10 µm.

Figure 4.3: Bayesian Inference (BI) phylogenetic tree based on partial nu 18S rDNA sequences. Phylogenetic analysis shows the relationships between various taxa from Eimeriidae, Lankesterellidae and Schellackiidae. The aligned rDNA sequences were analyses using a General Time-Reversible model (GTR + I + G, nst = 6). Bayesian Inference node support (probability) is indicated and all nodes support values above 0.50. The final alignment contained 578 nt from 44 sequences and was rooted with *Toxoplasma gondii*. The sequence obtained from this study is written in bold. The scale bar represents 0.03 nucleotide substitutions per site. The legend indicates the host species group. 93

Figure 4.4: Bayesian Inference (BI) phylogenetic tree based on mt cytochrome c oxidase subunit I (COI) sequences. Phylogenetic analysis shows the relationships between Eimeriidae and Lankesterellidae with *Toxoplasma gondii* as the outgroup. Analysis was performed using a reversible-jump MCMC algorithm (GTR + I + G, nst = mixed). Bayesian Inference node support (probability) is indicated and all nodes support values above 0.50. The final alignment contained 713 nt from 44 sequences. The scale bar represents 0.03 nucleotide substitutions per site. The legend indicates the host species group. 94

Figure 4.5: Bayesian Inference (BI) phylogenetic based on the concatenated nu 18S rDNA and mt COI sequences. Phylogenetic analysis shows the relationships between Eimeriidae and Lankesterellidae. Different analyses models were used on both alignments. The 18S rDNA sequences were analysed using a codon-based likelihood model (GTR + I + G (nst = 6) and the COI sequences were analysed using a reversible-jump MCMC algorithm GTR + I + G (nst = mixed). Bayesian Inference node support (probability) is indicated and all nodes support values above 0.50. The final alignment contained 1861 nt from 58 sequences and was rooted using *Toxoplasma gondii*. The scale bar represents 0.07 nucleotide substitutions per site. The legend indicates the host species group. 95

Figure 5.1: Sketch representing the 18S rRNA-ITS1-5.8S rRNA sequence with the used primer position. 101

Figure 5.2: Map of sampling localities of Common River frogs, *Amietia delalandii*, across the Soutpansberg Mountain Range, Limpopo, South Africa. The size of the circle demonstrates the number of frogs collected per site and the colour of the circle demonstrates the number of frogs that where infected with *Hepatozoon theileri* per site. 103

Figure 5.3: *Hepatozoon theileri* in the peripheral blood of *Amietia delalandii*. (A – E) Various stages of developing trophozoites. (F – J) Well-developed immature gamonts (slender form). (K – L) Mature gamonts. (M – N) Long, slender extracellular gamonts. (O) Possible extracellular merozoites before entering erythrocyte. 108

Figure 5.4: Median-joining network for the ITS-1 haplotypes of *Hepatozoon theileri* constructed using the Network software v10. Haplotypes are colour coded representing the two localities, the Soutpansberg (blue) and the Botanical Garden in Potchefstroom (green). Circles indicate longer ITS-1 sequences generated with method #1, the pentagon shapes represent the nested (#2) method and the stars represent shorter ITS-1 sequences using method #3. Samples that were used for different methods are shown in colour. Numbers on the branches indicate the number of nucleotide site substitutions between haplotypes. The size of the shapes is proportional to the haplotype frequency and the red square represents a hypothetical unsampled ancestor haplotype. 109

Figure 5.5: Sampling localities of haplotypes across the Soutpansberg. The coloured labels indicate haplotypes extracted from the same specimen. 109

Figure 5.6: Bayesian Inference (BI) phylogenetic relationship based on nu ITS-1 regions isolated from Hep*atozoon theileri* infecting *Amietia delalandii*. Phylogenetic analysis shows the relationship between *Hepatozoon* species. The Felsenstein's 1981 model with a discrete Gama distribution (F81 + G4) was used for analyses. BI node support (probability) values above 0.57. The final alignment contained 229 nt from 33 sequences. *Hepatozoon sipedon* was used as an outgroup. The scale bar represents 0.05 nt substitutions per site. 111

CHAPTER 1:

GENERAL INTRODUCTION

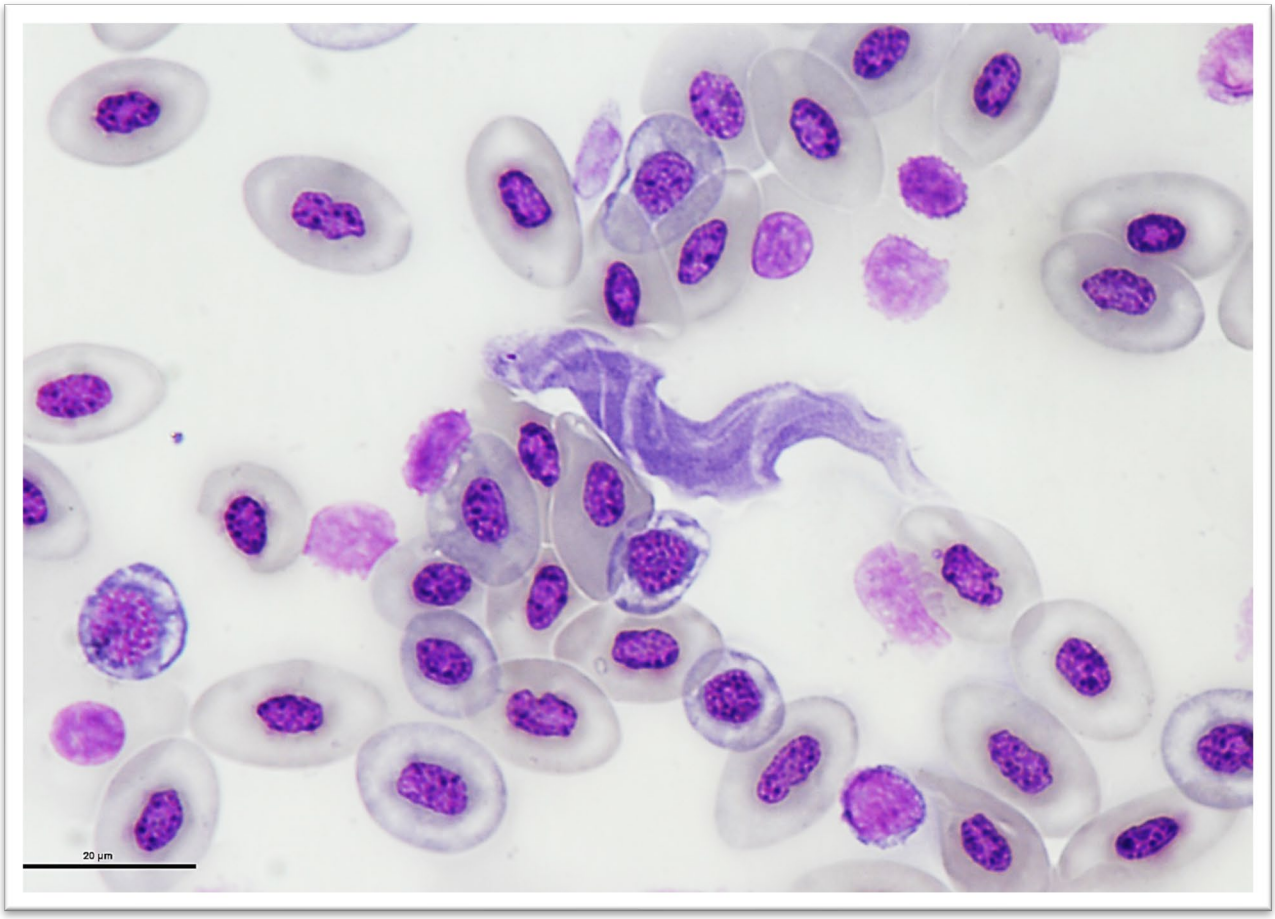

***Trypanosoma* species**

1.1 Introduction

Amphibians (Orders: Anura, Caudata and Gymnophiona) have a global distribution and are adapted for various habitats and terrestrial ecosystems, including tropical forests and semi-arid desert regions (Stebbins and Cohen, 1995; Frost *et al.*, 2006). The Anura is the only amphibian order present within South Africa, with the current study dedicating a chapter on the diversity and distribution of anuran species from northern South Africa. South Africa has a diverse landscape, with various climate conditions and unique habitat types resulting in a diverse amphibian fauna comprising 132 anuran species with 69 endemic species (Du Preez and Carruthers, 2017). The Soutpansberg Mountain range is the most northern mountain range in South Africa with a high fauna and flora diversity and endemism with various endangered species (Berger *et al.*, 2003). Nonetheless, this area has received little conservation support with less than 1% of the area being protected as a natural reserve in a fast growing agricultural and urban area. The Endangered Wildlife Trust recently embarked on an overall fauna and flora biodiversity survey of the mountain range as part of a long-term conservation project (Endangered Wildlife Trust, 2018, 2022). However, minimal information on amphibian diversity across the mountain range has been provided, with no formal anuran diversity survey conducted within the area. Based on the field guide of Du Preez and Carruthers (2017) at least 35 known frog species are expected to occur in the study area. However, only a few anecdotal records are available regarding the frogs in the study area, with limited data on their distribution across the Soutpansberg mountain range and even less information on the blood parasites that infect them.

Blood parasites have been reported on every continent within various vertebrate hosts ranging from mammals, birds, reptiles, amphibians, and fish. However, studies on anuran blood parasites from southern Africa have only recently become of interest to the science community (Readel and Goldberg, 2010; Netherlands, 2014, 2019; Netherlands *et al.*, 2014a; Netherlands *et al.*, 2015; Cook *et al.*, 2016; Netherlands *et al.*, 2018; Acosta *et al.*, 2020; Netherlands *et al.*, 2020a; Netherlands *et al.*, 2020b; Vanhove *et al.*, 2022). However, the majority of studies done on South African amphibian blood parasites was done in the tropical KwaZulu-Natal province on the east coast of South Africa (Netherlands, 2014, 2019). To date, no data is currently available on frog blood parasites from the far northern parts of South Africa, including the study area. This study will focus on the diversity of anuran blood parasite occurrence across their adult host diversity.

1.1.1 Research aims

The aims of this study are to:

1. document the anuran species diversity across the Soutpansberg Mountain Range, and;
2. document the anuran blood parasite diversity and occurrences across their host's diversity.

1.1.2 Research objectives

To achieve the aims of the study, the objectives are to:

1. undertake a comprehensive survey by means of active sampling to determine the anuran species diversity and richness;
2. document the blood parasite diversity using morphological and molecular techniques.

1.1.3 Study design

The current Master of Science dissertation includes six chapters. Chapter 1 is a brief introduction to the overall interests of the dissertation. Following Chapter 1, Chapter 2 mainly focuses on anurans whereas Chapter 3, 4 and 5 focuses on the blood parasites of these anuran hosts followed by Chapter 6 which is a short summative discussion. Chapter 2 to 5 consists of an introduction, materials and methods, results, a discussion. A complete reference list following the Harvard format of the NWU follows Chapter 6.

In ***Chapter 2***, the results of the diversity and distribution of anurans of the Soutpansberg mountain range are reported and compared with historical data on the species distribution range across the study area. In ***Chapter 3***, a detailed survey on the blood parasites infecting anuran hosts from the current study area are provided, along with the species richness and prevalence of the frog blood parasites observed. ***Chapter 4*** is a case study on haemococcidians infecting South African frogs including results on the descriptions of morphological and molecular characteristic of a *Lankesterella*-like species from the current study. In ***Chapter 5***, a detailed assessment on the molecular structure of species of *Hepatozoon* found in the current study (Chapter 3) is provided, the results are compared to haemogregarines found in South African anuran from a different geological region. ***Chapter 6***, include a brief summative discussion on the results of each chapter in the dissertation.

CHAPTER 2:

ANURAN DIVERSITY ACROSS THE SOUTPANSBERG MOUNTAIN RANGE

Breviceps adspersus

2.1 General introduction to amphibians

Amphibians comprise an ancient ectothermic vertebrate group that gave rise to all modern terrestrial vertebrates in the Devonian Period about 370 million years ago (Carroll, 2009; Dodd, 2010). These descendants have acquired adaptations to survive within diverse terrestrial environments. In doing so, amphibians have become globally distributed with representatives in nearly all terrestrial and freshwater habitats, with the exception of the polar regions and some remote oceanic islands (Stebbins and Cohen, 1995; Frost *et al.*, 2006; Du Preez and Carruthers, 2017; Wake and Koo, 2018).

Amphibian species are divided into three orders: Gymnophiona (caecilians) comprising 215 species, Caudata (salamanders and newts) 792 species and Anura (frogs and toads) with 7 524 species, making 8 531 in total (Frost, 2021). Caecilians are legless amphibians resembling large earthworms with reduced and/or no eyes and tails, populating tropical regions around the world, except for Madagascar and Oceania (Dodd, 2010). Most caecilian species are specialized for a fossorial lifestyle with exceptions of a few fully aquatic species. Little is known about these secretive creatures with most of our knowledge being obtained from observing museum specimens (Netherlands, 2019). Salamanders and newts are known as tailed amphibians and can be found in temperate and subtropical habitats of the Northern Hemisphere. They are either fully aquatic, terrestrial, amphibious, fossorial or arboreal (Dodd, 2010). Frogs and toads are the most diverse group within Amphibia and occur on every continent except for Antarctica. Anurans are terrestrial, aquatic, and amphibious and inhabit almost every environment, excluding marine habitats - with no known salt-water species.

Amphibians make up a large amount of the world's vertebrate population (Stebbins and Cohen, 1995; Frost *et al.*, 2006), but due to their secretive nature and mostly nocturnal behaviour, the number of amphibians per region can easily be misinterpreted. According to Stebbins and Cohen (1995), the number of amphibians per acre in tropical woodlands and forests, exceed those of all other terrestrial vertebrates, making amphibians the largest tissue and protein producers annually. With their large numbers, amphibians were found to be an important second-level consumer and a food source for higher vertebrates (mostly snakes and birds). The significant importance of the number of amphibians is linear to their role as primary predators of invertebrates in their ecosystem, both aquatic and terrestrial. Together with their role as predator and prey, they play an important role in energy flow and nutrient cycling in various ecosystems (Stebbins and Cohen, 1995). However, even with their numbers and their environmental importance, they are still the most threatened vertebrate group due to climate change, habitat loss, pollution and emerging diseases such as chytridiomycosis (Beebee and Griffiths, 2005).

2.1.1 South African amphibians

Anura is the only amphibian order found in southern Africa with 13 families, 34 genera and 177 species represented in southern Africa (Frost, 2021). One hundred-thirty-two anuran species can be found in South Africa, representing about 2% of the world's anuran population with 38% endemic (Frost, 2021). This diversity can be due to South Africa's high biological and landscape diversity which ranges from deserts to tropical forests. This includes nine biomes and three of the world's terrestrial biodiversity hotspots (Hrdina and Romportl, 2017). The frog distribution within South Africa is parallel to the rainfall of each region, increasing from West to East (Du Preez and Carruthers, 2017) with at least 44 anuran species in the Limpopo province.

2.1.2 Limpopo: the Vhembe Biosphere reserve

The UNESCO Vhembe Biosphere Reserve (Figure 2.1), proclaimed in 2009, makes up the northern part of the Limpopo province connecting with the borders of Botswana, Mozambique, and Zimbabwe (UNESCO, 2009). The Vhembe Biosphere Reserve consist of the species rich Blouberg- and Soutpansberg mountain ranges, the semi-arid Limpopo River Valley, Mapungubwe National Park, a UNESCO Mapungubwe Cultural Landscape World Heritage Site, the Makgabeng Plateau, a RAMSAR site namely Makuleke wetlands and the sub-tropical northern part of the Kruger National Park (UNESCO, 2009; Evans, 2017).

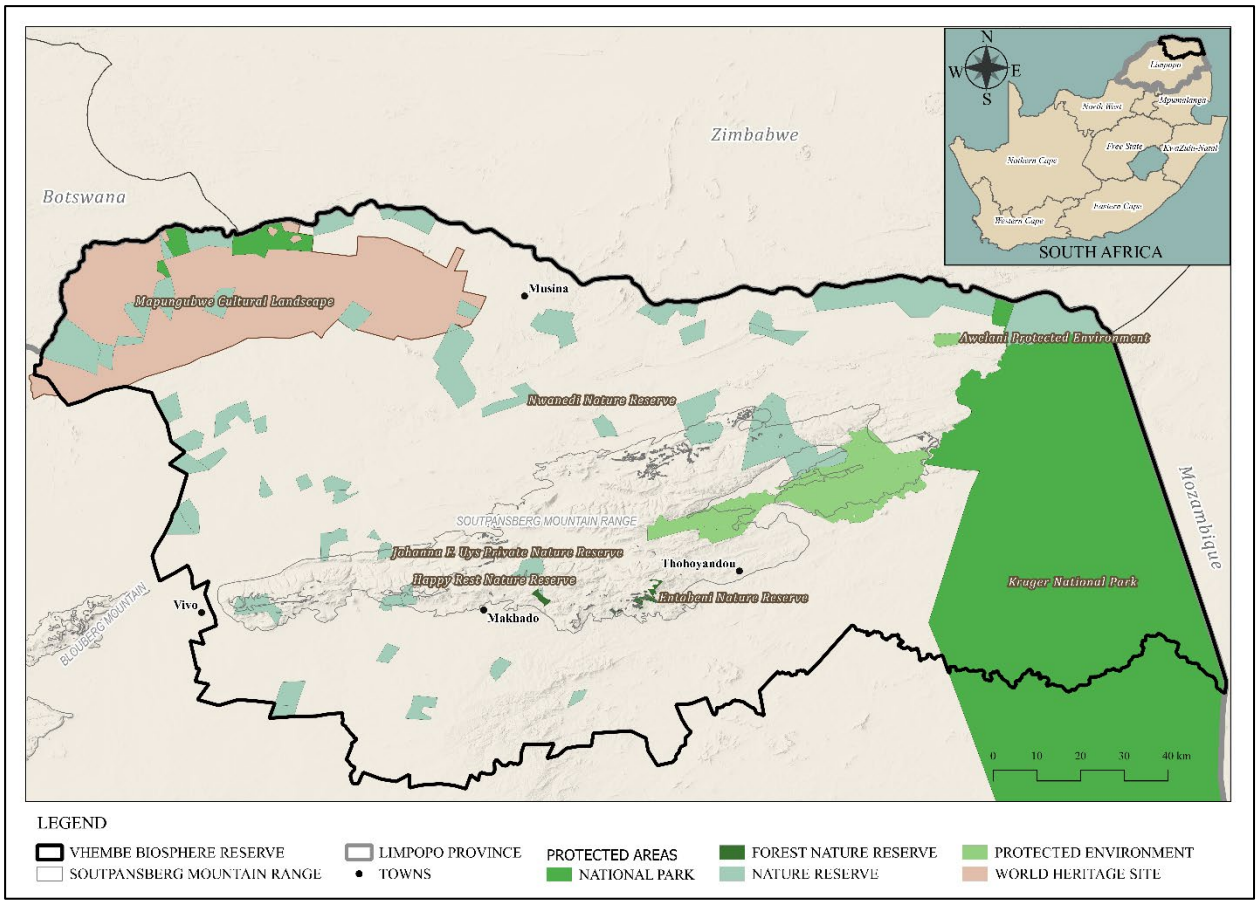

Figure 2.1: Nature reserves and protected areas within the Vhembe Biosphere Reserve, Limpopo province. The Soutpansberg Mountain Range lies within the Vhembe Biosphere Reserve (shown with a black boarder). Fifty-four Nature Reserves, four Forest Nature Reserves, two Protected areas, two National Parks and one Heritage site resides within the Vhembe Biosphere Reserve. Only seven Nature Reserves and one Protected area, the Mphaphuli Protected Environment, falls within the Soutpansberg Mountain Range.

The majority of the natural vegetation includes forests, grasslands, savannah and wetlands (Figure 2.2). The area has a rich biodiversity that includes roughly 3 000 plant species, 309 species of butterfly, 19 scorpion species, 133 species of ants, 550 species of spiders, 38 species of amphibians (Table 2.1), 140 reptile species, 542 bird species and 152 mammal species (Minter *et al.*, 2004; UNESCO, 2009; Du Preez and Carruthers, 2017; Evans, 2017; Endangered Wildlife Trust, 2018).

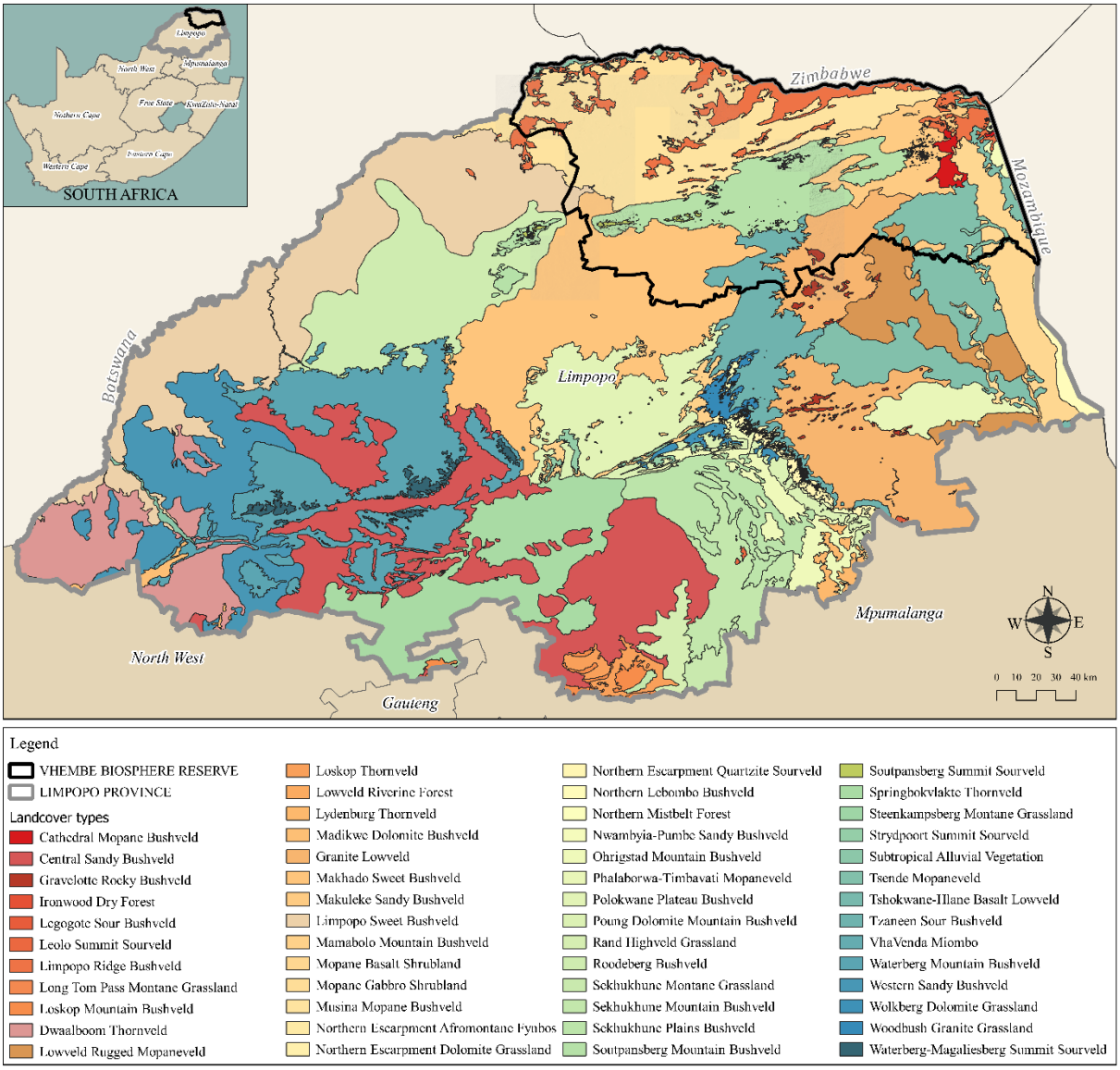

Figure 2.2: The various vegetation types within the Vhembe Biosphere Reserve, Limpopo province. The Limpopo province includes 53 vegetations types ranging from sandy bushvelds to mistbelt forests. Of these, 27 are within the Vhembe Biosphere Reserve.

2.1.3 Diversity within the Soutpansberg Mountain range

The Soutpansberg mountains is a unique mountain range situated in the extreme northern parts of South Africa in the Limpopo province. The mountains extend over 210 km, from Vivo in the West, to Punda Maria in the East - covering an approximate surface area of 6 800 km^2 (Berger *et al.*, 2003; Petford *et al.*, 2019). It ranges in altitude from roughly 200 m above sea level (asl) at Pafuri River camp, to Lajuma at 1 748 m as the highest point on the Soutpansberg mountain range (Petford *et al.*, 2019). On the south-western side of the mountain, the geological unit extends into Blouberg Mountain range and the Makgabeng Plateau, and forms part of the

sandstone Limpopo valley to the north and lastly forms part of the Kruger National Park in the east. The mountain range has a combination of different habitats and ecosystems due to the damp maritime air blowing in from the Indian Ocean on the eastern side (Figure 2.3).

Table 2.1: Frog species likely to occur in the Vhembe Biosphere listed in alphabetical order with family (adapted from Du Preez and Carruthers, 2017).

	Species name	Common name	Family		Species name	Common name	Family
1	*Arthroleptis stenodactylus*	Shovel-footed Squeaker	Arthroleptidae	20	*Hildebrandtia ornata*	Ornate frog	Ptychadenidae
2	*Leptopelis mossambicus*	Brown-backed Tree Frog	Arthroleptidae	21	*Ptychadena anchietae*	Plain Grass Frog	Ptychadenidae
3	*Breviceps adspersus*	Bushveld Rain Frog	Brevicipitidae	22	*Ptychadena mossambica*	Broad-banded Grass Frog	Ptychadenidae
4	*Breviceps sylvestris taeniatus*	Northern Forest Rain Frog	Brevicipitidae	23	*Ptychadena oxyrhynchus*	Sharp-nosed Grass Frog	Ptychadenidae
5	*Poyntonophrynus fenoulheti*	Northern Pygmy Toad	Bufonidae	24	*Ptychadena uzungwensis*	Udzungwa Grass Frog	Ptychadenidae
6	*Schismaderma carens*	Red Toad	Bufonidae	25	*Xenopus laevis*	Common Platanna	Pipidae
7	*Sclerophrys capensis*	Raucous Toad	Bufonidae	26	*Xenopus muelleri*	Müller's Platanna	Pipidae
8	*Sclerophrys garmani*	Eastern Olive Toad	Bufonidae	27	*Amietia delalandii*	Common River Frog	Pyxicephalidae
9	*Sclerophrys gutturalis*	Guttural Toad	Bufonidae	28	*Cacosternum boettgeri*	Boettger's Caco	Pyxicephalidae
10	*Sclerophrys pusilla*	Flat-backed Toad	Bufonidae	29	*Pyxicephalus adspersus*	Giant Bullfrog	Pyxicephalidae
11	*Hemisus guineensis*	Guinea Shovel-Nosed Frog	Hemisotidae	30	*Pyxicephalus edulis*	African Bullfrog	Pyxicephalidae
12	*Hemisus marmoratus*	Guinea Shovel-nosed Frog	Hemisotidae	31	*Strongylopus fasciatus*	Striped Stream Frog	Pyxicephalidae
13	*Hyperolius marmoratus*	Painted Reed Frog	Hyperoliidae	32	*Strongylopus grayii*	Clicking Stream Frog	Pyxicephalidae
14	*Hyperolius pusillus*	Water Lily Frog	Hyperoliidae	33	*Tomopterna adiastola*	Tremelo Sand Frog	Pyxicephalidae
15	*Kassina senegalensis*	Bubbling Kassina	Hyperoliidae	34	*Tomopterna krugerensis*	Knocking Sand Frog	Pyxicephalidae
16	*Phlyctimantis maculatus*	Vlei frog	Hyperoliidae	35	*Tomopterna marmorata*	Russet-backed Sand Frog	Pyxicephalidae
17	*Phrynomantis bifasciatus*	Banded Rubber Frog	Microhylidae	36	*Tomopterna natalensis*	Natal Sand Frog	Pyxicephalidae
18	*Phrynobatrachus mababiensis*	Dwarf Puddle Frog	Phrynobatrachidae	37	*Tomopterna tandyi*	Tandy's Sand Frog	Pyxicephalidae
19	*Phrynobatrachus natalensis*	Snoring Puddle Frog	Phrynobatrachidae	38	*Chiromantis xerampelina*	Southern Foam Nest Frog	Rhacophoridae

This air precipitates against the southern slopes and dissipates on the northern slopes, creating climate conditions ranging from Afromontane Forest and dense thickets on the south side to mountain grasslands and semi-deserts on the northern slopes (Berger *et al.*, 2003; Evans, 2017). Together with this, the archaeological-, geological- and biological components associated with the mountain and surrounding areas, resulted in the establishment of the Vhembe Biosphere reserve. As a result, the Soutpansberg Mountain Range has a high fauna and flora diversity on and around, the mountain range and is seen as a hotspot for diversity and endemism. The Soutpansberg Mountain Range is recognised as one of 18 of southern Africa's centres of endism. The Soutpansberg has the highest plant diversity of all 18 endemicity centres, making this area a valuable ecosystem for a variety of rare and endangered species. This led to the classification of the Soutpansberg as a Priority Conservation Area by the South African National Biodiversity Institute (SANBI) and a Critical Biodiversity Area by the Limpopo Department of Economic Development, Environment and Tourism (LEDET). The WWF also declared it a Strategic Water Source Area and it is part of the ongoing National Protected Area Expansion Strategy by South Africa's Department of Forestry, Fisheries, and Environment (DFFE).

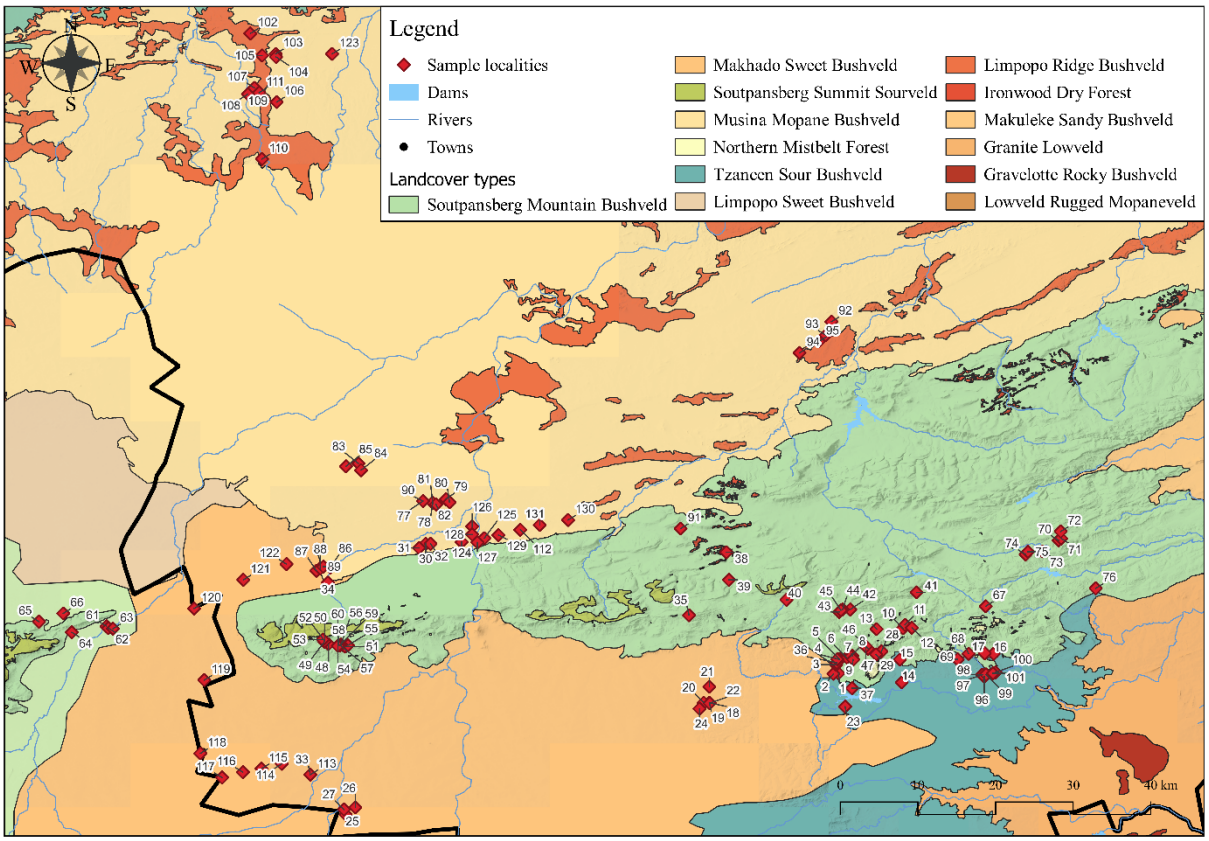

Figure 2.3: The mosaic of vegetation types across the Soutpansberg Mountain Range including the sample localities used in the present study. Thirteen vegetation types forms part of the Soutpansberg Mountain Range. A total number of 131 localities were visited, shown as red diamonds with its assigned locality number. The black boarder shows the Vhembe Biosphere which separates the Blouberg mountains from the Soutpansberg Mountain Range, excluding it from the study area.

2.1.4 Amphibian diversity across the Soutpansberg Mountain range

The anuran diversity of the mountain range is not well known with only a few anecdotal records on the different anuran species that might occur on the mountain range (Minter *et al.*, 2004). With a variety of climatic conditions and various habitat types, 11 anuran families, 19 genera and about 35 frog species (Table 2.2) are estimated to occur across the entire mountain; from the semi-desert plains of the west to more sub-tropical conditions in the east (Minter *et al.*, 2004; Du Preez and Carruthers, 2017). Only one frog species, *Breviceps sylvestris taeniatus* Poynton, 1963 is endemic to these mountains, with a limited distribution. *Breviceps s. taeniatus* inhabits the Afromontane Forest of Hanglip mountain peak at an altitude of 1 698 m asl, making it the second highest point on the mountain range.

Table 2.2: Frog species likely to occur on the Soutpansberg Mountain range listed in alphabetical order with family (adapted from Du Preez and Carruthers, 2017).

	Species name	Common name	Family		Species name	Common name	Family
1	*Arthroleptis stenodactylus*	Shovel-footed Squeaker	Arthroleptidae	19	*Ptychadena mossambica*	Broad-banded Grass Frog	Ptychadenidae
2	*Leptopelis mossambicus*	Brown-backed Tree Frog	Arthroleptidae	20	*Ptychadena oxyrhynchus*	Sharp-nosed Grass Frog	Ptychadenidae
3	*Breviceps adspersus*	Bushveld Rain Frog	Brevicipitidae	21	*Ptychadena uzungwensis*	Udzungwa Grass Frog	Ptychadenidae
4	*Breviceps sylvestris taeniatus*	Northern Forest Rain Frog	Brevicipitidae	22	*Xenopus laevis*	Common Platanna	Pipidae
5	*Poyntonophrynus fenoulheti*	Northern Pygmy Toad	Bufonidae	23	*Xenopus muelleri*	Müller's Platanna	Pipidae
6	*Schismaderma carens*	Red Toad	Bufonidae	24	*Amietia delalandii*	Common River Frog	Pyxicephalidae
7	*Sclerophrys capensis*	Raucous Toad	Bufonidae	25	*Cacosternum boettgeri*	Boettger's Caco	Pyxicephalidae
8	*Sclerophrys garmani*	Eastern Olive Toad	Bufonidae	26	*Pyxicephalus adspersus*	Giant Bullfrog	Pyxicephalidae
9	*Sclerophrys gutturalis*	Guttural Toad	Bufonidae	27	*Pyxicephalus edulis*	African Bullfrog	Pyxicephalidae
10	*Sclerophrys pusilla*	Flat-backed Toad	Bufonidae	28	*Strongylopus fasciatus*	Striped Stream Frog	Pyxicephalidae
11	*Hemisus marmoratus*	Guinea Shovel-nosed Frog	Hemisotidae	29	*Strongylopus grayii*	Clicking Stream Frog	Pyxicephalidae
12	*Hyperolius marmoratus*	Painted Reed Frog	Hyperoliidae	30	*Tomopterna adiastola*	Tremelo Sand Frog	Pyxicephalidae
13	*Hyperolius pusillus*	Water Lily Frog	Hyperoliidae	31	*Tomopterna krugerensis*	Knocking Sand Frog	Pyxicephalidae
14	*Kassina senegalensis*	Bubbling Kassina	Hyperoliidae	32	*Tomopterna marmorata*	Russet-backed Sand Frog	Pyxicephalidae
15	*Phrynomantis bifasciatus*	Banded Rubber Frog	Microhylidae	33	*Tomopterna natalensis*	Natal Sand Frog	Pyxicephalidae
16	*Phrynobatrachus mababiensis*	Dwarf Puddle Frog	Phrynobatrachidae	34	*Tomopterna tandyi*	Tandy's Sand Frog	Pyxicephalidae
17	*Phrynobatrachus natalensis*	Snoring Puddle Frog	Phrynobatrachidae	35	*Chiromantis xerampelina*	Southern Foam Nest Frog	Rhacophoridae
18	*Ptychadena anchietae*	Plain Grass Frog	Ptychadenidae				

2.2 Research methodology

2.2.1 Locality and site selection

The present study was conducted in northern Limpopo at various sites associated with the Soutpansberg Mountain Range. The Soutpansberg extends for 210 km from west to east. Due to the size and the various landscape and ecological changes, the study area is divided into almost equal transects including the arid northern and subtropical southern slopes. Both of which extend into bushveld plains. Three transects were erected and various location sites were identified within the study area (Figure 2.4). Transect 1 includes the west end of Vivo extending until Waterpoort on the north, where the Sand River cuts through the mountain. Transect 2 extends from east of the Sand River toward the Nzhelele dam in the north and lastly, transect three includes Albasini dam extending to the west all the way to Thohoyandou and the Luvuvhu river system. Overall, 132 sites across all three transects, including the northern and southern plains, were scouted (see appendix A). This included road sites that were noted while driving on rainy nights for acoustic sampling. The Blouberg Mountain is separate from the Soutpansberg, but, was still included as a sampling locality for a larger project on the biodiversity of anurans from

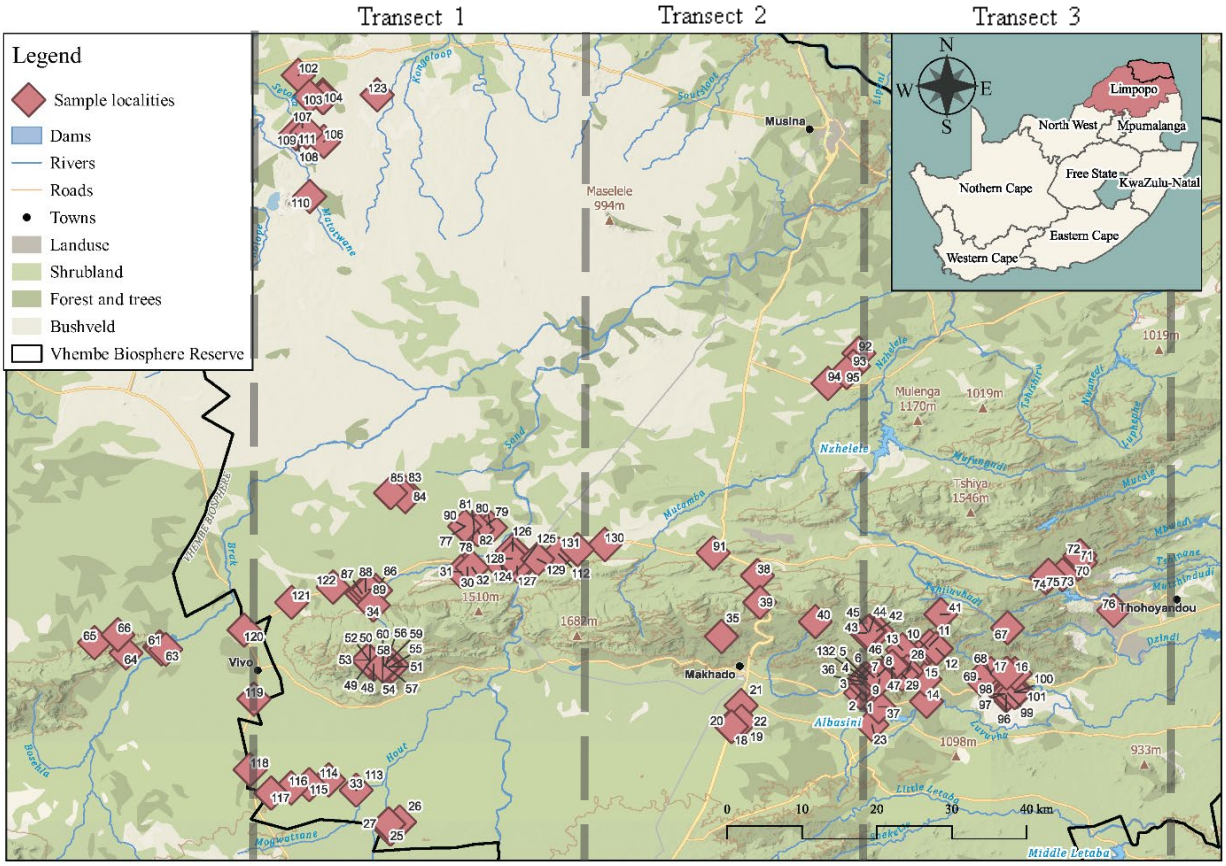

Figure 2.4: Sampling localities across the Soutpansberg Mountain Range across three transects. Transect 1 stretching for about 45 km from the most western mountain region. Transect 2 continues for about 35 km from the Sand River until just past the Nzhelele Nature Reserve. Transect 3 extending for 40 km from Albasini dam until Thohoyandou.

the Vhembe Biosphere. All specimens collected, however, were excluded from the current study due to the present study's focus on the distribution of anuran species across the Soutpansberg Mountain range. Equal efforts were made to sample as much as possible within all three transects, however, due to environmental and rainfall differences, some areas yielded more sampling locality opportunities with higher anuran sample counts. Transect one included 64 sampling localities, transect two included 16 sampling localities and, lastly, transect three included 46 sampling localities. A large area on the southern slopes within Transect 2 was not accessible to the public, resulting in lower sampling localities in the majority of the middle transect. One-hundred-thirty-two sampling localities were visited during sampling trips to determine the presence of adult frogs or tadpole species.

2.2.2 Sample collection

Frog collection by means of active sampling

All sampling techniques and data collection was done by Prof Louis du Preez and Dr Edward Netherlands on previous field trips throughout 2019 to 2021 (Ethics Number NWU-00380-16-A5). Adult frogs were collected at night by means of active sampling from sites across the Soutpansberg Mountain Range. These sites were visited during the warmer and wetter summer months of February 2019, February 2020, October – December 2020, February 2021, April 2021, and September 2021. According to permit regulations, 10 specimens per species per site was allowed to be collected. This was applied to all sites visited but not always fulfilled. Upon collection, specimens were individually placed in plastic bags or containers with sufficient water and damp vegetation. Specimens were assigned unique field numbers and transported back to a field laboratory. At the laboratory, specimens were identified to species level using du Preez and Carruthers's (2017) field guide, weighed and measured, then, once all the necessary data was collected, they were released at the site of capture once more. Tadpoles were collected with dip nets by means of actively sweeping various waterbodies and possible breeding sites.

Where possible, two voucher specimens per species per sampling locality were euthanised using MS222 and fixed in 10% neutral buffered formalin to be deposited into the African Amphibian Conservation Research Group (AACRG) anuran collection at the North-West University, Potchefstroom, South Africa. This collection forms part of the official South African Institute of Aquatic Biodiversity (SAIAB) museum collections. Muscle tissue and blood samples, collected from the hind ling of each adult specimen, was preserved in 99.6% molecular grade ethanol respectively, for future barcoding purposes within the scope of a larger study.

Passive acoustic sampling

Passive acoustic observations were also included at all sites visited and, while on the road on rainy nights on the N1, as well as on the R521, R522, R523. Frog calls were identified according to the Du Preez and Carruthers's frog app.

2.3 Results

2.3.1 Amphibian diversity across the Soutpansberg mountain

Specimens were collected successfully from 89 of the original 132 sampling localities. Several sites did not harbour any anuran species; this could be due to insufficient rainfall, or that seasonal preferences of species differed from when the sampling trips were executed.

Within the time frame of three years and seven sampling trips, 11 families, 19 genera and 29 frog species were collected or encountered throughout the Soutpansberg sampling localities (Table 2.4). A total of 540 adult frogs (Table 2.5) and 509 tadpoles (Table 2.6, also Appendix C for tadpole distribution across the transects) were collected and processed at 89 of the initial 132 sampling sites. Adult frogs were collected at 78/89 sites (Figure 2.5) of which 27 species were recorded, whereas, tadpole specimens were collected at 38/89 sites (Figure 2.6) comprising 24 species. However, the first sampling trip in 2019, was used as a scouting trip to identify potential sites. Opportunistic sampling occurred with no tadpoles collected during this time. Passive acoustic sampling was carried out at all sites visited, as well as at opportunistic sites along the road. Acoustic recordings at 56 localities and resulted in 20 species being recorded (Figure 2.7). Additionally, one species, *Leptopelis mossambicus* Poynton, 1985*,* was added to the list that was not initially observed by means of active sampling (Table 2.3). This method also confirmed that *Tomopterna adiastola* Channing & du Preez, 2020*, T. marmorata* Peters, 1854 and *T. tandyi* Channing & Bogart, 1996 do occur in the study area. *Tomopterna adiastola,* and *T. tandyi* are cryptic species and morphologically indistinguishable, thus, all *Tomopterna* species collected were preliminary identified as *Tomopterna* sp. Further work on the *Tomopterna* species within the Vhembe Biosphere is needed to determine the true distribution ranges of these species.

The highest diversity of adult frog species was collected across the mountain range, during 2020 and 2021 with 22 species for each year reported (Table 2.5), however, more individual specimens were collected during 2020 with the highest collection count occurring during the summer months in February. *Amietia delalandii* Duméril & Bibron, 1841 was the only species encountered on every sampling trip with a total of 109 adult frogs collected. This was followed by

Ptychadena anchietae Bocage, 1867 at 50 specimens, *Hyperolius marmoratus* Rapp, 1842 at 47, *Tomopterna* spp. at 37 and *Phrynomantis bifasciatus* Smith, 1847 at 26 specimens.

Table 2.3: All anuran species recorded calling from the Soutpansberg during the present study (adapted from Du Preez and Carruthers, 2017).

Species name	Family
Leptopelis mossambicus	Arthroleptidae
Breviceps sylvestris taeniatus	Brevicipitidae
Poyntonophrynus fenoulheti	Bufonidae
Schismaderma carens	Bufonidae
Sclerophrys pusilla	Bufonidae
Sclerophrys gutturalis	Bufonidae
Sclerophrys garmani	Bufonidae
Hyperolius marmoratus	Hyperoliidae
Kassina senegalensis	Hyperoliidae
Phrynomantis bifasciatus	Microhylidae
Phrynobatrachus mababiensis	Phrynobatrachidae
Ptychadena anchietae	Ptychadenidae
Amietia delalandii	Pyxicephalidae
Cacosternum boettgeri	Pyxicephalidae
Pyxicephalus edulis	Pyxicephalidae
Strongylopus fasciatus	Pyxicephalidae
Tomopterna adiastola	Pyxicephalidae
Tomopterna marmorata	Pyxicephalidae
Tomopterna tandyi	Pyxicephalidae
Chiromantis xerampelina	Rhacophoridae
20 anuran species	

.

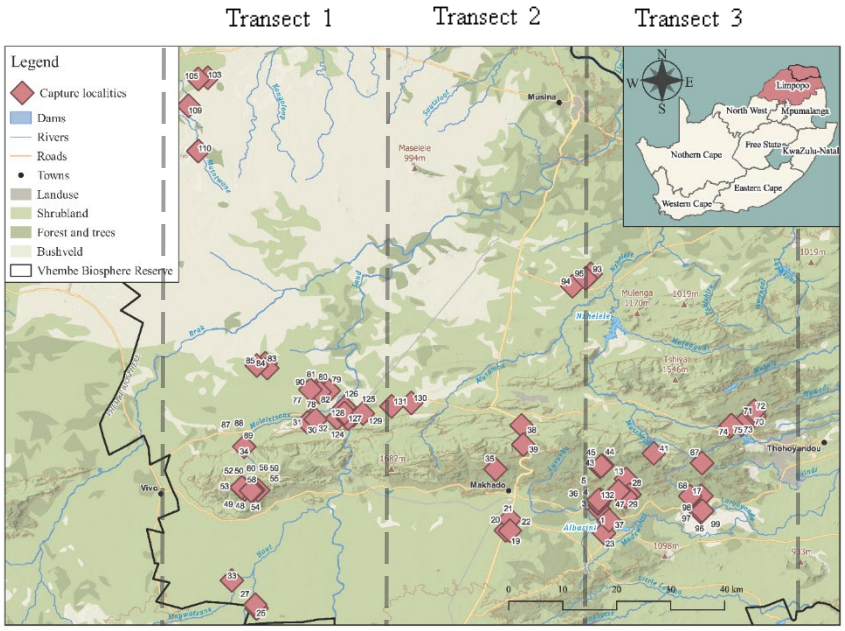

Figure 2.5: The distribution of capture localities of adult frog specimens. A total of 540 adult frogs, from 27 species, were collected at 78 sites within all three transects.

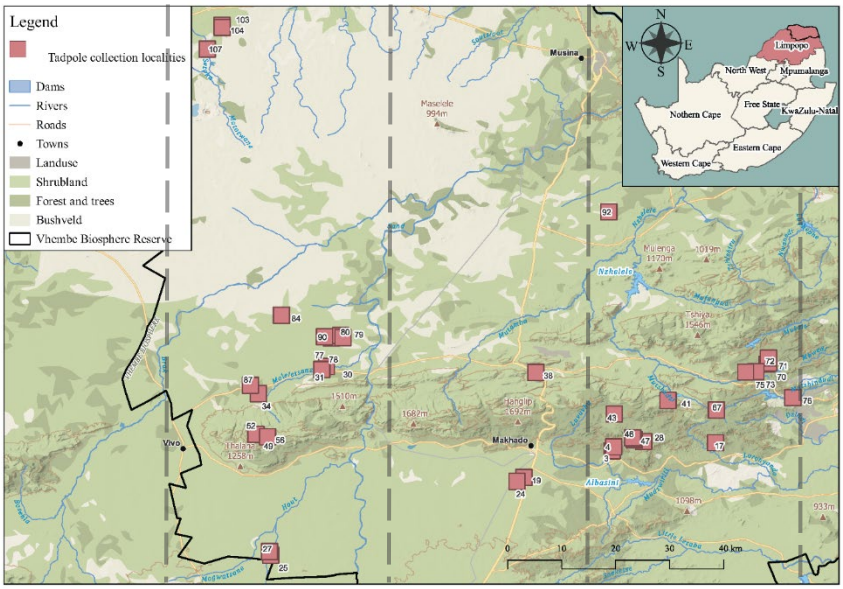

Figure 2.6: The distribution of tadpole collection localities. A total number of 509 tadpoles were collected at 38 sites comprising 24 species. Sampling occurred within all three transects.

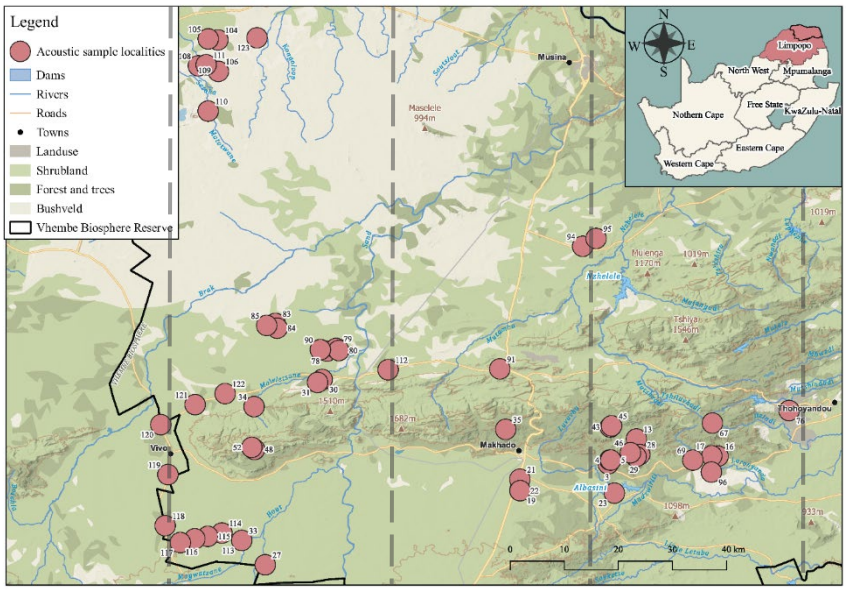

Figure 2.7: Acoustic sampling localities across the mountain range. Acoustic recordings were successfully conducted at 56 localities with 20 species recorded.

Table 2.4: All adult frog and tadpole species collected across the Soutpansberg Mountain range (adapted from Du Preez and Carruthers, 2017).

	Species name	Common name	Family		Species name	Common name	Family
1	*Arthroleptis stenodactylus*	Shovel-footed Squeaker	Arthroleptidae	19	*Ptychadena uzungwensis*	Udzungwa Grass Frog	Ptychadenidae
2	*Leptopelis mossambicus*	Brown-backed Tree Frog	Arthroleptidae	20	*Xenopus laevis*	Common Platanna	Pipidae
3	*Breviceps adspersus*	Bushveld Rain Frog	Brevicipitidae	21	*Xenopus muelleri*	Müller's Platanna	Pipidae
4	*Breviceps sylvestris taeniatus*	Northern Forest Rain Frog	Brevicipitidae	22	*Amietia delalandii*	Common River Frog	Pyxicephalidae
5	*Poyntonophrynus fenoulheti*	Northern Pygmy Toad	Bufonidae	23	*Cacosternum boettgeri*	Boettger's Caco	Pyxicephalidae
6	*Schismaderma carens*	Red Toad	Bufonidae	24	*Pyxicephalus adspersus*	Giant Bullfrog	Pyxicephalidae
7	*Sclerophrys garmani*	Eastern Olive Toad	Bufonidae	25	*Pyxicephalus edulis*	African Bullfrog	Pyxicephalidae
8	*Sclerophrys gutturalis*	Guttural Toad	Bufonidae	26	*Strongylopus fasciatus*	Striped Stream Frog	Pyxicephalidae
9	*Sclerophrys pusilla*	Flat-backed Toad	Bufonidae	27	*Strongylopus grayii*	Clicking Stream Frog	Pyxicephalidae
10	*Hemisus marmoratus*	Guinea Shovel-nosed Frog	Hemisotidae	28	*Tomopterna* sp.	Tremelo Sand Frog	Pyxicephalidae
11	*Hyperolius marmoratus*	Painted Reed Frog	Hyperoliidae	29	*Chiromantis xerampelina*	Southern Foam Nest Frog	Rhacophoridae
12	*Hyperolius pusillus*	Water Lily Frog	Hyperoliidae				
13	*Kassina senegalensis*	Bubbling Kassina	Hyperoliidae				
14	*Phrynomantis bifasciatus*	Banded Rubber Frog	Microhylidae				
15	*Phrynobatrachus mababiensis*	Dwarf Puddle Frog	Phrynobatrachidae				
16	*Phrynobatrachus natalensis*	Snoring Puddle Frog	Phrynobatrachidae				
17	*Ptychadena anchietae*	Plain Grass Frog	Ptychadenidae				
18	*Ptychadena mossambica*	Broad-banded Grass Frog	Ptychadenidae				

Table 2.5: Total number of adult frogs collected across the Soutpansberg Mountain Range throughout seven fieldtrips over three years.

		2019	*2020*				*2021*			
Species name	**Family**	**Feb**	**Feb**	**Oct**	**Nov**	**Des**	**Feb**	**Apr**	**Sept**	**Total**
Arthroleptis stenodactylus	Arthroleptidae							6		**6**
Breviceps adspersus	Brevicipitidae		1				1			**2**
Breviceps s. taeniatus	Brevicipitidae			6					1	**7**
Poyntonophrynus fenoulheti	Bufonidae		10				10			**20**
Schismaderma carens	Bufonidae	1	4		12		1	1		**19**
Sclerophrys garmani	Bufonidae	6					5	1		**12**
Sclerophrys gutturalis	Bufonidae	8		4	6	1				**19**
Sclerophrys pusilla	Bufonidae	1	4				9			**14**
Hemisus marmoratus	Hemisotidae			1						**1**
Hyperolius marmoratus	Hyperoliidae	14	8	10	8		7			**47**
Hyperolius pusillus	Hyperoliidae							1		**1**
Kassina senegalensis	Hyperoliidae	2	8	1	3	2	4			**20**
Phrynomantis bifasciatus	Microhylidae	8	11		1		6			**26**
Phrynobatrachus mababiensis	Phrynobatrachidae		4		10	1	1	5		**21**
Phrynobatrachus natalensis	Phrynobatrachidae							2		**2**
Xenopus laevis	Pipidae	1	2	3	4			2		**12**
Xenopus muelleri	Pipidae		2					11		**13**
Ptychadena anchietae	Ptychadenidae	12	3	7	14		12	2		**50**
Ptychadena mossambica	Ptychadenidae	4								**4**
Ptychadena uzungwensis	Ptychadenidae				14	6				**20**
Amietia delalandii	Pyxicephalidae	18	56	5	11	4	7	5	3	**109**
Cacosternum boettgeri	Pyxicephalidae		1	10	2					**13**
Pyxicephalus edulis	Pyxicephalidae		7				14			**21**
Strongylopus fasciatus	Pyxicephalidae				10				2	**12**
Strongylopus grayii	Pyxicephalidae				2				3	**5**
Tomopterna sp.	Pyxicephalidae		12	7	4		12	2		**37**
Chiromantis xerampelina	Rhacophoridae	2	9	1			15			**27**
Total frogs collected		77	142	55	101	14	104	38	9	
Total frog species		12	16	11	14	5	14	11	4	
Total frogs collected per year		77	312				151			
Total frog species per year		12	22				22			
Grand total		540 adult frogs collected								
Grand total species		27 species								

Table 2.6: Total number of tadpoles across the Soutpansberg Mountain Range throughout six fieldtrips over two years.

		2020				*2021*			
Species name	**Family**	**Feb**	**Oct**	**Nov**	**Des**	**Feb**	**Apr**	**Sept**	**Total**
Leptopelis mossambicus	Arthroleptidae		1					1	**2**
Poyntonophrynus fenoulheti	Bufonidae					10			**10**
Schismaderma carens	Bufonidae			2					**2**
Sclerophrys garmani	Bufonidae			1		3			**4**
Sclerophrys gutturalis	Bufonidae			3	1	22		8	**34**
Sclerophrys sp.	Bufonidae			1					**1**
Hemisus marmoratus	Hemisotidae	6				6		1	**13**
Hyperolius marmoratus	Hyperoliidae			3		5			**8**
Kassina senegalensis	Hyperoliidae	13			2	3	5	26	**49**
Phrynomantis bifasciatus	Microhylidae	19				8			**27**
Phrynobatrachus mababiensis	Phrynobatrachidae							1	**1**
Phrynobatrachus natalensis	Phrynobatrachidae				10				**10**
Xenopus laevis	Pipidae	10	3		1			1	**15**
Xenopus muelleri	Pipidae	5					6		**11**
Ptychadena anchietae	Ptychadenidae	7	1	10	15	62		23	**118**
Ptychadena uzungwensis	Ptychadenidae			4					**4**
Amietia delalandii	Pyxicephalidae	3	11	18	24	4		1	**61**
Cacosternum boettgeri	Pyxicephalidae	10					1	1	**12**
Pyxicephalus adspersus	Pyxicephalidae	8							**8**
Pyxicephalus edulis	Pyxicephalidae					1			**1**
Strongylopus fasciatus	Pyxicephalidae			4				1	**5**
Strongylopus grayii	Pyxicephalidae			4				4	**8**
Tomopterna sp.	Pyxicephalidae	7			2	25		16	**50**
Chiromantis xerampelina	Rhacophoridae	14				35	1	5	**55**
Total tadpoles collected		102	16	50	55	184	13	89	
Total tadpole species		11	4	10	7	12	4	13	
Total tadpoles collected per year		223				286			
Total tadpole species per year		21				19			
Grand total		509 tadpoles collected							
Grand total species		24 species							

2.3.2 Amphibian species distribution across the Soutpansberg

The distribution of anuran species collected was determined by the presence or absence of each species within the three transects. Ten species were present within all three transects and include: *A. delalandii, Chiromantis xerampelina* Peters, 1854*, H. marmoratus, Kassina senegalensis* Duméril & Bibron, 1841*, Phrynobatrachus mababiensis* FitzSimons, 1932*, P. bifasciatus, P. anchietae, Schismaderma carens* Smith, 1848*, Tomopterna* spp. and *Xenopus laevis* Daudin, 1802. This is in accordance with the distribution maps of Du Preez and Carruthers

(2017) field guide. Twenty-seven adult anuran species from 11 families were reported from the Soutpansberg (see Figures 2.9 – 2.29).

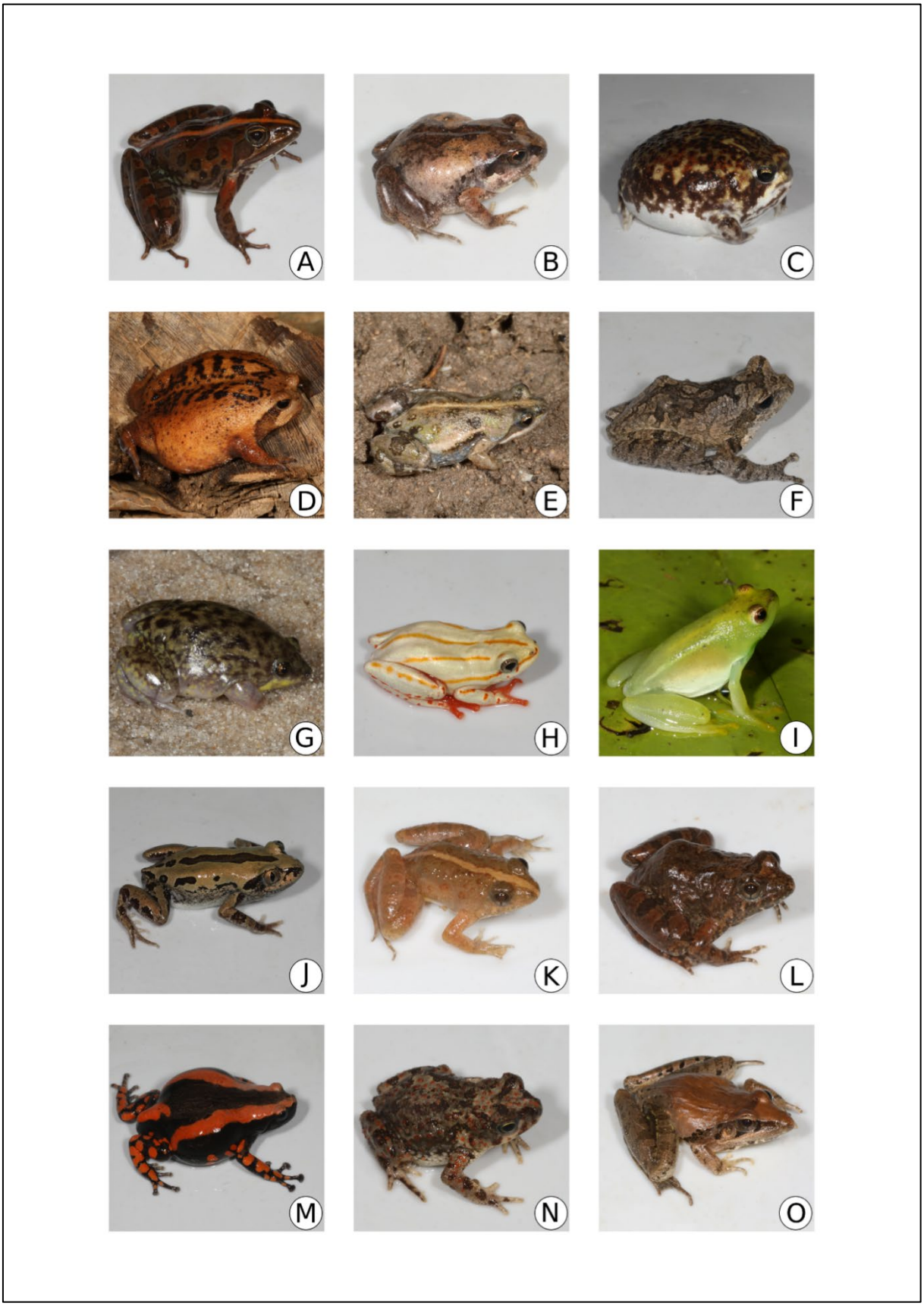

Figure 2.8: Adult frog species recorded during the current study across the Soutpansberg. (A) *Amietia delalandii,* (B) *Arthroleptis stenodactylus,* (C) *Breviceps adspersus,* (D) *Breviceps s. taeniatus,* (E) *Cacosternum boettgeri,* (F) *Chiromantis xerampelina,* (G) *Hemisus marmoratus,* (H) *Hyperolius marmoratus,* (I) *Hyperolius pusillus,* (J) *Kassina senegalensis,* (K) *Phrynobatrachus mababiensis*, (L) *Phrynobatrachus natalensis,* (M) *Phrynomantis bifasciatus,* (N) *Poyntonophrynus fenoulheti,* and (O) *Ptychadena anchietae.*

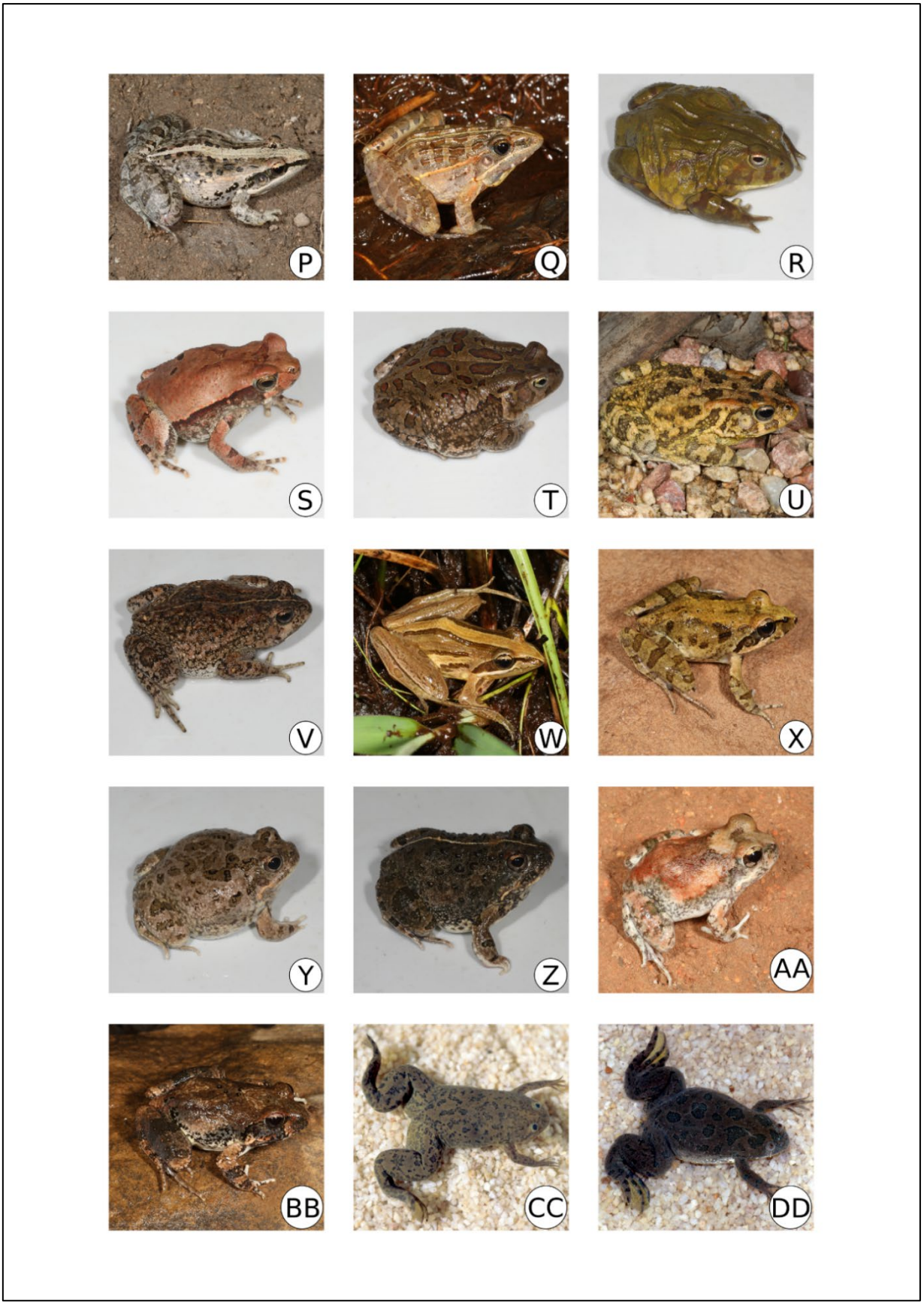

Figure 2.8 continued: (P) *Ptychadena mossambica,* (Q) *Ptychadena uzungwensis,* (R) *Pyxicephalus edulis,* (S) *Schismaderma carens,* (T) *Sclerophrys garmani,* (U) *Sclerophrys gutturalis,* (V) *Sclerophrys pusilla,* (W) *Strongylopus fasciatus,* (X) *Strongylopus grayii,* (Y – BB) *Tomopterna* spp., (CC) *Xenopus laevis,* and (DD) *Xenopus muelleri.*

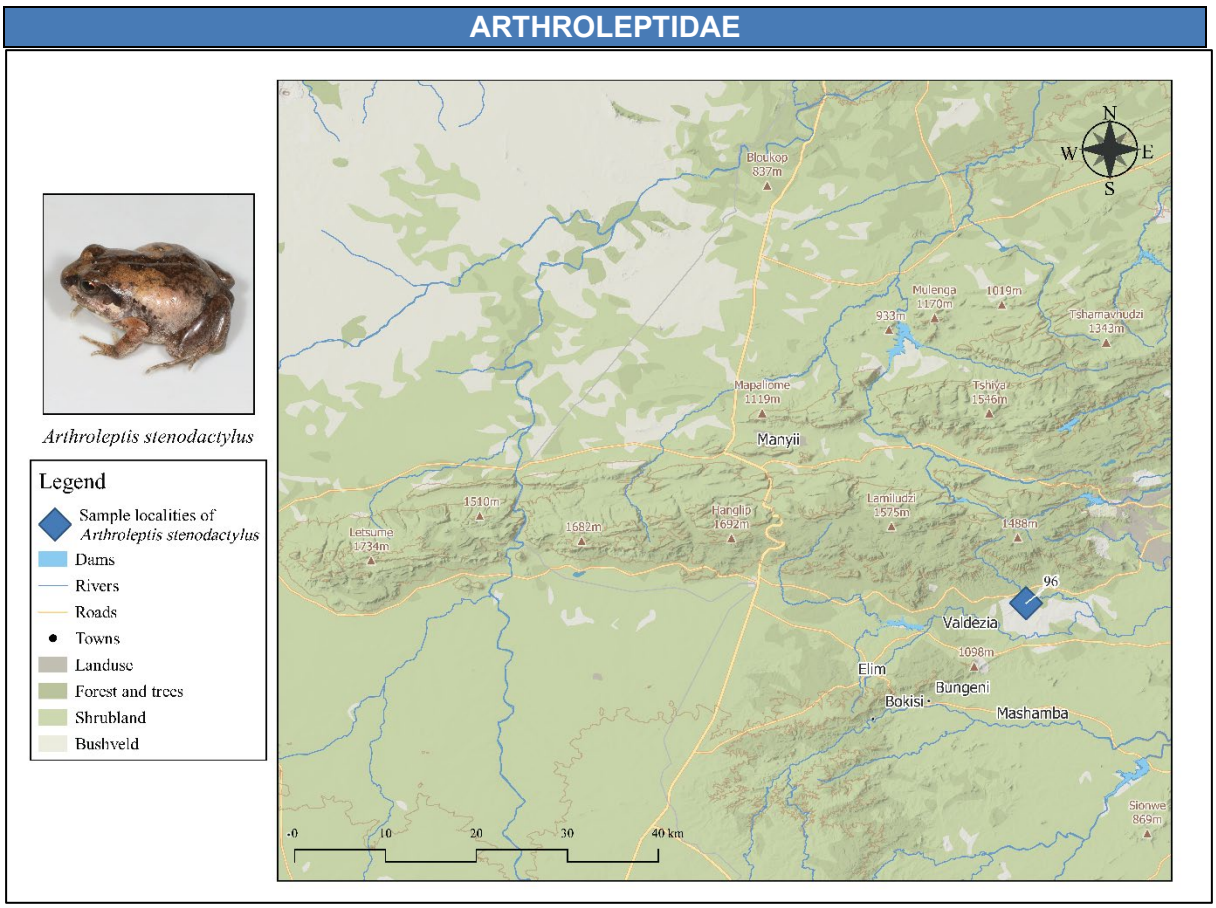

Figure 2.9: New site locality of *Arthroleptis stenodactylus* within the Luvuvhu catchment, Limpopo, South Africa. Six adult specimens were collected at this site.

The genus *Arthroleptis* forms part of the Arthroleptidae family and is more commonly known as squeakers. *Arthroleptis stenodactylus* Pfeffer, 1893 was reported at a farmhouse near Levubu (-23.07697, 30.25459), which forms part of the Luvuvhu catchment system (Figure 2.9). The species was not associated with a water body but frequented gardens in a farmstead. This is the first reported sighting of *A. stenodactylus* at the Soutpansberg mountain range and, thus, the distribution of *A. stenodactylus* has been extended to include the Luvuvhu system of the Soutpansberg in northern Limpopo (Figure 2.10).

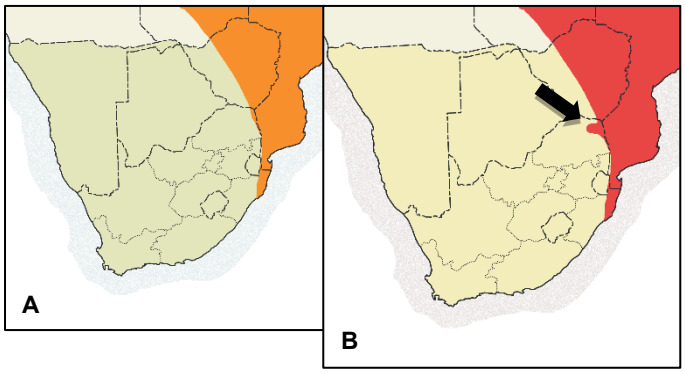

Figure 2.10: (A) *Arthroleptis stenodactylus* species distribution range as currently reported by Du Preez and Carruthers (2017). (B) Arrow showing newly extended species distribution from the current study.

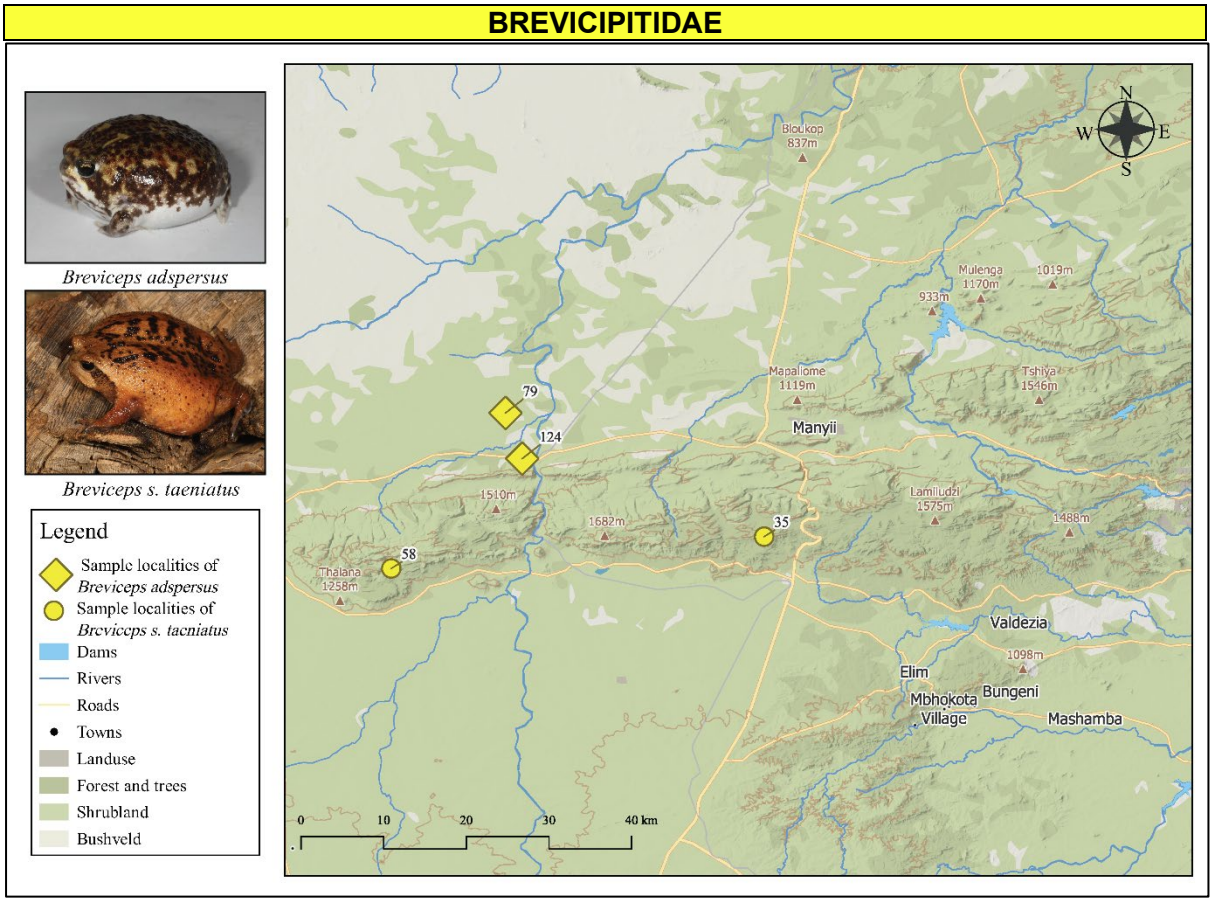

Figure 2.11: Site localities of *Breviceps adspersus* (yellow diamond) and *Breviceps s. taeniatus* (yellow circle) across the Soutpansberg. Both Breviceps species were collected at two sites each.

Breviceps adspersus Peters, 1882 is said to inhabit the entire Limpopo province and was found within the current study in the semi-arid grasslands of the northern plains of the Soutpansberg, as well as on one of the road sites (Figure 2.11). *Breviceps s. taeniatus* inhabits a small area in the Afromontane forests of the second highest mountain peak on the Soutpansberg, the Hanglip forest reserve (-22.99972, 29.88277). A healthy population was encountered and they were actively calling on a cool, foggy evening following a downpour. The highest mountain peak on the mountain range, Lajuma research centre (-23.03739, 29.44145) is found in the west and shares similarities in habitat types with the Hanglip reserve (Figure 2.11). This site is now known as the second site for the occurrence of *B. s. taeniatus.* This expands the distribution of *B. s. taeniatus* on the Soutpansberg mountain range to include the western mountain peaks (Figure 2.12).

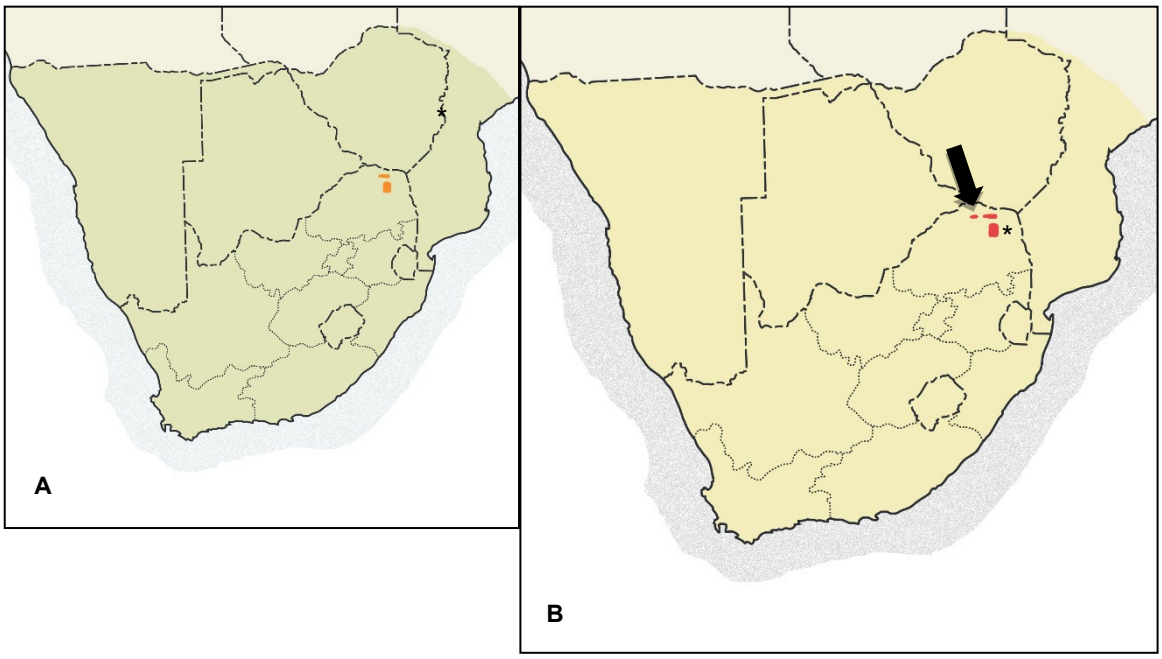

Figure 2.12 (A) *Breviceps s. taeniatus* species distribution range as currently reported by Du Preez and Carruthers (2017). (B) Arrow showing newly extended species distribution from the current study. The (*) asterisk indicates the distribution range of subspecies *Breviceps sylvestris sylvestris* that is not found on the mountain range.

BUFONIDAE

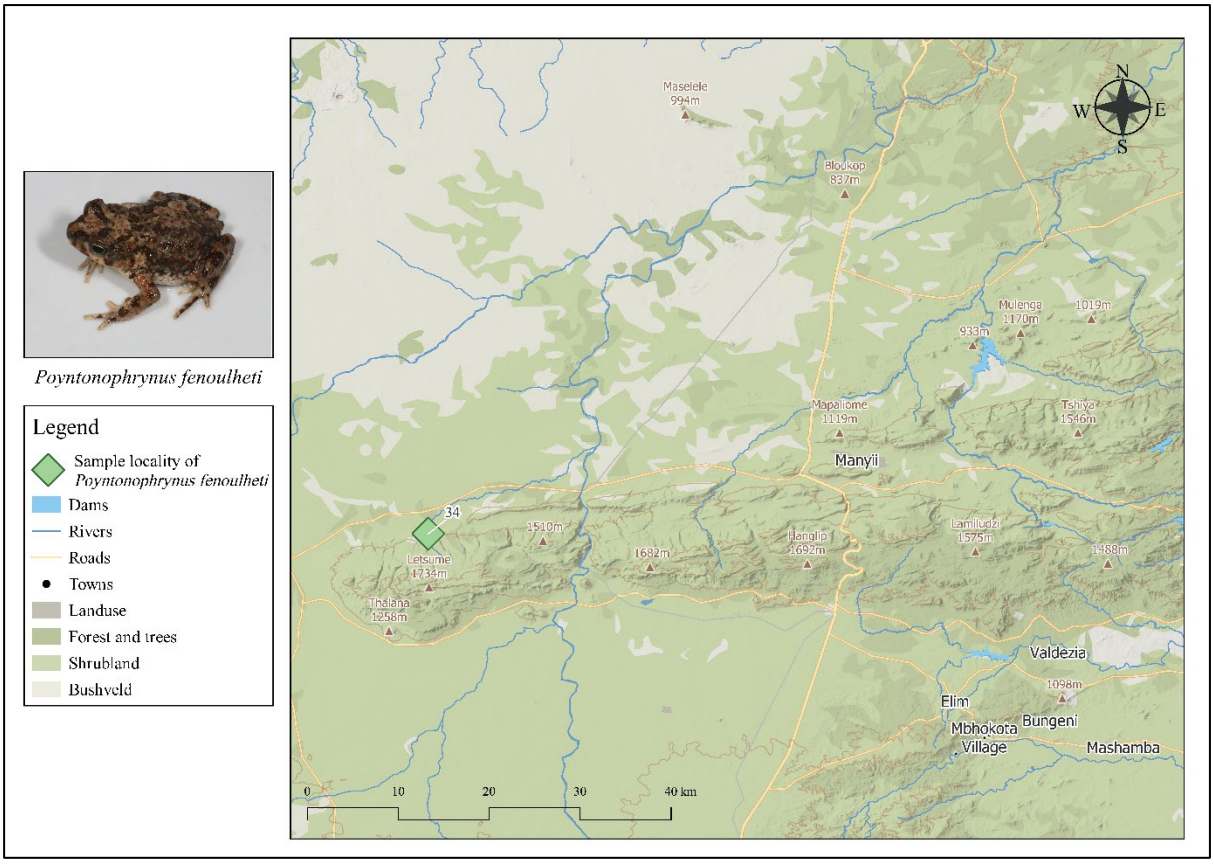

Figure 2.13: Site locality of *Poyntonophrynus fenoulheti* across the Soutpansberg. A healthy population was found at one site locality within the Goro Game Reserve.

Bufonidae is a relatively large toad family, of which the genera *Poyntonophrynus* (Pygmy toads), *Schismaderma* (Red toads) and *Sclerophrys* (Typical toads) were observed within the study area. *Poyntonophrynus fenoulheti* Hewitt & Methuen, 1913 was recorded at one site on the more arid northern side of the mountain at Goro Reserve (-22.9587, 29.428). Specimens were collected in small rock pools as part of a mountain seep (Figure 2.13). Males were actively calling and breeding in the very shallow rock pools was observed.

Schismaderma carens is distributed throughout Northern Limpopo and was collected within all three transects as well as on both the northern and the southern sides of the mountain (Figure 2.14). Red toads were collected on the roads and open areas where they foraged.

Three typical toad species (Figure 2.15), *Sclerophrys gutturalis* Power, 1927, *S. garmani* Meek, 1897, and *S. pusilla* Mertens, 1937 was collected from the Soutpansberg. All tree species were collected from the wetter eastern side of the mountain, with *S. gutturalis* being the most abundant with the widest distribution area. *Sclerophrys garmani* had a very small distribution area, collected only form one sampling locality and lastly *S. pusilla* was collected on both the wetter eastern side and the more arid western region at the Goro Reserve. Toads, especially *S. pusilla*, were collected around stagnant pools where the males formed choruses.

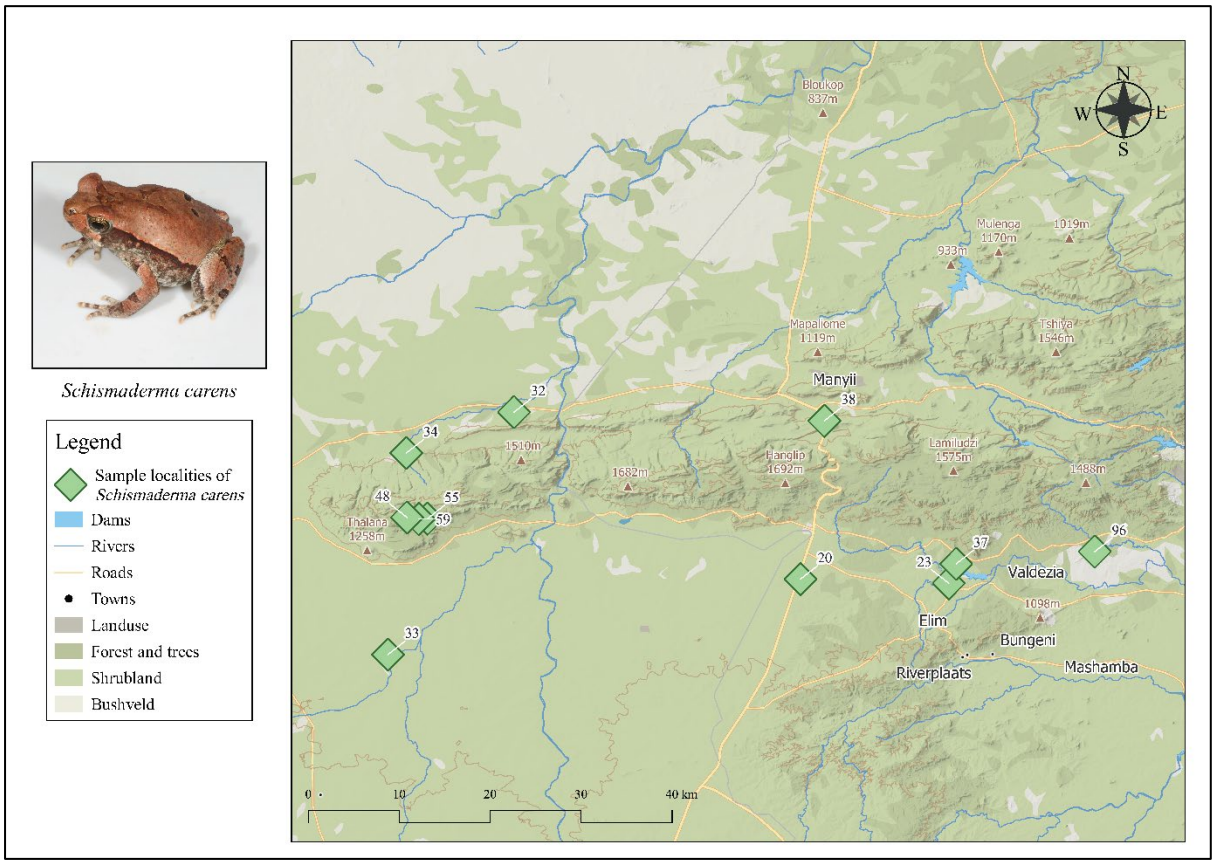

Figure 2.14: Site localities of *Schismaderma carens* across the Soutpansberg. Specimens were collected at 11 sites.

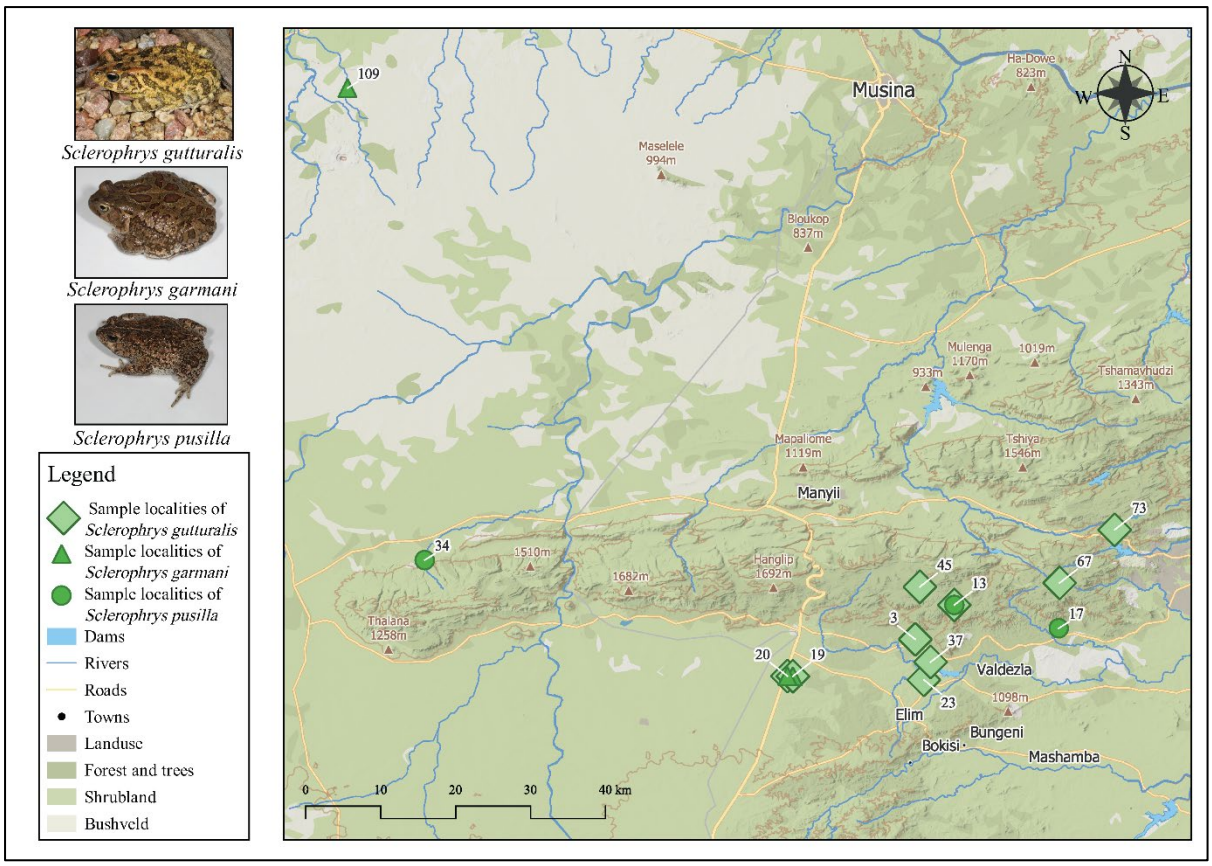

Figure 2.15: Site localities of *Sclerophrys gutturalis, S. garmani* and *S. pusilla* across the Soutpansberg. *Sclerophrys gutturalis* was collected at nine sites, *S. garmani* at two and *S. pusilla* at thee.

HEMISOTIDAE

Hemisus a monotypic genus within the Hemisotidae, includes *Hemisus marmoratus* Peters, 1854, distributed within the Soutpansberg region. Only a single specimen of *Hem. marmoratus* was found at the Piesanghoek site (-23.06198, 30.06808) where it was located on the periphery of a muddy pool (Figure 2.16).

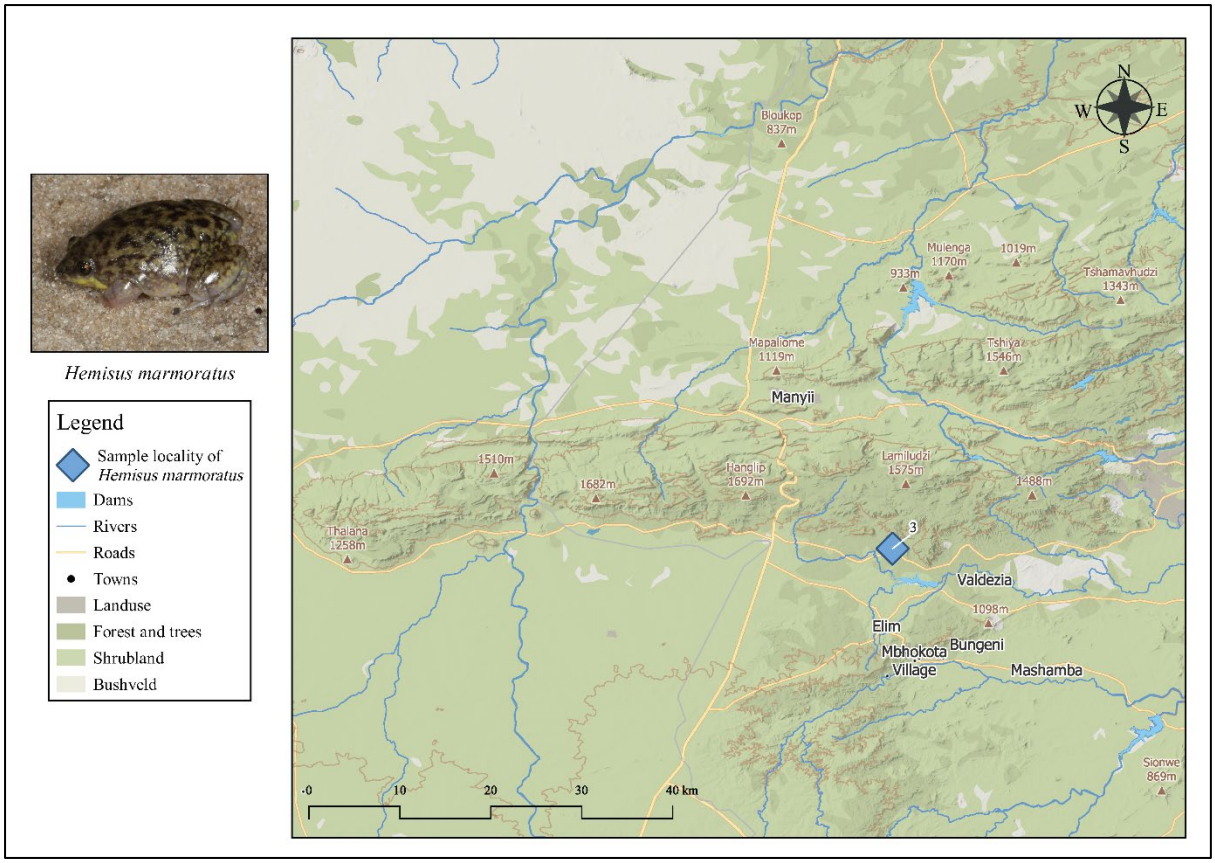

Figure 2.16: Site locality of *Hemisus marmoratus* across the Soutpansberg. Only a single specimen was collected at one site.

HYPEROLIIDAE

Hyperolius marmoratus was collected from three all transects and has a wide distribution across the mountain range, with the higher numbers occurring in the warmer and wetter eastern area (Figure 2.17). Reed frogs were found on dense vegetation, around clear stagnant pools, where big choruses formed. The species is very abundant in the area.

A single *Hyperolius pusillus* Cope, 1862 specimen was collected from the Luvuvhu catchment area. The frog was found on vegetation in a farmstead garden (Figure 2.17). During this study limited sampling was conducted east of Thohoyandou where the species is expected to occur in high density.

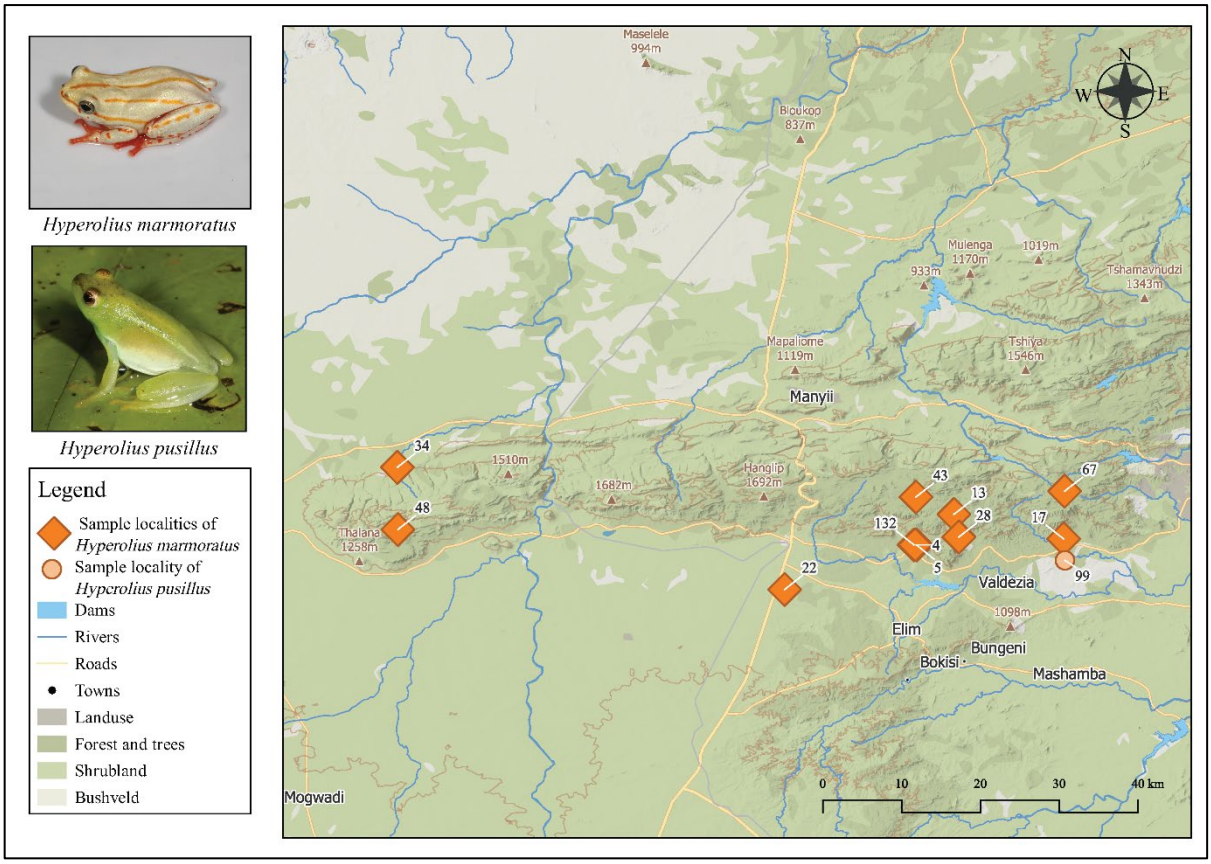

Figure 2.17: Site localities of *Hyperolius marmoratus* and *Hyp. pusillus* across the Soutpansberg. *Hyperolius marmoratus* was collected from three all transects. Only one specimen of *Hyp. pusillus* was collected.

Kassina senegalensis was collected over a wide distribution range, spanning all three transects, including the far north and south surrounding grasslands and from the low-lying bushveld surrounding the mountains to elevated sites high up on the mountain., However, *K. senegalensis* was not present in abundant numbers during the study (Figure 2.18).

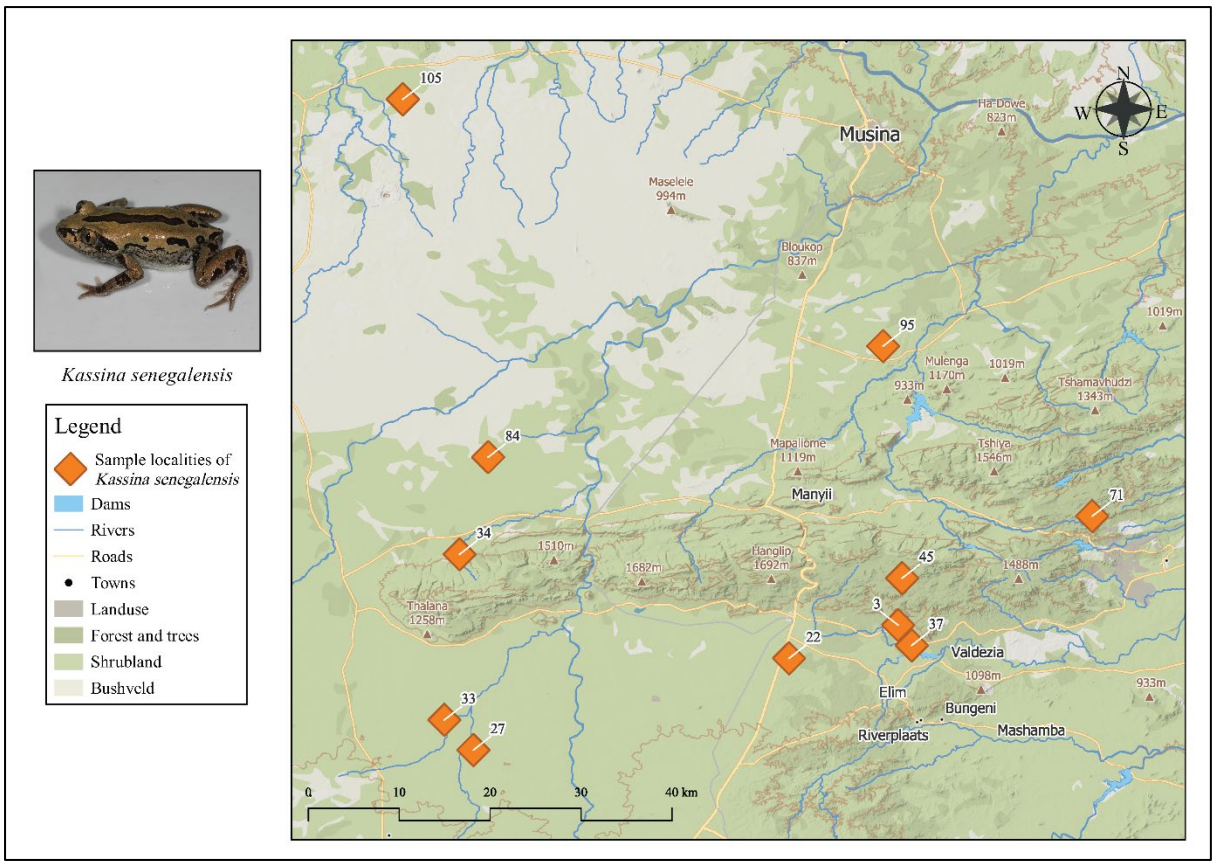

Figure 2.18: Site localities of *Kassina senegalensis* across the Soutpansberg. Specimens were collected over a wide distribution range, spanning all three transects.

MICROHYLIDAE

Phrynomantis, or Rubber frogs, are the only genus in the Microhylidae family. Only *Phrynomantis bifasciatus* occurs in South Africa, with a wide distribution across the study area. *Phrynomantis bifasciatus* was not present on the mountain, but, was collected in all three transects in the flatter, arid, grassland areas surrounding the mountain. (Figure 2.19).

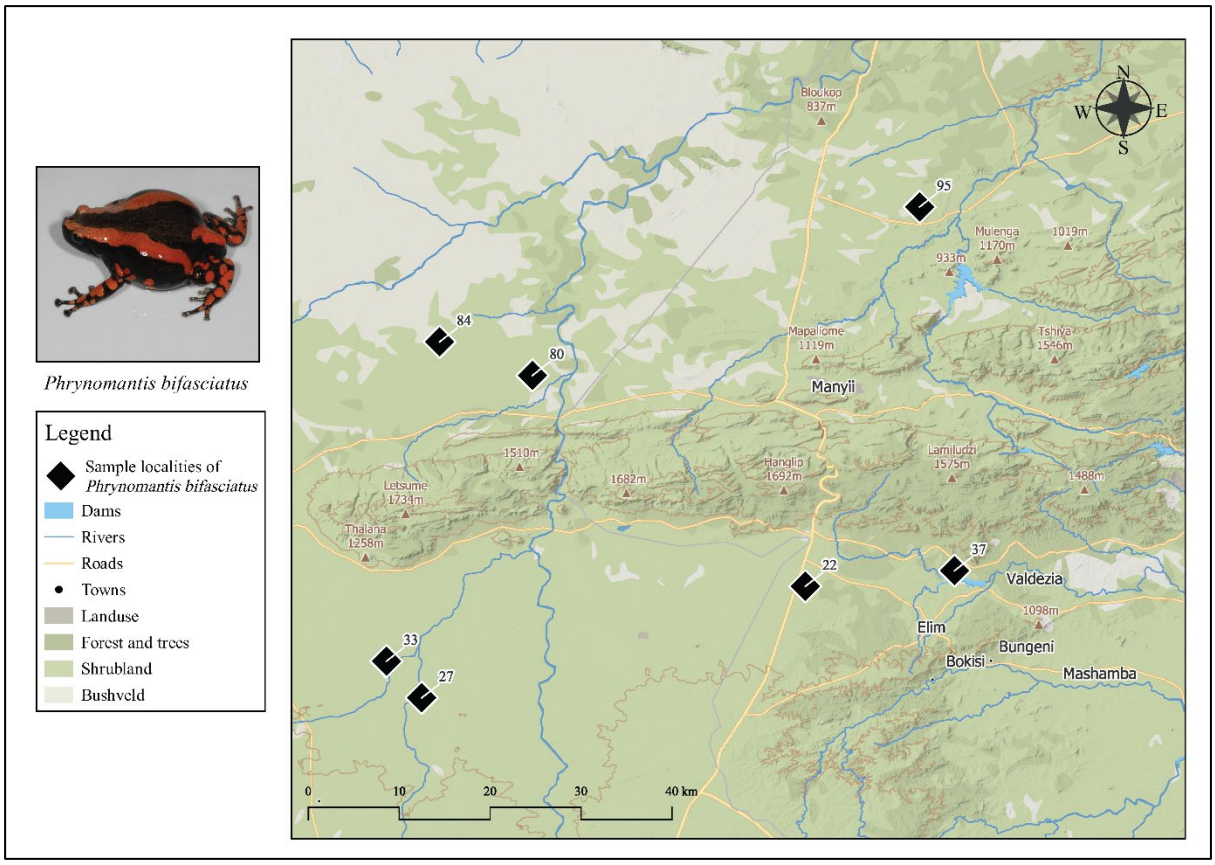

Figure 2.19: Site localities of *Phrynomantis bifasciatus* across the Soutpansberg. *Phrynomantis bifasciatus* was not present on the mountain, but, was collected in all three transects at seven sites.

PHRYNOBATRACHIDAE

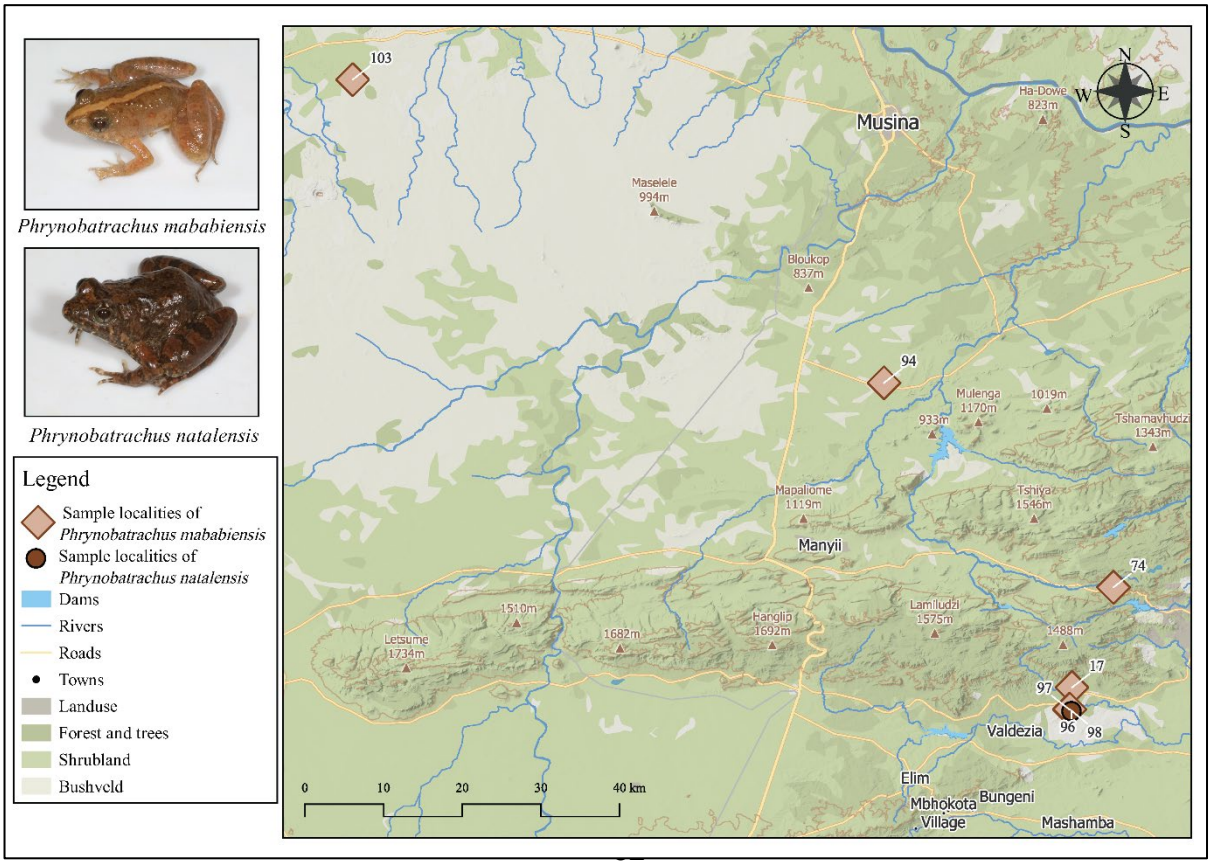

Figure 2.20: Site localities of *Phrynobatrachus mababiensis* and *Phry. natalensis* across the Soutpansberg. *Phrynobatrachus mababiensis* was collected at five sites and *Phry. natalensis* at one.

Puddle frogs are the only group within the Phrynobatrachidae family comprising only a single genus, *Phrynobatrachus*. Two species occur in and around, the study area namely, *Phry. mababiensis* and *Phry. natalensis* Smith, 1849. Both species were associated with muddy pools or the periphery of larger pools where they were located at ground level (Figure 2.20). Males were actively calling and, especially *Phry. mababiensis,* formed large choruses.

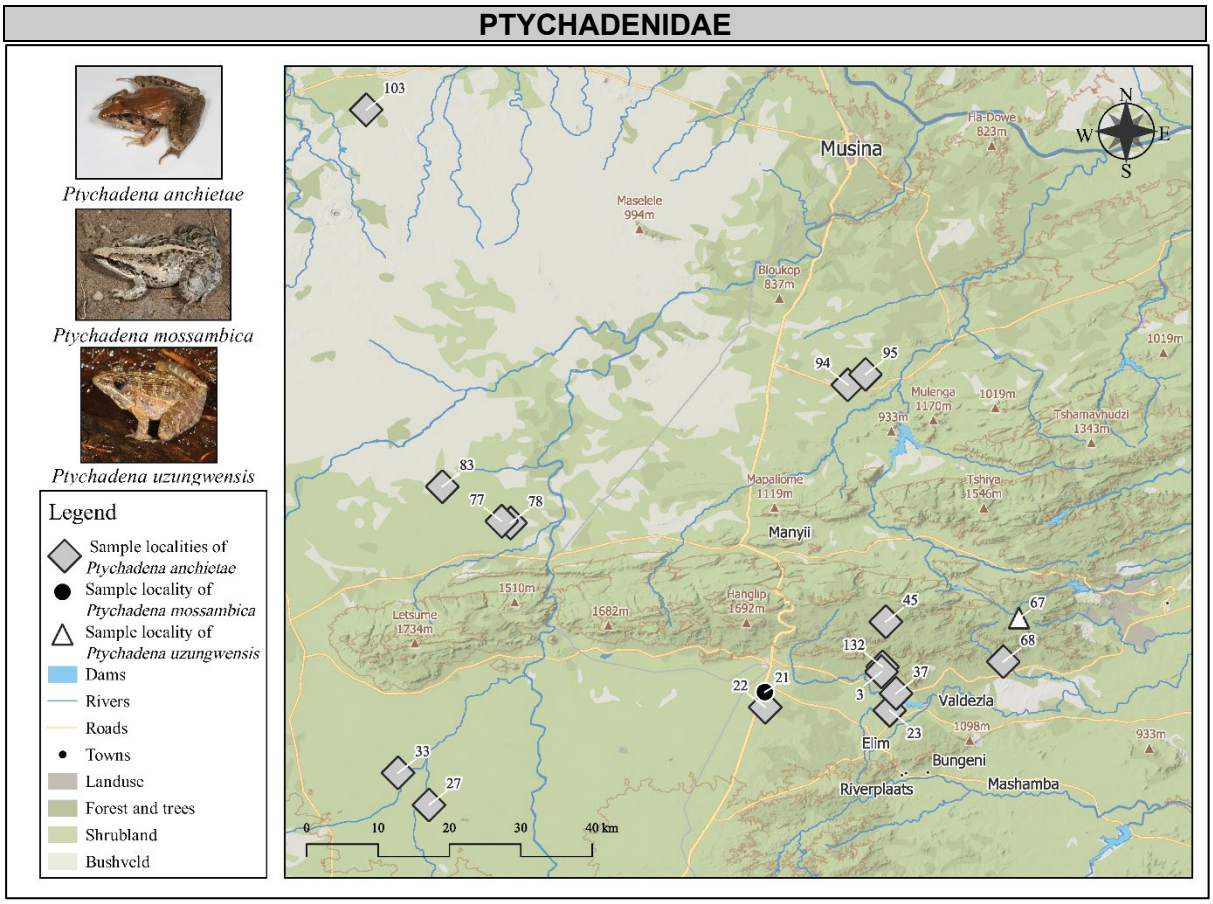

Figure 2.21: Site localities of *Ptychadena anchietae, Pt. mossambica* and *Pt. uzungwensis* across the Soutpansberg. *Ptychadena anchietae* was more abundant, collected at 15 sites whereas *Pt. mossambica* and *Pt. uzungwensis* were collected at one site each.

Ptychadenidae includes two genera, *Ptychadena* and *Hildebrandtia*, that occurs in the Limpopo province. *Ptychadena* species collected included *Pt. anchietae*, *Pt. mossambica* Peters, 1854, *Pt. oxyrhynchus* and *Pt. uzungwensis* Loveridge, 1932. *Ptychadena anchietae*, *Pt. oxyrhynchus* and *Pt. mossambica* were encountered on the low-lying bushveld surrounding the mountains with *Pt. anchietae* very abundant and widely distributed, across all the transects (Figure 2.21). *Ptychadena mossambica* was only observed at one locality within the second transect. *Ptychadena uzungwensis* was confirmed to be present at a locality high up on top of the mountain within the Entabeni state forest at Ebbedam (-22.98839, 30.25644), where a healthy population was found in seeps around the dam. Frogs were actively calling from late afternoon

well into the night. Finding the species confirms the presence of this species in South Africa and implies a significant range extension (Figure 2.22).

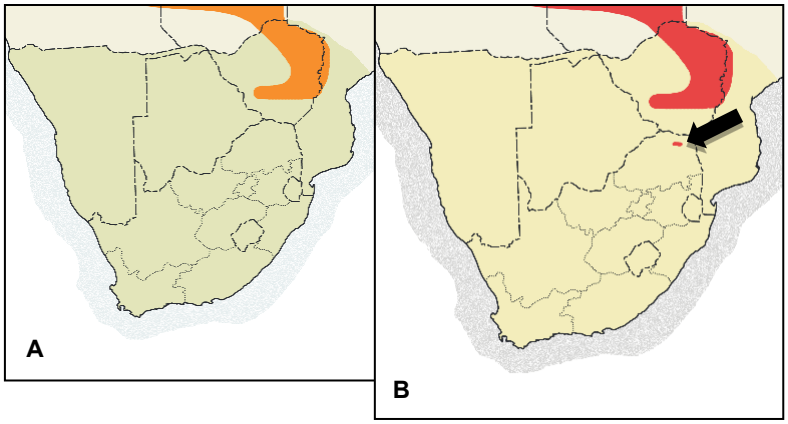

Figure 2.22: (A*) Ptychadena uzungwensis* species distribution range as currently reported by Du Preez and Carruthers (2017). (B) Arrow showing newly extended species distribution from the current study.

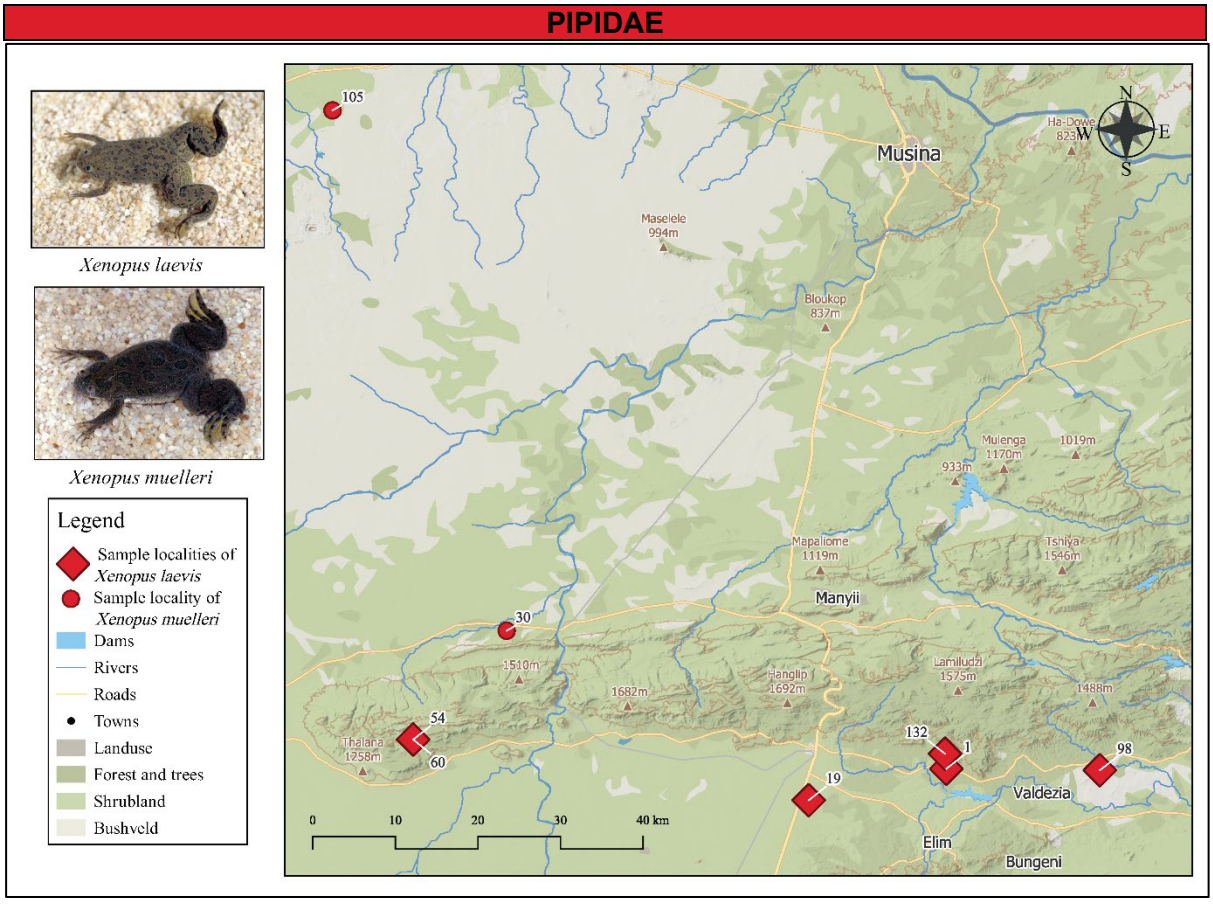

Figure 2.23: Site localities of *Xenopus laevis* and *X. muelleri* across the Soutpansberg. *Xenopus laevis* was collected from all transects with *X. muelleri* only present in one transect.

Species of *Xenopus* from part of the Pipidae of which two species, *Xenopus laevis* and *Xenopus muelleri* Peters, 1844 and were reported to occur within the study area. *Xenopus laevis* was collected from all transects, however, was only present at localities on the wetter southern slopes of the mountain (Figure 2.23). In contrast, *X. muelleri* was only present in transect one on the more arid and hotter, northern bushveld plains.

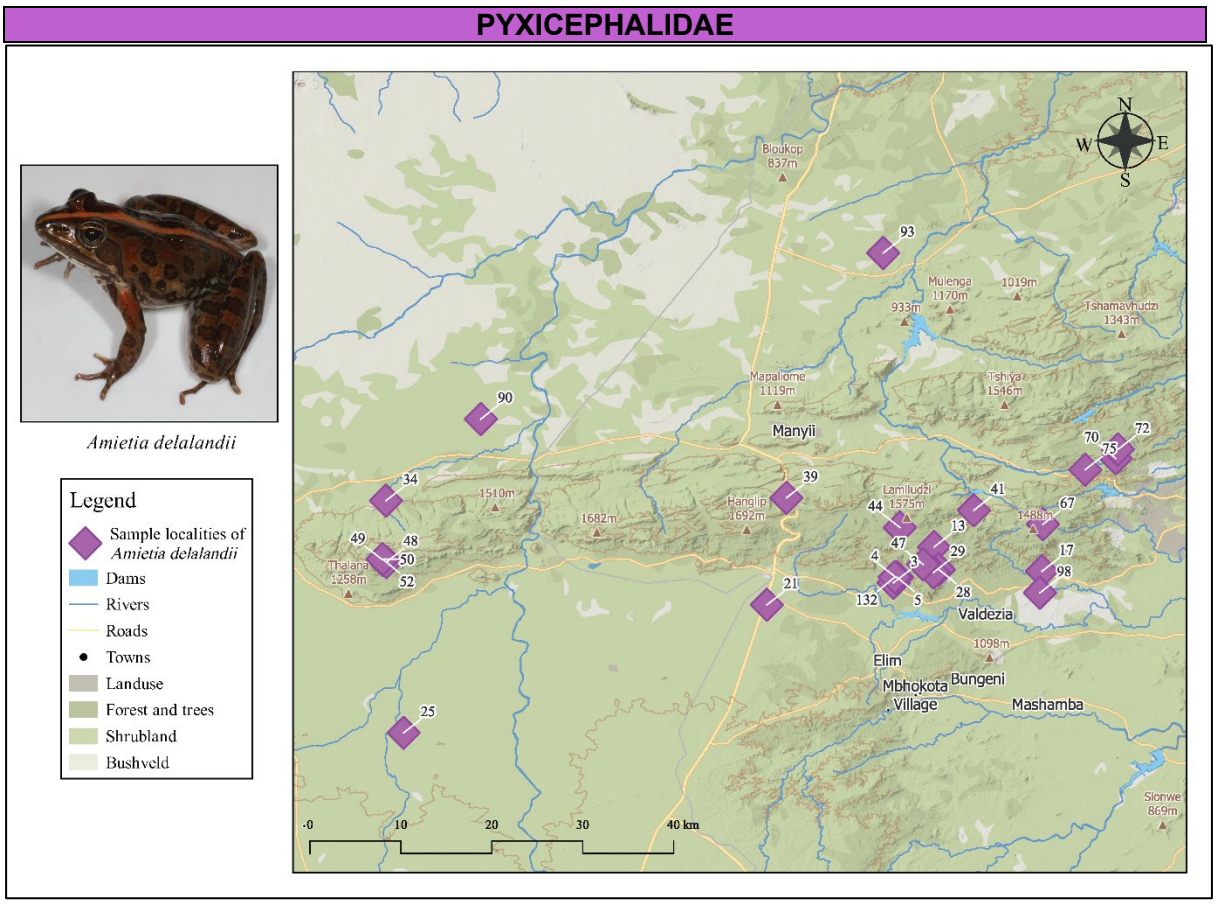

Figure 2.24: Site localities of *Amietia delalandii* across the Soutpansberg. *Amietia delalandii* was the most abundant throughout the sampling trips and was distributed across all three transects.

Six species of the Pyxicephalidae were recorded at the Soutpansberg, including *Amietia delalandii* (River frogs), *Cacosternum boettgeri* Boulenger, 1882 (Cacos), *Pyxicephalus edulis* Peters, 1854 (Bullfrogs), *Strongylopus fasciatus* Smith, 1849, *Strongylopus grayii* Smith, 1849 (Stream frogs) and *Tomopterna* spp. (Sand frogs). *Amietia delalandii* was the most abundant throughout the sampling trips and was distributed across all three transects as well as both north and south of the mountain (Figure 2.24) and encountered at stagnant pools as well as mountain streams. Healthy populations exist and large numbers of tadpoles were observed.

Cacosternum boettgeri was collected from two sites on the mountain and in the southern plains of the surrounding area (Figure 2.25). Where present, they were abundant at muddy pools, rain filled depressions, flooded grassland and roadside pools.

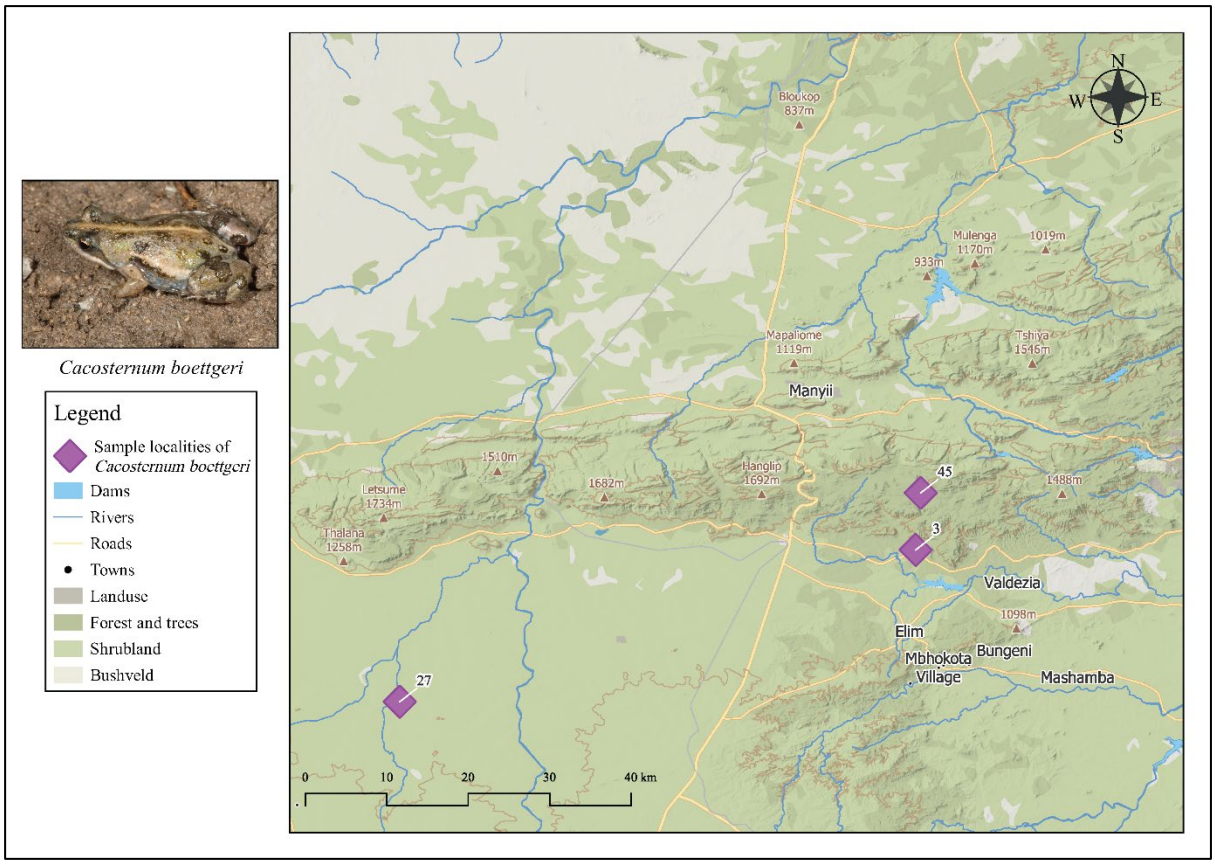

Figure 2.25: Site localities of *Cacosternum boettgeri* across the Soutpansberg. Specimens were collected from three sites.

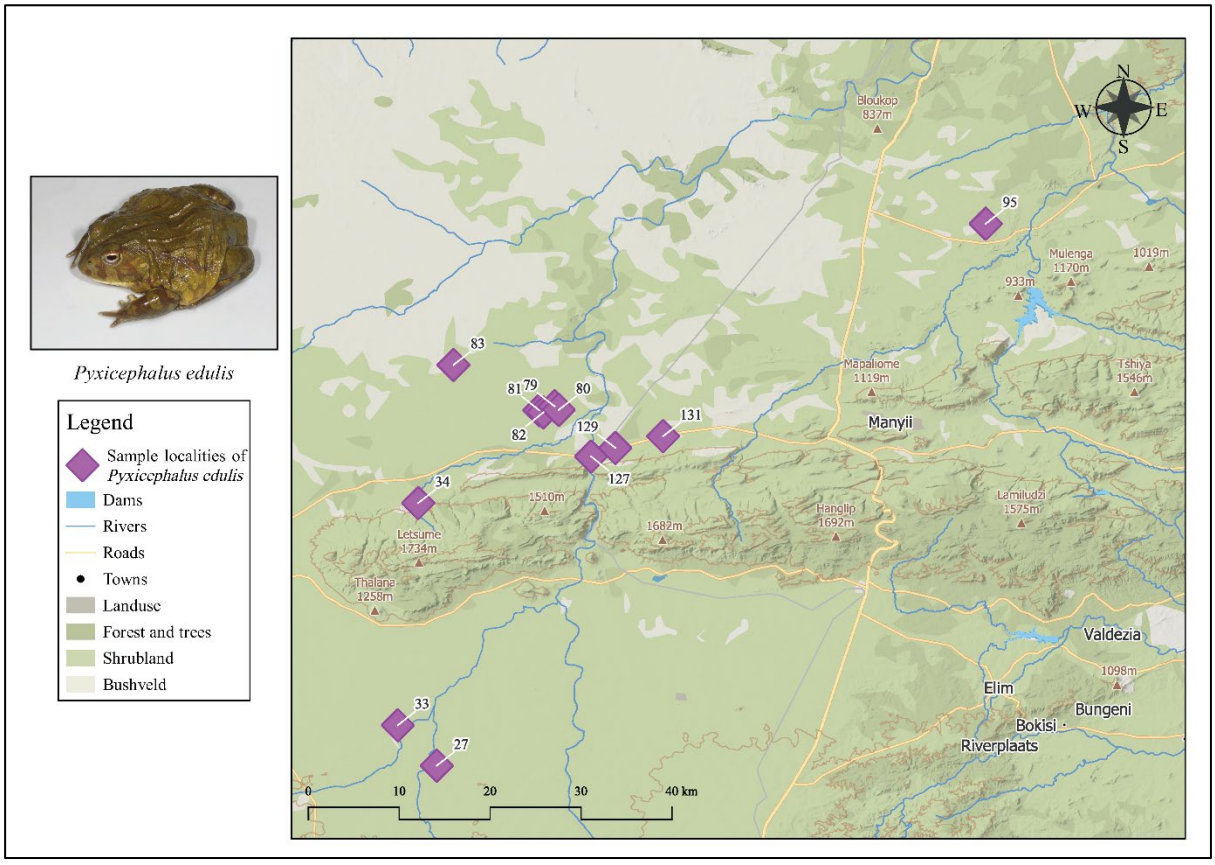

Figure 2.26: Site localities of *Pyxicephalus edulis* across the Soutpansberg. Specimens were collected mostly from the north-western area of the mountain range after heavy rains.

During the present study *Pyxicephalus edulis* was the only bullfrog collected from the study area at sample sites on the dry north-western area of the mountain range (Figure 2.26). Following a big rainfall event, bullfrogs emerged in their hundreds and were found in large numbers on the roads and in the veld, where they feasted on termites. A few breeding individuals were observed. Bullfrogs were not found on the mountain but along the foothills surrounding the mountain.

Of the six known *Strongylopus* species, both *S. fasciatus* and *S. grayii,* were encountered. *Strongylopus fasciatus* was collected in well-vegetated localities on both the southern and northern slopes within vlei areas (Figure 2.27). *Strongylopus grayii* was recorded from one elevated site on the southern slope and was restricted to a small, well vegetated mountain pool that formed against a vertical rock face. Even though the distribution range for *S. grayii* indicates the entire mountain range, it was only found at Lajuma (-23.03034, 29.4216). *Tomopterna* species, which are distributed throughout the entire mountain range including some mountain peaks, wetter and more arid areas, as well as the grassland and bushveld plains surrounding the mountain (Figure 2.28), were found from sites on the lowlands surrounding the mountain, as well as from elevated sites on the mountain.

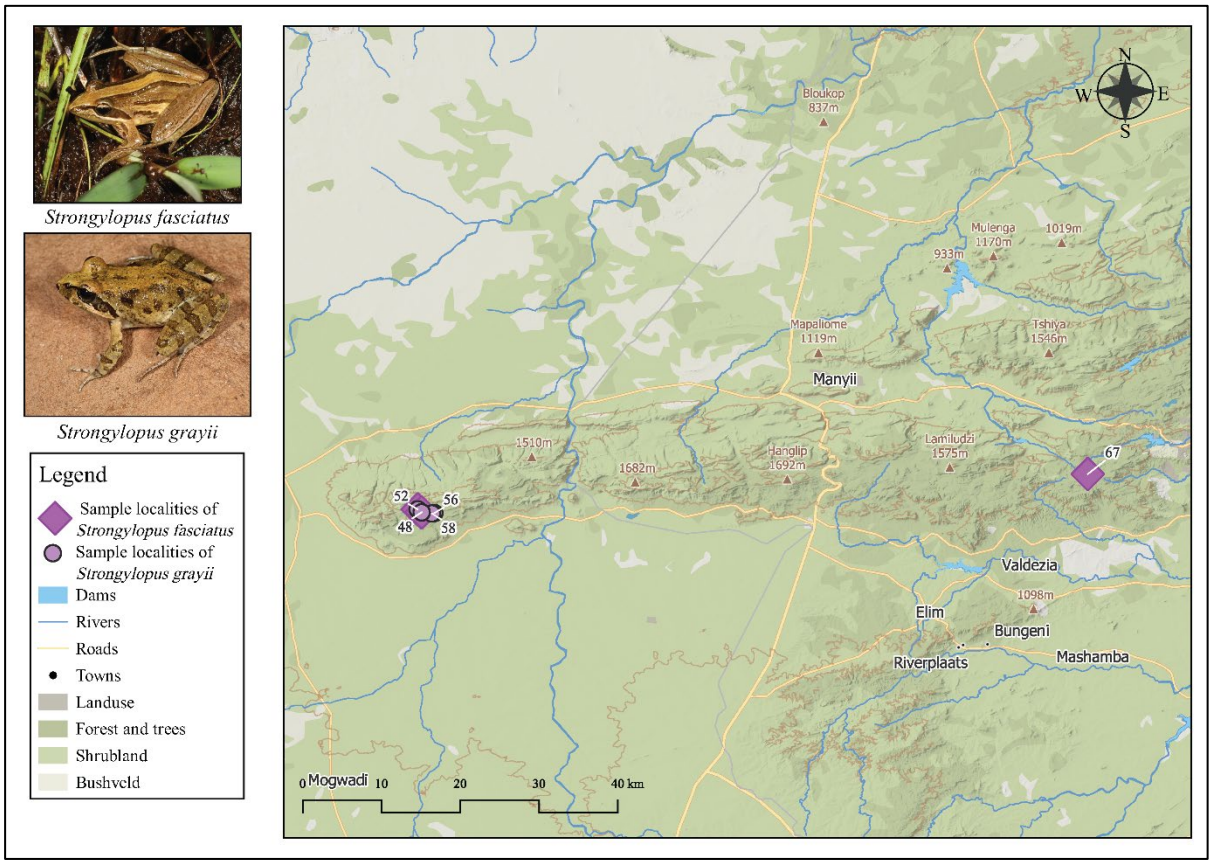

Figure 2.27: Site localities of *Strongylopus fasciatus* and *S. grayii* across the Soutpansberg. *Strongylopus fasciatus* was collected on both the southern and northern slopes areas whereas *S. grayii* was recorded from one elevated site on the southern slope.

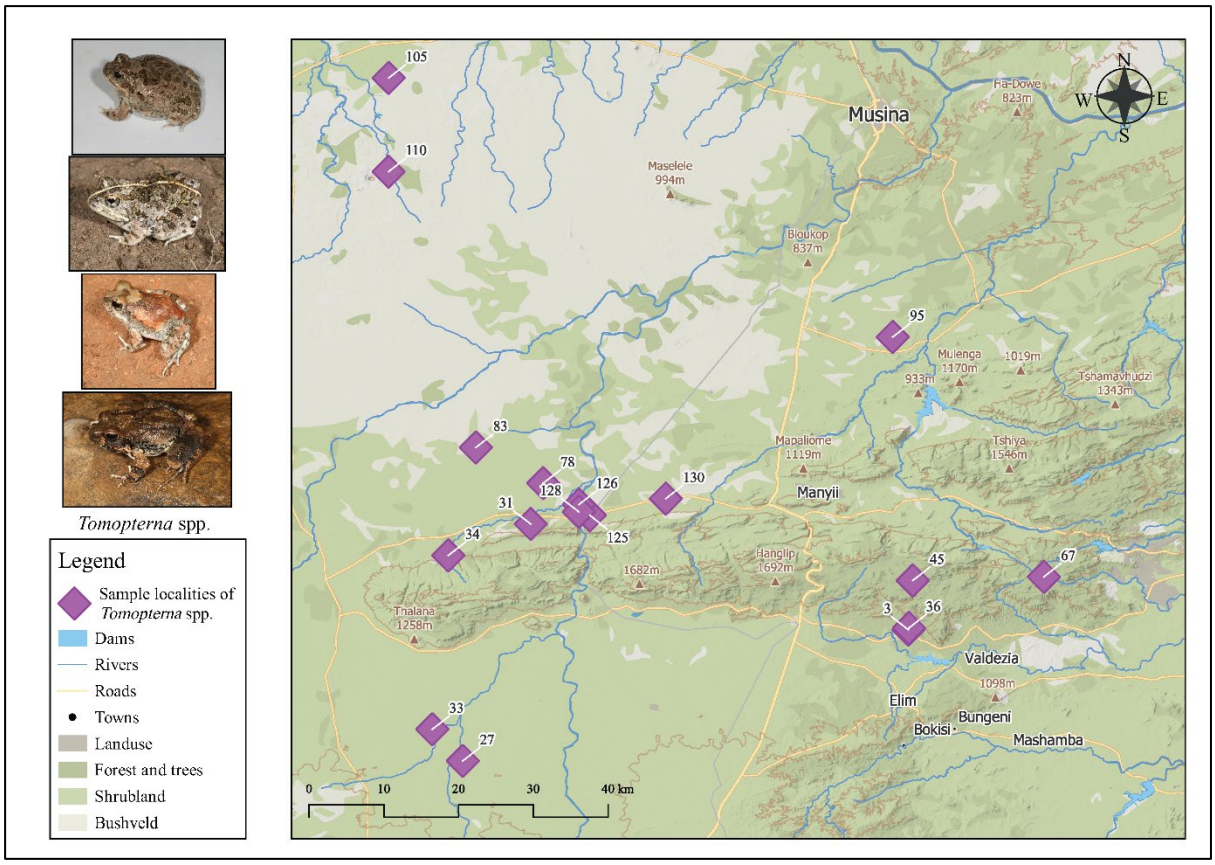

Figure 2.28: Site localities of *Tomopterna* spp. across the Soutpansberg. Specimens were distributed throughout the entire mountain range.

RHACOPHORIDAE

Chiromantis is a monotypic genus within the Rhacophoridae with *C. xerampelina* occurring in the study area. *Chiromantis xerampelina* was distributed across the study area, inhabiting the flatter, arid, bushveld regions in the west and was not collected on the mountain (Figure 2.29). Foam nest frogs were found in daytime, where they were sitting in trees around bushveld ponds and at night, where they were calling.

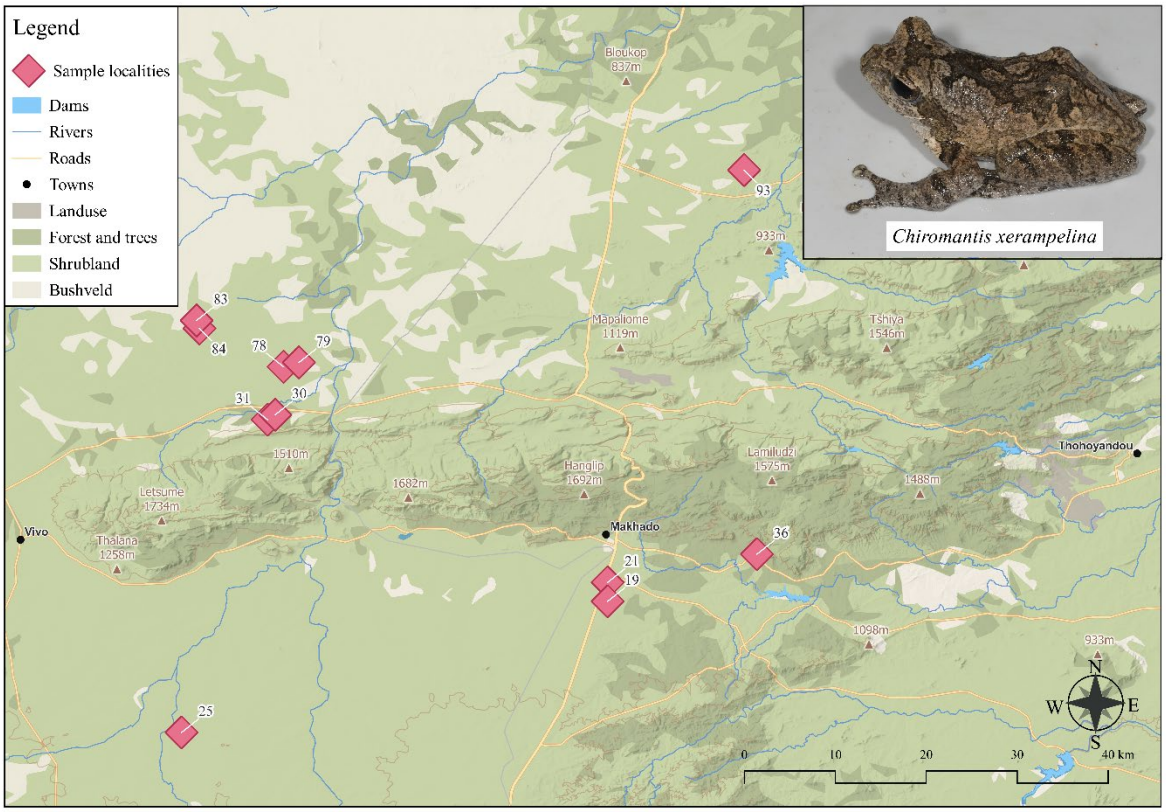

Figure 2.29: Site localities of *Chiromantis xerampelina* across the Soutpansberg. *Chiromantis xerampelina* was not collected on the mountain but distributed across the flatter, arid, bushveld regions.

2.3.3 Description of the amphibian community from the mountain range

General description of the sample

All calculations were performed in the R environment (R core Team 2022) using the package 'tidyverse' (Wickham *et al*., 2019) for manipulating and visualizing the data. The sample includes 540 adult frog specimens of 27 species (Figure 2.30) across 78 sampling localities. The number of amphibian specimens per site ranged from 1 to 43, with an average of 7.1. There are 40 sites with a small number (1 or 2) of collected frogs. The mean species richness was 2.2 which ranged from 1 to 8 amphibian species per site.

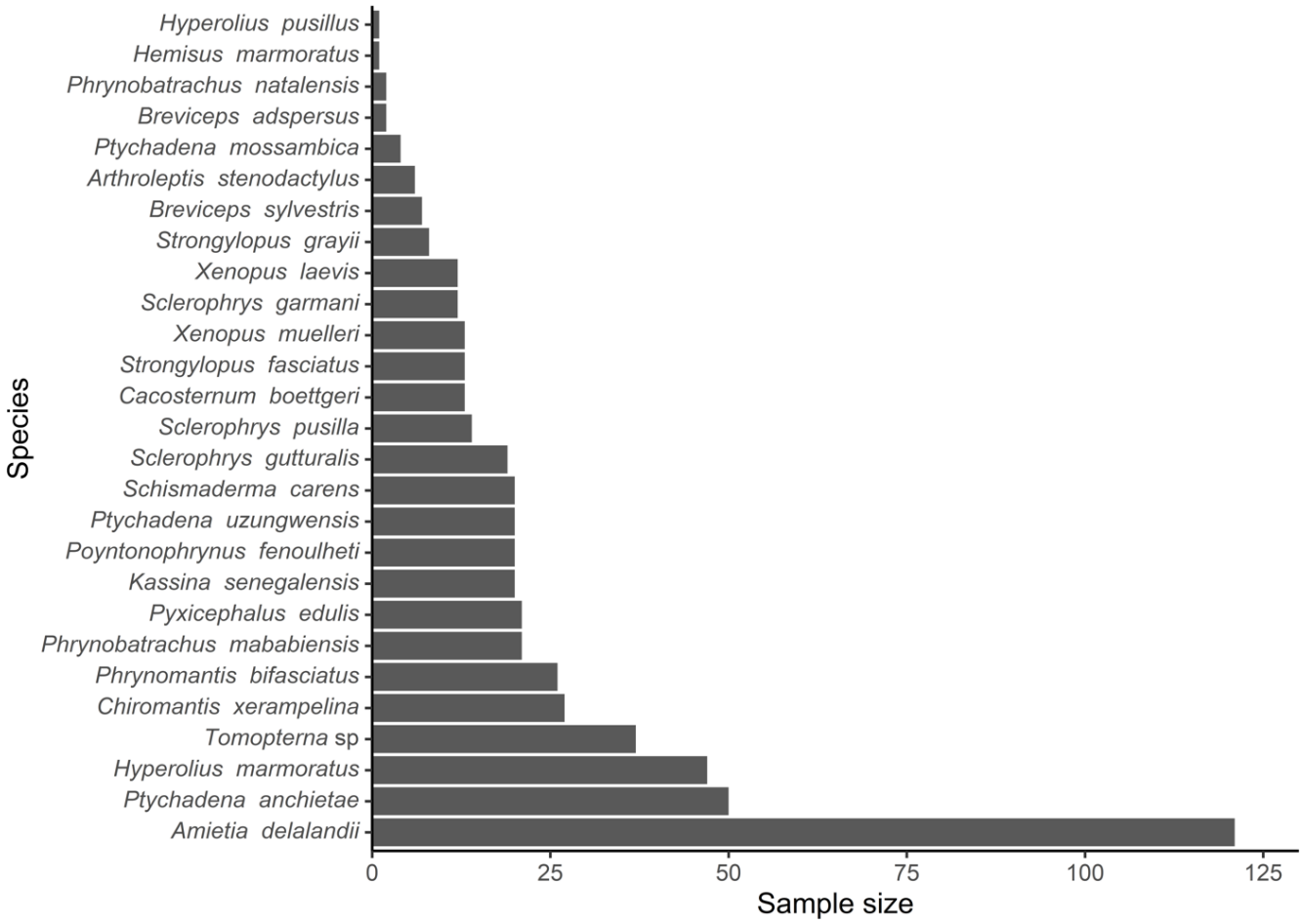

Figure 2.30: Sample size collected across 27 frog species throughout the Soutpansberg. The sample includes 540 adult frog specimens of 27 species across 78 sampling localities.

Alpha diversity

Alpha diversity indices were calculated with appropriate functions from packages 'vegan' (Oksanen *et al.,* 2022) and 'abdiv' (Bittinger, 2020). Sample's indices determined for the present study area: Shannon – 2.85, evenness – 0.87, Simpson – 0.92, Berger-Parker – 0.22. The results suggests that the sample is quite diverse (Magurran, 2004).

Estimation of true species richness

To evaluate whether our sample efforts were sufficient to reveal all species from the study area, the rarefaction curves approach was used, implemented in the package 'iNEXT' (Hsieh, Ma, and Chao 2022), namely functions *iNEXT* and *ggiNEXT*. The transect curves indicate that sample size and number of species are similar across the transects, but, the differences in species composition distinguishes them. The following species are present in Transect 1 but absent in Transect 2: *P. fenoulheti*, *S. pusilla*, *S. fasciatus*, and *S. grayii*. Species that are unique for

Transect 2 relative to Transect 1, include: *C. boettgeri*, *Pt. mossambica*, and *S. gutturalis*. Differences in species composition between Transects 1 and 3 include *B. adspersus*, *B. s. taeniatus*, *P. fenoulheti*, *P. edulis*, *S. garmani*, *S. grayii*, and *X. muelleri* and reversed the difference state that *A. stenodactylus*, *C. boettgeri*, *Hem. marmoratus*, *H. pusillus*, *P. natalensis*, *Pt. uzungwensis*, and *S. gutturalis* is unique to Transect 3. The differences in species composition between Transect 2 and Transect 3 included *B. adspersus*, *B. s. taeniatus*, *Pt. mossambica*, *P. edulis*, *S. garmani*, and *X. muelleri*, whereas *A. stenodactylus*, *Hem. marmoratus*, *H. pusillus*, *P. natalensis*, *Pt. uzungwensis*, *S. pusilla*, and *S. fasciatus* are only present in Transect 2 (also see appendix B for a full list of anuran species across the three transects). However, these differences cannot be considered significant as confidence intervals of transect curves overlapped. The rarefaction curve of the entire collection effort indicates that nearly all expected species were collected (Figure 2.31). However, the extrapolated part of the curve predicted a few unrevealed species on the territory, which we consider extremely rare or atypical for this region.

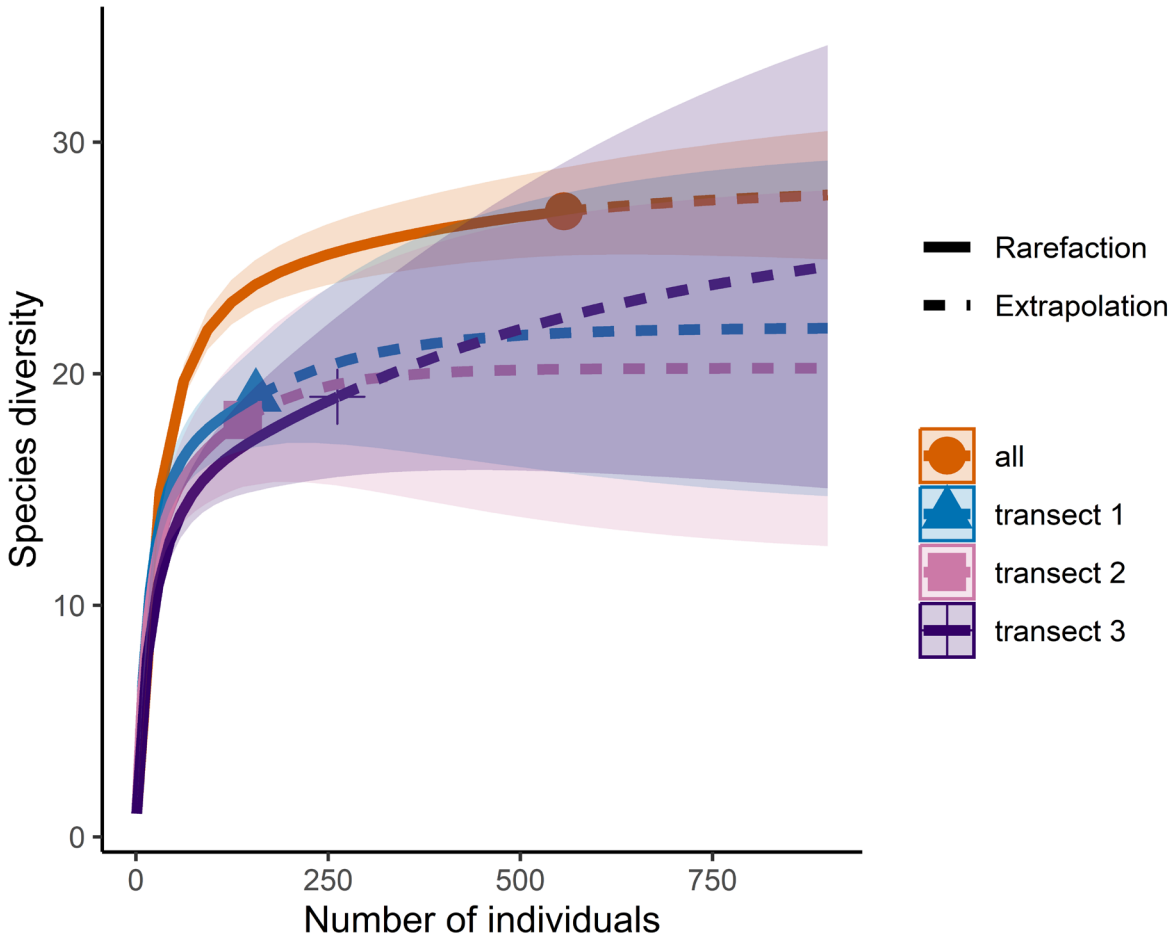

Figure 2.31: The rarefaction curves with 95% confidence intervals for the entire sample and separate transects. A monocoloured area around every curve marks the confidence intervals.

Classifying species as common or rare

To estimate whether frog species are common or rare in the dataset of the current study, the 'FuzzyQ' package was utilized (Balbuena *et al.,* 2021), which used a fuzzy clustering algorithm to classify species as common or rare. In the dataset cut-off of common index (representing the probability of each species being common) between clusters is near 0.5, however, some species have very wide confidence intervals, which make their belonging to certain clusters, unreliable. This phenomenon is caused by those species which were encountered frequently in different locations, although their abundance in each location was small in relation to the whole sample size (Figure 2.32).

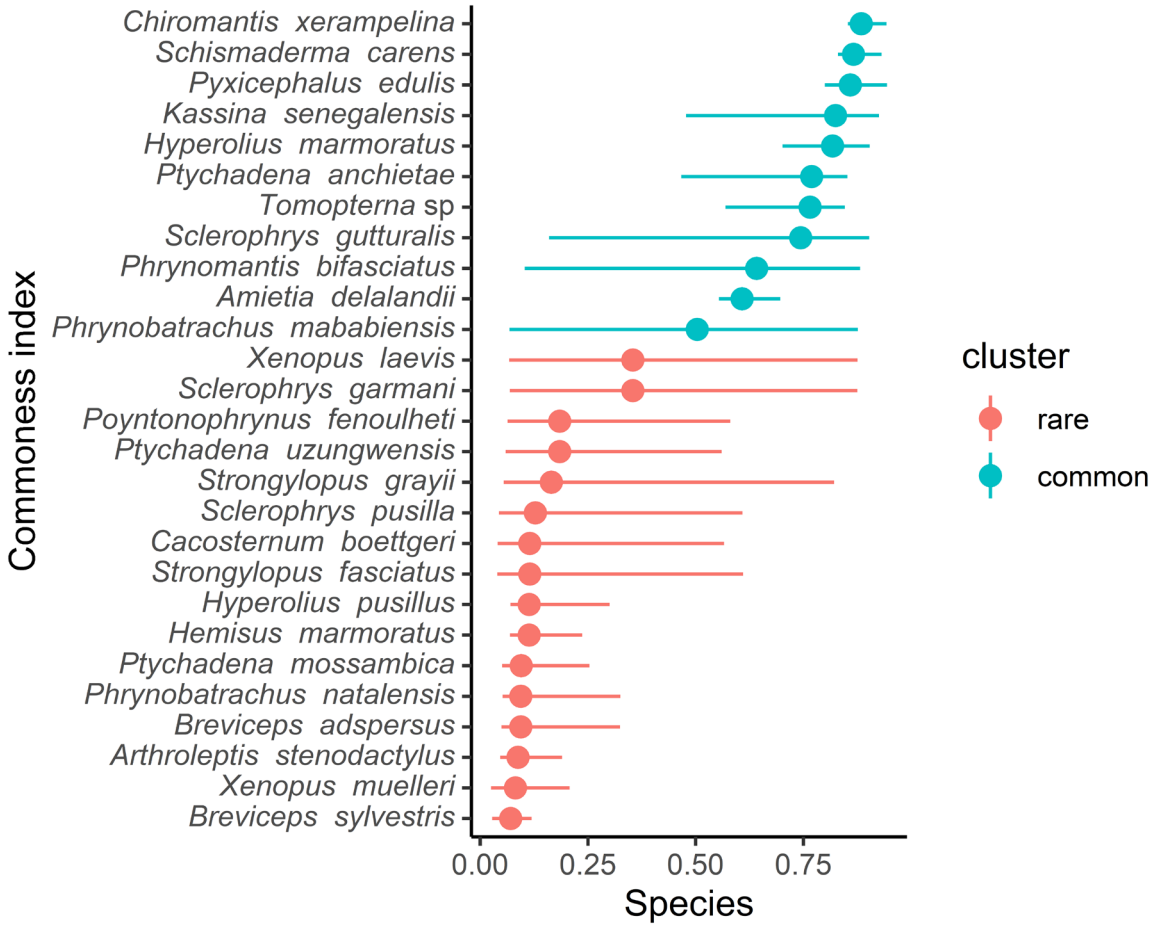

Figure 2.32: Each dot represents commonness indices of species for every frog species in the sample. Error bars represent bias-corrected and accelerated 95% confidence intervals computed with 1,000 bootstrap samples by row of the abundance matrix. Blue and pink indicate rare and common frog species, respectively.

Visualization of quality and quantity patterns in the dataset

Non-metrical multidimensional data scaling (nMDS) of abundance matrix was used for the visualization of the data structure of the sample. The analysis was performed with function *metaMDS* from 'vegan' package (Oksanen *et al.,* 2022). Before analysing the data, included sites with fewer than two species were removed from the dataset, as they are not very informative and cause unstable ordination. One dummy specimen was also added to each location site to make ordination more compact. This approach does not change data structure dramatically, as all records in the sample are transformed in the same way. Thus, the final data set for the analysis contained 38 locations, 26 species (plus one dummy species) and 508 specimens. Despite the reduction of the dataset, information on 91.2% of the specimens from original dataset was analysed.

The result (Figure 2.33) of nMDS shows that Transect 1 and Transect 2 are quite similar to eachother as the majority of their sites clustered close. Meanwhile Transect 3 clustered slightly separately. Also, all transects contain sites with rare species. Those sites are not clustered clearly and are located on the edge of the graph.

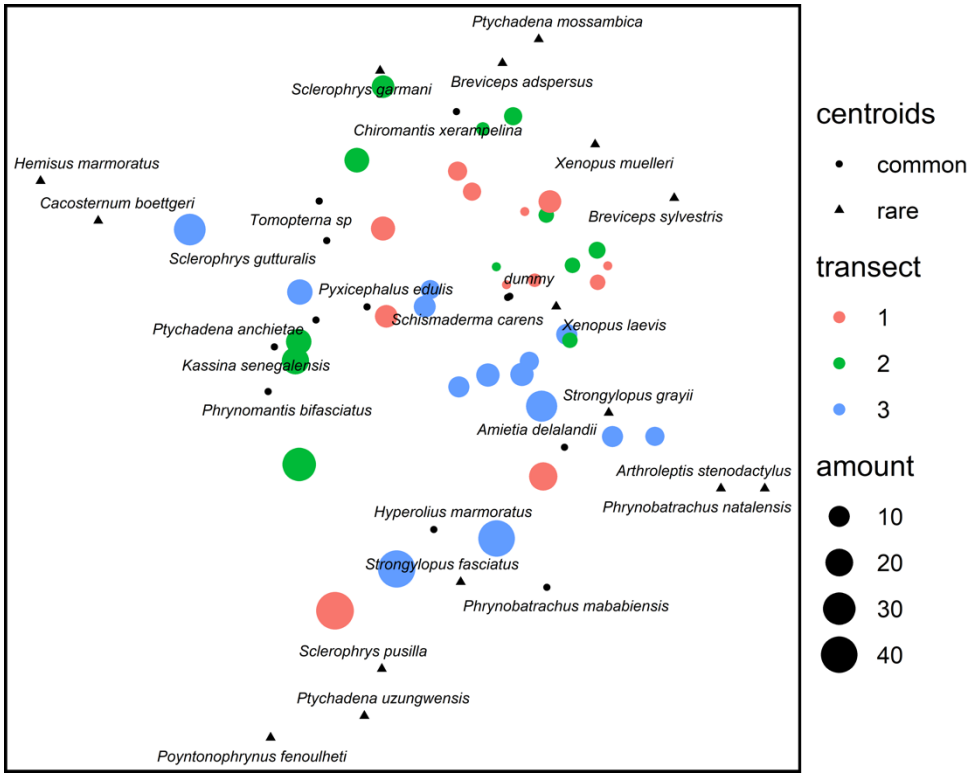

Figure 2.33: Non-metric multidimensional scaling. The nMDS was built on Bray-Curtis dissimilarity matrix generated based on the abundance matrix. Each coloured dot represents a separate site. The colour indicates to which transect the site is assigned and the size of the coloured dot shows the number of frogs collected in this site. Centroids show which frog species are represented in separate dots, namely the closer a site dot is to the centroid of a particular species, the greater probability that this species is present in this site (coloured dot) and vice versa.

2.4 Discussion

Biogeography is defined as the study of the geographic distribution of organisms, forming patterns as the species is distributed according to the geography of the area (see Minter *et al.,* 2004). This chapter focused on the biogeography of anurans on and around the Soutpansberg mountain range in the Vhembe Biosphere. The Soutpansberg Mountain range is recognised for its mosaic of habitats and ecosystems from the sub-tropical eastern region to the semi-arid west (Berger *et al.,* 2003) and is classified as a hotspot for diversity and endemism, including 35 possible frog species to occur there (Du Preez and Carruthers, 2017; Endangered Wildlife Trust, 2018). Limited research has been done on the amphibian biogeography in the most northern parts of South Africa (Minter *et al.,* 2004; Du Preez and Carruthers, 2017), with no detailed surveys recorded on the diversity of amphibians across the vast ecologically different habitats of the Soutpansberg (Endangered Wildlife Trust, 2018). Even though, the Soutpansberg is listed as a Priority Conservation Area by SANBI, only a few natural areas on the mountain range are protected (Berger *et al.,* 2003; Endangered Wildlife Trust, 2018). For future monitoring it is firstly important to identify the amphibian rich areas, species diversity, and their communities on the mountain range that need to be protected and monitored for conservation efforts.

The current study focused on the diversity and distribution of amphibians across the majority if the 6 800 km^2 surface area that the Soutpansberg mountain range covers. A total of 11 families, 19 genera and 31 out of a possible 35 anuran species were reported across the entire study area. This includes (in alphabetical order with family): *A. stenodactylus, L. mossambicus, B. adspersus, B. s. taeniatus, P. fenoulheti, S. carens, S. garmani, S. gutturalis, S. pusilla, Hem. marmoratus, Hyp. marmoratus, Hyp. pusillus, K. senegalensis, P. bifasciatus, P. mababiensis, P. natalensis, Pty. anchietae, Pty. mossambica, Pty. uzungwensis, X. laevis, X. muelleri, A. delalandii, C. boettgeri, P. adspersus, P. edulis, S. fasciatus, S. grayii, T. adiastola, T. marmorata, T. tandyi,* and *C. xerampelina*. This report included all sampling techniques such as active sampling for adult frogs, sweep netting for tadpoles as well as acoustic monitoring for calling males. Even though tadpoles and acoustic observations were opportunistically sampled, all tadpole and frog call data were excluded for the statistical analysis of this study.

Across all three sampling transects, 540 adult frog specimens were collected. Transect one and two both represented 18 frog species with 137 and 139 specimens collected, respectively. Transect three had the most individual frogs collected at 264 representing 19 species. The distribution and abundance of anurans are mirrored with the different ecological habitats on the Soutpansberg, with a single species difference in the sub-tropic region in the east compared to the semi-arid western region (see Berger *et al.,* 2003; Minter *et al*., 2004).

Even though at species level the transects did not show a significant difference, overall species composition within the transects included different species. Species unique for each transect included: *A. stenodactylus, Hem. marmoratus, Hyp. pusillus, P. natalensis*, and *Pt. uzungwensis* for transect three, which had the highest rare species composition; Transect two only had one unique species, *P. mossambica;* and lastly, transect one showed three rare species such as *B. adspersus, P. fenoulheti* and *S. grayii*. Most of the species listed above are in accordance with the species distribution range by Minter *et al.* (2004) however, almost all comparable data available was collected before 1996, with some exceptions of data collected between 1996 and 2002. Furthermore, no data was collected specifically for anuran distribution at the Soutpansberg since 2002. Species that were collected at localities unique to the current study included *A. stenodactylus, Hyp. pusillus, P. uzungwensis,* and *P. mossambica* (see Minter *et al*., 2004).

The species of *Tomopterna* has a wide distribution across Africa with eight of the 10 species occurring in southern Africa. Five out of eight species are reported to occur within the study area and include *T. adiastola*, *T. krugerensis* Passmore & Carruthers, 1975, *T. marmorata, T. natalensis,* and *T. tandyi*. Species of *Tomopterna* share similar morphological characteristics with some species morphologically indistinguishable, namely *T. adiastola* and *T. tandyi* (Du Preez and Carruthers 2017). To confirm species identification is accurate molecular work is encouraged to distinguish between cryptic species (Zimkus and Schick, 2010; Channing *et al.*, 2013), however, this was outside the scope of the present study. Even though the species of *Tomopterna* collected could not be identified to species level based on morphology, acoustic recordings confirmed that *T. adiastola, T. marmorata* and *T. tandyi* were collected within the study area.

The call of *T. adiastola* consists of a series of melodious high-pitch *ki-ki-ki-ki* notes, lasting several seconds, whereas the call of *T. marmorata* consist of rapid piping notes at variable rates; compared to *T. tandyi* who also has a high-pitched melodious call but consists of rapid metallic *ki-ki-ki-ki* notes (Du Preez and Carruthers, 2017; Bogart *et al.*, 2022). Acoustic monitoring can be used for different reasons such as identifying cryptic species or species that inhabit hard to reach sites. In the current study this was a valuable method to identifying species that are morphologically similar, concluding that at least three of the expected *Tomopterna* spp. were collected in the study area.

Due to sampling efforts from the current study, the species distribution range of three species, *A. stenodactylus, B. s. taeniatus* and *Pt. uzungwensis*, has been expanded to include new localities within the Soutpansberg. There are 13 known *Arthroleptis* species with four species recorded from southern Africa (Du Preez and Carruthers, 2017). Two of the four species, namely *A. stenodactylus and A. wahlbergii* Smith, 1849 occur in South Africa, however, neither species had previously been recorded within the study area. *Arthroleptis*

wahlbergii is reported to occur in the coastal forest of KwaZulu-Natal, whereas *A. stenodactylus* also inhabit Natal coastal forest as well as throughout Mozambique and extending into eastern Zimbabwe (Du Preez and Carruthers, 2017). In the current study six *A. stenodactylus* specimens were collected at one site in the Luvuvhu catchment system. No tadpoles were collected, and no calling males were recorded, thus only female frogs were collected. Calling males of *A. stenodactylus* males reported from Malawi were heard between November and March with a peak calling season in February, after heavy summer rainfall (Mercurio, 2009). The low calling activity recorded from the current study could be due to sampling effort being conducted out of breading season, in April. Records on *A. stenodactylus* found near the study area was located in the Kruger National Park with *A. stenodactylus* found within the leaf litter of riverine woodland (Minter *et al.*, 2004). Future sampling effort should be dedicated to the rest of the catchment system and more upstream, including all riverine woodlands towards Thohoyandou, to help determine the distribution range of *A. stenodactylus* across the Soutpansberg.

The genus *Breviceps* (rain frogs), are endemic to southern Africa with four species, namely *B. adspersus adspersus, B. sylvestris sylvestris, B. sylvestris taeniatus*, and *B. mossambicus* known to occur in Limpopo (Du Preez and Carruthers, 2017). However, only *B. adspersus* and *B. s. taeniatus* are reported form the Soutpansberg. *Breviceps s. taeniatus* inhabits the Afromontane forests and mountain grasslands from the second highest mountain peak on the Soutpansberg, the Hanglip forest reserve, at 1692m asl (Minter *et al.*, 2004; Du Preez and Carruthers, 2017). The highest mountain peak includes, Lajuma research centre (1 747 m asl) which also includes the damp Afromontane forests. Six specimens were collected at the Hanglip reserve and only a single specimen at Lajuma. At both localities the specimens were found within the damp forest under leaf foliage. According to Minter *et al.* (2004), *B. s. taeniatus* is likely to occur at all Afromontane Forest stretching from Blouberg, across Soutpansberg, to Thohoyandou, however, *B.s taeniatus* has only been recorder from a single locality at Blouberg and from the forests of the Hanglip reserve, with no detailed reports on *B.s taeniatus* collected at Lajuma Research Centre. This expands the species distribution of *B. s. taeniatus* to include both mountain peaks.

Currently the species distribution of *Pt. uzungwensis* mainly include the Udzungwa Mountains in Udzungwa National Park, Tanzania, Central Mozambique with only three anecdotal recordings from the Soutpansberg, including Bluegumspoort (-22.98611, 29.91667), Entabeni Forest Reserve (-23.0275, 30.20222) and Outlook (-22.99305, 30.10889) (Minter *et al.*, 2004). The distribution range of *Ptychadena uzungwensis* was expanded in the present study, with specimens collected at Ebbedam (-22.98839, 30.25644), a relatively small dam within the Entabeni forest on the eastern mountain peaks of the Soutpansberg (1 488 m asl). Entabeni forest is a strip of Afro-temperate mist-belt forest that is part of the Entabeni

plantation. *Ptychadena uzungwensis* is recorded at high altitude grasslands in proximity if pools and seepages (Stewart, 1967). Resultant, the species distribution range of *Pt. uzungwensis* is extended to include the most eastern part of the mountain mist-belt forest.

Collectively, 89% (31/35) of the expected frog species were reported during the current study, proving their species distribution includes the Soutpansberg. The three species that were absent from this biomonitoring survey includes *S. capensis* Tschudi, 1838*, Pt. oxyrhynchus, T. krugerensis* and *T. natalensis.* One of the reasons could possibly be that the sampling trips fell outside of their breading season (see Du Preez and Carruthers, 2017; Minter *et al.,* 2004).

The high anuran species diversity with multiple species range extensions on the Soutpansberg, that was reported in the current study supports the notion of why this region needs to be protected (see Endangered Wildlife Trust, 2018; Evans, 2017) This will ensure the protection of the natural environment of the anuran species in and around the Soutpansberg and will support the wellbeing and growth of anuran species composition and communities (UNESCO, 2009; Reserve, 2021). Vhembe Biosphere Reserve has a rapidly growing human population contributing to severe negative impacts on natural resources and destroying the ecosystems these frogs inhabit (Evans, 2017; Endangered Wildlife Trust, 2018; Reserve, 2021). It is thus important to implement an integrated approach to sustainable development to conserve the unique ecosystem and all of its fauna and flora species (Evans, 2017; Endangered Wildlife Trust, 2018). The Endangered Wildlife Trust (2018) plans on implementing socio-economic developmental opportunities to this under-developed region, by establishing a conservation-based economy to lesser the negative anthropogenic effects communities have on the environment without restricting community growth (Endangered Wildlife Trust, 2018).

CHAPTER 3:

BLOOD PARASITE DIVERSITY WITHIN VHEMBE FROGS

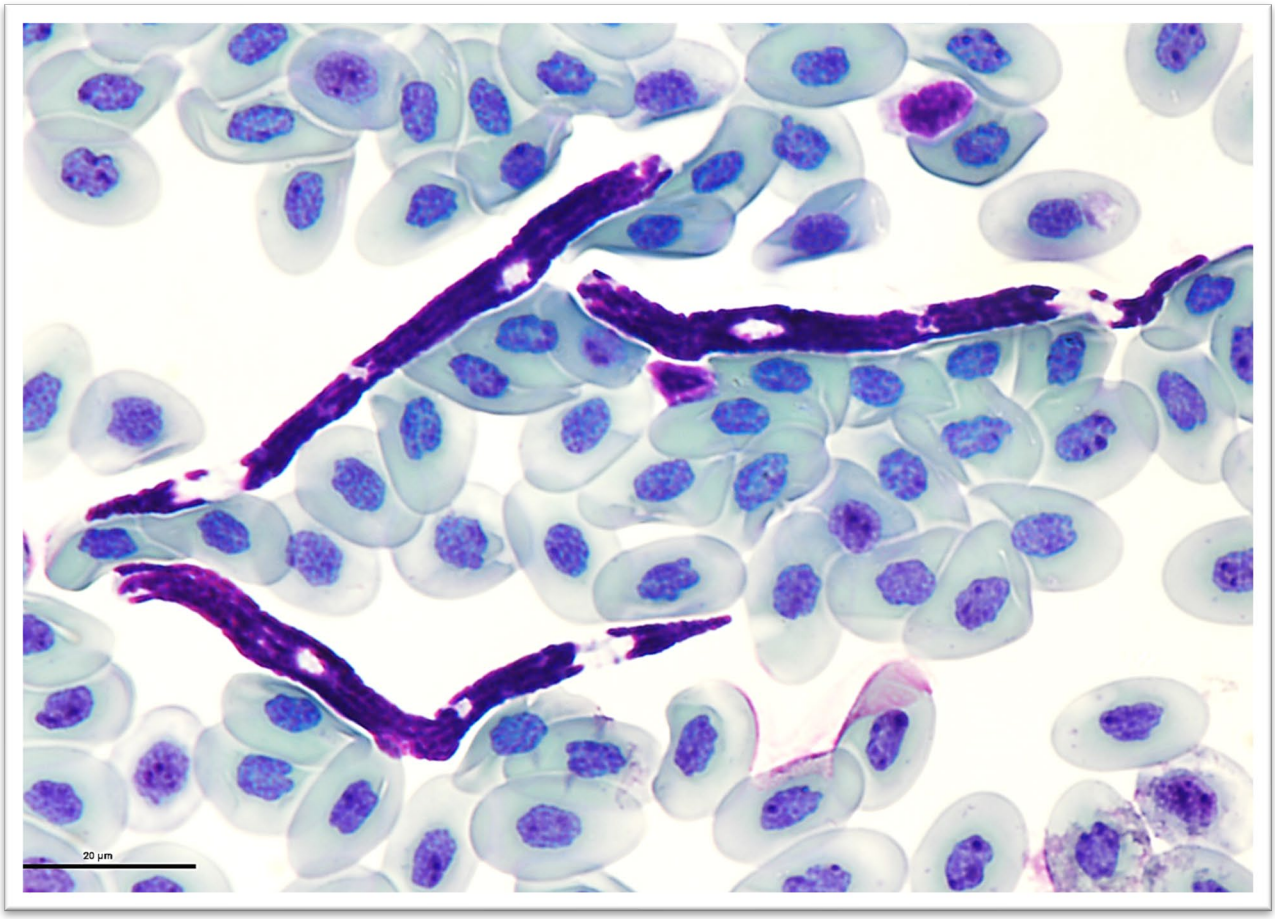

Neofoleyellides steyni

3.1 Introduction

3.1.1 General introduction to blood parasites

Amphibians are the among the most threatened vertebrate group, with a third of the estimated species in decline or facing extinction (Stuart *et al.*, 2004; Beebee and Griffiths, 2005; Silvano and Segalla, 2005; Chambouvet *et al.*, 2015). These large-scale declines could be due to numerous factors such as destruction and pollution of their natural habitats, global warming and diseases such as the frog killing fungal pathogen, *Batrachochytrium dendrobatidis* (Beebee and Griffiths, 2005; Readel and Goldberg, 2010). Alongside chytrid, amphibians are the preferred host for a variety of non-lethal, (at least according to current knowledge), intraerythrocytic and extracellular haemoparasites (Du Preez and Carruthers, 2009; Netherlands, 2014). Intraerythrocytic haemoparasites include protozoans such as apicomplexan haemogregarines, haemococcidia as well as rickettsial bacteria and viral infections. On the other hand, extracellular blood parasites consist of protozoan trypanosomatids and metazoan nematode microfilariae (Barta, 2000; Davies and Johnston, 2000; O'donoghue, 2017; Netherlands, 2019).

Research on anuran haemoparasites from southern Africa have increased in the past ten years, however, most of the recent African anuran haemoparasite surveys conducted to date, were focused on the biodiversity from the province of KwaZulu-Natal (Netherlands *et al.*, 2014a; Netherlands *et al.*, 2015). Thus, the far northern parts of South Africa have been neglected with regard studies on haemoparasite diversity within amphibian hosts. The Soutpansberg Mountain range forms part of the Vhembe Biosphere Reserve and is recognised as a hotspot of South African biodiversity and endemism.

Southern Africa has a diverse amphibian fauna comprising 172 species (Du Preez and Carruthers, 2017) of which 43% are endemic. Based on the field guide of Du Preez and Carruthers (2017) at least 35 species of known frog species are expected to occur in the Soutpansberg area. However, no data is currently available on the anuran haemoparasites from within the study area. This chapter will focus on the diversity of anuran haemoparasite occurrence across their anuran hosts diversity within the Soutpansberg Mountain range.

3.1.2 Introduction to frog blood parasites

A wide variety of intra- and extracellular blood parasites have been globally reported to infect anuran hosts (Du Preez and Carruthers, 2009; Netherlands, 2014). Anurans are exposed to several haematophagous vectors in their aquatic and terrestrial habitats. These vectors play the role of transmission of these blood parasites. Protozoan blood parasites are divided into the intracellular apicomplexan parasites and the extracellular euglenozoan flagellates and

extracellular nematode microfilariae. Intracellular apicomplexan parasites include haemogregarines, haemococcidia, haemosporidia, piroplasms, rickettsiae intraerythrocytic bacteria and intraerythrocytic viruses. Extracellular euglenozoan flagellates include trypanosomes and extracellular nematode microfilariae (Dutton *et al.*, 1907; Bardsley and Harmsen, 1973; Desser *et al.*, 1973; Barta and Desser, 1984; Desser, 2001; Silvano and Segalla, 2005).

Intraerythrocytic blood parasites

Haemogregarines (phylum Apicomplexa, suborder Adeleorina) are a diverse group of blood parasites divided into four families with eight genera (Jakes *et al.*, 2003; Barta *et al.*, 2012). The Haemogregarinidae include species of *Haemogregarina*, *Desseria*, and *Cyrillia;* the Dactylosomatidae comprise species of *Dactylosoma* and *Babesiosoma*; the Karyolysidae family include species of *Karyolysus* and *Hemoliva* and lastly, the Hepatozoidae family includes species of *Hepatozoon.* Three of the eight family groups have been reported to infect anurans, including species of *Dactylosoma, Babesiosoma*, *Hemoliva* and *Hepatozoon.* Haemogregarines have a heteroxenous lifecycle with transmission of all genera involving an intermediate vertebrate host and a haematophagous definitive invertebrate vector. Species of *Hepatozoon* are the most commonly reported haemogregarines known to parasitise anurans (Siddall, 1995; Smith, 1996; Netherlands *et al.*, 2018).

Haemococcidia (phylum Apicomplexa, suborder Eimeriorina) include the families Lankesterellidae and Schellackiidae, each comprising a single genus, *Lankesterella* and *Schellackia,* respectively (Davies and Johnston, 2000). Haemococcidia follow a heteroxenous lifecycle and complete their replication process within the gut cells of the definitive vertebrate host (Nöller, 1912; Nöller, 1920; Desser, 1993) with no development taking place within the intermediate invertebrate vector. Transmission occurs via a mechanical or paratenic haematophagous invertebrate vector such as dipterans, through ingestion of an infected invertebrate, or predation of an infected vertebrate host. Species of *Lankesterella* have been reported to infect various vertebrate hosts such as frogs, birds and lizards. Species of *Schellackia* mainly parasitize reptilian hosts, but, have also been reported from anuran hosts (Bonorris and Ball, 1955; Mansour and Mohammed, 1962; Paperna and Lainson, 1995; Upton, 2000; Telford, 2009; Megía-Palma *et al.*, 2013; Megía-Palma *et al.*, 2016; Megía-Palma *et al.*, 2017).

Rickettsial or bacteria-like infections are commonly reported from anurans (Barta and Desser, 1984; Zhang and Rikihisa, 2004). Little information is available on these small, gram-negative, intraerythrocytic organisms which have been referred to, among other designations, as species of *Aegyptianella,* Candidatus, *Hemobacterium, Chryseobacterium, Bertarellia,*

Cytamoeba and *Haemobaronella*. Morphological characteristics alone are not sufficient to correctly classify these organisms and molecular analyses are encouraged for use in future studies (Desser, 1987; Zhang and Rikihisa, 2004; Davis *et al.*, 2009; Netherlands, 2014; Cook *et al.*, 2015; Netherlands *et al.*, 2015).

Similarly, there is also limited knowledge available for intraerythrocytic viruses infecting amphibians, mainly due to the confusion and difficulty in their taxonomic classification. Thus, it has been suggested that all amphibian icosahedral iridovirus-like infections should be collectively referred to as Frog Erythrocyte Virus (FEV) until better diagnostic methods are readily available (Gruia-Gray *et al.*, 1989; Alves and Paperna, 1993; Telford Jr and Jacobson, 1993; Smith *et al.*, 1994). Gruia-Gray *et al*. (1992) explained that FEV is a cytoplasmic pox-like DNA virus which is mechanically transmitted between frogs by amphibian-feeding biting midges (Gruia-Gray *et al.*, 1992; Desser, 2001). Studies reported mycoplasma-like viruses such as *Toddia, Pirhemocyton* and other Rickettsiales (Barta and Desser, 1984; Davies and Johnston, 2000; Netherlands *et al.*, 2015) were similar to FEV species. As mentioned above, a combined approach of morphological characterisation and molecular analysis should be used to identify these organisms.

Extracellular blood parasites

The genus *Trypanosoma* Gruby, 1843 (Family: Trypanosomatidae; Order: Kinetoplasyida), are single cell flagellates with over 500 described species found in all vertebrate classes (Haag *et al.*, 1998; Martin *et al.*, 2002; Bernal and Pinto, 2016; Spodareva *et al.*, 2018). Prior to 1965, more than 70 anuran trypanosome species were recognized until Diamond (1965), constructed a comprehensive review, to reduce the species list to only 26 valid *Trypanosoma* species infecting anurans (Diamond, 1965; Desser, 2001). The genus *Trypanosoma* have been reported from numerous anurans, however, only limited research has been done on these trypanosomes (Bernal and Pinto, 2016). This is due to economically important, disease-causing, human and livestock trypanosomes, such as *Trypanosoma cruzi* and *T. brucei,* creating an attention split with less research focussing on wildlife, particularly amphibian trypanosomes (Bardsley and Harmsen, 1973; Desser and Yekutiel, 1986; Desser, 2001; Attias *et al.*, 2016; Bernal and Pinto, 2016; Spodareva *et al.*, 2018). Frog trypanosomes, however, provide further insight into the understanding of the group, both in ecological and evolutionary terms. Anuran trypanosomes played a significant historic role, with the first trypanosome observed by Gruby (1842) in a frog host. Furthermore, the genus name *Trypanosoma* was erected by Gruby (1843) with the description of the type species, *Trypanosoma sanguinis* Gruby 1843, now a junior synonym of *Trypanosoma rotatorium* (Mayer, 1843).

Trypanosomes are transmitted by a variety of haematophagous invertebrate vectors Arthropod and dipteran species infect mammals, birds, reptiles, and species of amphibians and hirudinean annelids infect fish (Martin *et al.*, 2002; Bernal and Pinto, 2016; Spodareva *et al.*, 2018). It has been reported that anuran trypanosomes are transmitted by both dipteran and annelid vectors due to their amphibious lifestyle (Bardsley and Harmsen, 1973; Martin and Desser, 1990; Desser, 2001; Spodareva *et al.*, 2018). Species of *Trypanosoma* have remarkable morphological plasticity and pleomorphism (Diamond, 1965; Desser, 2001; Martin *et al.*, 2002; Attias *et al.*, 2016; Spodareva *et al.*, 2018). This causes confusion in the literature regarding the taxonomy of anuran trypanosomes and species descriptions, without molecular characterisation, is discouraged (Desser, 2001; Martin *et al.*, 2002).

Filarial nematodes are long round worms found within the coelom, or tissue, of a broad range of hosts, including almost all vertebrate groups, excluding fish. Filarial nematodes are reported globally and are known for causing diseases within humans and livestock (Barta and Desser, 1984; Lefoulon *et al.*, 2015; Netherlands *et al.*, 2020b). Currently, anuran filarial nematodes are restricted to subfamilies, Icosiellinae and Waltonellinae, and comprise six genera and 41 described species (Netherlands, *et al.,* 2020). Adult filarial worms are located in the body cavity of the anuran host where sheathed microfilariae are released and migrate to the lymph or blood vessels (Bain, 2002; Bain et al., 2013). Transmission occurs when a haematophagous invertebrate vector, such as a mosquito, feeds on the infected, definitive vertebrate host and transmits the infective L3 stage to its next host during its blood meal (Netherlands *et al.*, 2020b).

3.2 Materials and Methods

3.2.1 Frog collection and blood sampling

Frogs were collected by means of active sampling during the night at various sampling localities across the Soutpansberg Mountain Range, Limpopo, South Africa (see Chapter 2). Following identification of specimens, small blood samples were taken via femoral venipuncture and thin blood smears were prepared (two smears per specimen) and processed, following methods described in Netherlands *et al.* (2015, 2018). Following processing, all specimens were released at the site of capture within 24 hours.

Blood samples were collected from 70 sample localities throughout the year 2020 – 2021, during the warm and wetter summer months of February 2020 and 2021, October – December 2020, colder autumn month of April 2021 and September 2021 during Spring.

3.2.2 Blood smear preparation and light microscopy screening

All microscopy preparations and techniques were done with the relevant ethical approval for the current study NWU-00429-21-A5. Thin blood smears were fixed with absolute methanol, air dried in a dust-proof container and stained using a modified Giemsa stain (FLUKA, Sigma-Aldrich, Steinheim, Germany). The remaining blood was preserved in 100% molecular grade ethanol for future use. Blood smears were screened for the presence of blood parasites using a 100x immersion oil objective on a Zeiss AX10 microscope and micrographs of the observed parasites were captured using a Zeiss Axiocam 305 color.

3.2.3 DNA extraction and PCR amplification

Total genomic DNA was extracted from whole blood preserved in 100% molecular grade ethanol from positive samples (confirmed with light microscopy) for all blood parasites. The standard protocol for human or animal tissue and cultured cells as detailed in the NucleoSpin Tissue Genomic DNA Tissue Kit (Macherey-Nagel, Düren, Germany) was used for DNA extractions. Polymerase chain reaction (PCR) amplification and sequencing, targeting a fragment of the nuclear 18S rRNA or the mitochondrial cytochrome c oxidase subunit I (COI) gene, was completed for samples found positive with blood parasites (see Table 3.1 for details about PCR primer sets and conditions).

A total volume of 25uL was used to perform the PCR amplification, using 1.25uL each of both primer sets, 12.5uL DreamTag Master Mix, between 3 – 7uL of the genomic DNA was used, depending on the quality of the extracted DNA product. Nuclease-free water was used to supplement the remaining volume. Amplification was performed in an Applied Biosystems SimpliAmp Thermal Cycler. Resulting amplicons were visualised under UV on a 1% agarose gel stained with gel red. The PCR product was pipetted into 1% agarose gel stained with SafeStain which made the resultant amplicons visible under ultraviolet light using an E-BOX CX5 imaging system (Vilber Lourmat Deutschland, Eberhardzell, Germany). The PCR product was sent to Inqaba Biotechnical Industries (Pty) Ltd, Pretoria, South Africa for purification and sequencing.

Table 3.1: List of primer sets and PCR conditions of different genotypes for all parasite groups observed in the current study.

Parasite group	Genotype	Forward primer	Reverse primer	PCR conditions																Citations
				x1				35x cycles								x1		∞		
Trypanosomatids	18S rRNA	SLF (5'- GCT TGT TTC AAG GAC TTAGC - 3')	S762 (5'- GAC TTT TGC TTC CTC TAA TG - 3')	Denaturation			+	Denaturation	+	Annealing	+	Extension	+	Final extension	+	Hold	(Maslov *et al.*, 1996; Mcinnes *et al.*, 2009)
				95°C	50°C	72°C		94°C		60°C		72°C		72°C		4°C				
				Min: 5	Min: 2	Min: 4		Sec: 30		Sec: 30		Min: 2, 20 sec		Min: 7		Pause				
		S825 F (5'-ACC GTT TCG GCT TTT GTT GG - 3')	SLIR (5'-AC- ATT GTA GTG CGC GTG TC - 3')	Denaturation			+	Denaturation	+	Annealing	+	Extension	+	Final extension	+	Hold	(Maslov *et al.*, 1996; Mcinnes *et al.*, 2009)
		B	I	95°C				95°C		57°C		72°C		72°C		4°C				
				Min: 3				Sec: 30		Sec: 30		Min: 1		Min: 7		Pause				
Haemogregarines	18S rRNA	HepF300 (5′-GTT TCT GAC CTA TCA GCT TTC GACG-3′)	HepR900 (5′-CAA ATC TAA GAA TTT CACCTC TGA C-3′)	Denaturation			+	Denaturation	+	Annealing	+	Extension	+	Final extension	+	Hold	(Ujvari *et al.*, 2004)
				95°C				95°C		60°C		72°C		72°C		4°C				
				Min: 3				Sec: 30		Sec: 30		Min: 1		Min: 10		Pause				
Haemococcidians	18S rRNA	HC-F (5′-TCT CTG GAG GGG CTG TGT TT- 3′)	ER (5′-CTT GCG CCT ACT AGG CAT TC- 3′)	Denaturation			+	Denaturation	+	Annealing	+	Extension	+	Final extension	+	Hold	(Kvičerová *et al.*, 2008)
				95°C				95°C		62°C		72°C		72°C		4°C				
				Min: 3				Sec: 30		Sec: 30		Min: 2		Min: 10		Pause				
	COI	COI 400F (5′- GGD TCA GGT RTT GGT TGG AC- 3′)	COI 500R (5′-CAT RTG RTG DGC CCA WAC-3′)	Denaturation			+	Denaturation	+	Annealing	+	Extension	+	Final extension	+	Hold	(El-Sherry *et al.*, 2013)
				96°C				94°C		55°C		72°C		72°C		4°C				
				Min: 5				Sec: 30		Sec: 30		Min: 1		Min: 10		Pause				

Parasite group	Genotype	Forward primer	Reverse primer	PCR conditions														Citations
				x1		35x cycles						x1		∞				
Microfilaria	18S rRNA	**F18ScF1** (5′-ACC GCC CTA GTT CTG ACC GTA AA-3′)	**F18ScR1** (5′-GGT TCA AGC CAC TGC GAT TAA AGC-3′)			40x cycles						X1		∞				(Lefoulon *et al.*, 2015)
						Denaturation		Annealing		Extension		Final extension		Hold				
						95°C	+	58°C	+	72°C	+	72°C	+	4°C				
						Sec: 30		Sec: 30		Sec: 90		Min: 10		Pause				

Table 3.2: Details on the phylogenetic analysis of the different parasite groups.

Parasite group	Genotype	Alignment tool	Final alignment: number of sequences	Final alignment: length of sequences	Most suitable nt substitution model (best BIC score)	MrBayes 3.2.7 algorithm	Outgroup
Haemogregarines	18S	ClustalW	46	1772 nt	GTR + I + G	lset nst=6 rates=invgamma; MCMC ngen=1000000	*Klossiella equi* (Úngari *et al.*, 2020)
Trypanosomatids	18S	ClustalW	104	1853 nt	GTR + I + G	lset nst=6 rates=invgamma; MCMC ngen=1000000	*Trypanosopma borreli* (Martin *et al.*, 2002)
Haemococcidians	18S	ClustalW	44	578 nt	GTR + I + G	lset nst=6 rates=invgamma; MCMC ngen=1000000	*Toxoplasma gondii* (Ogedengbe *et al.*, 2011)
	COI	ClustalW	44	713 nt	GTR + I + G	lset nst=mixed; MCMC ngen=1000000	*Toxoplasma gondii* (Ogedengbe *et al.*, 2011)
Microfilariae nematode	18S	MUSCLE	13	660 nt	K80 + I	lset nst=2 rates=propinv; MCMC ngen=1000000	*Filaria latala* (Lefoulon *et al.*, 2015)

3.2.4 Phylogenetic analysis

Resultant parasite 18S rDNA or COI sequences generated from the blood of infected individuals in the current study, were aligned with sequences of a diverse range of blood parasites downloaded from GenBank and used to construct phylogenetic trees. A combination of MEGA X and Geneious Pro (http://www.geneious.com) software was used for assembling and editing sequence fragments and compared with previously published sequences using the Basic Local Alignment Search Tool (BLAST). The GBlocks server (Castresana, 2000) was used to remove any alignment gaps, selecting the parameters to allow for smaller final blocks with gap positions. A model test was performed using RAxML, to determine the most suitable nucleotide substitution model with the best Bayesian information criterion (BIC) score. A Bayesian Inference analysis was performed using MrBayes 3.2.7 (Huelsenbeck and Ronquist, 2001). The alignment tool, number and length of sequences, the most suitable nucleotide substitution model, BI algorithm and the outgroups for all phylogenetic trees constructed of the different parasite groups, are listed in Table 3.2.

3.2.5 Statistical analysis of parasite fauna

All statistical analyses were calculated using the R programming platform (R core Team, 2022) using the package 'tidyverse' (Wickham *et al.,* 2019) to manipulate and visualise the data. To estimate Sterne confidence intervals for prevalence, function epi.prev was used from the package "epiR"(Stevenson *et al.,* 2022). Calculating the confidence intervals of mean species richness, which was considered the average number of species categories per individual of separate frog species, the bias-corrected and accelerated bootstrap method was calculated as implemented function BootCI from package "DescTools" (Signorell, 2022). To evaluate co-occurrence patterns of haemoparasites in host individuals, the Spearman correlation coefficient was calculated for each pair of frog specimens with function cor. The functions cor_pmat and ggcorrplot from the package "ggcorrplot" (Kassambara, 2022) were used for estimating the p-value of each coefficient and visualising results, respectively. Finally, factors (transects, year and host species) were tested to explain grouping frog individuals on base (dis)similarity in the quality composition of their parasites' infracommunities with the following approach. For each factor, the Gower similarity matrix was built with the function daisy from the package "cluster" (Maechler *et al.,* 2021). The on-base presence-absence blood parasite matrix and the Bray-Curtis dissimilarity matrix was calculated. As the presence-absence matrix was zero-inflated, the dissimilarity calculation for some pairs of individuals was impossible. These pairs were considered entirely dissimilar and the value 'one' was assigned to these cases in a matrix. Lastly, the Mantel test was run to get the correlation value and significance for each factor matrix and the Bray-Curtis matrix. The package

'vegan' (Oksanen *et al.,* 2022) was used for calculating the Bray-Curtis matrix and for all Mantel tests, with function vegdist and mantel, respectively.

3.3 Results

3.3.1 Overall prevalence and diversity of blood parasites

Blood samples were collected from frog specimens during the year 2020 – 2021 at the Soutpansberg Mountain Range across 70 sampling localities (Figure 3.1). Overall blood sample collection comprised 11 family, 18 genera and 25 anuran species from 387 individuals (see Table 3.3). From 20 sites, 38/387 (10%) frog specimens were found infected with intra- and extracellular blood parasites within 5/25 (20%) frog species. Data revealed a high blood parasite diversity with 25 possible parasite species belonging to five taxonomic groups including trypanosomatids, haemogregarines, haemococcidians, filariae nematodes and unknown non-protistan infections.

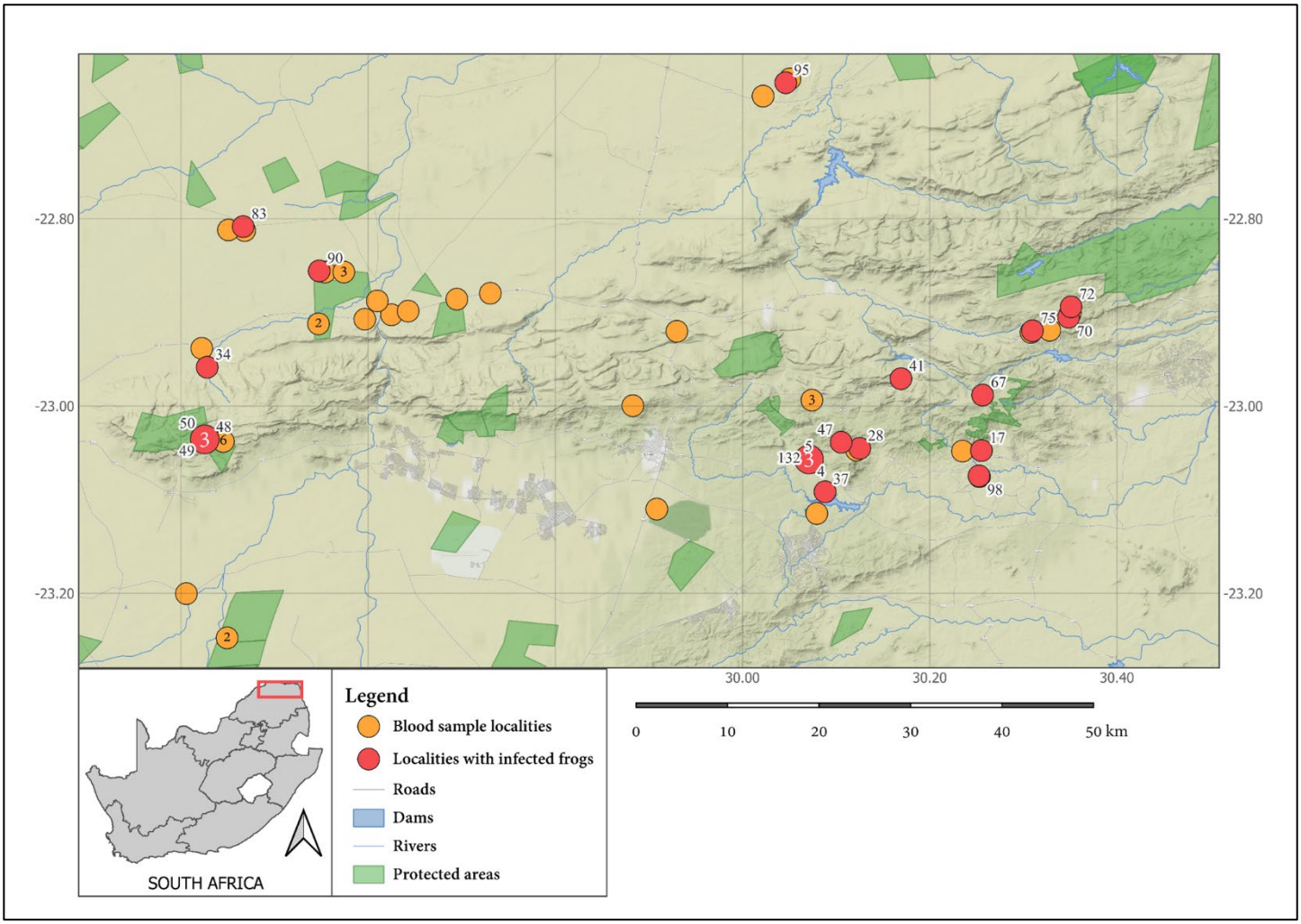

Figure 3.1: Sampling localities across the Soutpansberg Mountain range indicated by dots. Sites where no haemoparasites were detected indicated with an orange dot and in red where positive infections were detected. Multiple blood parasite species were observed within five frog species from 20 sample localities. The majority of the infections were located at the eastern sites.

Parasites belonging to the genera *Hepatozoon, Lankesterella, Trypanosoma* and *Neofoleyellides* were observed, as well as infections of uncertain status and non-protozoan organisms which couldn't be identified.

Anuran species that were not infected with one of the four classified parasite groups, included (the sample size of each frog species is in brackets): *A. stenodactylus* (n = 3), *B. adspersus* (n = 2), *B. sylvestris* (n = 5) *C. boettgeri* (n = 12) *C. xerampelina* (n = 20) *H. marmoratus* (n = 1), *K. senegalensis* (n = 14), *P. mababiensis* (n = 18), *P. natalensis* (n = 1), *P. bifasciatus* (n = 11) *P. fenoulheti* (n = 20), *Pt. uzungwensis* (n = 18), *P. edulis* (n = 19), *S. carens* (n = 16), *S garmani* (n = 6), *S. fasciatus* (n = 10), *S. grayii* (n = 2), *Tomopterna* spp. (n = 34), *X. laevis* (n = 5) and *X. muelleri* (n = 4). Frog species that were infected with at least one of the four parasite groups are listed in table 3.3.

Table 3.3: Blood parasites prevalence (with 95% confidence intervals limits - CI) of amphibians from the Soutpansberg Mountain Range. The sample size of each frog species is indicated between the brackets.

Species	**Prevalence (%)**	**Lower CI (%)**	**Upper CI (%)**
***Amietia delalandii* (n = 75)**			
Hepatozoon theileri	20.00	12.19	30.58
Lankesterella sp.	1.33	0.07	7.11
Neofoleyellides steyni	5.33	1.84	13.13
Trypanosoma A	1.33	0.07	7.11
Trypanosoma B	4.00	1.10	11.14
Trypanosoma C	5.33	1.84	13.13
Trypanosoma D	1.33	0.07	7.11
Trypanosoma E	1.33	0.07	7.11
Trypanosoma F	1.33	0.07	7.11
Trypanosoma G	2.67	0.48	9.14
Trypanosoma J	4.00	1.10	11.14
Trypanosoma K	4.00	1.10	11.14
Trypanosoma L	1.33	0.07	7.11
Trypanosoma M	6.67	2.66	15.11
Trypanosoma N	6.67	2.66	15.11
Trypanosoma O	1.33	0.07	7.11
Trypanosoma P	1.33	0.07	7.11
Trypanosoma R	1.33	0.07	7.11
Trypanosoma S	1.33	0.07	7.11
Trypanosoma T	1.33	0.07	7.11
***Hyperolius marmoratus* (n = 32)**			
Trypanosoma C	3.12	0.16	16.62
Trypanosoma H	6.25	1.12	20.01

Species	Prevalence (%)	Lower CI (%)	Upper CI (%)
***Ptychadena anchietae* (n = 38)**			
Hepatozoon ixoxo	2.63	0.13	14.00
Trypanosoma B	2.63	0.13	14.00
Trypanosoma U	5.26	0.94	18.00
***Sclerophrys gutturalis* (n = 11)**			
Hepatozoon ixoxo	9.09	0.47	40.45
***Sclerophrys pusilla* (n = 10)**			
Trypanosoma B	10.00	0.51	44.65
Trypanosoma J	20.00	3.68	55.35
Trypanosoma V	10.00	0.51	44.65

3.3.2 Frog blood parasites reported based on morphology

Trypanosoma species

Twenty-two morphologically different *Trypanosoma* spp. were observed infecting 32 specimens belonging to four species of anurans (Table 3.4 and Figure 3.2). Morphological features such as: overall size and shape, shape and position of the nucleus, flagellum, an undulating membrane, posterior kinetoplast and longitudinal striations are mostly used to distinguish between *Trypanosoma* species. However, it is encouraged to include both morphological characteristics as well as molecular analysis to accurately classify these species.

Table 3.4: A list of the 22 morphologically distinct morphotypes of *Trypanosoma* spp. observed in the current study. Characteristics such as overall shape and size, presence of a free flagellum, shape and position of nucleus, posterior kinetoplast, intensity of granulated cytoplasm and an undulating membrane, was used to characterize these *Trypanosoma* morphotypes.

Trypanosoma spp. morphotype	Description	Type host	Additional host
A	Oval or slightly elongated with an oval nucleus near the border of the parasite. A relatively large kinetoplast was adjacent to the nucleus with an undulating membrane that is double the diameter of the kinetoplast. No free flagellum was observed.	*Amietia delalandii* 1/75	n/a
B	Long body with a well-developed undulating membrane. The kinetoplast is near the more rounded posterior end and the long free flagellum extends from the tapering anterior end.	*Amietia delalandii* 2/75	*Ptychadena anchietae* 1/38
C	Rounded-body giant trypanosome. Large and flattened with a circular form. An almost spherical nucleus in the centre and an adjacent kinetoplast. Dense cytoplasm.	*Amietia delalandii* 4/75	*Hyperolius marmoratus* 1/32
D	Broad body and tapering ends. Well-developed undulating membrane. The widened anterior has a vacuolated cytoplasm and a small kinetoplast almost at the anterior end. A short free flagellum observed.	*Amietia delalandii* 1/75	**n/a**

Trypanosoma spp. morphotype	Description	Type host	Additional host
E	Flat S-shaped with easily visible oblique striations. The cytoplasm was vacuolated with an oval nucleus lying near the tapered anterior end. Narrow undulating membrane.	*Amietia delalandii* 1/75	**n/a**
F	Broad body with anterior end tapering to the pole opposite the undulating membrane. Granulated cytoplasm. The undulating membrane has sharp-pointed poles with a tail-like protrusion to both sides, a short flagellum extending from the one pole. Kinetoplast was centrally positioned.	*Amietia delalandii* 1/75	**n/a**
G	Oddly shaped extended body with a square like protrusion in the centre opposite the undulating membrane. Indents from the undulating membrane can be observed with the kinetoplast at the anterior point. No flagellum was visible.	*Amietia delalandii* 2/75	**n/a**
H	Large, extended body with coarsely granulated cytoplasm and well defined indents from undulating membrane. Flagellum was not observed and kinetoplast is closer to posterior end.	*Hyperolius marmoratus* 2/32	**n/a**
I	Fan-like shape with thick striated bands extending into well-defined undulating membrane. Kinetoplast was in the centre of the parasite and a short flagellum was in some cases visible.	*Ptychadena anchietae* 1/38	**n/a**
J	Elongated with an off-centre nucleus more towards the anterior end where the kinetoplast is situated. Vacuoles both sides of the nucleus. Cytoplasm slightly granulated near posterior end. Both ends tapering. Undulating membrane is well defined extending along half the body length of parasite. Long thin flagellum extending the body length.	*Sclerophrys pusilla* 2/10	*Amietia delalandii* **3/75**
K	Large, rounded body with light stained finely granulated cytoplasm. Short undulating membrane in the centre expanding from the centrally positioned kinetoplast. No vacuole or flagellum was observed.	*Amietia delalandii* 3/75	**n/a**
L	Large, centroided expanded body with finely granulated and lightly stained cytoplasm. Kinetoplast and vacuole is in the centre of the parasite with undulating membrane expanding from the kinetoplast, cutting across the surface of the parasite to both ends. No visible flagellum.	*Amietia delalandii* 1/75	**n/a**
M	Large, rounded body with dark stained granulated cytoplasm. Short undulating membrane in the centre expanding from the centrally positioned kinetoplast with adjacent vacuole. No visible flagellum.	*Amietia delalandii* 1/75	**n/a**
N	Medium sized rounded body with granulated cytoplasm. Kinetoplast is centrally positioned with short undulating membrane expanding from the centre. The edges ae flattened and appear translucent with no visible flagellum.	*Amietia delalandii* 5/75	**n/a**
O	Broad granulated body with tapering ends. Kinetoplast is positioned at the anterior pole. Well-defined undulating membrane extending from the posterior half of the body and no flagellum was visible.	*Amietia delalandii* 1/75	**n/a**
P	Rounded body with finely granulated cytoplasm. The kinetoplast is anterior with the vacuole centrally positioned. Some striations are visible on the outer edges. No flagellum or undulating membrane was observed.	*Amietia delalandii* 1/75	**n/a**

Trypanosoma spp. morphotype	Description	Type host	Additional host
Q	Slender, half-moon shaped body with dense, darkly stained cytoplasm. Twee large vacuoles are visible in the centre of the parasite. Well-developed undulating membrane extending from the middle of the body towards to the posterior point, tapering off into a short flagellum. Kinetoplast is positioned at the anterior pole.	*Amietia delalandii* 1/75	**n/a**
R	Slender body and tapering into sharp ends. Granulated cytoplasm with vacuolated anterior pole. Well-developed undulating membrane extending from the middle of the body towards the posterior end. A small kinetoplast almost at the anterior end. A short free flagellum was seen.	*Amietia delalandii* 1/75	**n/a**
S	Round, bean-shaped lightly granulated body. Well-developed undulating membrane forming indents, expanding from the central kinetoplast across the surface into a fine point. No flagellum was observed.	*Amietia delalandii* 1/75	**n/a**
T	Broad to narrow leaf-shaped body with finely granulated cytoplasm. Kinetoplast is positioned centrally from where the undulating membrane extends up the broader end. Posterior pole tapers into a sharp point opposite side of undulating membrane.	*Amietia delalandii* 1/75	**n/a**
U	Long tapering body towards posterior end with the cytoplasm staining dark. Well-developed undulating membrane extending from the centre of the body to the anterior pole. Long flagellum in some cases. The kinetoplast situated near the undulating membrane.	*Ptychadena anchietae* 2/38	**n/a**
V	Rather large, elongated body with almost centrally placed nucleus closer to anterior pole. Granulated cytoplasm with slight undulating membrane extending half the length of the organism. No flagellum was visible.	*Sclerophrys pusilla* 1/10	**n/a**

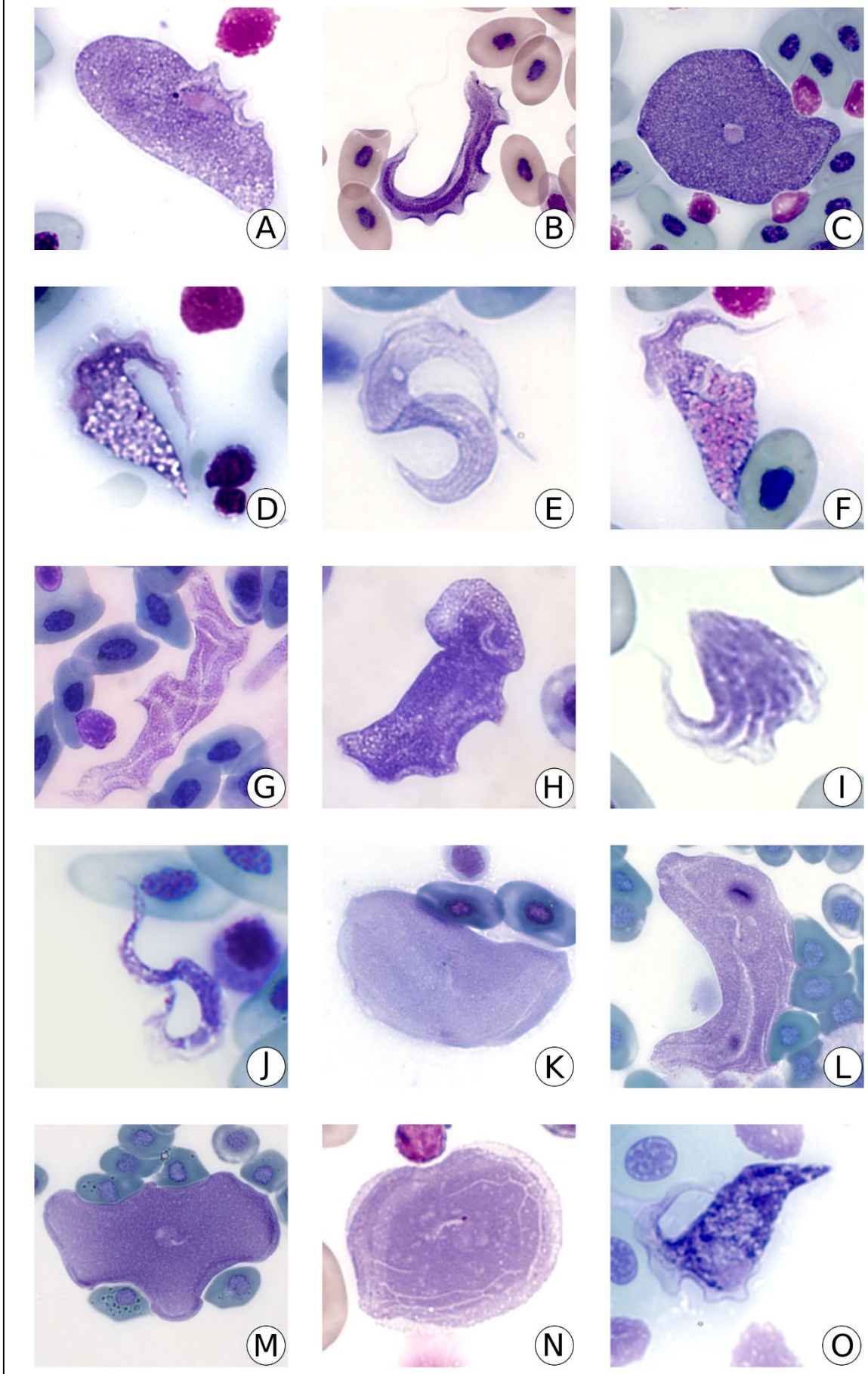

Figure 3.2: *Trypanosoma* species observed in the peripheral blood of anurans from the Soutpansberg Mountain range. (A – G, J – O) *Trypanosoma* spp. infecting *Amietia delalandii*. (B, I) *Trypanosoma* spp. infecting *Ptychadena anchietae*. *Trypanosoma* sp. I will be excluded from the dataset, from now on, due to the infected frog being collected from Blouberg, which falls outside of the study area. (C, H) *Trypanosoma* spp. infecting *Hyperolius marmoratus*. (J) *Trypanosoma* sp. infecting *Sclerophrys pusilla*. Scale bar: 20 µm.

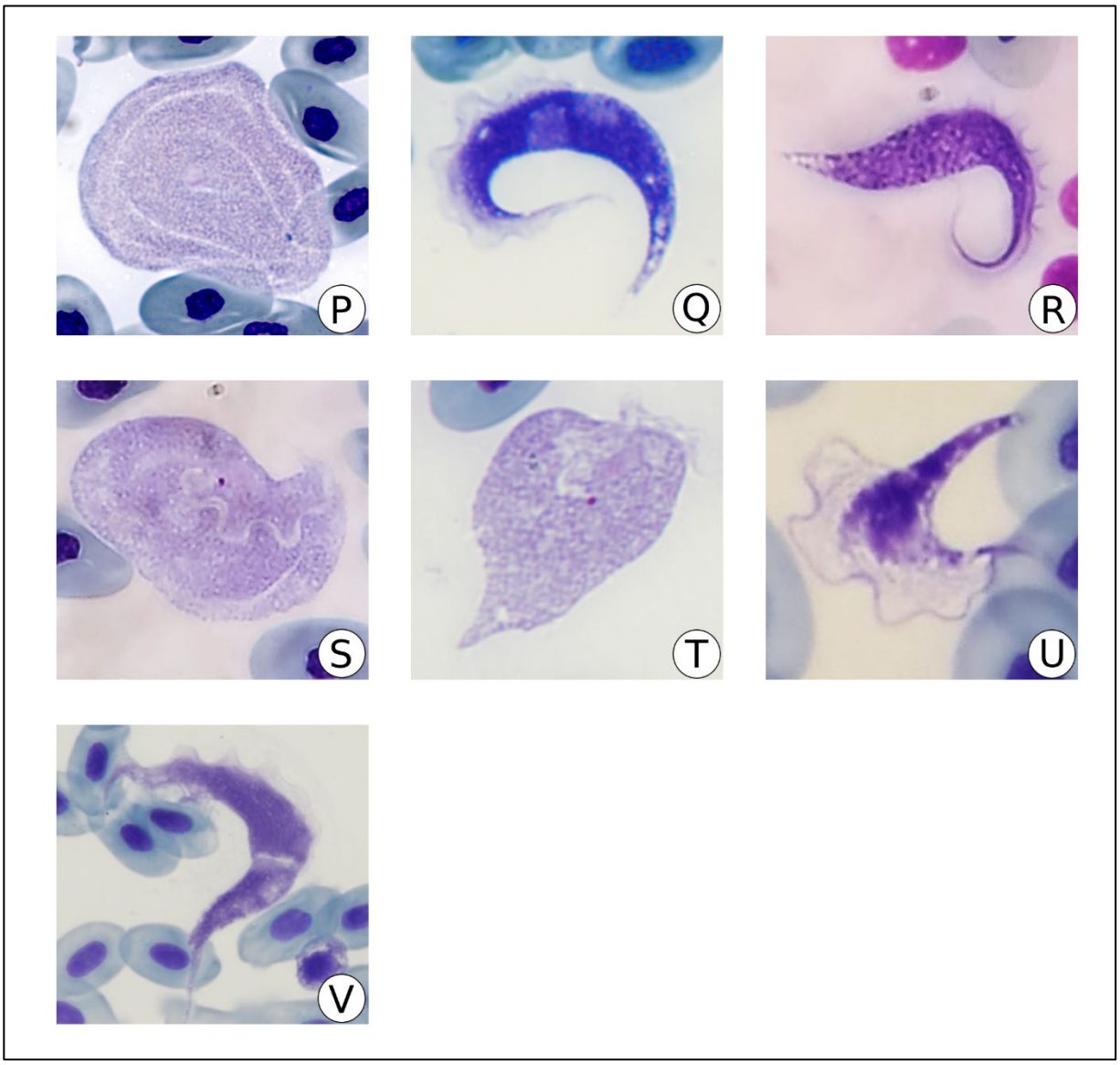

Figure 3.2 continued: *Trypanosoma* species observed in the peripheral blood of anurans from the Soutpansberg Mountain Range. (P – T) *Trypanosoma* spp. infecting *Amietia delalandii.* (U) *Trypanosoma* sp. infecting *Ptychadena anchietae.* (V) *Trypanosoma* sp. infecting *Sclerophrys pusilla.* Scale bar: 20 µm.

Hepatozoon species

Two haemogregarine species were observed, both belonging to the genus *Hepatozoon* - namely *Hepatozoon theileri* (Laveran, 1905) Smith, 1996 and *Hepatozoon ixoxo* Netherlands, Cook, and Smit, 2014 (Figure 3.3). *Hepatozoon theileri* was more abundant, infecting one frog species and 15 *Amietia delalandii* specimens. *Hepatozoon ixoxo* was observed in two frog species with only one specimen each, namely *Sclerophrys gutturalis* and *Ptychadena anchietae*.

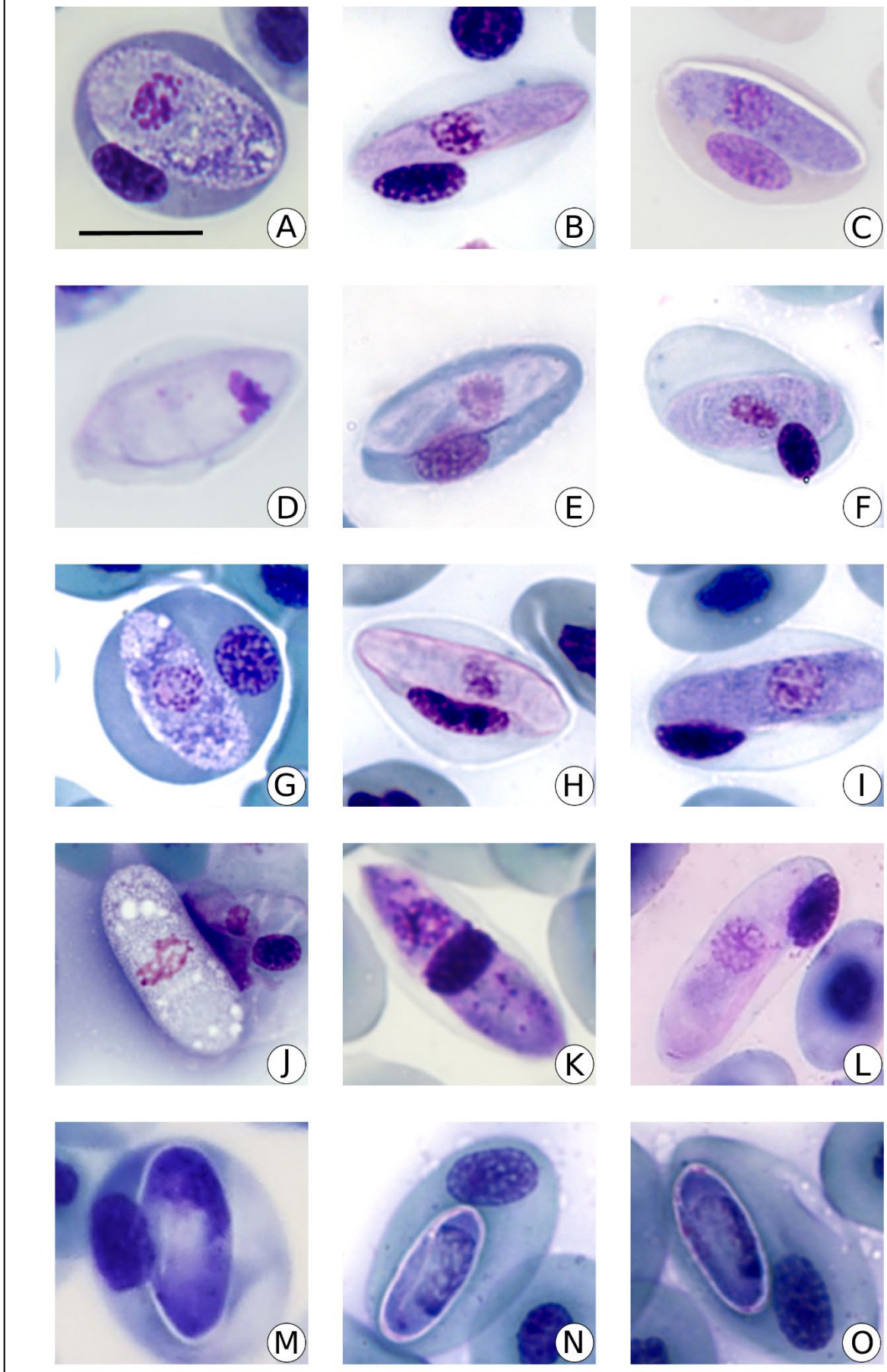

Figure 3.3: *Hepatozoon* spp. infecting three frog species across the Soutpansberg. (A – L) *Hepatozoon theileri* infecting *Amietia delalandii* (n = 15). (M) *Hepatozoon ixoxo* infecting *Ptychadena anchietae* (n = 1). (N – O) *Hepatozoon ixoxo* infecting a single *Sclerophrys gutturalis*. Scale bar is 20 µm.

Lankesterella species

A single *Amietia delalandii* was found infected by a haemococcidian parasite from the genus *Lankesterella*. Initially this specimen could not be classified to genus or species level, thus, a more detailed study was conducted to differentiate this species from other anuran haemococcidians and is considered to be a species of *Lankesterella* (Figure 3.4) (see Chapter 4).

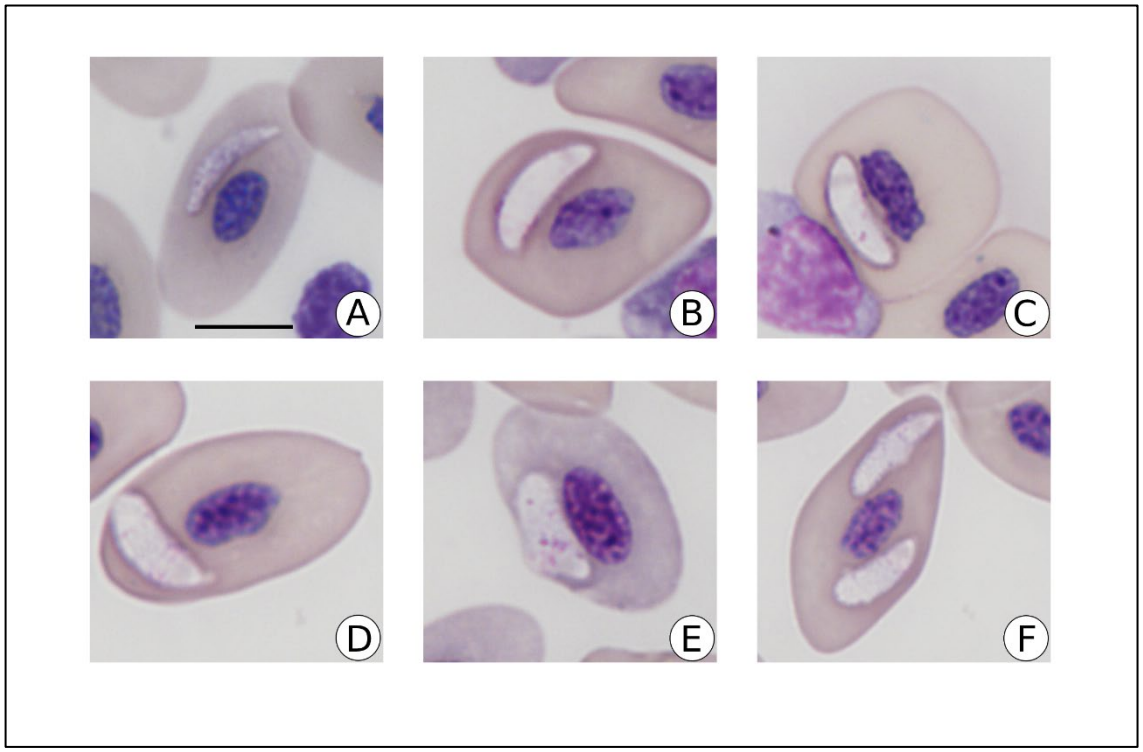

Figure 3.4: *Lankesterella* sp. observed in a single *Amietia delalandii* at the Soutpansberg. Scale bar is 10 µm.

***Neofoleyellides* species**

Four *Amietia delalandii* specimens were infected by the elongated, worm-like microfilariae nematode, *Neofoleyellides steyni.* These parasites are enclosed in a thick sheath and have coarsely granulated bodies staining dark purple, with Giemsa (Figure 3.5).

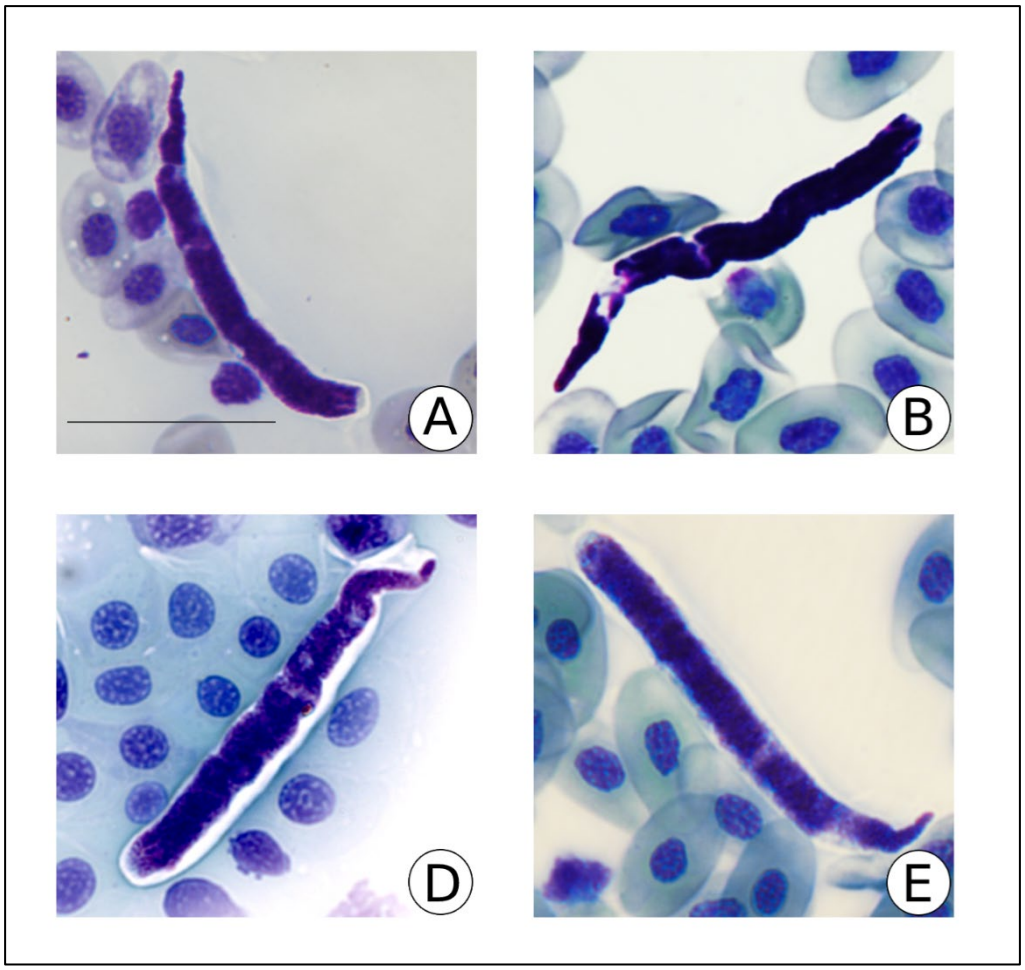

Figure 3.5: (A – E) *Neofoleyellides steyni* infecting four *Amietia delalandii* specimens across the Soutpansberg. Scale bar 20 µm.

Infections of Uncertain Status and Non-Protistan Infections

Non-protistan, intraerythrocytic organisms of unknown status were observed within the peripheral blood of 20 frog species (Table 3.5) (also see Figure 3.6). Large circular inclusions were observed, not staining with Giemsa stain, giving it an almost translucent appearance (Figure 3.6A, E), however, in some cases, a slightly purple stained border was visible (Figure 3.6A, D, K). Large, circular, purple-staining inclusions were also observed (Figure 3.6F) as well as smaller, circular inclusions staining white (Figure 3.6C, I, M). Other unidentified organisms observed had a slender shape and stained dark purple (Figure 3.6G, H, M). Lastly, small circular inclusions, staining from light pink to dark purple, infected the cytoplasm of erythrocytes (Figure 3.6J, L, M). Some infected erythrocytes showed disrupted cytoplasm with slightly distinct light and dark areas (Figure 3.6F). It is almost impossible to identify these organisms, based solely on morphology observed by means of light microscopy screening. Transmission electron microscopy (TEM) techniques need to be applied to accurately classify these infections (Davies and Johnston, 2000).

Table 3.5: Frog species infected with unknown non-protistan inclusions listed in alphabetical order with family.

Frog species	Family
Arthroleptis stenodactylus	Arthroleptidae
Breviceps adspersus	Brevicipitidae
Breviceps sylvestris	Brevicipitidae
Poyntonophrynus fenoulheti	Bufonidae
Schismaderma carens	Bufonidae
Sclerophrys garmani	Bufonidae
Sclerophrys gutturalis	Bufonidae
Sclerophrys pusilla	Bufonidae
Hyperolius marmoratus	Hyperoliidae
Kassina senegalensis	Hyperoliidae
Phrynomantis bifasciatus	Microhylidae
Phrynobatrachus mababiensis	Phrynobatrachidae
Xenopus laevis	Pipidae
Ptychadena anchietae	Ptychadenidae
Ptychadena uzungwensis	Ptychadenidae
Amietia delalandii	Pyxicephalidae
Pyxicephalus edulis	Pyxicephalidae
Strongylopus fasciatus	Pyxicephalidae
Strongylopus grayii	Pyxicephalidae
Tomopterna spp.	Pyxicephalidae

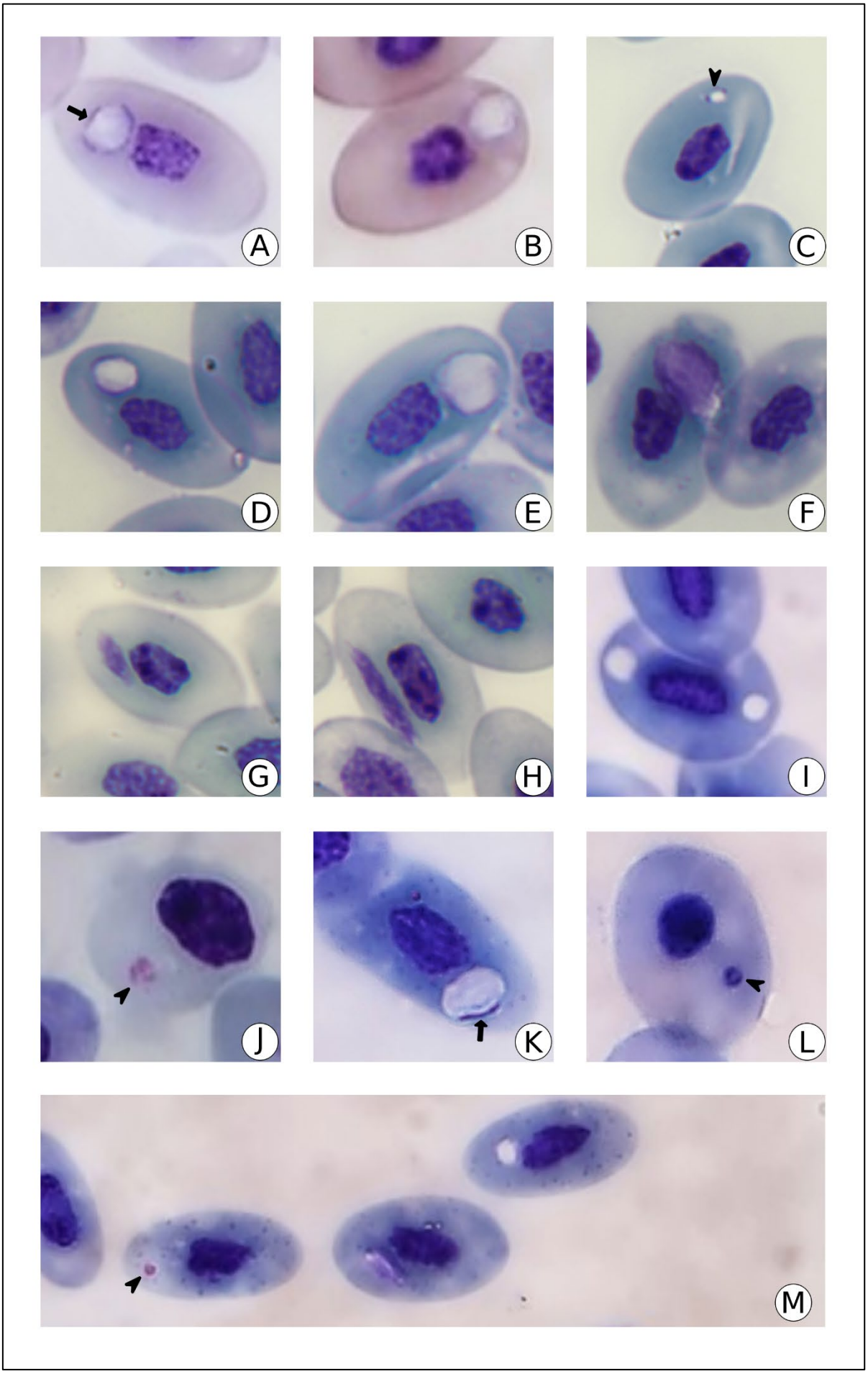

Figure 3.6: Infections of uncertain status and non-protistan infecting 20 frog species across the Soutpansberg. Arrow indicated slightly purple stained borders of the larger circular inclusions. Arrowhead shows small purple inclusions. (M) All three forms observed within *Amietia delalandii*. Scale bar is 10 µm.

3.3.3 Statistical results

Infections of uncertain status and non-protistan infections, were observed in the peripheral blood of 20 species of anurans with a total prevalence of 23%. Thus, the majority of frog species were infected by these unknown organisms. Due to uncertainties about this group, these infections will be excluded from the dataset from now on.

The reduced dataset was built to include only anuran species infected by non-viral parasites and contained 38 specimens from five anuran species. For all the following analyses, this dataset was used. The total infection prevalence for each frog species is presented in Figure 3.7. *Amietia delalandii* is the most infected species in the dataset. The prevalence of *A. delalandii* was considerably higher than *S. pusilla* and *Hyp. marmoratus* as the confidence intervals of *A. delalandii* did not overlap with the confidence intervals of *S. pusilla and Hyp. marmoratus*. The prevalence of the latter species did not differ significantly and confidence intervals of *S. gutturalis* and *P. anchietae* were quite broad, which was interpreted as a high level of uncertainty in the observed values. The reasons for the broad, confidence intervals were due to the small sample size and relatively small observed prevalence.

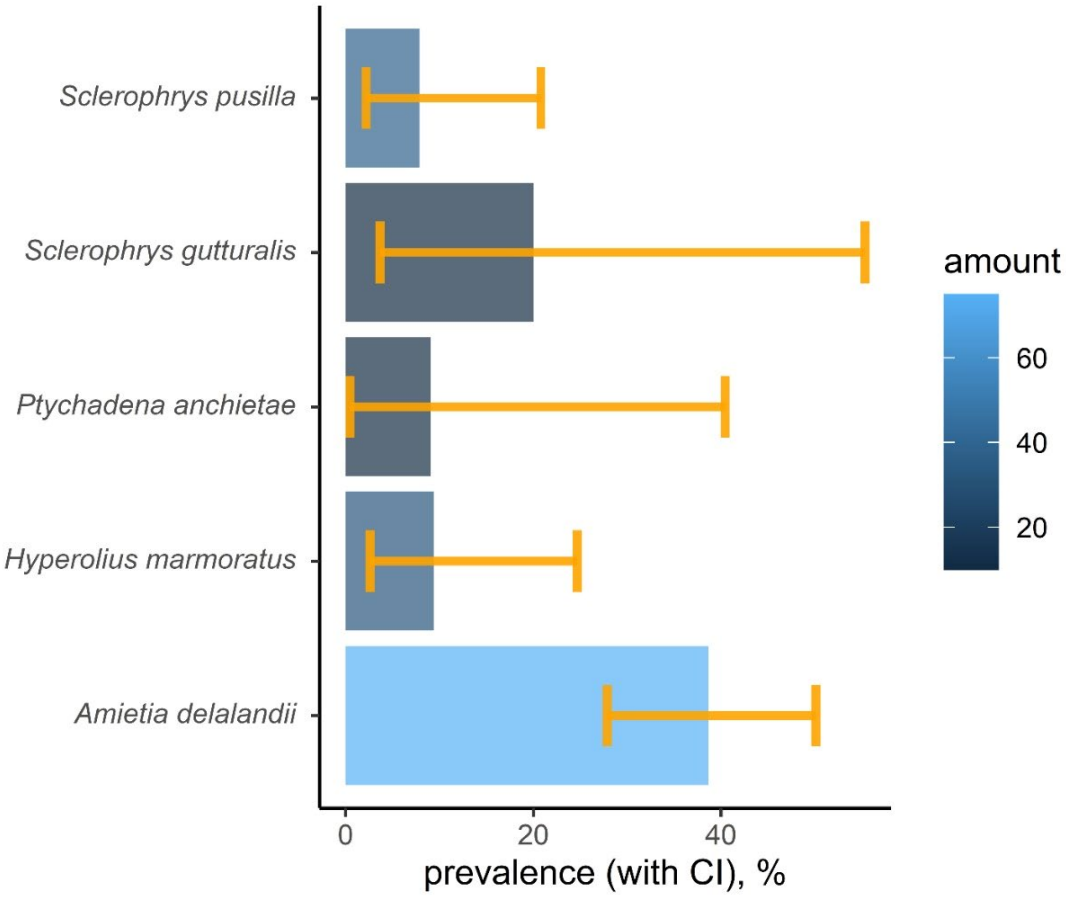

Figure 3.7: The overall infection prevalence for five frog species. The bars represent observed prevalence. The error bars show the Sterne confidence intervals. The colour of the bars reflects the sample size of frog species.

Figure 3.8 shows the quality and quantity character subset of each infected host species. The figure demonstrates that the most frequent parasites in the dataset were *Trypanosoma*, followed by *Hepatozoon theileri*. It shows *A. delalandii* to host the most diverse blood parasite fauna, comprising 20 of the 26 blood parasite species, found during the present study. Blood parasites found parasitising *A. delalandii*, included *Hepatozoon theileri*, *Lankesterella* sp., *Neofoleyellides steyni* and 17 possible *Trypanosoma* spp. Other host species were parasitised with the following blood parasite fauna: *Hyperolius marmoratus* – *Trypanosoma* spp. C and H, *Sclerophrys pusilla* – *Trypanosoma* spp. B, J, and V, *Ptychadena anchietae* – *Trypanosoma* spp. B and U and *Hepatozoon ixoxo* and *Sclerophrys gutturalis* – *Hepatozoon ixoxo*.

The observed average species richness ranged from 0.09 in *P. anchietae* to 0.75 in *A. delalandii* (Figure 3.9). Results revealed that all five species share a low index value. The comparison of confidence intervals indicated that the average species richness of *S. pusilla*, *Hyp. marmoratus* and *P. anchietae* did not differ significantly. In contrast, the species richness of *A. delalandii* was substantially higher relative to the latter three species. With regard to *S. gutturalis*, no conclusions could be made as this species had broad confident intervals.

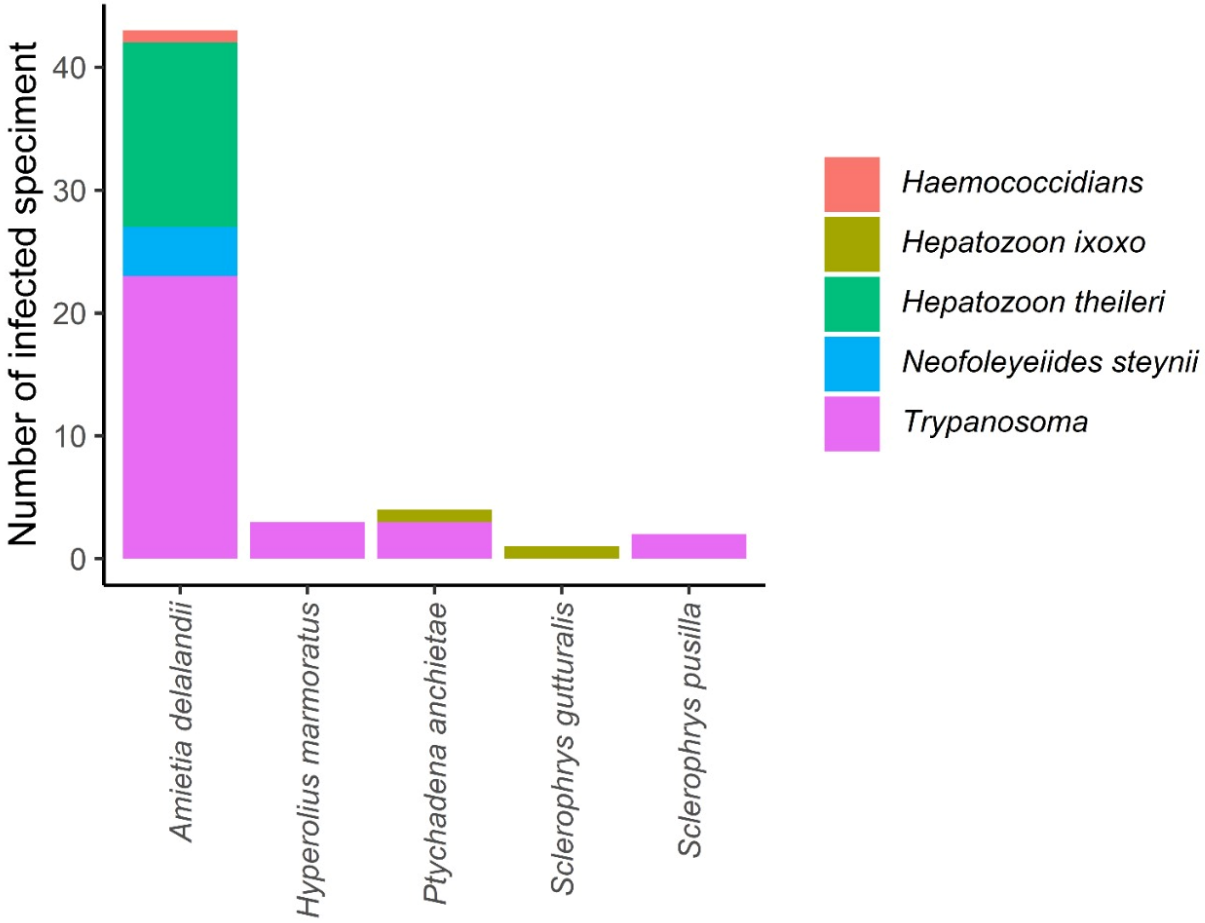

Figure 3.8: Number of infections by each parasite in five frog species. All *Trypanosoma* morphotypes are united in one group.

Although significant correlations were found in the co-occurrence of some parasite species (Figure 3.10), results should be interpreted with the following precautions. The correlations represent mostly patterns of *A. delalandii* as the host with the most significant sample size, the highest prevalence and the highest diversity of parasites. In the host, the prevalence of most parasite species is less than 6%. Thus, it was concluded that the results reflect random events which led to co-occurrence rather than some ecological link between parasites. The results, however, can't reject the possibility of such links and more data is necessary to test the hypothesis of such relationships.

The result of Mantell tests for the factors was the following: transect (r = 0.009, p = 0.313), year (r = -0.0081, p = 0.47) and host (r = 0.126, p = 0.001). Thus, only the host species factor was significant for explaining grouping of the frog individuals with a similar parasite species composition. In other words, the result showed some specialisation of the parasites to the anuran hosts, however, the correlation is weak. The following features of the dataset could explain this weak correlation: (1) approximately half of the frogs were not infected with any blood parasite species and (2) the mean species richness of individual frogs was low.

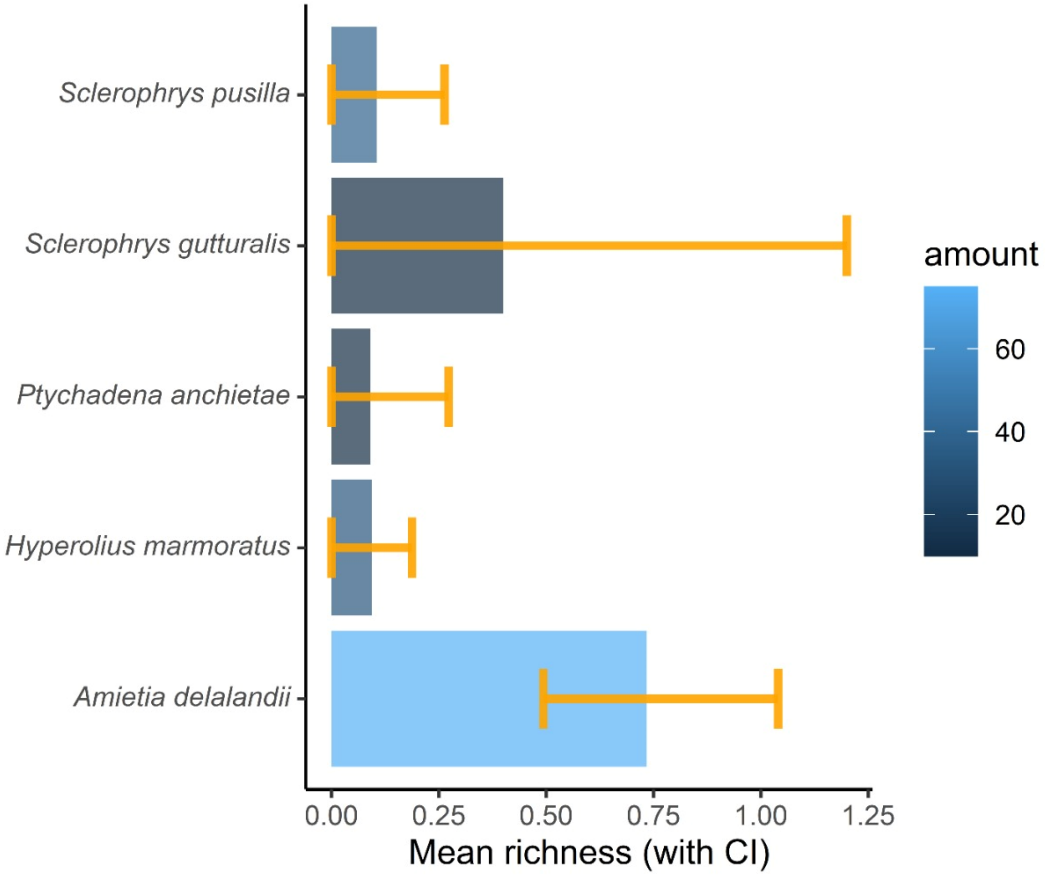

Figure 3.9: The average prevalence of species richness (number of parasite species per host individual) for five frog species. The error bars show the bootstrapped confidence intervals. The bars represent observed species richness. The colour of the bars meets the sample size of frog species.

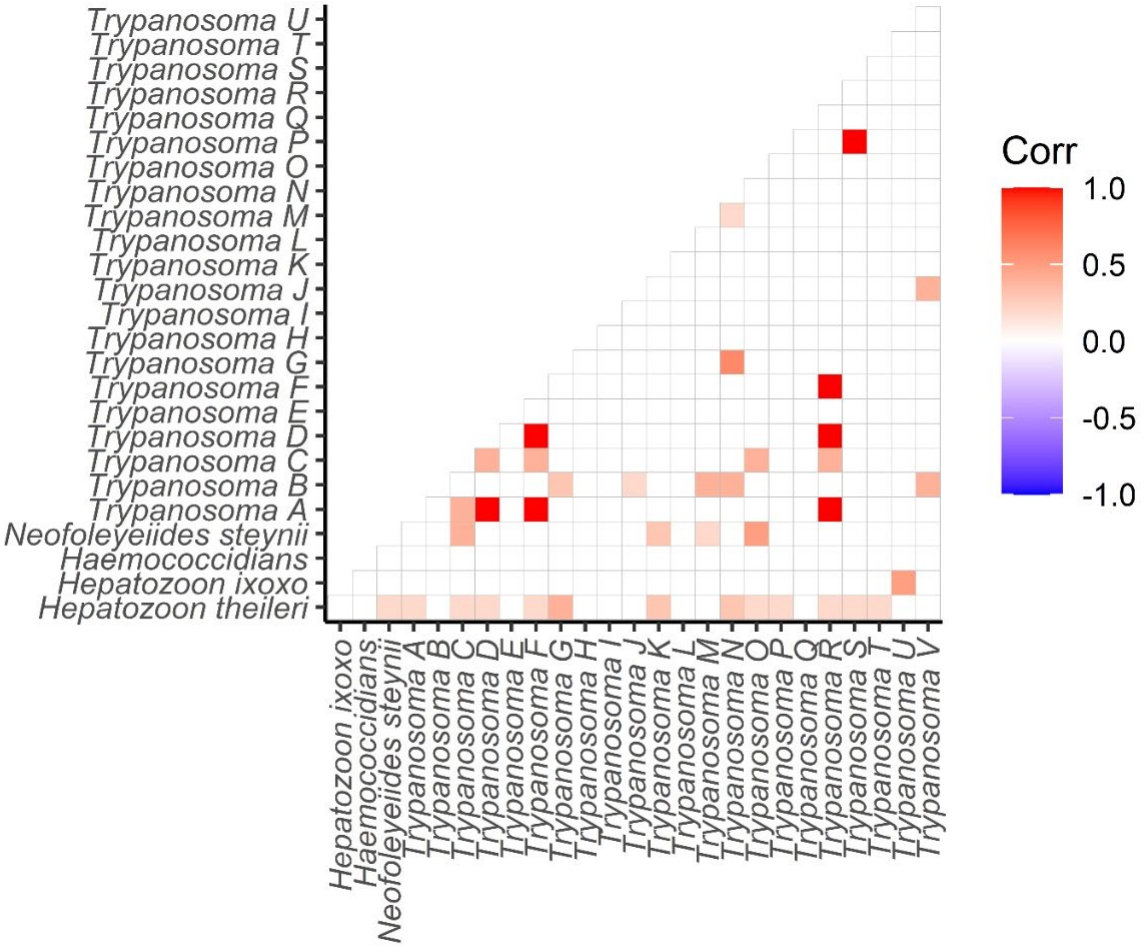

Figure 3.10: Visualisation of species co-occurrence patterns in data set of five frog species. For each parasite species pair, the Spearman correlation coefficient was calculated and the significance level was estimated (the alpha value level was equal to 0.05). Only significant correlations are shown in the plot.

3.3.4 Phylogenetic analyses

***Hepatozoon* spp.**

Amplicons of about 1 772 nt were generated for *H. theileri* and *H. ixoxo* from the blood of *Amietia delalandii* and *Sclerophrys gutturalis*, respectively. The *Hepatozoon* species observed in *Ptychadena anchietae* was not amplified. The phylogenetic analysis shows *Hepatozoon* species isolated from the same hosts formed well-supported monophyletic clades (Figure 3.11). Species of *Hepatozoon* isolated from anuran hosts formed a well-supported sister group with separate clades of *Hepatozoon* and *Hemolivia* spp. isolated from reptiles. The African *Hepatozoon* clade (A) formed a polytomy within the monophyletic anuran clade. *Hepatozoon ixoxo,* extracted from *Sclerophrys gutturals* from the current study (highlighted), formed a well-supported monophyletic clade with *H. ixoxo* isolated form *Sclerophrys pusilla* (syn. *Amietophrynus maculatus*)

(Netherlands *et al.*, 2014a). *Hepatozoon theileri* isolated form *Amietia delalandii* from the current study formed a well-supported clade with *H. theileri* (Netherlands *et al.*, 2014a) and a poorly supported polytomy with *H. thori* isolated from *Hyperolius argus* (Netherlands *et al.*, 2018). All *H. theileri* sequences generated from the current study were identical to *H. theileri* representative from Netherlands *et al*. (2014) and therefore only one sequence was included into the phylogenetic tree as a representative for all *H. theileri* sequences from the current study.

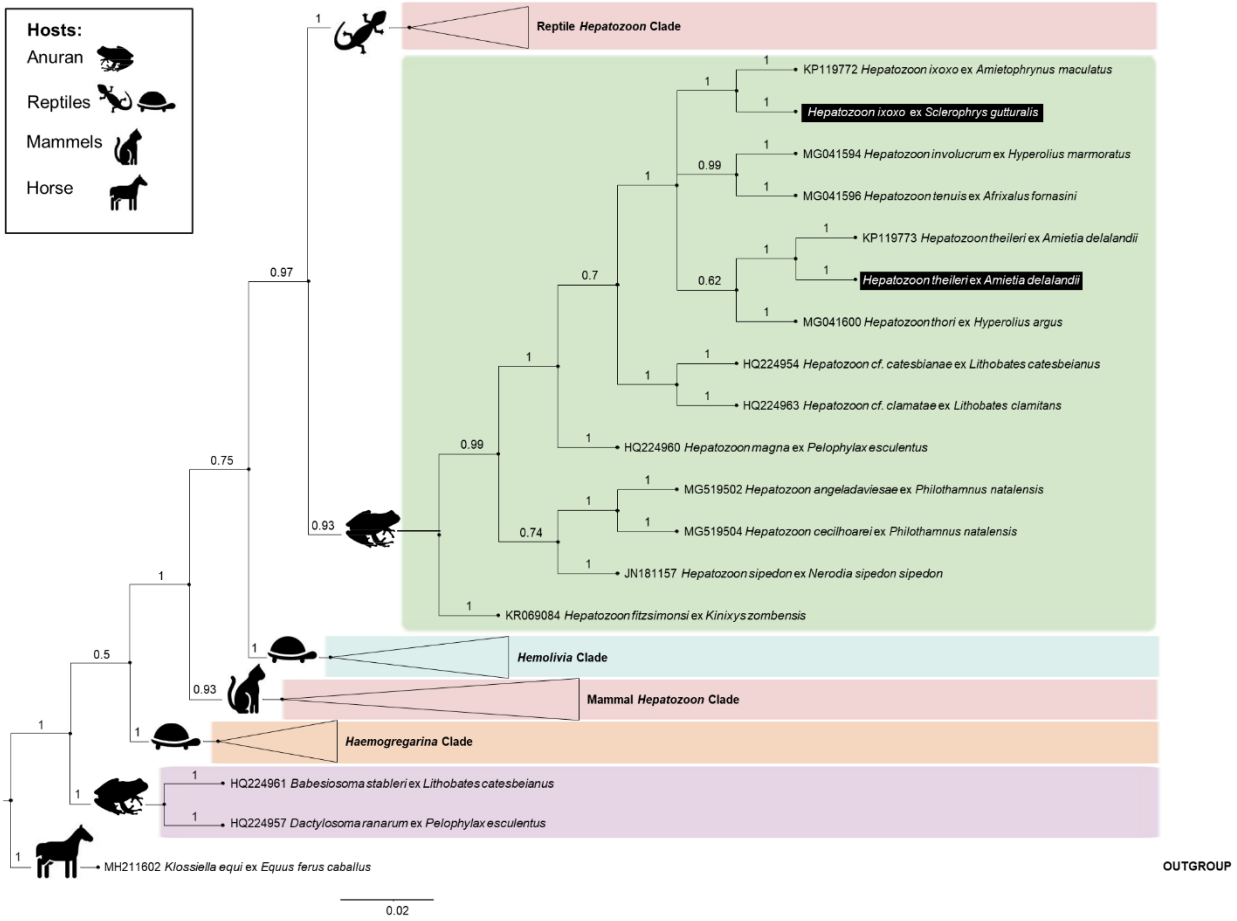

Figure 3.11: Bayesian inference (BI) phylogenetic tree based on 18S rDNA haemogregarine sequences. The phylogenetic analysis shows the positive identification of *Hepatozoon ixoxo* and *Hepatozoon theileri* isolates extracted from *Sclerophrys gutturalis* and *Amietia delalandii*, respectively. *Klossiella equi* was selected as the outgroup. General Time Reversible model (GTR + I + G) was used. The BI node support values (probability) above 0.50 is indicated. The scale bar represents 0.02 nucleotide substitutions per site. The legend indicates the host species group.

Trypanosoma spp.

Twenty-two *Trypanosoma* sequences were successfully amplified and sequenced from the blood of *Amietia delalandii* (n = 16 sequences), *Hyperolius marmoratus* (n = 3), *Ptychadena anchietae* (n = 1) and *Sclerophrys pusilla* (n = 2). Phylogenetic analysis shows a large anuran trypanosome clade generated using the sequences from the present study as well as *Trypanosoma* sequences

that were publicly available on GenBank (Figure 3.12). All anuran *Trypanosoma* isolates formed four large clades with the exception of *Trypanosoma loricatum*, forming a sister clade to the trypanosomes isolated from fish hosts, thereby making the frog trypanosomes paraphyletic. The majority of the *Trypanosoma* sequences form the current study formed separate clades from available data (Frog Clade 2 and 3). Frog Clade 2 consisted mostly of *Trypanosoma* spp. extracted from *Amietia delalandii* and formed a strongly supported sister taxon with *Trypanosoma*

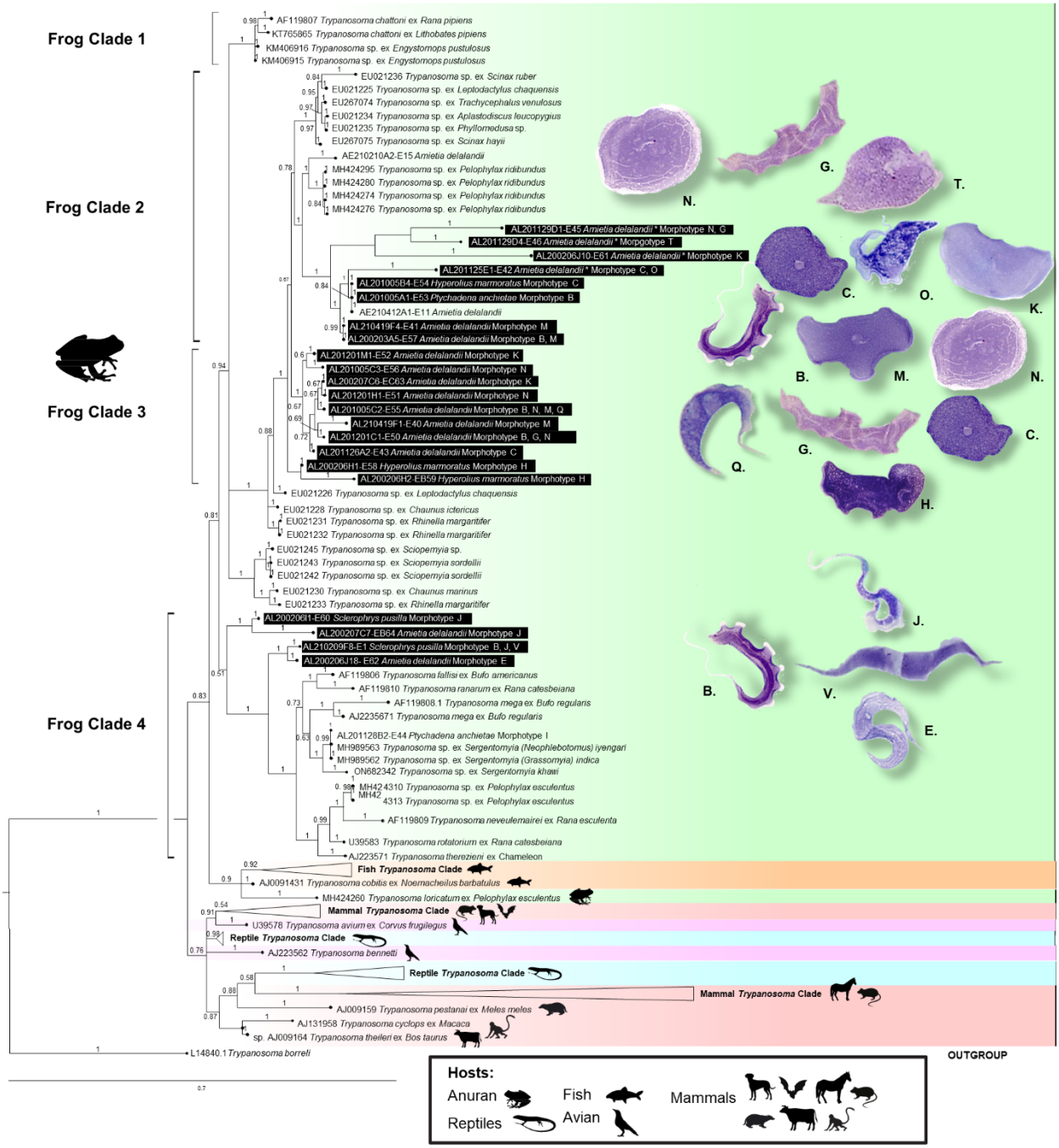

Figure 3.12: Bayesian inference (BI) phylogenetic tree based on 18S rDNA *Trypanosoma* spp. sequences. The phylogenetic analysis strongly supports the clustering of all anuran trypanosomes. *Trypanosoma borreli* was selected as an outgroup. The General Time Reversible model (GTR + I + G) was used with BI node support values above 0.50 indicated on the branch lengths. The scale bar represents 0.7 nucleotide substitutions per site. The legend indicates the host species group.

spp. extracted from *Pelophylax ridibundus* from Ukraine. Frog Clade 3 consisted entirely of *Trypanosoma* spp. form the current study and formed a sister taxon to Frog Clade 2. Among the known anuran trypanosomes, *T. chattoni* (Frog Clade 1) did not clade with any sequences from the current study or other known anuran species of *Trypanosoma*. In contrast, *T. fallisi, T. ranarum and T. mega* are closely associated with each other and four sequences isolated from *S. gutturalis* and *A. delalandii* (Frog clade 4). Only a few sequences generated were from anuran hosts that presented single infections. Single infection sequences, amplified successfully, included *Trypanosoma* morphotype B, C, E, H, J, K, M, N, and T.

***Lankesterella*-like sp.**

Amplicons for the 18S rRNA and the COI gene of approximately 578 nt and 713 nt respectively, were generated for a single *Lankesterella*-like species infecting *A. delalandii*. The 18S phylogenetic analysis of this species is elaborated on in the current chapter, however, more in-depth analysis is handled in Chapter 4.

The phylogenetic analyses of the 18S rRNA shows that the genus *Lankesterella* is paraphyletic with isolates separated from each other by a cluster of species from the Eimeriidae (Figure 3.13). *Lankesterella* species isolated from anurans formed a monophyletic clade with *Lankesterella* sp. extracted from birds and a reptile host (Clade B). Clade B formed a well-supported sister taxon to *Lankesterella* spp. isolated from reptiles (Clade C). The *Lankesterella*-like sp. sequence generated in the current study formed a well-supported clade with an unidentified *Eimeria*-like sp. from Brazil (Clade D).

***Neofoleyellides* spp.**

Amplicons of about 660 nt for *Neofoleyellides steyni* from the blood of *A. delalandii* was generated and compared to known microfilariae species infecting anuran hosts. All isolates obtained for *N. steynii* were identical to the representative sequence included in the analysis (Figure 3.14). For the BI analysis, isolates of filariae infecting anurans belonging to the Waltonellinae, formed paraphyletic clades of *Ochoterenella* spp. isolated from anurans from Venezuela and *Neofoleyellides* spp. isolated from African anurans, with the exception of one *Ochoterenella* sp. from French Guyana. *Neofoleyellides steyni* generated in the current study formed a well-supported polytomy with the *N. steynii* type specimen as well as *N. martini* (Kuzmin *et al.*, 2021). *Neofoleyellides* spp. formed a well-supported sister taxon to Icosiellinae isolated from anuran hosts.

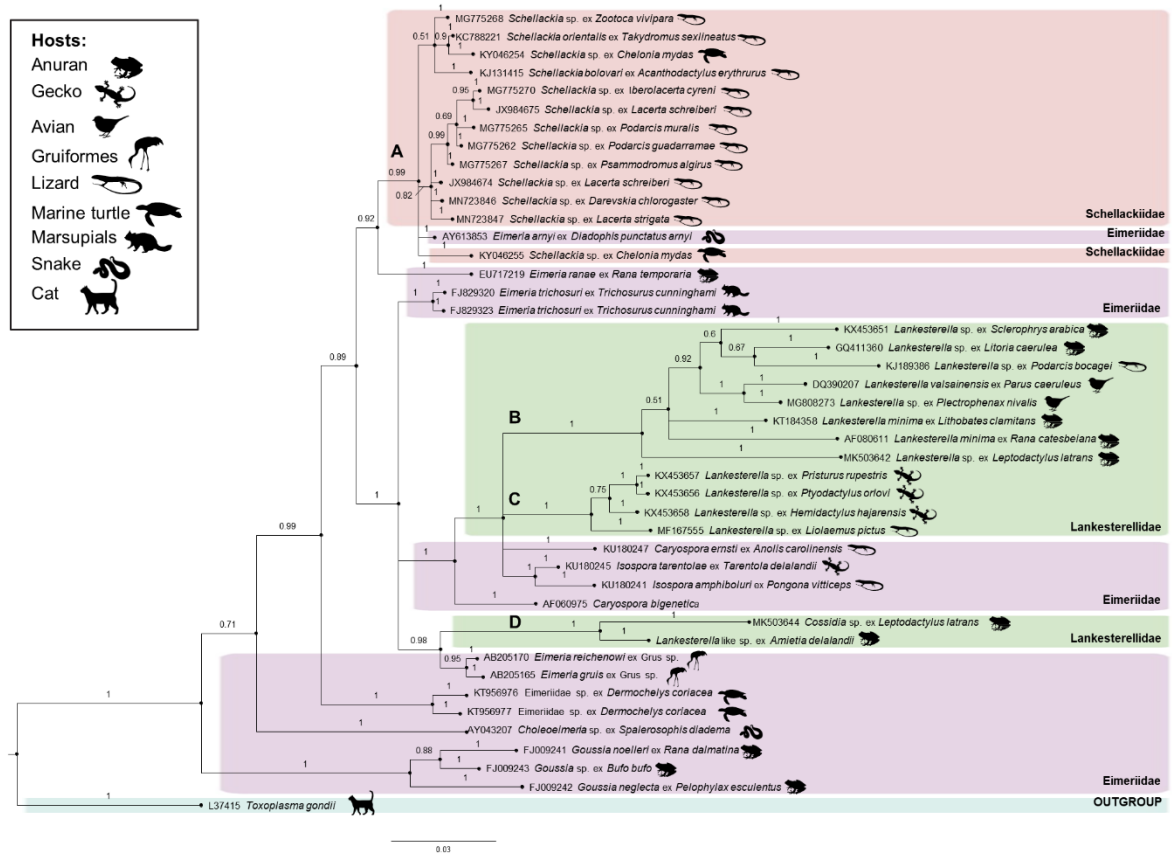

Figure 3.13: The BI phylogenetic tree based on 18S rDNA haemococcidian species sequences. The phylogenetic analysis shows a paraphyly in the *Lankesterella* genus. *Toxoplasma gondii* was selected as an outgroup. The General Time Reversible model (GTR + I + G) was used to generate the tree with the BI node support values above 0.50 displayed as the branch lengths. The scale bar represents 0.3 nucleotide substitutions per site. The legend indicates the host species group.

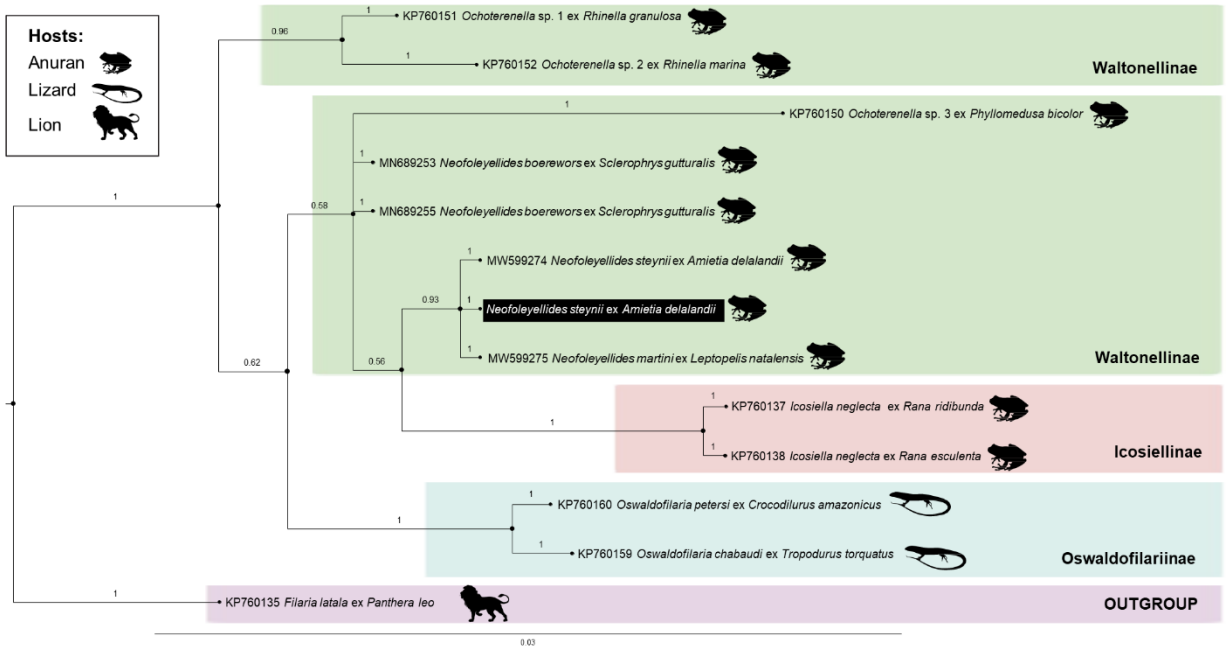

Figure 3.14: Bayesian Inference of 18S rRNA sequences of microfilariae, shows the relationship of *Neofoleyellides steyni* compared with anuran and reptile onchocercids. *Filaria latala* is chosen to root the tree. The Kimura 1980 model (K80 + I) was used to with the BI node support values above 0.50 displayed. The scale bar represents 0.03 nucleotide substitutions per site. The legend indicates the host species group.

3.4 Discussion

In the current study, attempts were not only made to estimate the blood parasite diversity within the study area, but, also to identify these parasite species by means of both morphological and molecular analysis. The present study revealed high parasite species richness and high infection prevalence in anuran hosts from within the study area. Only 10% (38/138) of anurans were infected with at least one of the five parasite groups observed, with some (14/38) harbouring more than one parasite group. Compared to other studies on blood parasite diversity in African anurans, the prevalence perceived in the current study was relatively low (Readel and Goldberg, 2010; Netherlands *et al.*, 2015). Netherlands *et al.* (2015) and Readel and Goldberg (2010) documented a 20% and 17% prevalence, respectively with both studies documented within National Parks or Protected Areas. The low prevalence in the current study may be explained by the lack of protected areas in and around the Soutpansberg mountain range (Endangered Wildlife Trust, 2018), possibly indicating the negative effects that anthropogenic influences have on the natural species composition. Only two nature reserves were included as sampling localities, namely the Goro reserve (site 34) and Lajuma research centre (site 48 – 50), with both sites showing mixed infections with up to 5 *Trypanosoma* morphotypes as well as *Hepatozoon* infections, in one host.

Trypanosoma spp. showed the highest prevalence, infecting 82% (31/38) of the overall infected anurans and the highest parasite species diversity with 22 possible *Trypanosoma* species observed. These finding are similar to other parasite diversity surveys done in Canada (Barta and Desser, 1984) but is in contrast to parasite diversity surveys done in Africa, demonstrating that species of *Hepatozoon* had a higher prevalence than *Trypanosoma* spp. (Readel and Goldberg, 2010). This may indicate that the Soutpansberg has a hidden parasite diversity and future studies should focus on uncovering the true parasite diversity and the prevalence within anuran hosts.

Little significant molecular data was generated in the current study due to the high prevalence of mixed trypanosome infections in the anuran hosts; 25% (8/31) of frogs were infected by more than one *Trypanosoma* spp. with the highest of up to five morphotypes in a single anuran host. Co-infections are not uncommon and have been reported from various aquatic vertebrates (Ferreira *et al.*, 2007; Gu *et al.*, 2007; Lemos *et al.*, 2008; Grybchuk-Ieremenko *et al.*, 2014; Dvořáková *et al.*, 2015; Fermino *et al.*, 2015; Spodareva *et al.*, 2018). Martin *et al*. (2002) speculates that these co-infections of *Trypanosoma* spp. may possibly be transmitted simultaneously from the same vector. Co-infections may also have misled many researchers prior to this knowledge and resulted in various species being classified as a single species with high pleomorphism (Tanabe, 1931; Martin *et al.*, 2002; Žičkus, 2002; Spodareva *et al.*, 2018).

The intraspecific variability of the morphology of anuran trypanosomes is a concern. The wide range of morphotypes lead to different isolates being assigned to single species. *Trypanosoma rotatorium* from Europe differs morphologically and phylogenetically from the two known *T. rotatorium* from Canada, supporting the Canadian trypanosome isolates as a separate species (Martin *et al.*, 2002; Bernal and Pinto, 2016; Spodareva *et al.*, 2018). Bernal and Pinto (2016) show that *T. tungarae* is morphologically similar to *T. rotatorium* and *T. ranarum,* but, is phylogenetically a sister taxon to *T. chattoni* with distinct morphological characters. This shows the importance of combining morphology and phylogenetics to get a better understanding of anuran trypanosomes (Desser, 2001; Martin *et al.*, 2002).

To determine the true diversity of *Trypanosoma* spp. in the study area, future work should include the elucidation of the life cycles within the anuran host and haematophagous dipteran vectors to be able to correctly identify and classify these species. Additionally, to review and to refine the phylogenetic methods that are used to be able to identify species accurately within mixed infections.

Of the two *Hepatozoon* species found, *Hepatozoon theileri* had a 20% prevalence infecting only *Amietia delalandii* and *Hepatozoon ixoxo* with a 2.63% and 9.09% prevalence in *Ptychadena anchietae* and *Sclerophrys gutturalis*, respectively. Even though *Hepatozoon* was the second most abundant parasite observed, the prevalence is similar to previous studies on African anuran parasite diversity (Ball, 1967; Readel and Goldberg, 2010; Netherlands *et al.*, 2015; Netherlands, 2019).

Microfilariae infections from the current study shows a low diversity, with only one species, *Neofoleyellides steyni*, observed and a low prevalence of 5.33% infecting four anuran hosts from one species, *Amietia delalandii*. These low results are seen to be similar to those of Netherlands *et al.* (2015) and Readel and Goldberg (2010).

Infections of other haemogregarine parasites not reported by Netherlands *et al*. (2015), but, reported in this study, included haemococcidian species. Haemococcidian species have, however, been reported by Netherlands (2019) with high prevalence in various frog species. In the current study only one infection of haemococcidians were reported with a 1.33% prevalence in *Amietia delalandii.*

Infections that were not recorded within the current study included *Dactylosoma* species, but have been reported by Netherlands *et al.* (2018) and Netherlands *et al.* (2020). The lack of species of *Dactylosoma* infections could be contributed to the absence of potential vectors throughout the study area. Netherlands *et al.* (2020) showed that *Dactylosoma kermiti* is potentially transmitted by sand flies (*Sergentomyia* sp.) and mosquitoes spp. (*Uranotaenia mashonaensis* and *U. montana*), however, no observations were made of these vectors feeding on anurans in the current study.

In addition, the data reported two *Hepatozoon* species infecting 17 anuran hosts from 3 species, *Amietia delalandii*, *Ptychadena anchietae* and *Sclerophrys gutturalis*. Of all frogs infected, 32/38 frogs (84%) were positive with at least one of 22 possible trypanosomes. However, the diversity of *Trypanosoma* spp. observed is not clear, as this group is known to be highly polymorphic and more molecular work is required to determine the true diversity with accuracy. Trypanosomes were observed in four anuran species, including *A. delalandii*, *P. anchietae*, *Hyp. marmoratus* and *S. pusilla*. Microfilariae species were only positive in four *A. delalandii* and the least abundant parasite species observed was the *Lankesterella*-like species, infecting a single *A. delalandii*. According to similar studies on African anuran parasite diversity (Netherlands, 2019; Netherlands *et al.*, 2020a; Netherlands *et al.*, 2020b), there are still more haemoparasites to be found within the anuran communities.

CHAPTER 4:

MORPHOLOGICAL AND MOLECULAR DATA OF AN UNKNOWN HAEMOCOCCIDIAN PARASITIZING THE COMMON RIVER FROG, *AMIETIA DELALANDII*, FROM THE NORTHERN PARTS OF SOUTH AFRICA

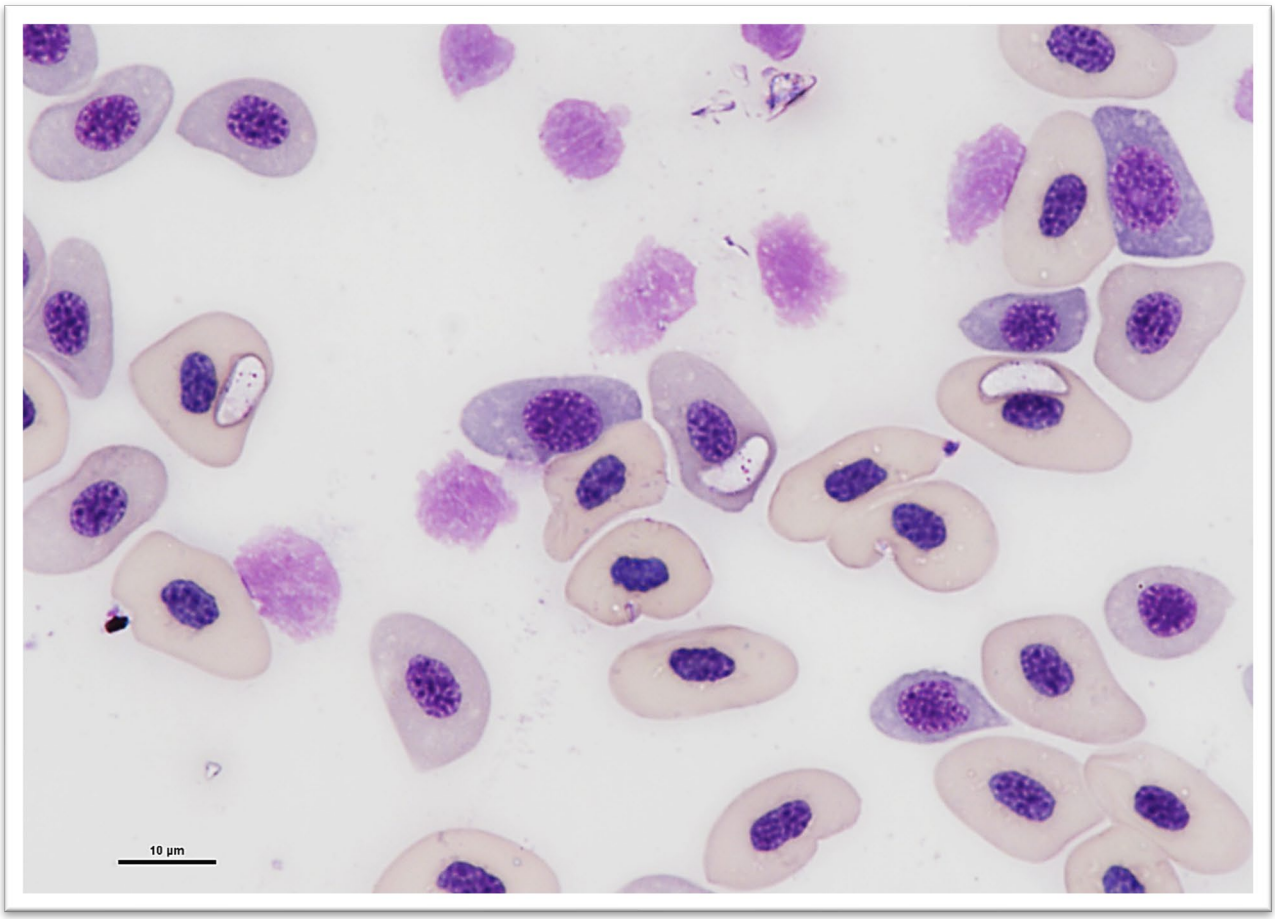

***Lankesterella*-like species**

4.1 Introduction

Amphibians host a variety of protozoan blood parasites and are exposed to several haematophagous vectors in their aquatic and terrestrial habitats (Du Preez and Carruthers, 2009, 2017; Netherlands, 2014; O'Donoghue, 2017). Protozoan blood parasites from the phyla Euglenozoa or Apicomplexa comprise five groups namely, trypanosomatids and haemogregarines, haemococcidia, haemosporidia and piroplasms, respectively (Barta, 2000; Davies and Johnston, 2000; Netherlands, 2019). However, due to the lack of research at a molecular level, the phylogenetic relationships between most protozoan species are still unresolved (Megía-Palma *et al*., 2013). Recent molecular studies on these apicomplexans (Megía-Palma *et al*., 2013, 2017; Cook *et al*., 2015, 2016; Netherlands *et al*., 2018) have provided useful insight into evolutionary relationships between species and genera.

Haemococcidia (Apicomplexa: Eimeriorina) are heteroxenous parasites comprising three genera namely, *Lankesterella* Labbé, 1899, *Schellackia* Reichenow, 1919 and *Lainsonia* Landau, 1973 (Telford, 2009; Megía-Palma *et al*., 2017). The parasite's entire replication process occurs within the vertebrate host's gut. Infectious sporozoites make their way into the vertebrate's bloodstream, ultimately penetrating the blood cells. Transmission occurs through a mechanical or paratenic, haematophagous invertebrate host (in which the parasite lies dormant and no development takes place). The invertebrate ingests the infected blood cells from the vertebrate host - mainly lizards or frogs. Transmission is accomplished when sporozoites are released into the bloodstream of a new host during feeding or via ingestion of infected vectors (Bonorris and Ball, 1955; Levine, 1980; Desser, 1993; Upton, 2000; Telford, 2009; Megía-Palma *et al*, 2013, 2017, 2018; Netherlands, 2019).

Species of *Lankesterella* are known to infect frog, bird and lizard hosts (Megía-Palma *et al*., 2013, 2016, 2017; Mansour and Mohammed, 1962; Paperna and Ogara, 1996; Merino *et al*., 2006). Nine species of *Lankesterella* are recognised from anurans, with four species recorded from Africa - *Lankesterella* cf. *minima*, *L. bufonis* Mansour and Mohammed 1962, *L. dicroglossi* Paperna and Ogara 1996 and *L. ptychadeni* Paperna and Ogara 1996 (see Schwetz, 1930, Mansour and Mohammed, 1962; Paperna and Ogara, 1996) (also see Table 4.1).

Twelve species of *Schellackia* have been described from the blood of reptiles and frogs globally, including Africa, America, Asia, and Europe (Paperna and Lainson, 1995; Bonorris and Ball, 1955; Upton, 2000; Telford, 2009; Megía-Palma *et al*., 2013, 2014, 2017; Zechmeisterova *et al.*, 2019). Of the twelve described and named species of *Schellackia*, only a single species has been recorded from anuran hosts, namely, *Schellackia balli* Le Bail & Landau, 1974 which infects the cane toad (*Rhinella marina*) from French Guyana. Additionally, there is a report of an unnamed *Schellackia* sp. which infected a pepper treefrog (*Trachycephalus typhonius*) from

Brazil (Le Bail and Landau, 1974; Paperna and Lainson, 1995). To date, there are no reported *Schellackia* species from African anuran hosts.

The genus *Lainsonia* is found parasitising host erythrocytes of South American lizards (Telford, 2009). However, according to some authors, *Lainsonia* (*Lainsonia iguana* Landau, 1973 and *Lainsonia legeri* Landau *et al*., 1974) is considered a synonym for *Schellackia* (*Schellackia iguana* Landau, 1973 and *Schellackia weinbergi* Levine, 1980), due to similar life cycle characteristics and similar morphological characteristics of the oocyst (Levine, 1980; Upton, 2000; Telford, 2009; Megía-Palma *et al*., 2017). In the present study, *Lainsonia* is considered to be a junior synonym of a species of *Schellackia.*

Studies on the ultrastructure of various species of *Schellackia* and *Lankesterella* infecting reptile and amphibian hosts (Sinden, and Moore, 1974; Tse *et al*., 1986; Paperna and Ostroska, 1989; Bristovetzky and Paperna, 1990; Desser *et al*., 1990; Paperna, 1992; Paperna, and Ogara, 1996; Telford, 2009; Megía-Palma *et al.,* 2014) have found differences between the two species. Diagnostic characteristics that may vary include, host and host species type and the presence of and a differing total number of refractile bodies (Megía-Palma *et al.* 2017). However, these differences alone have been deemed unreliable due to inconsistencies (Telford, 2009; Megía-Palma *et al.,* 2017; Ogedengbe *et al*., 2018). As stated by Megía-Palma *et al.* (2017) the main morphological difference between *Lankesterella* and *Schellackia* is the total number of sporozoites within the intestinal oocyst during the endogenous development of the parasite (Telford, 2009). Within the lamina propria of the intestine of the vertebrate host, *Schellackia* has eight naked sporozoites present in the oocyst, whereas *Lankesterella* contains 32 or more sporozoites. The number of sporozoites in the final host is considered a diagnostic characteristic for both genera (Telford, 2009; Megía-Palma *et al*., 2014; 2017; 2018). Thus, proper identification of haemococcidia requires a combined approach of molecular analysis, sporozoite morphology, life cycle patterns, host associations and geographic distribution (Zechmeisterová *et al*., 2019).

Molecular characterisation of haemococcidians has provided further insight into the evolutionary relationships of these parasites, helping to distinguish between species within distantly related genera such as *Lankesterella* and *Schellackia* (Megía-Palma *et al*., 2013, 2017, 2018; Cook *et al*., 2015, 2016; Netherlands *et al*., 2018) as well as showing their close relationship to other coccidia (Merino *et al*., 2006; Biedrzycka *et al*., 2013; Megía-Palma *et al*., 2013, 2014, 2017; Martinez *et al*., 2018; Ogedengbe *et al*., 2018).

Table 4.1: A summary of currently recognized anuran haemococcidian species.

Species	Family	Type locality	Type host
Lankesterella alencari Costa and Pereira, 1971	Lankesterellidae	Rio de Janeiro, Brazil	*Leptodactylus latrans*
Lankesterella bufonis Mansour and Mohammed 1962	Lankesterellidae	Giza Province, Egypt	*Sclerophrys regularis*
Lankesterella canadensis Fantham, Porter and Richardson 1942	Lankesterellidae	Quebec and Ontario, Canada	*Rana catesbeiana*
Lankesterella dicroglossi Paperna and Ogara 1996	Lankesterellidae	Lake Baringo, Kenya	*Dicroglossus occipitalis*
Lankesterella hylae Cleland and Johnston 1910	Lankesterellidae	Sydney, Australia	*Litoria caerulea*
Lankesterella minima (Chaussat 1850) Hintze 1902	Lankesterellidae	Paris, France	*Pelophylax kl. esculentus*
Lankesterella petiti Lainson and Paperna, 1995	Lankesterellidae	Pará, North Brazil	*Rhinella marina*
Lankesterella poeppigii Paperna, Bastien, Chavatte and Landau, 2009	Lankesterellidae	Peru	*Rhinella poeppigii*
Lankesterella ptychadeni Paperna and Ogara 1996	Lankesterellidae	Lake Victoria, Kenya	*Ptychadena nilotica*
Schellackia balli Le Bail & Landau, 1974	Schellackiidae	French Guyana	*Bufo marinus*
Schellackia sp. Paperna and Lainson, 1995	Schellackiidae	North Brazil	*Phrynohyas venulosa*

The taxonomic placement of coccidia parasitizing amphibians is still uncertain. However, the use of phylogenetic approaches (such as Ogedengbe *et al*., 2015; 2016; 2018) and through building large genetic datasets with nuclear 18S rDNA and mitochondrial cytochrome c oxidase subunit I (COI) sequence data, may help resolve uncertainties among apicomplexan taxa.

Currently, no information on the molecular diversity and the phylogenetic relationships of haemococcidia that infect anurans from the northern part of South Africa is available. This study aimed to use morphological and molecular characterisation to identify and estimate the phylogenetic placement of an anuran haemococcidia found parasitising *Amietia delalandii* from the Soutpansberg mountain range.

4.2 Materials and Methods

4.2.1 Study area and sample collection

A total of 75 *Amietia delalandii* were collected at night through active sampling from several localities (n=20) throughout the Soutpansberg Mountain Range, Limpopo, South Africa (Figure 4.1). Specimens were placed individually in labelled containers with sufficient water and damp vegetation and transported back to a field laboratory. Blood samples were taken from the specimens via femoral venipuncture at the field laboratory and the frogs were released the next day, at the site of capture. This study has received the relevant ethical approval from the North-

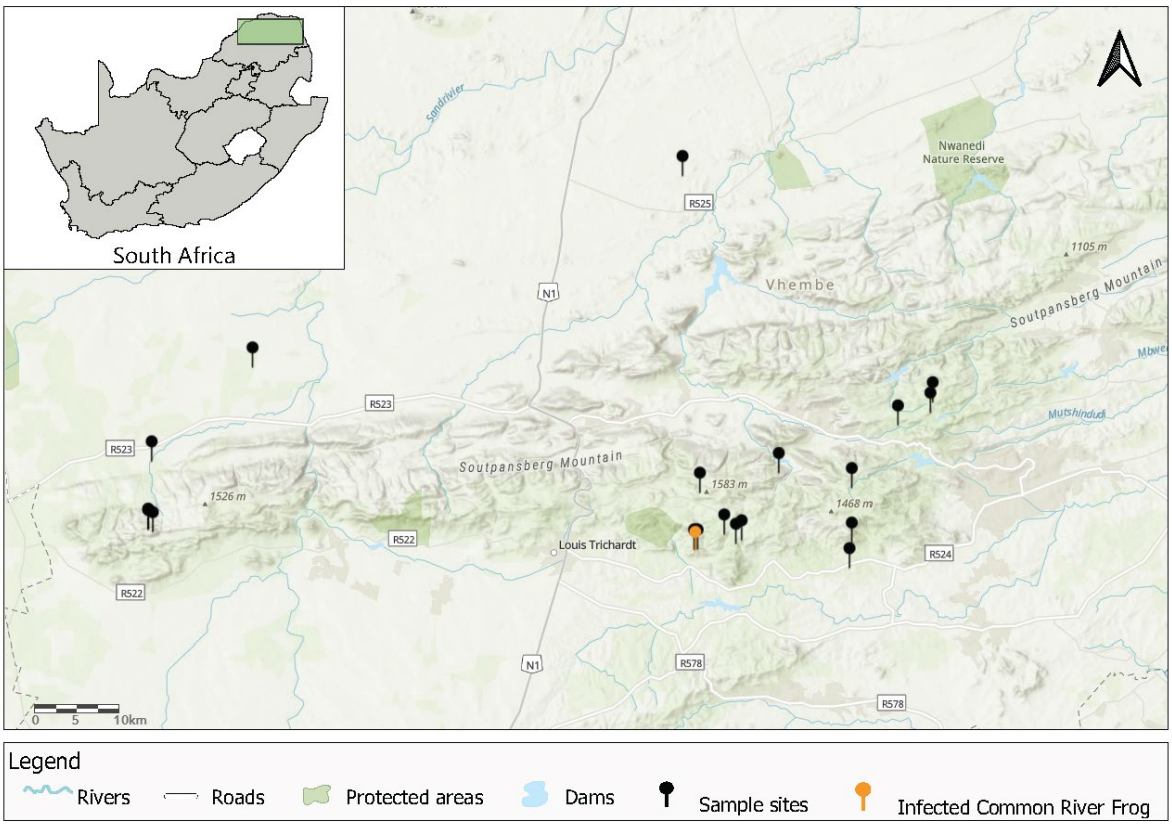

Figure 4.1: Map of various sample localities across the Soutpansberg Mountain range, Limpopo, South Africa. Black pins indicate all sampling localities of Common River Frogs, *Amietia delalandii* and the orange pin indicates the locality of the infected *Amietia delalandii*.

West University's AnimCare ethics committee with ethics numbers: NWU-00429-21-A5 and NWU-00372-16-A5.

4.2.2 Sample processing and light microscopy screening

Thin blood smears were prepared, fixed with absolute methanol, air dried, and stained using a modified Giemsa stain (FLUKA, Sigma-Aldrich, Steinheim, Germany) for approximately 15 – 20 minutes. The slides were screened for haemococcidian parasites using a compound microscope. The remaining blood was stored in cryovials filled with 100% molecular grade EtOH for molecular work. Micrographs and measurements for morphological characterisation and comparison were taken of peripheral blood-stage sporozoites using the Zeiss microscope. Measurements were taken in micrometres (um), across the longest and widest points following the curvature of the parasite. Measurements consisted of the length and width of the parasite and the length and width of the parasitophorous vacuole (PV), if present.

4.2.3 DNA extraction and PCR amplification

Total genomic DNA was extracted from whole blood, preserved in 100% molecular grade alcohol, from samples positive (confirmed with light microscopy) for haemococcidian blood parasites. The standard protocol detailed in the NucleoSpin® Tissue Genomic DNA Tissue Kit (Macherey-Nagel) for nucleated blood samples, was followed. Extracted DNA was used for polymerase chain reaction (PCR), amplification and sequencing. The PCR targeting a fragment of the nuclear 18S rRNA and mitochondrial COI gene was completed and amplified using the primer sets HC-F (5′-TCT CTG GAG GGG CTG TGT TT-3′) and ER (5′-CTT GCG CCT ACT AGG CAT TC-3′), and COI 400F (5′- GGD TCA GGT RTT GGT TGG AC-3′) and COI 500R (5′-CAT RTG RTG DGC CCA WAC-3′), respectively. These primer sets were chosen due to their amplification success rate across a wide range of apicomplexan taxa. For the HC-F and ER primer sets, PCR conditions were as follows: initial denaturation at 95 °C for 3 min, followed by 35 cycles of 95 °C for 30 sec, with an annealing temperature of 62 °C for 30 sec and an extension of 72 °C for 2 min and lastly a final extension step of 72 °C for 10 min. PCR conditions for the COI 400F and COI 500R primer set were: initial denaturation at 96 °C for 5 min, followed by 35 cycles of 94 °C for 30 sec, with an annealing temperature of 55 °C for 30 sec and an extension step of 72 °C for 1 min and a final extension of 72 °C for 10 min. A total volume of 25uL was used to perform the PCR reactions, using 1.25uL of each of the primer sets, 12.5uL DreamTag Master Mix, 5uL of nuclease-free water and lastly 5uL of the extracted DNA. Amplification was done by an Applied Biosystems SimpliAmp Thermal Cycler. The PCR product was visualized under ultraviolet light in a 1% agarose gel stained with SafeStain using an E-BOX CX5 imaging system. The PCR product

was sent to Inqaba Biotechnical Industries (Pty) Ltd, Pretoria, South Africa for purification and sequencing. A combination of MEGA X and Geneious Prime software was used for assembling sequence fragments and compared against previously published sequences using the Basic Local Alignment Search Tool (BLAST).

4.2.4 Phylogenetic analysis

In the present study, three datasets were analysed: (1) a partial nu 18S rDNA sequence alignment; (2) a partial mt COI sequence alignment and (3) a concatenated sequence alignment with both nu 18S r DNA and mt COI sequences (see Appendix D). Publicly available 18S rDNA and COI sequence data were obtained from GenBank and aligned with sequence data generated from this study following previous studies (Ogedengbe, *et al*., 2017).

The resultant 18S rDNA sequences generated from the blood of an infected *Amietia delalandii* specimen were aligned and compared to a diverse range of apicomplexan parasites, containing families such as Schellackiidae, Eimeriidae and Lankesterellidae. The tree was rooted with *Toxoplasma gondii* (L37415) following previous studies on Eimeriidae (Ogedengbe *et al*., 2011; Megía-Palma *et al*., 2017). Sequences were aligned using the ClustalW alignment tool within MEGA X. The GBlocks tool on the NGPhylogeny.fr server (https://ngphylogeny.fr/) was used to remove any alignment gaps, selecting the parameters to allow for smaller final blocks with gap positions resulting in an alignment containing 578 nt from 44 sequences. The most suitable nucleotide substitution model was determined using RAxML. The results for the model test indicate that the Tamura-Nei model with invariable sites and gamma distribution of G4 (TrN + I + G4) had the best score according to the Bayesian information criteria (BIC). However, following Lecocq *et al.* (2013) the TIM1, TIM2, TIM3, TPM1uf, TPM2uf, TPM3uf and TrN models were replaced by the General Time Reversible model (GTR) model (Tavaré, 1986). Results showed the best model for the 18S rDNA sequence alignment to be the GTR model, with estimates of invariable sites and gamma distribution (GTR + I + G). Bayesian inference (BI) analysis was performed in MrBayes (Huelsenbeck and Ronquist, 2001) using the GTR + I + G as the selected model, with the Markov chain Monte Carlo (MCMC) algorithm set to run for 1 million generations with the first 25% of the trees discarded as 'burn-in'. Results were visualized and edited using FigTree v1.4.4.

The COI gene sequences generated in the present study, as well as publicly available COI sequences from GenBank, were aligned using the ClustalW and edited as stated above. The final alignment contained 713 nt from 44 sequences with *Toxoxplasma gondii* (HM771689) as the outgroup, following Ogedengbe *et al.* (2015). BI analysis was performed in MrBayes with the GTR + I + G as the selected model according the RAxML. However, due to a large number of resultant polytomies, a reversible-jump MCMC algorithm (nst = mixed) was used instead of the GTR model.

As stated above the MCMC algorithm was run in MrBayes and results were visualized in FigTree v1.4.4.

A concatenated sequence alignment was constructed using the 18S rDNA and the COI sequences within Geneious following Ogedengbe *et al*. (2018). The concatenation of sequences was created with separately aligned 18S rDNA and COI sequences without modifying the alignments after concatenation. The 18S rDNA sequences contained 1387 nt and the COI mt sequences contained 473 nt. The GBlocks server was used to trim the final alignment containing 1861 nt from 58 sequences. *Toxoplasma gondii* was used to root the tree (Ogedengbe *et al*., 2018). The BI analysis was performed in MrBayes using the GTR model for the 18S rDNA sequences [lset applyto = (1) nst = 6 rates = invgamma] and for the COI sequences [lset applyto = (2) nst = mixed rates = invgamma]. The characters for the 18S rDNA sequences were set at 1 to 1387 basepairs within the concatenated alignment (charset 18S = 1 – 1387) and the characters for the COI was set at 1388 to 1861 basepairs (charset COI = 1388 – 1861). The MCMC algorithm was set to run for 1 million generations with the first 25% of the trees discarded as 'burn-in', as stated above.

4.3 Results

From a total of 75 *Amietia delalandii* individuals collected and screened for blood parasites, of which only a single individual was infected with a haemococcidian. The haemococcidia observed was identified as an undescribed species of *Lankesterella* (*Lankesterella* sp.)

Species classifications

Phylum: Apicomplexa Levine, 1970
Class: Conoidasida Levine, 1988
Subclass: Coccidiasina Leuckart, 1879
Order: Eucoccidiorida Léger, 1911
Suborder: Eimeriorina Léger & Duboscq, 1911
Family: Lankesterellidae Grassé 1953,
Genus: *Lankesterella* Labbé, 1899

Differential diagnosis

The type species: *Lankesterella minima* (Chaussat, 1850) Hintze, 1902
Hosts: Amphibians, reptiles and avians

Description

Immature sporozoites (Figure 4.2B – D): slender crescent-shaped parasites, rounded or semicircle shape on one end and tapering off on the opposite end; cytoplasm staining blueish-purple with dark purplish-pink chromatin granules; the parasite extends the length and curves towards the blood cell nucleus; some refractile bodies are visible (Figure 4.2C); some individuals showed a slight PV (Figure 4.2D); no cytopathological effect visible. Immature stages measured at 9,66 ± 1,14 (2,50 – 11,11) long by 2,41 ± 1,07 (1,68 – 9,59) wide (n = 51).

Mature sporozoites (Figure 4.2E – L): similar crescent-shape as the immature sporozoites but larger; cytoplasm staining a light purplish-pink with occasional dark purple stained spots and/or a dark purple stained border; a single refractile body visible staining white (Figure 4.2H – L); slightly enlarged PV for some individuals (Figure 4.2E – F) extending away from the parasite within, in some cases the cytoplasm or the PV did not stain, causing a white vacuole-like appearance (Figure 4.2G); no visible cytopathological effects on the host cell but some individuals caused the displacement of the cell nucleus as well as changed the host cell shape (Figure 4.2G). The mean average measurements of mature sporozoites with a PV, measured at 9,56 ± 1,50 (7,65 –11,33) long by 3,62 ± 1,34 (3,02 – 4,55) wide (n = 61). Mature stages without the PV measured at 9,07 ± 0,88 (7,74 – 10,44) long (n = 10) by 3,04 ± 0,45 (2,17 – 3,7) wide (n = 14). No nuclei were visible within immature or mature sporozoites.

Remarks

Life cycle: Morphological characteristics for the genus *Lankesterella* have been described from the sporozoites in the blood of the final host. According to studies (Mansour and Mohammed 1962; Megía-Palma *et al.,* 2014), the general shape of *Lankesterella* sporozoites varies from elongated to somewhat oval, single or multiple refractile bodies visible in the granulated cytoplasm, the nucleus shape is band-like and situated on the walls of the sporozoite but varies in placement and lastly, some individuals are encased in a parasitophorous vacuole (PV). Sporozoites enter the bloodstream and penetrate the erythrocytes of vertebrate hosts. *Lankesterella* is considered a heteroxenous protozoan endoparasite due to the manner of transmission which includes haematophagous vectors such as mites, ticks, mosquitoes and/or leeches. Haematophagous vectors ingest the infected blood from the vertebrate host and go on to infect other hosts, completing the life cycle (Levine, 1980; Desser *et al*., 1990; Davies and Johnston, 2000; Upton, 2000).

Lankesterella sp. is characterized by its shape, ranging from crescent shape to elongated ellipsoid, with a slightly enlarged PV; unbalanced semicircle on one end and tapering off on the opposite end (with extended PV); has a white vacuole-like appearance and dark purple stained boards when colourant did not stain the PV; one to two refractile bodies visible, staining white. Based on the size, *Lankesterella* sp. (7,74 – 10,44 µm long and 2,17 – 3,7 µm wide) can be

distinguished from all nine species of *Lankesterella* infecting frogs, but is most similar to *L. hylae* (7 – 11 µm in length and 1 – 3 µm in width) from Australia. Based on morphometrics, the mature sporozoites of *L. hylae* are generally more slender in comparison to *Lankesterella* sp.*,* with a distinct nucleus, centrally placed, whereas no definitive nucleus was observed in *Lankesterella* sp. When looking at size and morphology, it is safe to say that *Lankesterella* sp. does not fit with the other frog lankesterellids.

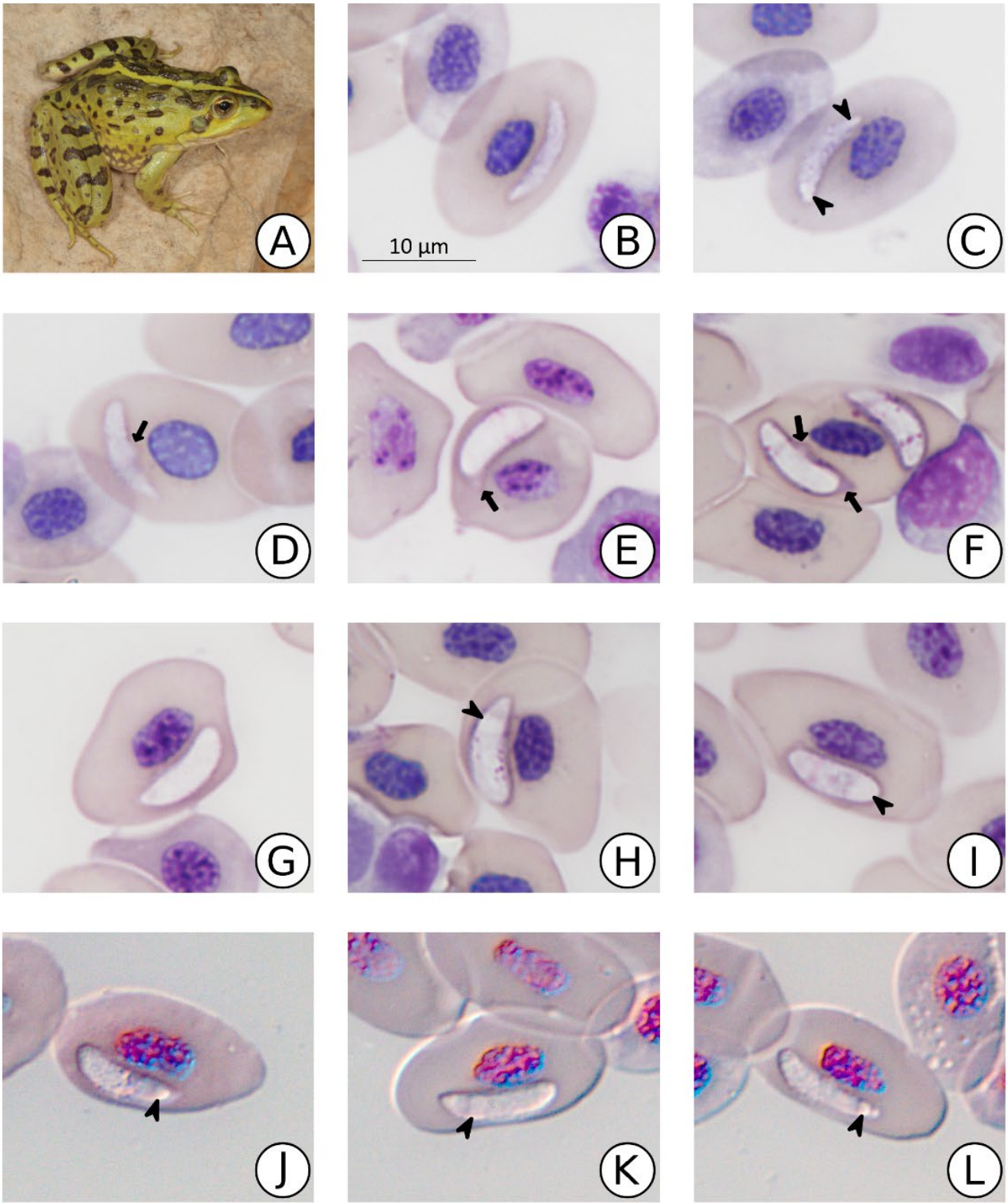

Figure 4.2: *Lankesterella* sp. observed in the peripheral blood of (A) *Amietia delalandii* from Limpopo, South Africa. (B – D) Immature sporozoites. (E – L) Mature sporozoites with (E – F, H – I) purplish-pink stained spots at random and dark purple stained borders. (D – F) Arrow showing slightly enlarged PV. (F) Double infection of a single erythrocyte. (G) Cytoplasm or PV not stained, causing a white vacuole-like appearance. (G) Deformation of host cell shape. (C, H – L) Arrowhead showing visible refractile bodies in immature and mature sporozoites. Scale bar: 10 µm.

Lankesterella sp. from the current study can be distinguished from frog *Schellackia* species, *Schellackia balli* (see Le Bail and Landau, 1974) and *Schellackia* sp. (see Paperna and Lainson, 1995), based on the enlarged PV forming around the crescent shape parasite and the presence of refractile bodies in the mature sporozoites within the peripheral blood of the host. Although *Lankesterella* sp. and *Schellackia balli,* are morphologically similar in size (9.07 x 3.04 and 9.18 x 3.06, respectively) they are distinguishable from each other based on the presence of a PV and refractile bodies.

Anuran *Lankesterella* species can also be distinguished by the ±32 sporozoites within the oocyst found in the cells of the host's reticuloendothelial system (Davies and Johnston, 2000; Megía-Palma *et al*., 2014, 2017), however, this study formed part of a larger project on non-lethal surveying of anurans, thus, no anurans were dissected to screen for additional life cycle stages within the host's organs. Only sporozoites found in the peripheral blood were compared with relevant studies.

4.3.1 Phylogenetic result analysis

Phylogenetic analysis for the 18S rDNA gene shows that different haemococcidian families, Lankesterellidae (shown in green) and Schellackiidae (shown in pink), formed separated clades between clusters of Eimeriidae (shown in purple) (Figure 4.3). The Lankesterellidae is divided into polyphyletic clades (clade B, C and D) clustering with species of the Eimeriidae isolated from reptile hosts. Clade B comprises *Lankesterella* species isolated from avians, anurans and a lizard host *Podarcis bocagei*. Clade C recovered as sister to clade B contains species isolated from geckos and the orange-bellied lizard *Liolaemus pictus*. Clade D comprises the *Lankesterella*-like sequence from the present study and an undescribed coccidian species isolated from a Brazilian frog and forms a well-supported clade sister to species of *Eimeria* isolated from avian hosts. Clade A forms a polytomy comprising the Schellackiidae isolated from reptiles and *Eimeria arnyi* from a snake host. Furthermore, Clade A also forms a sister taxon with *Eimeria ranae* isolated from a frog host. Lastly, within Eimeriidae, genera *Eimeria* and *Caryospora* are shown to be polyphyletic and *Isospora* and *Goussia* monophyletic (Morrison *et al*., 2004; Ogedengbe *et al.,* 2011; Megía-Palma *et al*., 2014; Ogedengbe *et al*., 2015). *Toxoplasma gondii* was used as an outgroup following Ogedengbe *et al*. (2011) and Megía-Palma *et al*. (2017).

For the phylogenetic analysis of the COI gene (Figure 4.4), the two families, Lankesterellidae and Eimeriidae are polyphyletic. The species of *Lankesterella* from the present study is separated from other species of *Lankesterella* isolated from anurans (Clade C) forming a cluster of *Isospora, Eimeria,* and *Caryspora* isolated from lizards, marsupials and snakes, respectively (Clade B). The *Lankesterella* sp. from the present study formed a sister taxon to *Isospora amphibolouri* with 91.67% similarity. Clade A revealed that *Isospora* species isolated

from birds formed a sister taxon to *Eimeria* species isolated from rodents and a chicken and formed a polytomy with a larger *Eimeria* clade isolated from various hosts and *Cyclospora cayetanensis* isolated from humans. This phylogenetic tree has poorly supported branch length probability values and thus a concatenated approach was recommended to attempt to solve this problem.

Sequences from the nu 18S rDNA and mt COI genes were used to construct a concatenated alignment. Results of the BI phylogenetic analysis shows Eimeriidae to be polyphyletic and Lankesterellidae monophyletic (Figure 4.5). Despite the lack of monophyletic clades among the Eimeriidae, species of *Eimeria* parasitizing closely related definitive hosts such as marsupials and ruminants, formed well-supported clades. Species of *Lankesterella* form a polytomy with *Lankesterella minima* isolated from frogs and *Lithobates clamitans* from Canada.

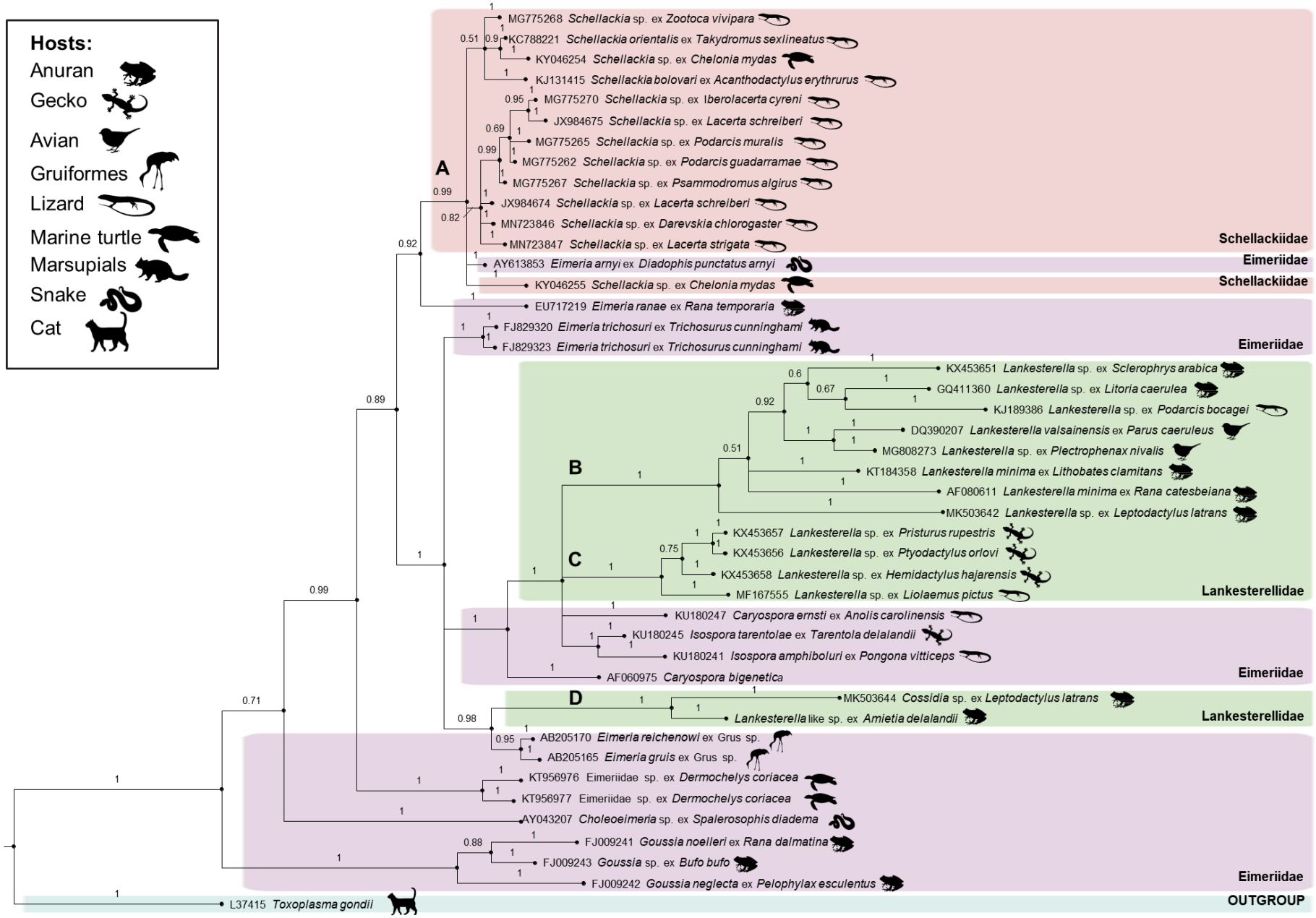

Figure 4.3: Bayesian Inference (BI) phylogenetic tree based on partial nu 18S rDNA sequences. Phylogenetic analysis shows the relationships between various taxa from Eimeriidae, Lankesterellidae and Schellackiidae. The aligned rDNA sequences were analyses using a General Time-Reversible model (GTR + I + G, nst = 6). Bayesian Inference node support (probability) is indicated and all nodes support values above 0.50. The final alignment contained 578 nt from 44 sequences and was rooted with *Toxoplasma gondii*. The sequence obtained from this study is written in bold. The scale bar represents 0.03 nucleotide substitutions per site. The legend indicates the host species group.

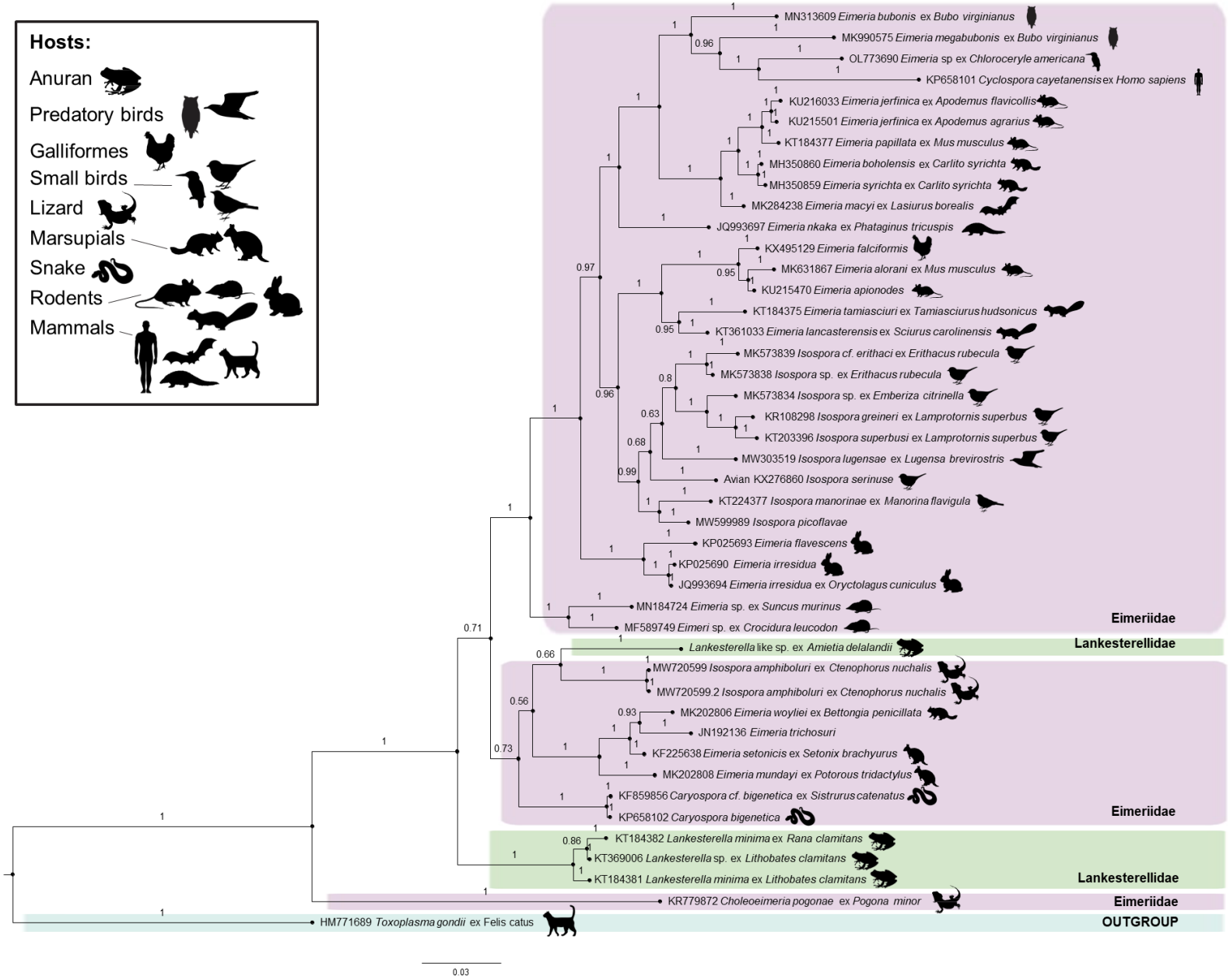

Figure 4.4: Bayesian Inference (BI) phylogenetic tree based on mt cytochrome c oxidase subunit I (COI) sequences. Phylogenetic analysis shows the relationships between Eimeriidae and Lankesterellidae with *Toxoplasma gondii* as the outgroup. Analysis was performed using a reversible-jump MCMC algorithm (GTR + I + G, nst = mixed). Bayesian Inference node support (probability) is indicated and all nodes support values above 0.50. The final alignment contained 713 nt from 44 sequences. The scale bar represents 0.03 nucleotide substitutions per site. The legend indicates the host species group.

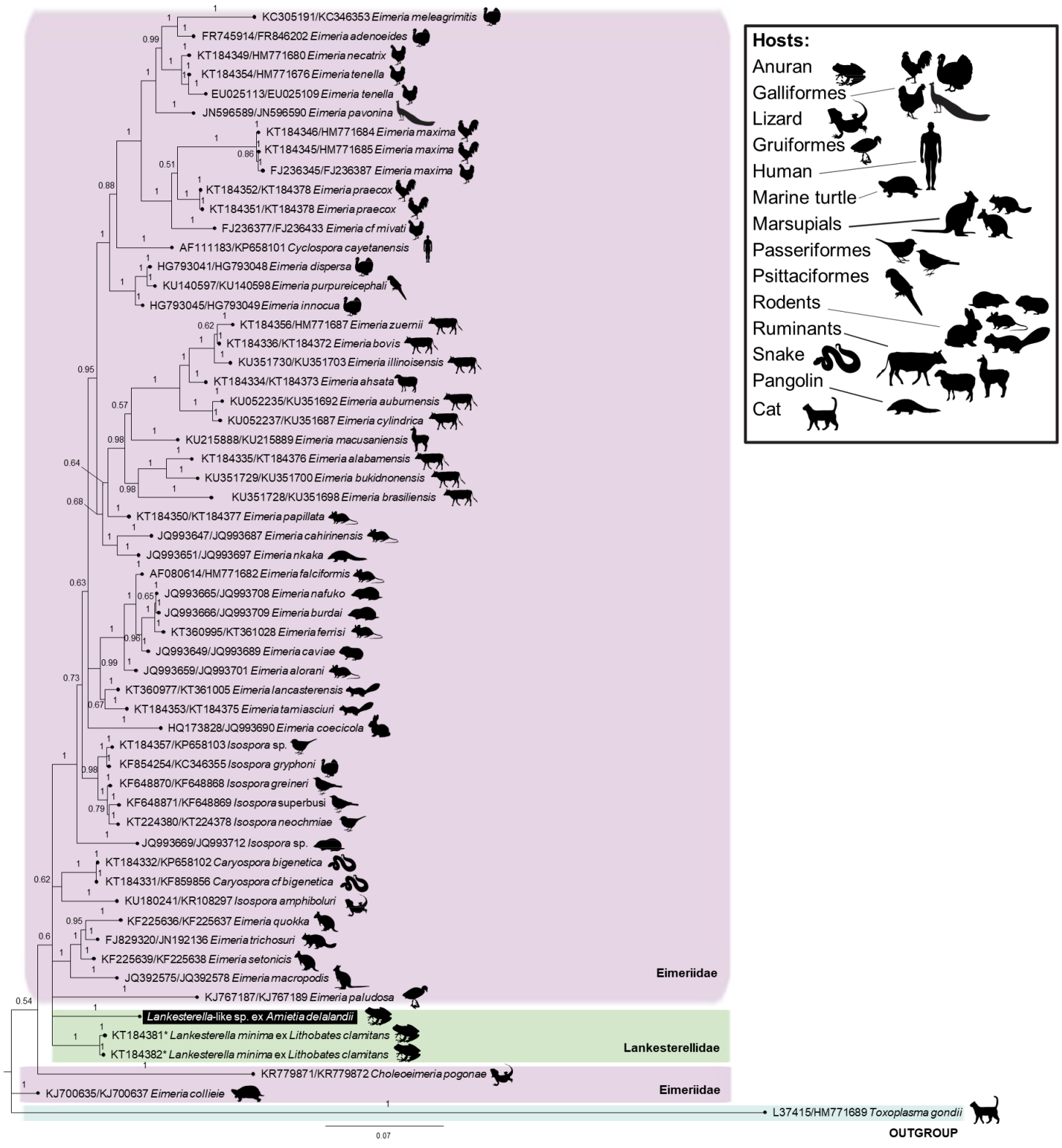

Figure 4.5: Bayesian Inference (BI) phylogenetic based on the concatenated nu 18S rDNA and mt COI sequences. Phylogenetic analysis shows the relationships between Eimeriidae and Lankesterellidae. Different analyses models were used on both alignments. The 18S rDNA sequences were analysed using a codon-based likelihood model (GTR + I + G (nst = 6) and the COI sequences were analysed using a reversible-jump MCMC algorithm GTR + I + G (nst = mixed). Bayesian Inference node support (probability) is indicated and all nodes support values above 0.50. The final alignment contained 1861 nt from 58 sequences and was rooted using *Toxoplasma gondii.* The scale bar represents 0.07 nucleotide substitutions per site. The legend indicates the host species group.

4.4 Discussion

In this study, attempts were made to phylogenetically characterize an undescribed haemococcidian species isolated from the frog host *A. delalandii*. The sequence fragments of the nu 18S rRNA gene and the mt COI gene, revealed that this species does not form a monophyly with other anuran haemococcidians. To provide better resolution a concatenated phylogenetic analysis of both 18S rDNA and COI sequences was used, revealing that the species from this study is, however, still closely related to the genus *Lankesterella*. Additionally, when compared to other currently recognised anuran *Lankesterella* species, it is clear that based on the morphological and molecular data, the species from the present study is most probably an undescribed species of *Lankesterella*.

Phylogenetic analysis of partial 18S rDNA sequences recover a well-supported monophyletic clade of *Schellackia* isolated from reptiles, but, with polyphyletic clades for species of *Eimeria* isolated from reptiles, avians, and marsupials, as well as species of *Lankesterella* isolated from anuran, reptiles and avian hosts. According to several previous studies, these polyphyletic traits of eimeriids are a common occurrence within the family (Ogedengbe *et al*., 2011; Megía-Palma *et al.,* 2014; Ogedengbe *et al*., 2015). Surprisingly, *Eimeria arnyi* and *E. ranae*, from snake and frog hosts respectively, clustered in the same clade as species of *Schellackia* isolated from reptiles. This either indicates that *E. arnyi* and *E. ranae* shared a common ancestor with the genus, or that these samples were misidentified (see Megía-Palma *et al.,* 2014), or as result of contamination with infected host blood.

Within the polyphyletic Eimeriidae clades, a monophyly was recovered between species isolated from the same hosts, such as *Isospora* isolated from reptiles, *Eimeria* isolated from gruiformes, marsupials and sea turtles and *Goussia* isolated from anurans.

The phylogenetic analysis shows that *Lankesterella* sp. and an undescribed coccidian species isolated from a Brazilian frog, *Leptodactylus latrans,* are monophyletic (de Abreu Reis Ferreira, 2020) and formed a well-supported clade with *Eimeria* species isolated from avian species. This suggests that certain species of *Lankesterella* from anuran hosts are closely related to certain species of *Eimeria*.

Phylogenetic analysis of mt COI sequences also supported the polyphyly of the eimeriid genera *Eimeria* and *Isospora*, as well as the polyphyly of *Lankesterella* isolated from anurans. The *Lankesterella* sp. from this study is separated from the anuran lankesterellid clade by a cluster of eimeriid genera *Isospora amphiboluri* isolated from bearded dragons, *Eimeria* isolated from marsupials and *Caryospora bigenetica* isolated from snakes. *Lankesterella* sp. forms a sister clade with *Isospora amphiboluri.*

The phylogenetic analysis of the concatenated 18S rDNA and COI sequences support the polyphyly of the Eimeriidae revealing that lankesterellids isolated from anurans formed a monophyletic clade. The *Lankesterella* sp. from the present study, form a monophyly with other species of *Lankesterella* isolated from Canadian frogs. Despite the lack of available data for haemococcidia in general, phylogenetic analyses suggest that the concatenated phylogeny is better resolved and more robust, for determining the phylogenetic relationships between species of eimeriids (Ogedengbe *et al*., 2018).

Although similarities between different eimeriid taxa seem to be persistently high, the small differences continue to be supported by the molecular phylogeny. In this study, phenotypic differences have been established in the peripheral blood stages of *Lankesterella* sp. and those of other *Lankesterella* and *Schellackia* specimens. Even though, only the blood stages were observed, these findings support the separation of *Lankesterella* sp. from known anuran haemococcidian species that contain intraerythrocytic sporozoites enveloped by an expanded PV. Future work is needed and should prioritize the clarification of the life cycles as well as mode of transmission. Additionally, it is important to increase the number of mitochondrial COI gene sequences of haemococcidia from anurans to get a clear understanding of the phylogenetic relationship between anuran haemococcidians and other coccidian taxa.

CHAPTER 5:

INTERNAL TRANSCRIBED SPACER 1 (ITS-1) NUCLEOTIDE SEQUENCE VARIATION OF TWO *HEPATOZOON THEILERI* POPULATIONS IN SOUTH AFRICA

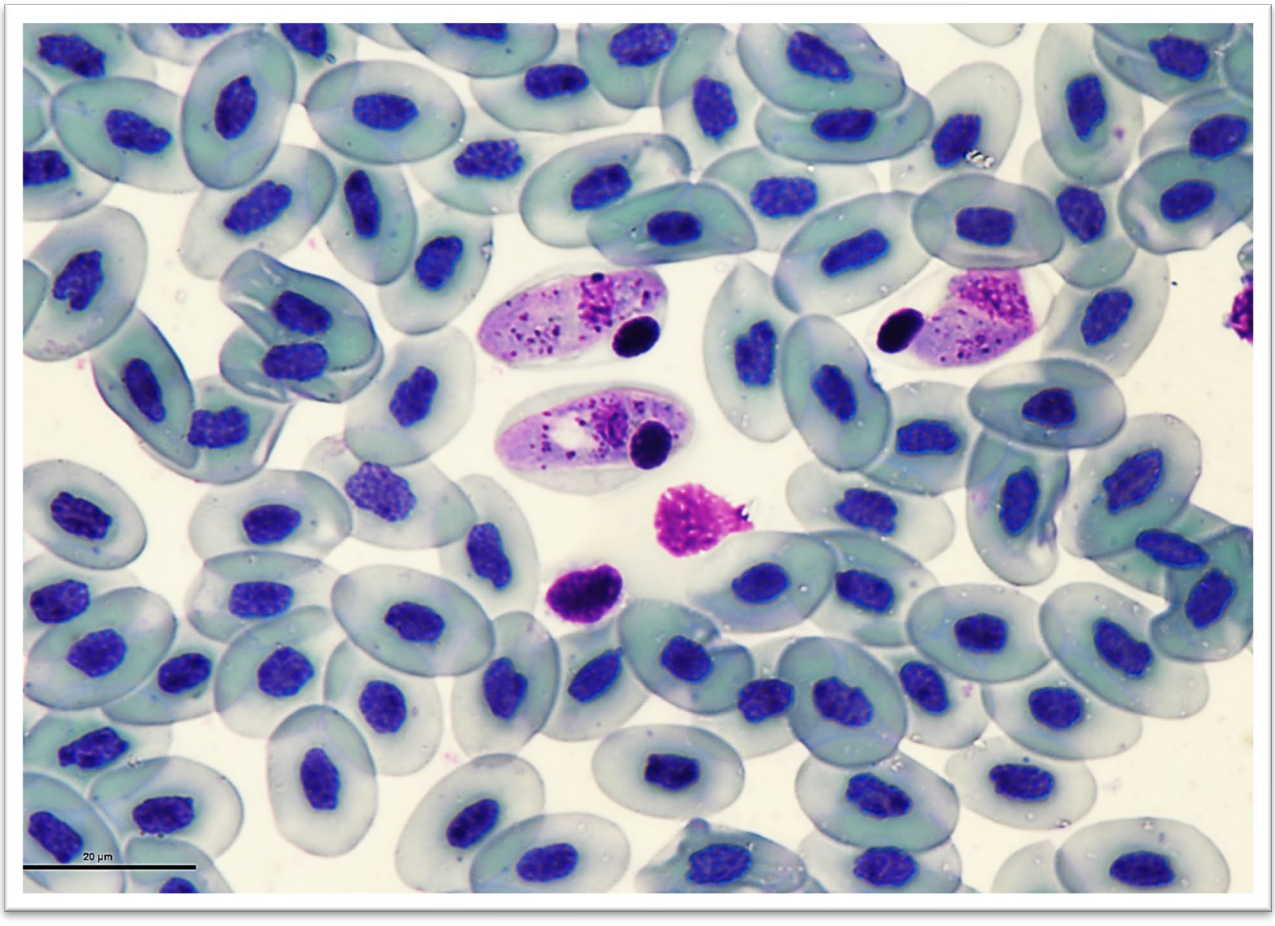

Hepatozoon theileri

5.1 Introduction

Haemogregarines (Apicomplexa: Adeleorina) are a diverse group of blood parasites, reported from almost all vertebrate classes, divided into four families and eight genera (Jakes *et al.*, 2003; Barta *et al.*, 2012). All haemogregarine species share a similar lifecycle, of which all are heteroxenous and involve an intermediate vertebrate host and a haematophagous definitive invertebrate host (Smith, 1996; Kim *et al.*, 1998; Boulianne *et al.*, 2007). Anuran haemogregarines are among the most commonly reported apicomplexan parasite to parasitise frogs (Netherlands *et al.*, 2014b; Netherlands *et al.*, 2018). Four of the eight genera have been recorded from anuran hosts and include species of *Dactylosoma* Labbé,1894*, Babesiosoma* Jakowska and Nigrelli, 1956, *Hemolivia* Petit, Landau, Baccam and Lainson, 1990, and *Hepatozoon* Miller, 1908 (Davies and Johnston, 2000). In 1996, Smith revised the genus *Hepatozoon* leading to 42 frog *Hepatozoon* species being transferred from *Haemogregarina* to *Hepatozoon* based on developmental stages. This expanded the genus to include all species of *Haemogregarina* that infect amphibians, reptiles (lizards, snakes, and crocodiles), birds and mammals (Siddall, 1995; Smith, 1996). Currently there are 48 known species of *Hepatozoon* infecting anurans globally, with at least 18 species reported in Africa (Table 5.1) (Smith, 1996; Netherlands *et al.*, 2014a; Netherlands *et al.*, 2014b; Úngari *et al.*, 2021). Of these 18 species, five species, *Hepatozoon involucrum* Netherlands, Cook et Smit 2018*, Hepatozoon tenuis* Netherlands, Cook et Smit 2018*, Hepatozoon thori* Netherlands, Cook et Smit 2018, *Hepatozoon ixoxo* Netherlands, Cook et Smit, 2014, and *Hepatozoon theileri* (Laveran, 1905) Smith, 1996 are reported from South African frogs. The majority of African anuran *Hepatozoon* infections occur within the Bufonidae family (12/18), followed by Hyperoliidae (4/18), Ptychadenidae (1/18) and Pyxicephalidae (1/18).

The genus *Hepatozoon* are intraerythrocytic apicomplexan parasites with transmission occurring via the ingestion of infected invertebrate definitive hosts such as mosquitoes, sandflies, ticks and mites (Smith, 1996; Kim *et al.*, 1998; Davies and Johnston, 2000; Netherlands *et al.*, 2014b). Sporogony occurs within the gut of these dipteran and arthropod definitive hosts and infects the vertebrate host on ingestion. After ingestion, merogonic development occurs within endothelial cells of various organs, especially the liver, of their vertebrate host. Eventually, these merozoites enter the bloodstream and develop into gamonts within erythrocytes, or rarely, within leukocytes (Desser *et al.*, 1995; Smith, 1996; Kim *et al.*, 1998; Van As *et al.*, 2013; Netherlands *et al.*, 2014b).

Table 5.1: *Hepatozoon* species recorded from African amphibians.

Parasite species	No.	Host family	Type host	Locality	References
***Hepatozoon aegyptia* (Mohammed et Mansour, 1963) Smith, 1996**	1	Bufonidae	*Sclerophrys regularis* (syn., *Amietophrynus regularis, Bufo regularis*)	Cairo, Egypt; Khartoum, Sudan	Mohammed and Mansour (1963); Younis and Saoud (1969)
***Hepatozoon assiuticus* (Abdel-Rahman, El-Naffer, Sakla et Khalifa, 1978) Smith, 1996**	2	Bufonidae	*Sclerophrys regularis*	Assuit, Egypt	Abdel-Rahman *et al* (1978)
***Hepatozoon boueti* (França, 1910) Smith, 1996**	3	Bufonidae	*Sclerophrys regularis*	Guinea-Bissau; Cairo and Giza, Egypt	Franca (1910); Mohammed and Mansour (1966)
***Hepatozoon epuluensis* (Van den Berghe, 1942) Smith, 1996**	4	Ptychadenidae	*Ptychadena oxyrhynchus* (syn., *Rana oxyrhynchus*)	D.R.C.	Levine and Nye (1977); Smith (1996)
***Hepatozoon faiyumensis* (Mansour et Mohammed, 1966) Smith, 1996**	5	Bufonidae	*Sclerophrys regularis*	Faiyum, Egypt	Mansour and Mohammed (1966)
***Hepatozoon francai* (Abdel-Rahman, El-Naffer, Sakla et Khalifa, 1978) Smith, 1996**	6	Bufonidae	*Sclerophrys regularis*	Assuit, Egypt	Abdel-Rahman *et al* (1978)
***Hepatozoon froilanoi* (França, 1925) Smith, 1996**	7	Bufonidae	*Sclerophrys regularis*	Luanda, Angola	França (1925)
***Hepatozoon hyperolii* Hoare, 1932**	8	Hyperoliidae	*Hyperolius* spp.	Uganda	Hoare (1932); Levine and Nye (1977)
***Hepatozoon involucrum* Netherlands, Cook et Smith 2017**	9	Hyperoliidae	*Hyperolius marmoratus*	South Africa	Netherlands *et al* (2018)
***Hepatozoon ixoxo* Netherlands, Cook et Smit, 2014**	10	Bufonidae	*Sclerophrys pusilla* (syn., *Amietophrynus maculatus*)	Ndumo and Jozini, South Africa	Netherlands *et al* (2014)
***Hepatozoon lavieri* (Tuzet et Grjebine, 1957) Smith, 1996**	11	Bufonidae	*Sclerophrys regularis*	Pointe-Noire, Congo	Tuzet and Grjebine (1957)
***Hepatozoon magni* (Hassan, 1992) Smith, 1996**	12	Bufonidae	*Sclerophrys regularis*	Qena, Egypt	Hassan (1992)
***Hepatozoon moloensis* (Hoare, 1920) Smith, 1996**	13	Bufonidae	*Sclerophrys* sp.	Molo, Kenya	Hoare (1920)
***Hepatozoon pestanae* (França, 1910) Smith, 1996**	14	Bufonidae	*Sclerophrys regularis*	Guinea-Bissau; Giza, Egypt	França (1910); Mohammed and Mansour (1966)
***Hepatozoon tenius* Netherlands, Cook and Smit 2018**	15	Hyperoliidae	*Afrixalus fornasini*	St. Lucia on Monzi Farm, KwaZulu-Natal, South Africa	Netherlands et al (2018)
***Hepatozoon theileri* (Laveran, 1905) Smith, 1996**	16	Pyxicephalidae	*Amietia delalandii* (syns., *A. quecketti, Rana angolensis*)	South Africa and Tanzania	Averinzew (1949); Ball (1967); Laveran (1905); Netherlands *et al* (2014)
***Hepatozoon thori* Netherlands, Cook et Smit, 2018**	17	Hyperoliidae	*Hyperolius marmoratus*	KwaNyamazane Conservancy (KNC), KwaZulu-Natal, South Africa	Netherlands *et al* (2018)
***Hepatozoon tunisiensis* (Nicolle, 1904) Smith, 1996**	18	Bufonidae	*Sclerophrys mauritanicus* (syns., *Amietophrynus regularis, Bufo regularis*)	Tunis, Tunisia	Nicolle (1904)

Former studies, between the 1900's until about the 1970's, only used the morphology of gamont stages in the peripheral blood to characterize anuran *Hepatozoon* species. Most of these descriptions were based on incomplete or poorly illustrated sketches causing confusion among researchers. Since 2014, Netherlands *et al.,* 2014 was the first study to include molecular analysis as a means of identifying African anuran *Hepatozoon* species. Although morphology is still a vital aspect to include when characterizing haemogregarines, a combination of morphological and molecular analysis should be considered when classifying species of *Hepatozoon*. Only a few studies (Laveran, 1905; Fantham *et al.*, 1942; Netherlands *et al.*, 2014a; Netherlands *et al.*, 2014b; Netherlands *et al.*, 2015; Netherlands *et al.*, 2018) have been conducted on haemogregarines parasitizing South African amphibians with Netherlands *et al*. (2014a, 2014b, 2015, 2018) contributing most of the available molecular data for anuran haemogregarines from Africa.

Phylogenetic studies provide useful insight into the evolutionary relationship of apicomplexan parasites, as well as assisting in distinguishing between closely related species. The 18S rRNA gene is a relatively conserved marker and is widely used for barcoding protozoan parasites. However, to be able to differentiate between closely related species, or populations on a genetic level, a less conserved DNA sequence is required (Cai *et al.*, 1992). The internal transcribed spacer 1 (ITS-1) is located downstream of the 18S rRNA gene and upstream of the 5.8S rRNA gene (Figure 5.1). Although several studies have focused on characterising the ITS region of different apicomplexans (Shippen-Lentz *et al.*, 1987; Cai *et al.*, 1992; Goggin, 1994; Payne and Ellis, 1996), only recently has some research been completed on the ITS-1 region of species of *Hepatozoon* (Kim *et al.*, 1998; Smith *et al.*, 1999; Boulianne *et al.*, 2007; Leveille *et al.*, 2021). Currently, there is no ITS-1 data available for species of *Hepatozoon* from Africa.

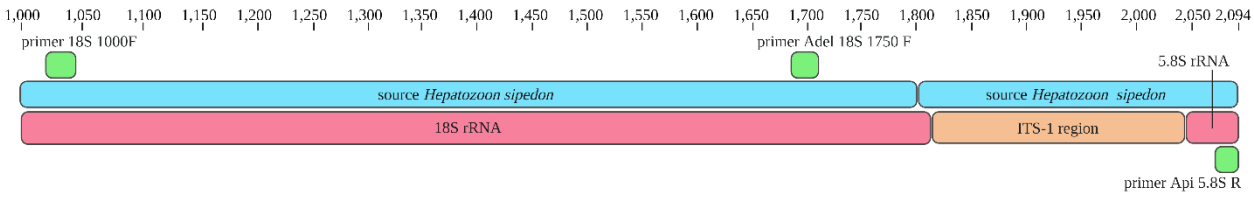

Figure 5.1: Sketch representing the 18S rRNA-ITS1-5.8S rRNA sequence with the used primer position.

The Common River frog, *Amietia delalandii* Duméril & Bibron, 1841*,* has a wide distribution within South Africa, occurring from the northern parts of Limpopo southwards to the Eastern Cape, including all eastern provinces, as well as the upper parts of the Northern Cape, avoiding the more arid climates to the west (Du Preez and Carruthers, 2017). *Amietia delalandii* is not restricted to a specific microhabitat and is reported from various habitats (Viviers, 2013). With its wide distribution, relatively large size and its extended seasonal activity, *A. delalandii* is an ideal host for haemogregarine infections. *Hepatozoon theileri* has been reported to infect *A. delalandii*

from North-West (Netherlands *et al.*, 2014b) and Kwazulu-Natal (Netherlands *et al.*, 2015; Netherlands *et al.*, 2018), but, no data is available for the study area in the Limpopo province. The aim of the study was to molecularly compare the highly variable ITS-1 region of *H. theileri* from different populations within South Africa. Data from Potchefstroom in the North-West province [collected as part of a previous study (Conradie *et al.*, 2017)] and the Soutpansberg Mountain Range, Limpopo (this study), was used to compare *H, theileri* populations from two very different habitats.

5.2 Materials and Methods

5.2.1 Sampling areas and frog collection

Comparisons were done between two ecologically different sampling areas from two South African provinces. The first site of collection is the Botanical Gardens of the North-West University in Potchefstroom, North-West province (-26.68185, 27.09423). Potchefstroom is located in the Grassland Biome along the Mooi River system with surrounding wetlands. Potchefstroom experiences cold dry winters with regular frost and warm summers accompanied by frequent thunderstorms, making the annual rainfall about 767 millimetres. The NWU Botanical Garden is a member of Botanic Gardens Conservation International (BGCI) and covers a surface area of about 30 000m^2. The garden is sectioned into ecological niches and includes a natural veld, a swampy area, a vlei, an indigenous species garden, an invasive species garden and, lastly, a succulent rockery. The garden houses more than 1 500 plant species (most being indigenous), making it suitable for a variety of animals and insects (Viviers, 2013). A total of 162 adult *A. delalandii* were collected in the Botanical Gardens during 2015 as part of a different study (Conradie *et al.*, 2017).

The second collection area expanded across the Soutpansberg Mountain Range in the Vhembe Biosphere, Limpopo. The Soutpansberg Mountain Range is the northernmost mountain range in South Africa with an approximate surface area of 6 800 km^2 (Berger *et al.*, 2003; Petford *et al.*, 2019). Damp air blowing in from the Indian Ocean creates precipitation against the southern slopes with an annual rainfall of up to 2 000 mm. However, this damp air dissipates when reaching the northern slopes, causing semi-desert conditions in the north (leeward side). These extremities allow for a mosaic of climate conditions, creating Afromontane forests, dense thickets, mountain grasslands and semi-deserts (Berger *et al.*, 2003; Evans, 2017). This results in an area with high diversity and endemism. A total of 75 *A. delalandii* were collected from 20 sites (Table 5.2) across the Soutpansberg Mountain Range (Figure 5.2).

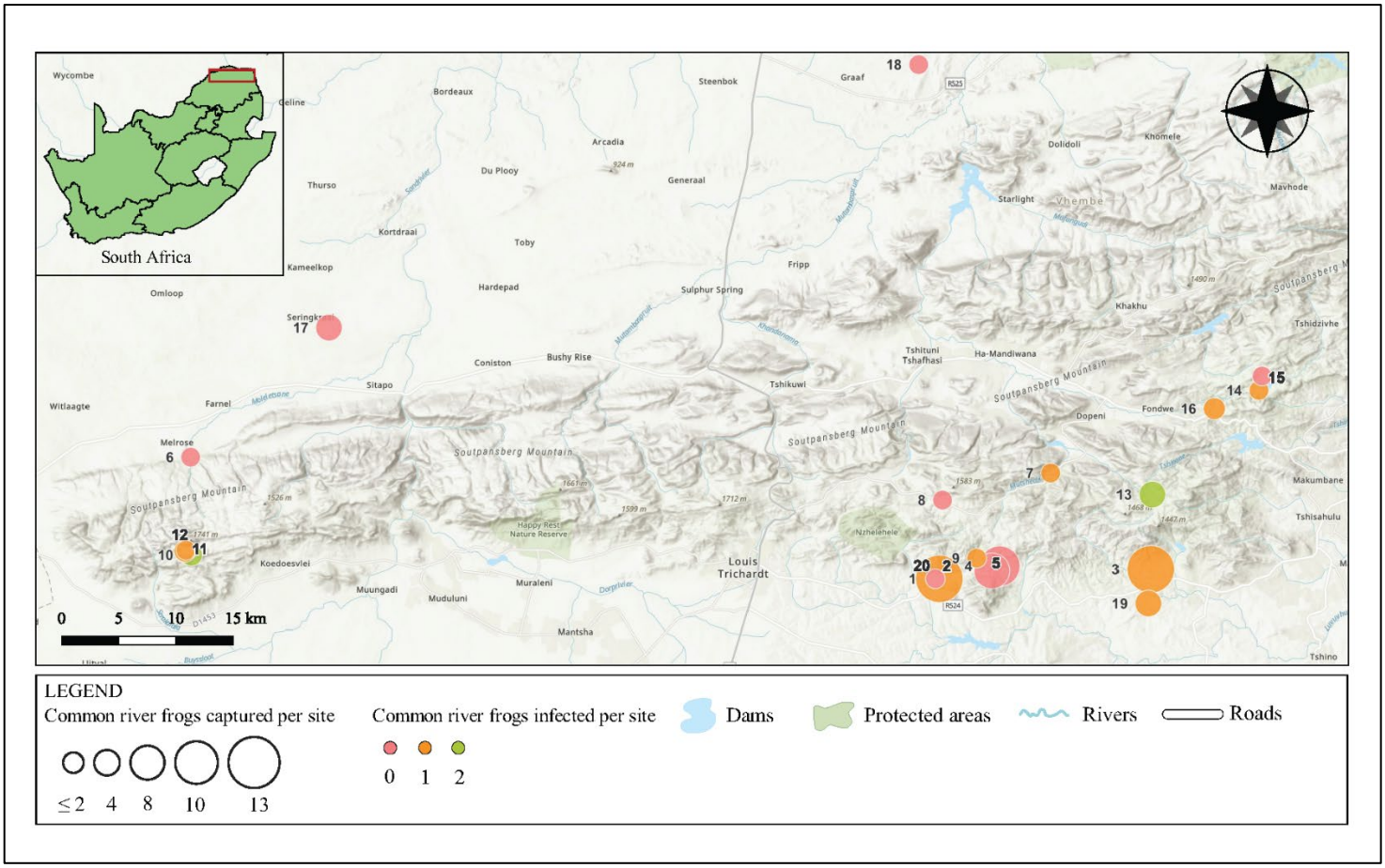

Figure 5.2: Map of sampling localities of Common River frogs, *Amietia delalandii,* across the Soutpansberg Mountain Range, Limpopo, South Africa. The size of the circle demonstrates the number of frogs collected per site and the colour of the circle demonstrates the number of frogs that where infected with *Hepatozoon theileri* per site.

Table 5.2: Sample collection sites where *Amietia delalandii* was collected at the Soutpansberg Mountain range, Limpopo.

Site	Description of site	Longitude	Latitude	Elevation
1	Well & swampy area	30.0708	-23.0550	827
2	Pond and stream	30.0727	-23.0553	830
3	Pond - Malume dam 2	30.2552	-23.0476	720
4	Luande Mountain - School Pond	30.1252	-23.0453	917
5	Luande Mountain - pool	30.1184	-23.0491	1209
6	Goro reserve	29.4280	-22.9587	854
7	Mountain stream N	30.1692	-22.9709	924
8	Vlei area	30.0761	-22.9925	1210
9	Concrete dam small	30.1054	-23.0388	1024
10	Lajuma - wetland	29.4287	-23.0360	1324
11	Lajuma - rock pool	29.4235	-23.0330	1350
12	Lajuma - forest stream	29.4239	-23.0322	1368
13	Ebbedam	30.2564	-22.9884	1300
14	Forestry - Mountain stream	30.3483	-22.9053	1084
15	Forestry - Mountain stream	30.3509	-22.8942	1109
16	Stream	30.3096	-22.9197	1042
17	Stream	29.5477	-22.8559	754
18	Game trough	30.0550	-22.6468	614
19	Levubu - Small stream, muddy	30.2526	-23.0746	678
20	Vlei & spring	30.0695	-23.0551	819

Active sampling was used during the night to capture a total of 237 adult Common River frogs. When captured, frogs were placed into disposable plastic bags with sufficient water and vegetation. Each specimen was given a unique field number and transported back to a field laboratory where they were identified using Du Preez and Carruthers (2017). After processing, specimens were released at site of capture within the following days. This study received the relevant ethical approval from the North-West University's AnimCare ethics committee [Ethics number for Conradie *et al.* (2017): NWU-00006-14-A3; Ethics numbers for current study: NWU-00429-21-A5 and NWU-00372-16-A5].

5.2.2 Blood sample collection, preparation and light microscopy

Blood samples were taken from each frog via femoral venipuncture. Thin blood smears were prepared, air-dried, fixed and stained using Giemsa-stain - following protocol as stated by Netherlands *et al*. (2015). Remaining blood was stored in cryovials topped with 100 molecular grade EtOH to be used for future molecular analysis. Stained blood smears were screened by means of light microscopy using a 100x immersion oil objective on a Nikon compound microscope for the presence of haemogregarine parasites within the peripheral blood. Images were taken of samples showing haemogregarine gamonts using a Zeiss microscope.

5.2.3 DNA extraction, PCR amplification and phylogenetic analysis

EtOH-preserved blood samples showing haemogregarine parasites (n = 17) were used for molecular analysis. Genomic DNA of haemogregarines were extracted from whole blood samples using the nucleated blood samples protocol within the NucleoSpin® Tissue Genomic DNA Tissue Kit (Macherey-Nagel). Following extraction, DNA was used for polymerase chain reaction (PCR), amplification and sequencing. The ITS-1 region lays downstream from the 18S rRNA gene and upstream from the 5.8S rRNA gene. Three different approaches were utilized to isolate the ITS-1 sequence region (Table 5.3). The first approach (1) selected a forward primer which lays upstream from the ITS-1 region, including about 1 000 bp of the adjacent 18S rRNA gene and a reverse primer that includes the end region of the downstream 5.8S rRNA gene. Primer sets Adel_18S_1000_F (5'-AGATACCGTCGTAGTCTTAACT-3') and Api_5.8S_R (5'-CGATGAAGRMCGYAGC-3') was used for this purpose. Conditions for the PCR were as follows: initial denaturation at 98 °C for 30 sec, followed by 35 cycles of denaturation at 98 °C for 10 sec, annealing at 62 °C for 30 sec with an end extension at 72 °C for 2 min and a final extension of 72 °C for 10 min. With the second method (2), a nested PCR reaction was performed with the PCR products of the first approach for samples that both failed and was successful in the first PCR round. Primer set, Adel_18S_1750_F (5'-TATCACTTAGAGGAAGRAG-3') and Api_5.8S_R was

used and resulted in a shorted fragment of the ITS-1 region (Leveille *et al.*, 2021). Lastly, the third PCR amplifications (3) were performed by using only the second primer set, Adel_18S_1750_F and Api_5.8S_R. The PCR conditions for both the second and third method were as follow: initial denaturation at 98 °C for 3 min, followed by 35 cycles of denaturation at 98 °C for 30 sec, annealing at 54 °C for 30 sec with an end extension at 72 °C for 1 min and a final extension of 72 °C for 10 min. PCR reactions were performed with a total volume of 25 µL, entailing 12.5 µL DreamTaq PCR master mix (Thermo Scientific), 1.25 µL of each of the primer sets mentioned above, 1-7 µL DNA (depending on the quality of the sample), with the final reaction volume topped up with nuclease-free water. Reactions were undertaken in a Thermal Cycler PCR machine and resulting products were visualized under ultraviolet light in a 1 agarose gel stained with SafeStain using an E-BOX CX5 imaging system. Resultant PCR products were sent to a commercial sequencing company (Inqaba Biotechnical Industries) for purification and sequencing. Geneious prime was used to assemble sequence fragments, creating an alignment with consensus sequences. The Basic Local Alignment Search Tool (BLAST) was used to compare sequences to previously published data.

For comparison, ITS-1 sequences of anuran *Hepatozoon* species, publicly available from GenBank, was downloaded and aligned with sequences generated from the current study (Table 5.3). Species of *Hepatozoon* from anuran hosts included *H. catesbianae* and *H. clamatae* from Nova Scotia and Ontario, Canada (Smith *et al.*, 1999; Boulianne *et al.*, 2007). *Hepatozoon sipedon* (AF110248) isolated from a snake was used as an outgroup following previous studies (Smith *et al.*, 1999; Boulianne *et al.*, 2007). Sequences were aligned using the MUSCLE alignment tool and edited within Geneious Prime. The alignment consisted of 33 sequences containing 229 nt (with gaps). A model test was performed using RAxML to determine the most suitable nucleotide substitution models. The model with the best Bayesian information criterion (BIC) score was the Felsenstein's 1981 model with a discrete Gama distribution (F81 + G4). Bayesian inference (BI) was performed within MrBayes (Huelsenbeck and Ronquist, 2001) using the Markov Chain Monte Carlo (MCMC) algorithm running for 1 million generations, sampling every 1 000 generations and using the default parameters (lset nst=1; rates=gamma; mcmc ngen=1 000 000; nchains=4; temp=0.2). First 25% of the sampled trees were discarded as relative ‘burn-in’. Results were visualized and edited using FigTree v1.4.4 and Inkscape v1.1.2, respectively.

Lastly, a phylogenetic median-joining haplotype network was estimated to conclude the relationships among haplotypes with Network software v.10. (fluxusengineering.com), applying the default settings.

Table 5.3: List of the ITS-1 sequences from amphibians used in the current study. Sequences generated from the same sample: 1_SPB6 and 3_SPB1; 1_P11, 2_P5 and 3_P1; 1_P14 and 3_P2; 2_SPB4 and 3_SPB3; 2_P6 and 3_P4.

Method #_Sample code	Species	Host	Locality	Primers	Reference
1_SPB1	*Hepatozoon theileri*	*Amietia delalandii*	Soutpansberg Mountain range, South Africa	Adel_18S_1000_; Api_5.8S_R	Current study
1_SPB4	*Hepatozoon theileri*	*Amietia delalandii*	Soutpansberg Mountain range, South Africa	Adel_18S_1000_; Api_5.8S_R	Current study
1_SPB5	*Hepatozoon theileri*	*Amietia delalandii*	Soutpansberg Mountain range, South Africa	Adel_18S_1000_; Api_5.8S_R	Current study
1_SPB6	*Hepatozoon theileri*	*Amietia delalandii*	Soutpansberg Mountain range, South Africa	Adel_18S_1000_; Api_5.8S_R	Current study
2_SPB3	*Hepatozoon theileri*	*Amietia delalandii*	Soutpansberg Mountain range, South Africa	Adel_18S_1750_F; Api_5.8S_R	Current study
3_SPB1	*Hepatozoon theileri*	*Amietia delalandii*	Soutpansberg Mountain range, South Africa	Adel_18S_1750_F; Api_5.8S_R	Current study
3_SPB2	*Hepatozoon theileri*	*Amietia delalandii*	Soutpansberg Mountain range, South Africa	Adel_18S_1750_F; Api_5.8S_R	Current study
3_SPB3	*Hepatozoon theileri*	*Amietia delalandii*	Soutpansberg Mountain range, South Africa	Adel_18S_1750_F; Api_5.8S_R	Current study
1_P1	*Hepatozoon theileri*	*Amietia delalandii*	Potchefstroom, South Africa	Adel_18S_1000_; Api_5.8S_R	Current study
1_P2	*Hepatozoon theileri*	*Amietia delalandii*	Potchefstroom, South Africa	Adel_18S_1000_; Api_5.8S_R	Current study
1_P5	*Hepatozoon theileri*	*Amietia delalandii*	Potchefstroom, South Africa	Adel_18S_1000_; Api_5.8S_R	Current study
1_P6	*Hepatozoon theileri*	*Amietia delalandii*	Potchefstroom, South Africa	Adel_18S_1000_; Api_5.8S_R	Current study
1_P7	*Hepatozoon theileri*	*Amietia delalandii*	Potchefstroom, South Africa	Adel_18S_1000_; Api_5.8S_R	Current study
1_P8	*Hepatozoon theileri*	*Amietia delalandii*	Potchefstroom, South Africa	Adel_18S_1000_; Api_5.8S_R	Current study
1_P9	*Hepatozoon theileri*	*Amietia delalandii*	Potchefstroom, South Africa	Adel_18S_1000_; Api_5.8S_R	Current study
1_P10	*Hepatozoon theileri*	*Amietia delalandii*	Potchefstroom, South Africa	Adel_18S_1000_; Api_5.8S_R	Current study
2_P1	*Hepatozoon theileri*	*Amietia delalandii*	Potchefstroom, South Africa	Adel_18S_1750_F; Api_5.8S_R	Current study
2_P4	*Hepatozoon theileri*	*Amietia delalandii*	Potchefstroom, South Africa	Adel_18S_1750_F; Api_5.8S_R	Current study
3_P1	*Hepatozoon theileri*	*Amietia delalandii*	Potchefstroom, South Africa	Adel_18S_1750_F; Api_5.8S_R	Current study
3_P2	*Hepatozoon theileri*	*Amietia delalandii*	Potchefstroom, South Africa	Adel_18S_1750_F; Api_5.8S_R	Current study
3_P3	*Hepatozoon theileri*	*Amietia delalandii*	Potchefstroom, South Africa	Adel_18S_1750_F; Api_5.8S_R	Current study
3_P4	*Hepatozoon theileri*	*Amietia delalandii*	Potchefstroom, South Africa	Adel_18S_1750_F; Api_5.8S_R	Current study
T3	*Hepatozoon theileri*	*Amietia delalandii*	Potchefstroom, South Africa	Adel_18S_1000_; Api_5.8S_R	Unpublished data
T1	*Hepatozoon ixoxo*	*Sclerophrys gutturals*	Soutpansberg Mountain range, South Africa	Adel_18S_1000_; Api_5.8S_R	Current study
T2	*Hepatozoon tenuis*	*Afrixlus fornasinii*	KwaZulu-Natal, South Africa	Adel_18S_1000_; Api_5.8S_R	Netherlands *et al.,* 2018
AF110241	*Hepatozoon catesbianae*	*Rana clamitans*	Ontario, Canada, North America	"ITS-7; ITS-8"	Smith *et al.,* 1999

5.3 Results

A total of 237 adult *A. delalandii* individuals were captured and screened for haemogregarines from the Botanical Gardens in Potchefstroom (n = 162) and the Soutpansberg Mountain Range (n = 75). Twenty-seven frogs (11%) were infected with haemogregarines, confirmed with light microscopy and according to the descriptions by Netherlands *et al*. (2014), the gamonts observed in the peripheral blood were those of *H. theileri* (Figure 5.3). Different developmental stages [as described by Netherlands *et al.* (2014)] of *Hepatozoon theileri* were found parasitizing the erythrocytes and, in some cases, extracellular stages were observed. Mature (i) and well-developed, immature (ii) gamonts were most prevalent, however, trophozoites (iii) and immature (iv) gamonts were also recorded parasitising erythrocytes and less frequently, leukocytes. The well-developed immature gamonts had a slender, elongated shape and the mature gamonts had a more elliptical shape. Disruption of the host blood cell was observed as well as dehaemoglobinisation, making the blood cell appear light blue in colour and even translucent.

5.3.1. Phylogenetic analysis

Sequences between 119 and 209 nt (without gaps) were isolated from *H. theileri* from the blood of 17 Common River frogs. Additionally, sequences of *H. ixoxo* isolated from *Sclerophrys gutturals* from the Soutpansberg Mountain Range and *H. tenuis* isolated from *Afrixlus fornasinii* Bianconi, 1849, from KwaZulu-Natal, part of a previous study (Netherlands *et al.*, 2018), were provided for comparison.

The phylogenetic analysis (Figure 5.6) showed that anuran *Hepatozoon* species isolated from South Africa and Canada, formed separate well-supported monophyletic clades (clade A and B) and each is a sister taxon to the other. The South African isolates formed two separate well-supported monophyletic clades of *H. theileri* from the Botanical Gardens in Potchefstroom (clade C) and the Soutpansberg Mountain Range in Limpopo (clade D). The monophyletic cluster of *H. theileri,* from both South African localities, formed a well-supported sister taxon with *H. tenuis* and *H. ixoxo*. *Hepatozoon catesbianae* and *H. clamatae* from Canada formed a well-supported monophyletic clade (clade A). *Hepatozoon sipedon* isolated from an Ontarian snake, *Thamnophis s. septentrionalis*, was used as an outgroup.

Distance matrix tables show the percentage difference (see Appendix E) and the number difference of nucleotide bases (see Appendix F) between the haemogregarine sequences used in the current study. The distance matrix analysis indicates an up to 20% difference in ITS-1 sequences when comparing *H. theileri* isolates form both localities. Isolates from the Botanical Gardens, Potchefstroom had a 1 – 15% difference and differed from each other by 1 – 35 nucleotide sites.

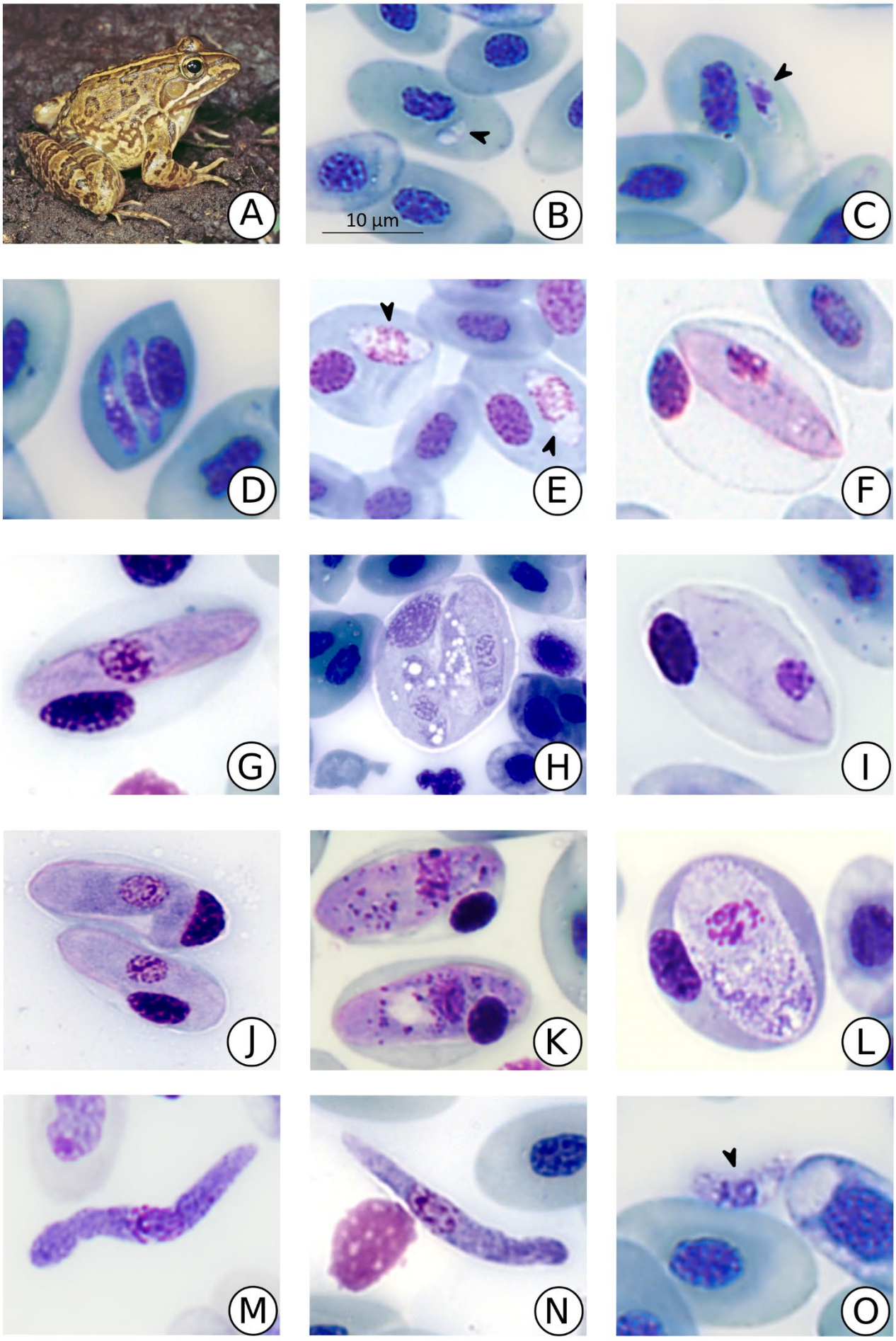

Figure 5.3: *Hepatozoon theileri* in the peripheral blood of *Amietia delalandii*. (A – E) Various stages of developing trophozoites. (F – J) Well-developed immature gamonts (slender form). (K – L) Mature gamonts. (M – N) Long, slender extracellular gamonts. (O) Possible extracellular merozoites before entering erythrocyte. Scale bar: 10 µm.

Differences between isolates from the Soutpansberg Mountain Range is reported with 1 – 12% difference with 1 – 27 nucleotide site differences.

5.3.2 Statistical analysis of haplotype network

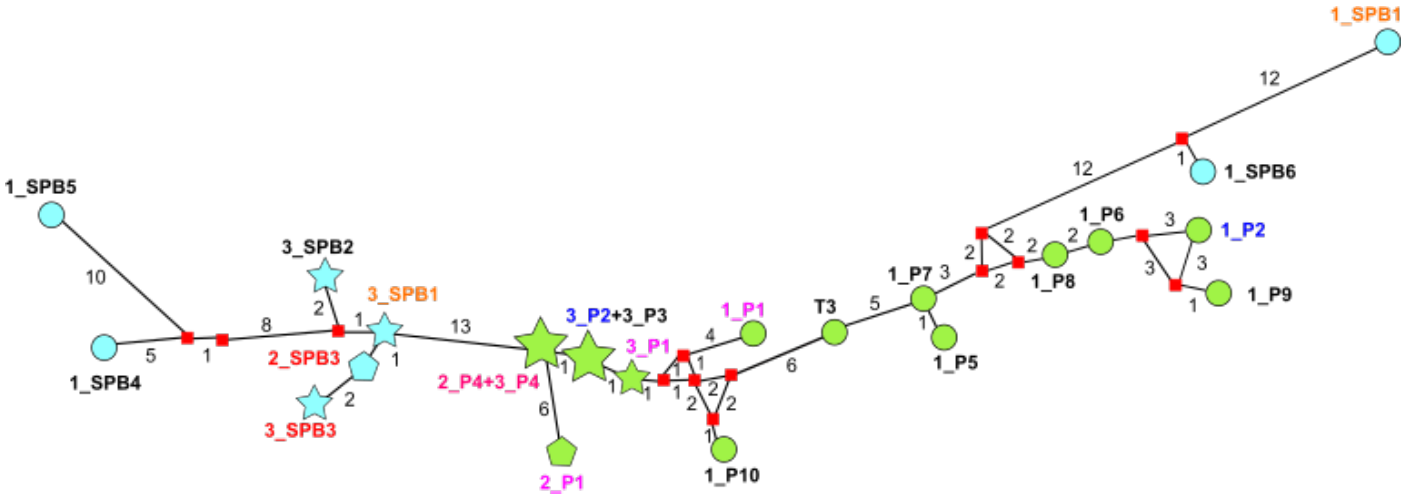

Figure 5.4: Median-joining network for the ITS-1 haplotypes of *Hepatozoon theileri constructed* using the Network software v10. Haplotypes are colour coded representing the two localities, the Soutpansberg (blue) and the Botanical Garden in Potchefstroom (green). Circles indicate longer ITS-1 sequences generated with method #1, the pentagon shapes represent the nested (#2) method and the stars represent shorter ITS-1 sequences using method #3. Samples that were used for different methods are shown in colour. Numbers on the branches indicate the number of nucleotide site substitutions between haplotypes. The size of the shapes is proportional to the haplotype frequency and the red square represents a hypothetical unsampled ancestor haplotype.

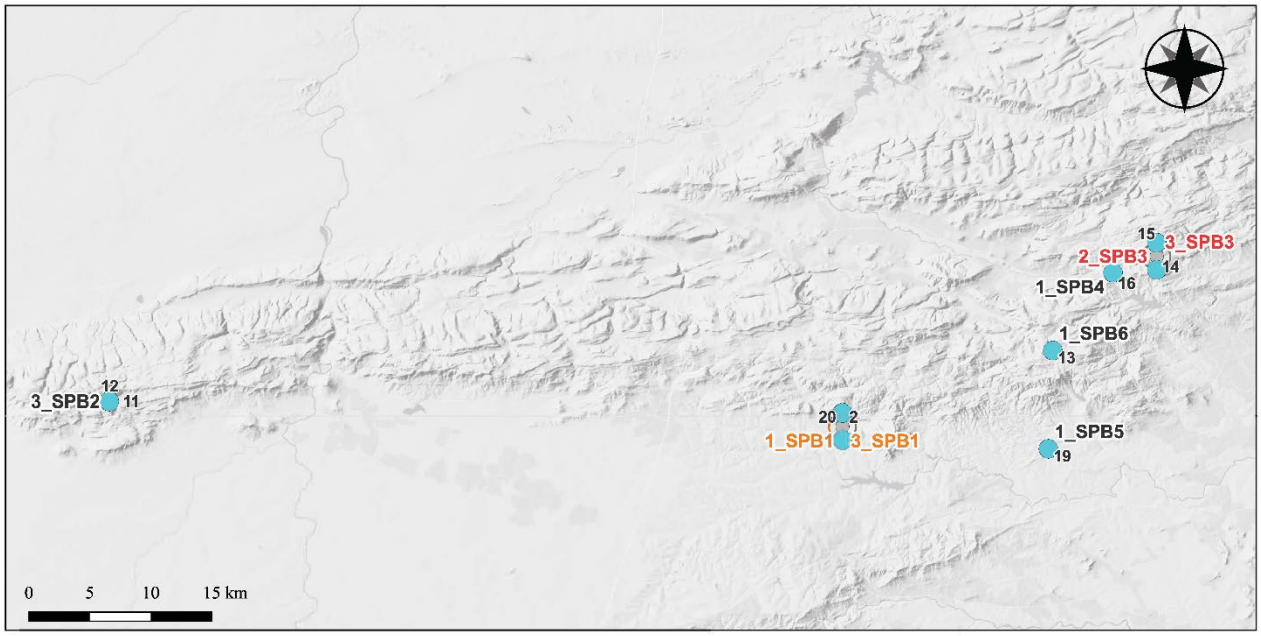

Figure 5.5: Sampling localities of haplotypes across the Soutpansberg. The coloured labels indicate haplotypes extracted from the same specimen.

The median-joining haplotype network generated, using the partial 18S rRNA sequences obtained in the current study from the two localities, displayed polymorphisms and nucleotide diversity. Only two small clusters formed between haplotype 2_P4 and 3_P4, and 3_P2 and 3_P3, respectively. All the other specimens formed single haplotypes. Haplotypes from the same localities didn't clade together, however, haplotypes from the same localities still grouped closely. Haplotype 1_SPB1 and 1_SPB6 did not group together with the rest of the SPB samples. Haplotypes extracted using method 1 (circles) generally grouped together on the right-hand side, with the exception of 1_SPB4 and 1_SBP5. Haplotypes extracted using method 2 and 3 mixed and grouped in the middle.

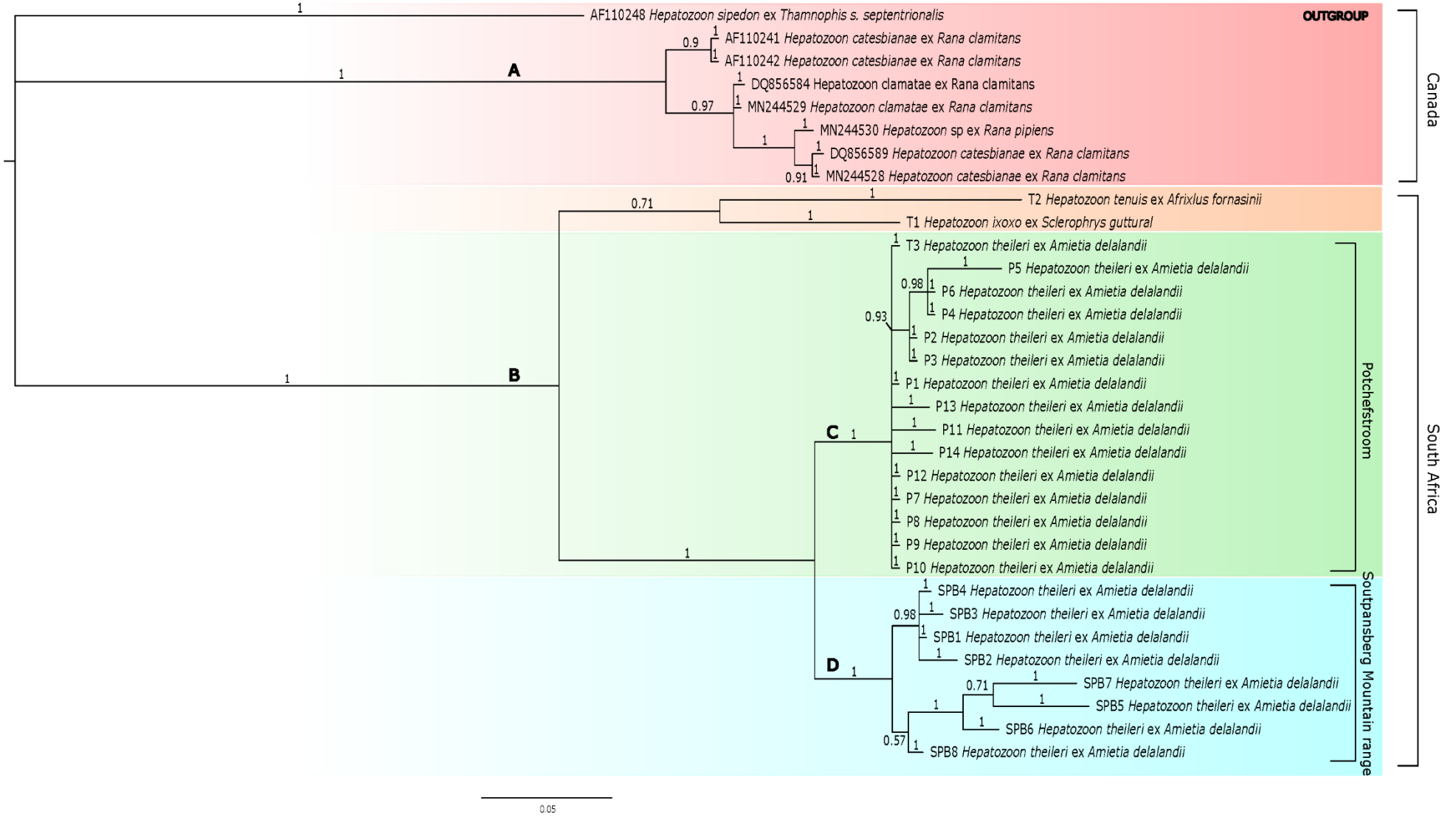

Figure 5.6: Bayesian Inference (BI) phylogenetic relationship based on nu ITS-1 regions isolated from *Hepatozoon theileri* infecting *Amietia delalandii*. Phylogenetic analysis shows the relationship between *Hepatozoon* species. The Felsenstein's 1981 model with a discrete Gama distribution (F81 + G4) was used for analyses. BI node support (probability) values above 0.57. The final alignment contained 229 nt from 33 sequences. *Hepatozoon sipedon* was used as an outgroup. The scale bar represents 0.05 nt substitutions per site.

5.4 Discussion

Species of the genus *Hepatozoon* have been reported from almost all vertebrate groups, including mammals, birds, reptiles, and amphibians (Smith, 1996), however, anuran *Hepatozoon* species are relatively under-studied, especially when regarding African anuran species. The latest contributions toward South African anuran *Hepatozoon* species have been increased hugely since 2014 by Netherlands *et al.* (2014a, 2014b, 2015, 2018). One of the collective aims of the latter studies was to determine the diversity and distribution of anuran haemogregarines in KwaZulu-Natal and their findings suggested that there is a vast blood parasite diversity of amphibians and that studies on anuran haemoparasites should continue across South Africa. No other studies have been conducted on the anuran blood parasites from the study area in Limpopo, concluding that this study is the first to determine the presence of *H. theileri* in *A. delalandii* across the Soutpansberg Mountain Range.

A total of 27/237 *A. delalandii* specimens were found infected with *H. theileri.* This expands the species distribution range for *H. theileri* with the first report from the Soutpansberg Mountain Range in the Vhembe Biosphere. Low prevalence was found with 11% of all frogs infected. The frogs from the Soutpansberg Mountain Range had higher prevalence at 19% (14/75), as compared to the population of Potchefstroom with 8% (13/162) prevalence. Even though the Soutpansberg sampling area was larger, with fewer frogs collected, more individual frogs were found positive with *H. theileri* than frogs collected from Potchefstroom.

Phylogenetic analysis shows that African and North American species formed separate monophyletic clades. Comparison of the ITS-1 region between the two localities provides evidence that there are differences (20%) between the isolates from the two populations. Comparisons among the 22 sequences, reveal 7 nucleotide polymorphisms that provided useful characters to determine the relationship between *H. theileri* from the different sites. All *H. theileri* sequences from the Soutpansberg Mountain Range shared the same nucleotides, accounting for a 3.3% intraspecific divergence from the *H. theileri* sequences from Potchefstroom. The isolates of *H. theileri* from the Soutpansberg Mountain Range and Potchefstroom were united as separate monophyletic groups.

The haplotype network analyses show that the two *Hepatozoon* populations, separated by geographical distance, not only differ from each other, but, also show nucleotide polymorphisms within each population. When comparing populations to each other the ITS-1 region is a conserved region within these populations demonstrating polymorphism. This is why it became necessary to compare ITS-1 regions from two populations of *H. theileri* to account for the differences, however, it shows differences between individuals within a population vary when using different primer sets, to amplify the ITS-1 region. It was suspected that the Potchefstroom

and the Soutpansberg samples would form separate, well-supported clusters indicating similarity within a population, however, this changed when amplifying different genotypes.

The results showed ITS-1 sequences provide useful insight into nucleotide differences between individuals from the same species. These character differences distinguish species from different localities; therefore, the analysis of ITS-1 sequences is helpful to determine the relationship between highly similar parasites (see Boulianne *et al*., 2007) and between individuals of the same species as shown in the current study. In the past, sequences of the ITS-1 region were used to distinguish between similar species such as *H. catesbianae* and *H. clamatae* (Boulianne *et al.*, 2007) when morphology and lifecycle characteristics failed to do so. This study shows that the ITS-1 region can be used to determine the intraspecific divergence between populations of species of *Hepatozoon*. Further work is still required to determine the exact variability of nucleotide sites between different sampling localities across South Africa, but, the data provided in the present study provides important insight into the differences that *H. theileri* share across two distinct populations.

CHAPTER 6:

SUMMATIVE DISCUSSION

Breviceps sylvestris taeniatus

The Soutpansberg mountain range lays within the Vhembe Biosphere in the Limpopo provinces which is known for its diverse terrestrial environment, ultimately supporting one of the most florally rich ecosystems (Berger *et al.*, 2003; Measey, 2011; Endangered Wildlife Trust, 2018). Not surprisingly the mountain range also boasts a high faunal diversity, including serval spices of amphibians (Minter *et al.*, 2004; UNESCO, 2009; Du Preez and Carruthers, 2017; Evans, 2017; Endangered Wildlife Trust, 2018)

The overall aim of the current study was to determine the biodiversity, habitat utilisation and distribution of the anurans and their associated blood parasites that occur across the Soutpansberg Mountain Range. This was achieved by conducting a comprehensive survey the anurans and their blood parasites in the study area over a three-year period, which included 132 sampling localities. In ***Chapter 2,*** the diversity and abundance of frog species were recorded by means of different sampling methods (see Chapter 2), and results indicate that 32 of the possible 35 frog species were confirmed to occurred across the Soutpansberg. With only four species not accounted for during the present study namely *S. capensis, Pt. oxyrhynchus, T. krugerensis* and *T. natalensis*. This is likely due to some areas that were not accessible such as the rural areas of Thohoyandou on the far eastern region of the mountain range, as well as restricted access to the majority of the central region of the mountain range that is closed for public access (private land). Additionally, three frog species were encountered outside their known distribution range and thus, confirmed the extension of the distribution range of *A. stenodactylus, B. s. taeniatus* and *P. uzungwensis* to include the Soutpansberg (see Du Preez and Carruthers, 2017; Minter *et al.,* 2004).

Furthermore, ***Chapter 2*** shows a high diversity of amphibian species that occur within the study area, warranting further monitoring of this sensitive vertebrate class. The results showed that the majority of the anuran species estimated to occur in the study area by anecdotal records, are still present and abundant. A total of 540 adult frog specimens were collected across the three sampling transects. The distribution and abundance of collected anurans are mirrored by the different ecological habitats found across the Soutpansberg, with only a single species not found to occur in the semi-arid western region, that was found in the sub-tropical eastern region (see Berger *et al.,* 2003; Minter *et al*., 2004).

In terms of anuran blood parasites, the present study focused on the diversity and occurrence within and around the Soutpansberg. Only a small number of studies have been conducted on the anuran blood parasite diversity in South Africa, with most studies occurring in the province of KwaZulu-Natal, a biodiversity hotspot (Netherlands, 2014; Netherlands *et al.*, 2015; Netherlands, 2019). The present study was thus, the first survey of anuran blood parasite diversity across the Soutpansberg. Blood parasites were documented by means of light

microscopy and identified, when possible, to genus level by using a combined approach of morphological and molecular characterisation.

Chapter 3, provides a detailed survey on the anuran blood parasite groups encountered in during the present study, namely trypanosomatids, haemogregarines, haemococcidians, filarial nematodes and unknown non-protistan infections. High blood parasite diversity with 25 possible species and an overall prevalence of 10% (38/387) across all host species screened was recorded in the present study. Infection prevalence of the various blood parasite species and groups varied across host species and even within certain individuals. Species of *Trypanosoma* and *Hepatozoon* were the most abundant with microfilariae and haemococcidians being the least prevalent. These findings could possibly be due to different life history strategies followed by the different blood parasite groups or the longevity of the parasites. Netherlands *et al*. (2014) found infections of *Hepatozoon ixoxo* to remain constant over the course of a year, with parasitaemia peaking within the first several months and then steadily decreasing to similar parasitaemia levels as when first recorded a year earlier. This could explain why species of *Hepatoozoon* were more abundant as infections may last more than a year without reinfection. On the other hand, trypanosomes are known to replicate extracellularly within the peripheral blood of their host (Bardsley and Harmsen, 1973; Martin and Desser, 1990; Desser, 2001; Spodareva *et al.*, 2018). This may explain why trypanosomes may be so abundant and why some individuals hosted several species or morphotypes. Furthermore, microfilariae of the recently described *Neofoleyellides steyni*, were observed infecting *Amietia delalandii* (see Kuzmin *et al*., 2021). Additionally, infections of unknown status and non-protozoan infections were observed, but could not be identified, in 20 frog species with a prevalence of 23%. This chapter represents the first multispecies blood parasite survey done on anurans from the Soutpansberg in the Limpopo province, highlighting the importance of biomonitoring surveys and that a lot of work still need to be done on blood parasites in different provinces across South Africa.

Provided in ***Chapter 4*****,** is a case study of an undescribed haemococcidian species isolated from the frog host *A. delalandii*. The sequence fragments of the nu 18S rRNA gene and the mt COI gene, revealed that this species does not cluster with other haemococcidians. Phylogenetic analysis of both 18S rDNA and COI sequences, show the species to be closely related to the genus *Lankesterella*, and was thus preliminarily designated as a species of *Lankesterella*. Future work should focus on the clarification of this parasite's life history and developmental stages.

Chapter 5, focused on an in-depth study of the genetic variation of *Hepatozoon theileri* between two district populations, using for the first time the internal transcribed spacer 1 (ITS-1)

region located downstream of the 18S rRNA gene and upstream of the 5.8S rRNA gene. Results showed ITS-1 sequence data may provide useful insight into nucleotide differences between individuals from the same species from various populations. These finding are similar to finding between two closely related species of *Hepatozoon* from Canada (see Boulianne *et al*., 2017). Further work should be extended to more populations across South Africa to determine the exact variability of nucleotide sites for this species.

Future work and perspectives

This study provides a baseline for future studies of diversity, ecological, and phylogenetic, relationships the anurans and their blood parasites within the Soutpansberg mountain range. With no officially protected areas forming part of the Soutpansberg mountain range, future work should focus on the importance of continues monitoring, especially for species sensitive to habitat change, such as amphibians. Furthermore, comparing parasite diversity and distribution to host distribution may provide insight on the parasite sensitivity to varying ecosystem. This area is particularly vulnerable to habitat fragmentation due to the high demand for clearing land for agriculture and plantations. Comparisons of these data inside and outside formally protected areas will also provide invaluable data in determining the impact that human activities have on the diversity, prevalence and distribution of blood parasites. Additionally, it is important to increase the number barcodes of blood parasites from anurans from different areas to get a clear understanding of the phylogenetic relationship between species of anuran blood parasites.

REFERENCES

Acosta, A.A., Netherlands, E.C., Retief, F., De Necker, L., Du Preez, L.H., Truter, M., Alberts, R., Gerber, R., Wepener, V. & Malherbe, W. 2020. Conserving freshwater biodiversity in an African subtropical wetland: South Africa's lower Phongolo river and floodplain. *Managing Wildlife in a Changing World.* IntechOpen London, UK.

Alves, A.P. & Paperna, I. 1993. Ultrastructure of erythrocytic virus of the South African anuran *Ptychadena anchietae*. *Diseases of Aquatic Organisms,* 16**:**105–109.

Attias, M., Sato, L.H., Ferreira, R.C., Takata, C.S., Campaner, M., Camargo, E.P., Teixeira, M.M. & De Souza, W. 2016. Developmental and ultrastructural characterization and phylogenetic analysis of *Trypanosoma herthameyeri* n. sp. of Brazilian Leptodactilydae frogs. *Journal of Eukaryotic Microbiology,* 63(5)**:**610–622.

Ball, G.H. 1967. Blood sporozoans from east African amphibia. *The Journal of Protozoology,* 14(3)**:**521–527.

Bardsley, J.E. & Harmsen, R. 1973. The trypanosomes of anura. *Advances in Parasitology,* 11**:**1–73.

Barta, J.R. & Desser, S.S. 1984. Blood parasites of amphibians from Algonquin Park, Ontario. *Journal of Wildlife Diseases,* 20(3)**:**180–189.

Barta, J.R. 2000. Adeleorina. *In:* Lee, J.J., Leedale, G.F., Bradbury, P.C. (ed.) *An illustrated Guide to the Protozoa.* 305–318.

Barta, J.R., Ogedengbe, J.D., Martin, D.S. & Smith, T.G. 2012. Phylogenetic position of the adeleorinid coccidia (Myzozoa, Apicomplexa, Coccidia, Eucoccidiorida, Adeleorina) inferred using 18S rDNA sequences. *Journal of Eukaryotic Microbiology,* 59(2)**:**171–180.

Beebee, T.J. & Griffiths, R.A. 2005. The amphibian decline crisis: A Watershed for Conservation Biology. *Biological Conservation,* 125(3)**:**271–285.

Berger, K., Crafford, J.E., Gaigher, I., Gaigher, M.J., Hahn, N. & Macdonald, I. 2003. *A first Synthesis of the Environmental, Biological and Cultural assets of the Soutpansberg,* Louis Trichardt, South Africa, Leach Printers & Signs.

Bernal, X.E. & Pinto, C.M. 2016. Sexual differences in prevalence of a new species of trypanosome infecting túngara frogs. *International Journal for Parasitology: Parasites and Wildlife,* 5(1)**:**40–47.

Biedrzycka, A., Kloch, A., Migalska, M. & Bielański, W. 2013. Molecular characterization of putative *Hepatozoon* sp. from the sedge warbler (*Acrocephalus schoenobaenus*). *Parasitology,* 140:695–698.

Bogart, J.P., Dawood, A., Becker, F.S. & Channing, A. 2022. Chromosomes in the African frog genus *Tomopterna* (Pyxicephalidae) and probing the origin of tetraploid *Tomopterna tandyi*. *Genome,* (1)**:**1–29.

Bonorris, J.S. & Ball, G.H. 1955. *Schellackia occidentalis* n. sp., a blood-inhabiting coccidian found in lizards in southern California. *The Journal of Protozoology,* 2(1)**:**31–34.

Boulianne, B., Evans, R.C. & Smith, T.G. 2007. Phylogenetic analysis of *Hepatozoon species* (Apicomplexa: Adeleorina) infecting frogs of Nova Scotia, Canada, determined by ITS-1 sequences. *Journal of Parasitology,* 93(6)**:**1435–1441.

Bristovetzky, M. & Paperna, I. 1990. Life cycle and transmission of *Schellackia cf. agamae,* a parasite of the starred lizard *Agama stellio*. *International Journal for Parasitology,* 20(7):883–892.

Cai, J., Collins, M.D., Mcdonald, V. & Thompson, D.E. 1992. PCR cloning and nucleotide sequence determination of the 18S rRNA genes and internal transcribed spacer 1 of the protozoan parasites *Cryptosporidium parvum* and *Cryptosporidium muris*. *Biochimica et Biophysica Acta (BBA)-Gene Structure and Expression,* 1131(3)**:**317–320.

Carroll, R.L. 2009. *The rise of amphibians: 365 million years of evolution,* Baltimore, The Johns Hopkins University Press.

Castresana, J. 2000. Selection of conserved blocks from multiple alignments for their use in phylogenetic analysis. *Molecular Biology and Evolution,* 17(4)**:**540–552.

Chambouvet, A., Gower, D.J., Jirků, M., Yabsley, M.J., Davis, A.K., Leonard, G., Maguire, F., Doherty-Bone, T.M., Bittencourt-Silva, G.B. & Wilkinson, M. 2015. Cryptic infection of a broad taxonomic and geographic diversity of tadpoles by *Perkinsea* protists. *Proceedings of the National Academy of Sciences,* 112(34)**:**4743–4751.

Channing, A., Hillers, A., Lötters, S., Rödel, M., Schick, S., Conradie, W., Rödder, D., Mercurio, V., Wagner, P. & Dehling, J. 2013. Taxonomy of the super-cryptic *Hyperolius nasutus* group of long reed frogs of Africa (Anura: Hyperoliidae), with descriptions of six new species. *Zootaxa,* 3620(3)**:**301–350.

Conradie, R., Cook, C.A., Du Preez, L.H., Jordaan, A. & Netherlands, E.C. 2017. Ultrastructural comparison of *Hepatozoon ixoxo* and *Hepatozoon theileri* (Adeleorina: Hepatozoidae), parasitising South African anurans. *Journal of Eukaryotic Microbiology,* 64(2)**:**193–203.

Cook, C.A., Netherlands, E.C. & Smit, N.J. 2015. First *Hemolivia* from southern Africa: reassigning chelonian *Haemogregarina parvula* Dias, 1953 (Adeleorina: Haemogregarinidae) to *Hemolivia* (Adeleorina: Karyolysidae). *African Zoology,* 50(2)**:**165–173.

Cook, C.A., Netherlands, E.C. & Smit, N.J. 2016. Redescription, molecular characterisation and taxonomic re-evaluation of a unique African monitor lizard haemogregarine *Karyolysus paradoxa* (Dias, 1954) n. comb. (Karyolysidae). *Parasites & Vectors,* 9(1)**:**347.

Davies, A.J. & Johnston, M.R.L. 2000. The biology of some intraerythrocytic parasites of fishes, amphibia and reptiles. *Advances in Parasitology,* 45**:**107.

Davis, A.K., Devore, J.L., Milanovich, J.R., Cecala, K., Maerz, J.C. & Yabsley, M.J. 2009. New findings from an old pathogen: Intraerythrocytic bacteria (family Anaplasmatacea) in red-backed salamanders *Plethodon cinereus*. *EcoHealth,* 6(2)**:**219–228.

de Abreu Reis Ferreira, D., Perles, L., Machado, R.Z., Prado, C.P.A. & André, M.R. 2020. Molecular detection of Apicomplexan haemoparasites in anurans from Brazil. *Parasitology Research*, 119(10):3469–3479.

Desser, S.S. 1993. The Haemogregarinidae and Lankesterellidae, *In*: Kreier, J.P. eds. *Parasitic Protozoa,* 2nd ed., 247–272.

Desser, S.S. & Yekutiel, D. 1986. Blood parasites of amphibians and reptiles in Israel. *Israel Journal of Ecology and Evolution,* 34(1–2)**:**77–90.

Desser, S.S. 1987. *Aegyptianella ranarum* sp. n. (Rickettsiales, Anaplasmataceae): ultrastructure and prevalence in frogs from Ontario. *Journal of Wildlife Diseases,* 23(1)**:**52–59.

Desser, S.S. 1993. The haemogregarinidae and lankesterellidae. *Parasitic Protozoa*, 247–272.

Desser, S.S. 2001. The blood parasites of anurans from Costa Rica with reflections on the taxonomy of their trypanosomes. *Journal of Parasitology,* 87(1)**:**152–160.

Desser, S.S., Hong, H. & Martin, D.S. 1995. The life history, ultrastructure, and experimental transmission of *Hepatozoon catesbianae* n. comb., an apicomplexan parasite of the bullfrog, *Rana catesbeiana* and the mosquito, *Culex territans* in Algonquin Park, Ontario. *The Journal of Parasitology***,** 212–222.

Desser, S.S., Mciver, S.B. & Ryckman, A. 1973. *Culex territans* as a potential vector of *Trypanosoma rotatorium*. I. Development of the flagellate in the mosquito. *The Journal of Parasitology,* 1**:**353–358.

Desser, S.S., Siddall, M.E., Barta, J.R. 1990. Ultrastructural observations on the developmental stages of *Lankesterella minima* (Apicomplexa) in experimentally infected *Rana catesbeiana* tadpoles. *The Journal of Parasitology,* 76(1):97–103.

Diamond, L.S. 1965. A study of the morphology , biology and taxonomy of the trypanosomes of anura. *Wildlife Diseases,* 44**:**1–77.

Dodd, C.K. 2010. *Amphibian Ecology and Conservation: A Handbook of Techniques*, Oxford University Press.

Du Preez, L.H. & Carruthers, V.C. 2009. *A Complete Guide to the Frogs of Southern Africa,* Cape Town, Struik Nature.

Du Preez, L.H. & Carruthers, V.C. 2017. *Frogs of Southern Africa,* Cape Town, Struik Nature: Penguin Random House.

Dutton, J.E., Todd, J.L. & Tobey, E.N. 1907. Concerning certain parasitic protozoa observed in Africa: Being the eighth interim report of the expedition of the Liverpool school of tropical medicine to the Congo, 1903–5. *Annals of Tropical Medicine & Parasitology,* 1(1–5)**:**286–371.

Dvořáková, N., Čepička, I., Qablan, M.A., Gibson, W., Blažek, R. & Široký, P. 2015. Phylogeny and morphological variability of trypanosomes from African pelomedusid turtles with redescription of *Trypanosoma mocambicum* Pienaar, 1962. *Protist,* 166(6)**:**599–608.

El-Sherry, S., Ogedengbe, M.E., Hafeez, M.A. & Barta, J.R. 2013. Divergent nuclear 18S rDNA paralogs in a turkey coccidium, *Eimeria meleagrimitis*, complicate molecular systematics and identification. *International Journal for Parasitology,* 43(8)**:**679–685.

Evans, S.W. 2017. An assessment of land cover change as a source of information for conservation planning in the Vhembe Biosphere Reserve. *Applied Geography,* 82**:**35–47.

Fantham, H.B., Porter, A. & Richardson, L.R. 1942. Some haematozoa observed in vertebrates in eastern Canada. *Parasitology,* 34(2)**:**199–226.

Fermino, B.R., Paiva, F., Soares, P., Tavares, L.E.R., Viola, L.B., Ferreira, R.C., Botero-Arias, R., De-Paula, C.D., Campaner, M. & Takata, C.S. 2015. Field and experimental evidence of a new caiman trypanosome species closely phylogenetically related to fish trypanosomes and

transmitted by leeches. *International Journal for Parasitology: Parasites and Wildlife,* 4(3)**:**368–378.

Ferreira, R., Campaner, M., Viola, L.B., Takata, C.S.D.A., Takeda, G. & Teixeira, M.M.G. 2007. Morphological and molecular diversity and phylogenetic relationships among anuran trypanosomes from the Amazonia, Atlantic Forest and Pantanal biomes in Brazil. *Parasitology,* 134(11)**:**1623–1638.

Frost, D.R. 2021. Amphibian Species of the World: an Online Reference.

Frost, D.R., Grant, T., Faivovich, J., Bain, R.H., Haas, A., Haddad, C.F., De Sa, R.O., Channing, A., Wilkinson, M. & Donnellan, S.C. 2006. The amphibian tree of life. *Bulletin of the American Museum of natural History,* 297**:**1–291.

Goggin, C.L. 1994. Variation in the two internal transcribed spacers and 5.8 S ribosomal RNA from five isolates of the marine parasite *Perkinsus* (Protista, Apicomplexa). *Molecular and Biochemical Parasitology,* 65(1)**:**179–182.

Gruia-Gray, J., Petric, M. & Desser, S. 1989. Ultrastructural, Biochemical and Biophysical Properties of an Erythrocytic virus of frogs from Ontario, Canada. *Journal of Wildlife Diseases,* 25(4)**:**497–506.

Gruia-Gray, J., Ringuette, M. & Desser, S.S. 1992. Cytoplasmic localization of the DNA virus frog erythrocytic virus. *Intervirology,* 33(3)**:**159–164.

Grybchuk-Ieremenko, A., Losev, A., Kostygov, A.Y., Lukes, J. & Yurchenko, V. 2014. High prevalence of trypanosome co-infections in freshwater fishes. *Folia Parasitologica,* 61(6)**:**495.

Gu, Z., Wang, J., Li, M., Zhang, J., Ke, X. & Gong, X. 2007. Morphological and genetic differences of *Trypanosoma* in some Chinese freshwater fishes: difficulties of species identification. *Parasitology Research,* 101(3)**:**723–730.

Haag, J., O'huigin, C. & Overath, P. 1998. The molecular phylogeny of trypanosomes: evidence for an early divergence of the Salivaria. *Molecular and Biochemical Parasitology,* 91**:**37–49.

Hrdina, A. & Romportl, D. 2017. Evaluating global biodiversity hotspots–Very rich and even more endangered. *Journal of Landscape Ecology,* 10(1)**:**108–115.

Huelsenbeck, J.P. & Ronquist, F. 2001. MRBAYES: Bayesian inference of phylogenetic trees. *Bioinformatics,* 17(8)**:**754–755.

Jakes, K., O'donoghue, P.J. & Cameron, S.L. 2003. Phylogenetic relationships of *Hepatozoon* (Haemogregarina) *boigae*, *Hepatozoon* sp., *Haemogregarina clelandi* and *Haemoproteus chelodina* from Australian reptiles to other Apicomplexa based on cladistic analyses of ultrastructural and life-cycle characters. *Parasitology,* 126(6)**:**555–559.

Kim, B., Smith, T.G. & Desser, S.S. 1998. The Life History and Host Specificity of *Hepatozoon clamatae* (Apicomplexa: Adeleorina) and ITS-1 Nucleotide Sequence Variation of *Hepatozoon* Species of Frogs and Mosquitoes from Ontario. *The American Society of Parasitologists,* 84(4)**:**789–797.

Kuzmin, Y., Netherlands, E.C., Du Preez, L.H. & Svitin, R. 2021. Two new species of *Neofoleyellides* (Nematoda: Onchocercidae) parasitising anuran amphibians in South Africa. *International Journal for Parasitology: Parasites and Wildlife,* 14**:**298–307.

Kvičerová, J., Pakandl, M. & Hypša, V. 2008. Phylogenetic relationships among *Eimeria* spp. (Apicomplexa, Eimeriidae) infecting rabbits: evolutionary significance of biological and morphological features. *Parasitology,* 135(4)**:**443–452.

Laveran, A. 1905. Contribution a l'etude des grandes hemogregarines des grenouilles. *Comptes Rendus des Séances de la Société de Biologie et de Ses Filiales,* 59**:**172–175.

Le Bail O, Landau I. 1974. Description and experimental life cycle of *Schellackia balli* n. sp. (Lankesterellidae) a parasite of toads in Guyana (author's transl*). Annales de Parasitologie Humaine et Comparee,* (6):663–668.

Lecocq, T., Vereecken, N.J., Michez, D., Dellicour, S., Lhomme, P., Valterova, I., Rasplus, J.Y. & Rasmont, P. 2013. Patterns of genetic and reproductive traits differentiation in mainland vs. Corsican populations of bumblebees. *PLoS One*, 8(6):65642.

Lefoulon, E., Bain, O., Bourret, J., Junker, K., Guerrero, R., Cañizales, I., Kuzmin, Y., Satoto, T.B.T., Cardenas-Callirgos, J.M. & De Souza Lima, S. 2015. Shaking the tree: multi-locus sequence typing usurps current onchocercid (filarial nematode) phylogeny. *PLOS Neglected Tropical Diseases,* 9(11)**:**4233.

Lemos, M., Morais, D.H., Carvalho, V.T. & D'agosto, M. 2008. First record of *Trypanosoma chattoni* in Brazil and occurrence of other *Trypanosoma* species in Brazilian frogs (Anura, Leptodactylidae). *Journal of Parasitology,* 94(1)**:**148–151.

Leveille, A.N., Zeldenrust, E.G. & Barta, J.R. 2021. Multilocus Genotyping of Sympatric *Hepatozoon s*pecies Infecting the Blood of Ontario Ranid Frogs Reinforces Species Differentiation and Identifies an Unnamed *Hepatozoon* species. *Journal of Parasitology,* 107(2)**:**246–261.

Levine, N.D. 1980. Some corrections of coccidian (Apicomplexa: Protozoa) nomenclature. *The Journal of Parasitology*, 66(5):830–834.

Mansour, N.S. & Mohammed, A.H. 1962. *Lankesterella bufonis* sp. nov. parasitizing toads, *Bufo regularis* Reuss, in Egypt. *The Journal of Protozoology,* 9(2)**:**243–248.

Martin, D.S. & Desser, S.S. 1990. A light and electron microscopic study of *Trypanosoma fallisi* n. sp. in toads (*Bufo americanus*) from Algonquin Park, Ontario. *The Journal of Protozoology,* 37(3)**:**199–206.

Martin, D.S., Wright, A.-D.G., Barta, J.R. & Desser, S.S. 2002. Phylogenetic position of the giant anuran trypanosomes *Trypanosoma chattoni, Trypanosoma fallisi, Trypanosoma mega, Trypanosoma neveulemairei*, and *Trypanosoma ranarum* inferred from 18S rRNA gene sequences. *Journal of Parasitology,* 88(3)**:**566–571.

Martínez, J., Merino, S., Badás, E.P., Almazán, L., Moksnes, A. & Barbosa, A. 2018. Hemoparasites and immunological parameters in Snow Bunting (*Plectrophenax nivalis*) nestlings. *Polar Biology*, 41(9):1855–1866.

Maslov, D.A., Lukeš, J., Jirku, M. & Simpson, L. 1996. Phylogeny of trypanosomes as inferred from the small and large subunit rRNAs: Implications for the evolution of parasitism in the trypanosomatid protozoa. *Molecular and Biochemical Parasitology,* 75(2)**:**197–205.

Mcinnes, L.M., Gillett, A., Ryan, U.M., Austen, J., Campbell, R.S.F., Hanger, J. & Reid, S.A. 2009. *Trypanosoma irwini* n. sp (Sarcomastigophora: Trypanosomatidae) from the koala (*Phascolarctos cinereus*). *Parasitology,* 136(8)**:**875–885.

Measey, G. 2011. *Ensuring a Future for South Africa's Frogs,* Pretoria, South African National Biodiversity Institute.

Megía-Palma, R., Martınez, J. & Merino, S. 2014. Molecular characterization of haemococcidia genus *Schellackia* (Apicomplexa) reveals the polyphyletic origin of the family Lankesterellidae. *Zoologica Scripta*, 43:304–312.

Megía-Palma, R., Martinez, J. & Merino, S. 2013. Phylogenetic analysis based on 18S rRNA gene sequences of *Schellackia* parasites (Apicomplexa: Lankesterellidae) reveals their close relationship to the genus *Eimeria*. *Parasitology,* 140(9)**:**1149–1157.

Megía-Palma, R., Martínez, J., Cuervo, J.J., Belliure, J., Jiménez-Robles, O., Gomes, V., Cabido, C., Pausas, J.G., Fitze, P.S., Martín, J. & Merino, S. 2018. Molecular evidence for host–parasite co-speciation between lizards and *Schellackia* parasites. *International Journal for Parasitology*, 48(9–10):709–718.

Megía-Palma, R., Martínez, J., Nasri, I., Cuervo, J.J., Martín, J., Acevedo, I., Belliure, J., Ortega, J., García-Roa, R. & Selmi, S. 2016. Phylogenetic relationships of *Isospora*, *Lankesterella*, and *Caryospora* species (Apicomplexa: Eimeriidae) infecting lizards. *Organisms Diversity & Evolution,* 16(1)**:**275–288.

Megía-Palma, R., Martinez, J., Paranjpe, D., D'amico, V., Aguilar, R., Palacios, M.G., Cooper, R., Ferri-Yanez, F., Sinervo, B. & Merino, S. 2017. Phylogenetic analyses reveal that *Schellackia* parasites (Apicomplexa) detected in American lizards are closely related to the genus *Lankesterella*: is the range of *Schellackia* restricted to the Old World? *Parasites & Vectors,* 10(1)**:**470.

Mercurio, V. 2009. Advertisement calls of three species of *Arthroleptis* (Anura: Arthroleptidae) from Malawi. *Journal of Herpetology,* 43(2)**:**345–350.

Merino, S., Martínez, J., Martínez-de la Puente, J., Criado-Fornelio, Á., Tomás, G., Morales, J., Lobato, E., & García-Fraile, S. 2006. Molecular characterization of the 18S rDNA gene of an avian *Hepatozoon* reveals that it is closely related to *Lankesterella*. *Journal of Parasitology*, 92:1330–1335.

Minter, L., Burger, M., Harrison, J.A., Braack, H.H., Bishop, P.J. & Kloepfer, D. 2004. *Atlas and Red Data Book of the Frogs of South Africa, Lesotho and Swaziland*, Smithsonian Institute and Avian Demography Unit.

Morrison, D.A., Bornstein, S., Thebo, P., Wernery, U., Kinne, J. & Mattsson, J.G. 2004. The current status of the small subunit rRNA phylogeny of the coccidia (Sporozoa). *International Journal for Parasitology*, 34(4):501–514.

Mutinga, M.J. & Dipeolu, O.O. 1989. Saurian malaria in Kenya: description of new species of Haemoproteid and Haemogregarine parasites, Anaplasma-like and Pirhemocyton-like organisms in the blood of lizards in West Pokot District. *International Journal of Tropical Insect Science*, 10(3):401–412.

Netherlands, E.C. 2014. *Species diversity, habitat utilization and blood parasites of amphibians in and around Ndumo Game Reserve.* Magister Scientiae, North-West University.

Netherlands, E.C. 2019. *Ecology, systematics and evolutionary biology of frog blood parasites in northern KwaZulu-Natal.* PhD, North-West University.

Netherlands, E.C., Cook, C.A. & Smit, N.J. 2014a. *Hepatozoon* species (Adeleorina: Hepatozoidae) of African bufonids, with morphological description and molecular diagnosis of *Hepatozoon ixoxo* sp. nov. parasitising three *Amietophrynus* species (Anura: Bufonidae). *Parasites & Vectors,* 7**:**552.

Netherlands, E.C., Cook, C.A., Du Preez, L.H., Vanhove, M.P., Brendonck, L. & Smit, N.J. 2020a. An overview of the Dactylosomatidae (Apicomplexa: Adeleorina: Dactylosomatidae), with the description of *Dactylosoma kermiti* n. sp. parasitising *Ptychadena anchietae* and *Sclerophrys gutturalis* from South Africa. *International Journal for Parasitology: Parasites and Wildlife,* 11**:**246–260.

Netherlands, E.C., Cook, C.A., Du Preez, L.H., Vanhove, M.P.M., Brendonck, L. & Smit, N.J. 2018. Monophyly of the species of *Hepatozoon* (Adeleorina: Hepatozoidae) parasitizing (African) anurans, with the description of three new species from hyperoliid frogs in South Africa. *Parasitology,* 145(8)**:**1039–1050.

Netherlands, E.C., Cook, C.A., Kruger, D.J., Du Preez, L.H. & Smit, N.J. 2015. Biodiversity of frog haemoparasites from sub-tropical northern KwaZulu-Natal, South Africa. *International Journal for Parasitology: Parasites and Wildlife,* 4(1)**:**135–141.

Netherlands, E.C., Cook, C.A., Smit, N.J. & Du Preez, L.H. 2014b. Redescription and molecular diagnosis of *Hepatozoon theileri* (Laveran, 1905) (Apicomplexa: Adeleorina: Hepatozoidae), infecting *Amietia quecketti* (Anura: Pyxicephalidae). *Folia Parasitologica,* 61(4)**:**293–300.

Netherlands, E.C., Svitin, R., Cook, C.A., Smit, N.J., Brendonck, L., Vanhove, M.P. & Du Preez, L.H. 2020b. *Neofoleyellides boerewors* n. gen. n. sp. (Nematoda: Onchocercidae) parasitising common toads and mosquito vectors: Morphology, life history, experimental transmission and host-vector interaction in situ. *International Journal for Parasitology,* 50(3)**:**177–194.

Nöller, W. 1912. *Über eine neue Schizogonie von Lankesterella minima Chaussat*, G. Fischer.

Nöller, W. 1913. Die Blutprotozoen des Wasserfrosches und ihre Übertragung. *Archiv für Protistenkunde*, 31:169–240.

Nöller, W. 1920. Kleine beobachtungen an parasitischen protozoen. *Archiv für Protistenkunde,* 41**:**169–189.

O'donoghue, P. 2017. Haemoprotozoa: Making biological sense of molecular phylogenies. *International Journal for Parasitology: Parasites and Wildlife,* 6(3)**:**241–256.

Ogedengbe, J.D., Hanner, R.H. & Barta, J.R. 2011. DNA barcoding identifies *Eimeria* species and contributes to the phylogenetics of coccidian parasites (Eimeriorina, Apicomplexa, Alveolata). *International Journal for Parasitology,* 41(8)**:**843–850.

Ogedengbe, J.D., Ogedengbe, M.E., Hafeez, M.A. & Barta, J.R. 2015. Molecular phylogenetics of eimeriid coccidia (Eimeriidae, Eimeriorina, Apicomplexa, Alveolata): a preliminary multi-gene and multi-genome approach. *Parasitology Research*, 114(11):4149–4160.

Ogedengbe, M.E., El-Sherry, S., Ogedengbe, J.D., Chapman, H.D. & Barta, J.R. 2017. Phylogenies based on combined mitochondrial and nuclear sequences conflict with morphologically defined genera in the eimeriid coccidia (Apicomplexa). *International Journal of Parasitology*, 48:59–69.

Ogedengbe, M.E., Ogedengbe, J.D., Whale, J.C., Elliot, K., Juárez-Estrada, M.A. & Barta, J.R. 2016. Molecular phylogenetic analyses of tissue coccidia (Sarcocystidae; Apicomplexa) based on nuclear 18S rDNA and mitochondrial COI sequences confirms the paraphyly of the genus *Hammondia*. *Parasitology Open,* 2.

Paperna, I. 1992. Ultrastructural studies on oocysts, sporulation and sporozoites of *Schellackia cf. agamae* from the intestine of the starred lizard *Agama stellio*. *International Journal for Parasitology*, 22(3):361–368.

Paperna, I. & Lainson, R. 1995. *Schellackia* (Apicomplexa: Eimeriidae) of the Brazilian tree-frog, *Phrynohyas venulosa* (Amphibia: Anura) from Amazonian Brazil. *Memórias do Instituto Oswaldo Cruz*, 90(5):589–592.

Paperna, I. & Ogara, W. 1996. Description and ultrastructure of *Lankesterella* species infecting frogs in Kenya. *Parasite*, 4:341–349.

Paperna, I. & Ostroska, K. 1989. Ultrastructural studies on sporozoite stages of *Schellackia cf. agamae* from liver and blood of the starred lizard *Agama stellio*. *International Journal for Parasitology,* 19(1):13–19.

Payne, S. & Ellis, J. 1996. Detection of *Neospora caninum* DNA by the polymerase chain reaction. *International Journal for Parasitology,* 26(4)**:**347–351.

Petford, M.A., Alexander, G.J. & Van Huyssteen, R. 2019. Influences of ecology and climate on the distribution of restricted, rupicolous reptiles in a biodiverse hotspot. *African Journal of Herpetology,* 68(2)**:**118–133.

Readel, A.M. & Goldberg, T.L. 2010. Blood parasites of frogs from an equatorial African montane forest in western Uganda. *Journal of Parasitology,* 96(2)**:**448–450.

Vhembe Biosphere Reserve. 2021. *Vhembe Biosphere Reserve: Limpopo* [Online]. Available: https://www.vhembebiosphere.org/ [Accessed November 29, 2022].

Schwetz, J. 1930. Notes protozoologiques. Les hématozoaires des grenouilles et des crapauds de Stanleyville (Congo Belge). *Annales de Parasitologie Humaine et Comparée*, 8(2):122–134.

Shippen-Lentz, D., Ray, R., Scaife, J.G., Langsley, G. & Vezza, A.C. 1987. Characterization and complete nucleotide sequence of a 5.8 S ribosomal RNA gene from *Plasmodium falciparum*. *Molecular and Biochemical Parasitology,* 22(2–3)**:**223–231.

Siddall, M.E. 1995. Phylogeny of adeleid blood parasites with a partial systematic revision of the haemogregarine complex. *Journal of Eukaryotic Microbiology,* 42(2)**:**116–125.

Silvano, D.L. & Segalla, M.V. 2005. Conservation of Brazilian amphibians. *Conservation Biology,* 19(3)**:**653–658.

Sinden, R.E. & Moore, J. 1974. Fine structure of the sporozoite of *Schellackia occidentalis*. *The Journal of Parasitology,* 60(4):666–673.

Smith, T.G. 1996. The genus *Hepatozoon* (Apicomplexa: Adeleina). *The Journal of Parasitology***,** 565–585.

Smith, T.G., Desser, S.S. & Hong, H. 1994. Morphology, ultrastructure and taxonomic status of *Toddia* sp. in northern water snakes (*Nerodia sipedon sipedon*) from Ontario, Canada. *Journal of Wildlife Diseases,* 30(2)**:**169–175.

Smith, T.G., Kim, B. & Desser, S.S. 1999. Phylogenetic relationships among *Hepatozoon* species from snakes, frogs and mosquitoes of Ontario, Canada. *International Journal for Parasitology,* 29**:**293–304.

Spodareva, V.V., Grybchuk-Ieremenko, A., Losev, A., Votýpka, J., Lukeš, J., Yurchenko, V. & Kostygov, A.Y. 2018. Diversity and evolution of anuran trypanosomes: insights from the study of European species. *Parasites & Vectors,* 11(1)**:**1–12.

Stebbins, R.C. & Cohen, N.W. 1995. *A Natural History of Amphibians*, Princeton University Press.

Stewart, M.M. 1967. *Amphibians of Malawi,* State University of New York Press, Albany., SUNY Press.

Stuart, S.N., Chanson, J.S., Cox, N.A., Young, B.E., Rodrigues, A.S., Fischman, D.L. & Waller, R.W. 2004. Status and trends of amphibian declines and extinctions worldwide. *Science,* 306(5702)**:**1783–1786.

Tanabe, M. 1931. Studies on the blood inhabiting Protozoa of the frog. *Keijo Journal of Medicine,* 2**:**53–71.

Tavaré, S. 1986. Some probabilistic and statistical problems in the analysis of DNA sequences. *Lectures on Mathematics in the Life Sciences,* 17:57–86.

Telford Jr, S.R. & Jacobson, E.R. 1993. Lizard erythrocytic virus in east African chameleons. *Journal of Wildlife Diseases,* 29(1)**:**57–63.

Telford, S.R. 2009. *Hemoparasites of the Reptilia Color Atlas and Text*, CRC Press.

Endangered Wildlife Trust. 2018. *Soutpansberg Protected Area: A Unique Mountain Paradise*.

Endangered Wildlife Trust. 2022. *Soutpansberg Protected Area*. https://ewt.org.za/what-we-do/conserving-habitats/spa-programme/. Date of acces: 29 November, 2022

Tse, B., Barta, J., Desser, S. 1986. Comparative ultrastructural features of the sporozoite of *Lankesterella minima* (Apicomplexa) in its anuran host and leech vector. *Canadian Journal of Zoology,* 64(10):2344–2347.

Ujvari, B., Madsen, T. & Olsson, M. 2004. High prevalence of *Hepatozoon* spp. (Apicomplexa, Hepatozoidae) infection in water pythons (*Liasis fuscus*) from tropical Australia. *Journal of Parasitology,* 90(3)**:**670–672.

UNESCO. 2009. *Vhembe Biosphere Reserve, South Africa.* https://en.unesco.org/biosphere/Vhembe/Vhembe. Date of access: 29 November, 2022.

Úngari, L.P., Netherlands, E.C., Santos, A.L.Q., De Alcantara, E.P., Emmerich, E., Da Silva, R.J. & O'dwyer, L.H. 2020. A new species, *Dactylosoma piperis* n. sp. (Apicomplexa, Dactylosomatidae), from the pepper frog *Leptodactylus labyrinthicus* (Anura, Leptodactylidae) from Mato Grosso State, Brazil. *Parasite,* 27.

Úngari, L.P., Netherlands, E.C., Santos, A.L.Q., De Alcantara, E.P., Emmerich, E., Da Silva, R.J. & O'dwyer, L.H. 2021. New insights on the diversity of Brazilian anuran blood parasites: With the description of three new species of *Hepatozoon* (Apicomplexa: Hepatozoidae) from Leptodactylidae anurans. *International Journal for Parasitology: Parasites and Wildlife,* 14**:**190–201.

Upton, S.J. 2000. Suborder Eimeriorina Léger, 1911. *The Illustrated Guide to the Protozoa.* 2nd ed. Allen Press Inc., Lawrence, KA, 1:318–339.

Van As, J., Davies, A.J. & Smit, N.J. 2013. *Hepatozoon langii* n. sp. and *Hepatozoon vacuolatus* n. sp. (Apicomplexa: Adeleorina: Hepatozoidae) from the crag lizard (Sauria: Cordylidae) *Pseudocordylus langi* from the North Eastern Drakensberg escarpment, Eastern Free State, South Africa. *Zootaxa,* 3608(5)**:**345–356.

Vanhove, M.P.M., Kmentová, N., Luus-Powell, W.J., Netherlands, E.C., De Buron, I. & Barger, M.A. 2022. A snapshot of parasites in tropical and subtropical freshwater wetlands: modest attention for major players. *Fundamentals of Tropical Freshwater Wetlands.* Elsevier, 417–485.

Viviers, J. 2013. *Seasonal migration and reproductive behaviour of the Common River Frog (Amietia quecketti).* PhD, North-West University.

Wake, D.B. & Koo, M.S. 2018. Amphibians. *Current Biology,* 28(21)**:**1237–1241.

Zechmeisterova, K., de Bellocq, J.G & Siroky, P. 2019. Diversity of *Karyolysus* and *Schellackia* from the Iberian lizard *Lacerta schreiberi* with sequence data from engorged ticks. *Parasitology,* 146(13):1690–1698.

Zhang, C. & Rikihisa, Y. 2004. Proposal to transfer *Aegyptianella ranarum*, an intracellular bacterium of frog red blood cells, to the family Flavobacteriaceae as *Candidatus hemobacterium ranarum* comb. nov. *Environmental Microbiology,* 6(6)**:**568–573.

Žičkus, T. 2002. The first data on the fauna and distribution of blood parasites of amphibians in Lithuania. *Acta Zoologica Lituanica,* 12(2)**:**197–202.

Zimkus, B.M. & Schick, S. 2010. Light at the end of the tunnel: insights into the molecular systematics of East African puddle frogs (Anura: Phrynobatrachidae). *Systematics and Biodiversity,* 8(1)**:**39–47.

Appendix A

Table A1: List of all 132 sample localities across the Soutpansberg mountain range.

Site	Description	Owner	Latitude	Longtitude	Elevation	Transect
1	Pond 1 in Luvuvhu River	Hannes Badenhorst	-23.07283	30.07105	808	3
2	Pond 2 in Luvuvhu River	Hannes Badenhorst	-23.07351	30.06461	789	3
3	Quarry; Very shallow	Koos Steyn	-23.06198	30.06808	831	3
4	Well & swampy area	Koos Steyn	-23.05502	30.07083	827	3
5	Pond and stream	Frans du Toit (Welgevonden)	-23.05526	30.07268	830	3
6	Irrigation pond	Alan White	-23.05316	30.08173	849	3
7	Stream		-23.05085	30.08879	863	3
8	Pond	Fritz Arends	-23.05157	30.08643	867	3
9	Nursery pond	Gate	-23.05553	30.08959	898	3
10	Forestry stream	Andre Kruger	-23.01608	30.15228	1118	3
11	Big dam on border	Andre Kruger	-23.01183	30.15477	1099	3
12	Big dam in forest	Andre Kruger	-23.01551	30.16342	1135	3
13	Big dam in forest	Andre Kruger	-23.01718	30.11901	1112	3
14		Maclands dam	-23.08441	30.15063	722	3
15	Crocs and Hippo	Mueried dam - Jaco Roux	-23.05554	30.1483	774	3
16	Pond - Malume dam 1	Elsje Joubert	-23.04831	30.26634	703	3
17	Pond - Malume dam 2	Elsje Joubert	-23.04759	30.2552	720	3
18	Garden pond	Andre Olwage	-23.1101	29.90837	919	2
19	Garden pond 10m apart	Andre Olwage	-23.1101	29.90837	919	2
20	Game pond	Adrian de Beer	-23.10991	29.90127	903	2
21	Pool on road next to fence, muddy pool	Adrian de Beer	-23.089783	29.908337	916	2
22	Grassy pan	Andre Olwage	-23.110477	29.908861	919	2
23	Sunset lodge	Murray Stewart	-23.114843	30.079296	764	3

24	Borrow pit	Along N1	-23.117464	29.896009	914	2
25	Muddy pool 1 Vivo	Pieter Klopper	-23.250922	29.450407	897	1
26	Muddy pool 2 Vivo	Pieter Klopper	-23.241774	29.46246	946	1
27	Grassy pan	Pieter Klopper	-23.244329	29.448209	933	1
28	Luande Mountain - School pond	Murray Stewart	-23.045264	30.125178	917	3
29	Luande Mountain - pool	Murray Stewart	-23.049057	30.118416	1209	3
30	Muddy pond	Francois Pauer	-22.909694	29.551077	745	1
31	Muddy pond	Francois Pauer	-22.914985	29.542766	770	1
32	Hunter camp	Francois Pauer	-22.909727	29.557249	765	1
33	Unknown farmer	Pond near road	-23.200395	29.405795	921	1
34	Goro reserve	Dave Dewsnap	-22.9587	29.428	854	1
35	Hangklip picnic site	Hanglip	-22.99972	29.88277	1520	2
36	Koos Steyn House	Koos Steyn	-23.05944	30.06888	849	3
37	Sunset road	Sunset road	-23.09164	30.08808	267	3
38	Bola Bola	Paul Roux	-22.92031	29.92983	927	2
39	Wallicedale farm	Brian O Regan	-22.95513	29.93301	1018	2
40	Bass dam	Theo Schlieben	-22.98025	30.00542	1217	2
41	Mountain stream N		-22.97087	30.16923	924	3
42	Rubber lined pond	Andrew Smit	-22.99251	30.08576	1291	3
43	Eart walled pond	Pierre Thomas	-22.99552	30.07191	1184	3
44	Vlei area	Pierre Thomas	-22.99252	30.0761	1210	3
45	Small burrow pit	Pierre Thomas	-22.99351	30.07407	1194	3
46	Concrete dam big	Gerco Serfontein	-23.04193	30.10829	986	3
47	Concrete dam small	Gerco Serfontein	-23.03876	30.10535	1024	3
48	Lajuma - wetland	Jabu & Bibi	-23.03599	29.42872	1324	1
49	Lajuma - rock pool	Jabu & Bibi	-23.033004	29.42352	1350	1
50	Lajuma - forest stream	Jabu & Bibi	-23.032175	29.4239	1368	1

51	Lajuma - Camp	Jabu & Bibi	-23.03925	29.44934	1311	1
52	Lajuma - Pool above rondawel	Jabu neighbour	-23.03224	29.42384	1350	1
53	Lajuma - Forest stream	Jabu neighbour	-23.03034	29.4216	1364	1
54	Lajuma - Ian's house	Jabu & Bibi	-23.03833	29.44051	1304	1
55	Lajuma - Stream south of camp	Jabu & Bibi	-23.03752	29.45322	1297	1
56	Lajuma - Pool against rock face	Jabu & Bibi	-23.03678	29.44447	1327	1
57	Lajuma - Pool below rock face	Jabu & Bibi	-23.03714	29.44269	1258	1
58	Lajuma - Forest patch	Jabu & Bibi	-23.03739	29.44145	1304	1
59	Lajuma - Student camp	Jabu & Bibi	-23.03788	29.4428	1319	1
60	Lajuma - Garden pond 1	Jabu & Bibi	-23.03831	29.44053	1295	1
61	Blouberg - Floodplain	Johan van Wyk	-23.01354	29.14903	841	Blouberg
62	Blouberg - Floodplain	Johan van Wyk	-23.01585	29.1514	836	Blouberg
63	Blouberg - Floodplain pan pump	Johan van Wyk	-23.01662	29.15722	832	Blouberg
64	Blouberg - Pumped water hole	Johan van Wyk	-23.02121	29.10537	889	Blouberg
65	Blouberg - Sand road	Johan van Wyk	-23.00778	29.0641	921	Blouberg
66	Blouberg - Buffelpan	Johan van Wyk	-22.99739	29.09465	901	Blouberg
67	Ebbedam	Forestry	-22.98839	30.25644	1300	3
68	Roadside pool	Forestry	-23.0482	30.23491	719	3
69	Pond and vlei are	Forestry	-23.05529	30.2211	743	3
70	Forestry - Mountain stream	Tatenda	-22.90531	30.34828	1084	3
71	Big mountain lake	Tatenda	-22.90297	30.35149	1084	3
72	Forestry - Mountain stream	Tatenda	-22.89419	30.35094	1109	3
73	Mountain seep	Tatenda	-22.91918	30.32814	1206	3
74	Grassland	Tatenda	-22.92306	30.30678	1062	3
75	Stream	Tatenda	-22.91972	30.30964	1042	3
76	Pool	Tatenda	-22.96585	30.39497	638	3
77	Cango hunting camp	Gerhard du Plesis	-22.85586	29.54781	752	1

78	Muddy pan	Gerhard du Plesis	-22.85821	29.56	744	1
79	Muddy pan	Gerhard du Plesis	-22.85349	29.57663	740	1
80	Muddy pan	Gerhard du Plesis	-22.85733	29.58113	743	1
81	On road in game camp	Gerhard du Plesis	-22.8578	29.55987	750	1
82	Near gate between farms	Gerhard du Plesis	-22.86007	29.56423	754	1
83	Semi permanent pool	Nico Konig	-22.80849	29.46644	767	1
84	Well vegetated pan	Nico Konig	-22.81697	29.46972	774	1
85	Dirt road on farm	Nico Konig	-22.8121	29.45074	780	1
86	Goro reserve - Game trough	Dave Dewsnap	-22.93965	29.43107	813	1
87	Goro reserve - Game pond	Dave Dewsnap	-22.94361	29.41348	817	1
88	Goro reserve - Clear stream crossing road	Dave Dewsnap	-22.94076	29.4183	819	1
89	Goro reserve - Small puddle on road	Dave Dewsnap	-22.93853	29.42223	815	1
90	Stream below house, clear water	Lourens Botes	-22.85587	29.54771	754	1
91	Tilapia pond	Lourens Botes	-22.89052	29.87216	822	2
92	Big muddy farm dam	Johan en Marietha Botha	-22.62986	30.0622	599	2
93	Game trough	Johan en Marietha Botha	-22.64684	30.05504	614	2
94	Stream in sandy area	Johan en Marietha Botha	-22.66917	30.02192	641	2
95	Dam and seep	Johan en Marietha Botha	-22.65491	30.04615	622	2
96	Levubu - Hoffman house	Francois & Le Roux Hoffman	-23.07697	30.25459	738	3
97	Levubu - Seep	Francois & Le Roux Hoffman	-23.07476	30.25197	679	3
98	Levubu - Small stream, muddy	Francois & Le Roux Hoffman	-23.07463	30.25262	678	3
99	Levubu - Vlei area with seep	Francois & Le Roux Hoffman	-23.07428	30.25688	675	3
100	Levubu - Big dam	Francois & Le Roux Hoffman	-23.07152	30.26883	658	3
101	Levubu - Garden pond, grandma house	Francois & Le Roux Hoffman	-23.07288	30.26565	692	3
102	Faure base camp	Guide Isaiah	-22.26694	29.33027	620	1
103	Muddy pan	Guide Isaiah	-22.29263	29.36215	618	1
104	Muddy pan	Guide Isaiah	-22.29637	29.36256	615	1

105	Concrete walled dam	Guide Isaiah	-22.29465	29.34511	614	1
106	Dam at Werner house	Guide Isaiah	-22.35326	29.36349	640	1
107	Big dam, red water	Guide Isaiah	-22.33544	29.33546	597	1
108	Overflow big dam	Guide Isaiah	-22.34320	29.32720	593	1
109	Bank of big dam, pool	Guide Isaiah	-22.34322	29.32720	593	1
110	River crossing	Guide Isaiah	-22.425	29.345	518	1
111	River	Guide Isaiah	-22.34138	29.34138	614	1
112	N1 Road	Highway	-22.89212	29.670302	771	1
113	N1 Road	Highway	-23.20043	29.4058	921	1
114	N1 Road	Highway	-23.18692	29.36991	944	1
115	N1 Road	Highway	-23.19301	29.34436	968	1
116	N1 Road	Highway	-23.19738	29.32089	968	1
117	N1 Road	Highway	-23.20418	29.2947	984	1
118	N1 Road	Highway	-23.17369	29.26735	943	1
119	N1 Road	Highway	-23.0814	29.27221	915	1
120	N1 Road	Highway	-22.99119	29.25948	829	1
121	N1 Road	Highway	-22.9551	29.32148	796	1
122	N1 Road	Highway	-22.93525	29.37573	820	1
123	N1 Road	Highway	-22.29258	29.43331	821	1
124	N1 Road	Highway	-22.907433	29.59647	763	1
125	N1 Road	Highway	-22.902661	29.6249	740	1
126	N1 Road	Highway	-22.88786	29.60975	735	1
127	N1 Road	Highway	-22.908	29.61632	745	1
128	N1 Road	Highway	-22.89799	29.60962	738	1
129	N1 Road	Highway	-22.89873	29.64272	759	1
130	N1 Road	Highway	-22.879694	29.73049	801	2
131	N1 Road	Highway	-22.88601	29.69473	783	1

132	Vlei & spring	Koos Steyn	-23.055094	30.069498	819	3

Appendix B

Table B1: Full list of anuran species across the three transects from 2019 – 2021.

		2020	2021	2019	2020	2021	2019	2020	2021
Species name	**Family**	**Transect 1**		**Transect 2**			**Transect 3**		
Amietia delalandii	Pyxicephalidae	4	4	1	1	6	17	71	5
Arthroleptis stenodactylus	Arthroleptidae								6
Breviceps adspersus	Brevicipitidae	1	1						
Breviceps s. taeniatus	Brevicipitidae		1		6				
Cacosternum boettgeri	Pyxicephalidae				1			12	
Chiromantis xerampelina	Rhacophoridae	4	7	2	5	8		1	
Hemisus marmoratus	Hemisotidae							1	
Hyperolius marmoratus	Hyperoliidae	3	7	10			4	23	
Hyperolius pusillus	Hyperoliidae								1
Kassina senegalensis	Hyperoliidae	5	3	2	3	2		6	
Phrynobatrachus mababiensis	Phrynobatrachidae		1			1		15	4
Phrynobatrachus natalensis	Phrynobatrachidae								2
Phrynomantis bifasciatus	Microhylidae	1	2	8	10	4		1	
Poyntonophrynus fenoulheti	Bufonidae	10	10						
Ptychadena anchietae	Ptychadenidae	2	7	12	1	7		21	
Ptychadena mossambica	Ptychadenidae			4					
Ptychadena uzungwensis	Ptychadenidae							20	
Pyxicephalus edulis	Pyxicephalidae	3	5		4	9			
Schismaderma carens	Bufonidae	5	1	1	6			5	1
Sclerophrys garmani	Bufonidae		4	6		2			
Sclerophrys gutturalis	Bufonidae			4			4	11	
Sclerophrys pusilla	Bufonidae		9				1	4	
Strongylopus fasciatus	Pyxicephalidae		2					10	
Strongylopus grayii	Pyxicephalidae	2	3						
Tomopterna sp.	Pyxicephalidae	10	7		2	6		12	
Xenopus laevis	Pipidae	4			2		1	3	2
Xenopus muelleri	Pipidae		11		2				
Total frogs collected		54	83	50	43	46	27	216	21
Total frog species		13	17	10	12	10	5	16	7
Total frogs collected per transect		137		139			264		
Total frog species per transect		18		18			19		
Grand total		540 adult frogs collected							
Grand total species		27 species							

Appendix C

Table C1: Distribution of tadpoles collected across the three transects from 2020 – 2021.

		2020	***2021***	***2020***	***2021***	***2020***	***2021***
Species name	**Family**	**Transect 1**		**Transect 2**		**Transect 3**	
Amietia delalandii	Pyxicephalidae	3	3		2	53	
Cacosternum boettgeri	Pyxicephalidae	1	1	10			
Chiromantis xerampelina	Rhacophoridae	14	9		27		5
Hemisus marmoratus	Hemisotidae		6	6			1
Hyperolius marmoratus	Hyperoliidae		1		4	3	
Kassina senegalensis	Hyperoliidae		8	13		2	26
Leptopelis mossambica	Arthroleptidae					2	
Phrynobatrachus mababiensis	Phrynobatrachidae						1
Phrynobatrachus natalensis	Phrynobatrachidae					10	
Phrynomantis bifasciatus	Microhylidae	18	8	1			
Poyntonophrynus fenoulheti	Bufonidae		10				
Ptychadena anchietae	Ptychadenidae	3	1	4	1	26	83
Ptychadena uzungwensis	Ptychadenidae					4	
Pyxicephalus adspersus	Ptychadenidae	8					
Pyxicephalus edulis	Pyxicephalidae				1		
Schismaderma carens	Bufonidae			2			
Sclerophrys garmani	Bufonidae		2	1	1		
Sclerophrys gutturalis	Bufonidae		2		22	4	6
Sclerophrys sp.	Bufonidae					1	
Strongylopus fasciatus	Pyxicephalidae		1			4	
Strongylopus grayii	Pyxicephalidae	4	4				
Tomopterna sp.	Pyxicephalidae	7	28		1	2	12
Xenopus laevis	Pipidae			10		4	1
Xenopus muelleri	Pipidae	5	6				
Total tadpoles collected		63	90	47	59	115	135
Total tadpole species		9	15	8	8	12	8
Total tadpole collected per transect		153		106		250	
Total tadpole species per transect		18		18		19	
Grand total		509 tadpoles collected					
Grand total species		24 tadpole species					

Appendix D

Table D1: List of sequence data used to create the 18S-COI concatenated tree.

	18S						COI					
	Assesion code	Species name		Host	Locality	Souce	Assesion code	Species name		Host	Locality	Souce
1	KC305191	*Eimeria*	*meleagrimitis*	Turkey	USA	El-Sherry et al., 2013	KC346353	*Eimeria*	*meleagrimitis*	Turkey	USA	El-Sherry et al., 2013
2	FR745914	*Eimeria*	*adenoeides*	Turkey	Czech Republic	Poplstein & Vrba, 2011	FR846202	*Eimeria*	*adenoeides*	Turkey	Czech Republic	Poplstein & Vrba, 2011
3	KT184349	*Eimeria*	*necatrix*	Chicken	Canada	Ogedengbe et al., 2016	HM771680	*Eimeria*	*necatrix*	Chicken	Canada	Ogedengbe et al., 2016
4	KT184354	*Eimeria*	*tenella*	Chicken	Canada	Ogedengbe et al., 2016	HM771676	*Eimeria*	*tenella*	Chicken	Canada	Ogedengbe et al., 2011
5	KT184346	*Eimeria*	*maxima*	Red junglefowl; *Gallus gallus*	Canada	Ogedengbe et al., 2011	HM771684	*Eimeria*	*maxima*	Red junglefowl; *Gallus gallus*	Canada	Ogedengbe et al., 2011
6	KT184345	*Eimeria*	*maxima*	Red junglefowl; *Gallus gallus*	Canada	Ogedengbe et al., 2011	HM771685	*Eimeria*	*maxima*	Red junglefowl; *Gallus gallus*	Canada	Ogedengbe et al., 2011
7	KT184352	*Eimeria*	*praecox*	Red junglefowl; *Gallus gallus*	Canada	Ogedengbe et al., 2016	KT184378	*Eimeria*	*praecox*	Red junglefowl; *Gallus gallus*	Canada	Ogedengbe et al., 2016
8	KT184356	*Eimeria*	*zuernii*	Cattle; *Bos taurus*	Canada	Ogedengbe et al., 2016	HM771687	*Eimeria*	*zuernii*	Cattle; *Bos taurus*	Canada	Ogedengbe et al., 2011
9	KT184357	*Isospora*	*sp.*	*Canary; Serinus canaria*	Canada	Ogedengbe et al., 2016	KP658103	*Isospora*	*sp.*	Voucher	Canada	Ogedengbe et al., 2015
10	KF854254	*Isospora*	*gryphoni*	x	x	unpiblish by Ogedengbe	KC346355	*Isospora*	*gryphoni*	Turkey	USA	El-Sherry et al., 2013
11	KF648870	*Isospora*	*greineri*	Superb Glossy Starling; *Lamprotornis superbus*	Canada	Hafeez et al., 2013	KF648868	*Isospora*	*greineri*	Superb Glossy Starling; *Lamprotornis superbus*	Canada	Hafeez et al., 2013
12	KF648871	*Isospora*	*superbusi*	Superb Glossy Starling; *Lamprotornis superbus*	Canada	Hafeez et al., 2013	KF648869	*Isospora*	*sp.*	Superb Glossy Starling; *Lamprotornis superbus*	Canada	Hafeez et al., 2013
13	KT184332	*Caryospora*	*cf. bigenetica*	Massasauga snake; *Sistrurus catenatus*	Canada	Ogedengbe et al., 2016	KP658102	*Caryospora*	*bigenetica*	voucher	Canada	Ogedengbe & Barta, 2015
14	KT184331	*Caryospora*	*cf. bigenetica*	Massasauga snake; *Sistrurus catenatus*	Canada	Ogedengbe et al., 2016	KF859856	*Caryospora*	*cf. bigenetica*	Snake; *Sistrurus catenatus*	Canada	Ogedengbe et al., unpublish
15	L37415	*Toxoplasma*	*gondii*	strain	Australia	Luton et al., 1995	HM771689	*Toxoplasma*	*gondii*	Cat; *Felis catus*	Canada	Ogedengbe et al., 2011
16	KT224380	*Isospora*	*neochmiae*	Red-browed finch; *Neochmia temporalis*	Australia	Yang et al., 2016	KT224378	*Isospora*	*neochmiae*	red-browed finch; *Neochmia temporalis*	Australia	Yang et al., 2016
17	JQ993669	*Isospora*	*sp.*	European mole; *Talpa europaea*	Czech Republic	Kvicerova & Hypsa, 2013	JQ993712	*Isospora*	*sp.*	Mole; *Talpa europaea*	Czech Republic	Kvicerova & Hypsa, 2013
18	KJ700635	*Eimeria*	*collieie*	Oblong turtle; *Chelodina colliei*	Australia	Yang et al., 2015	KJ700637	*Eimeria*	*collieie*	Freshwater turtle; *Chelodina colliei*	Australia	Yang et al., 2015
19	KT184335	*Eimeria*	*alabamensis*	Cattle; *Bos taurus*	Canada	Ogedengbe et al., 2016	KT184376	*Eimeria*	*alabamensis*	Cattle; *Bos taurus*	Canada	Ogedengbe et al., 2016
20	KU215888	*Eimeria*	*macusaniensis*	Llama, *Lama guanicoe*	Argentina	Petrigh & Fugassa, 2015	KU215889	*Eimeria*	*macusaniensis*	Llama, *Lama guanicoe*	Argentina	Petrigh & Fugassa, 2015
21	AF080614	*Eimeria*	*falciformis*	x	x	Barta et al., 2001	HM771682	*Eimeria*	*falciformis*	Rodent; *Mus musculus*	Canada	Ogedengbe et al., 2011
22	JQ993665	*Eimeria*	*nafuko*	Silver mole rat; *Heliophobius argenteocinereus*	Czech Republic	Kvicerova & Hypsa, 2013	JQ993708	*Eimeria*	*nafuko*	Mole rat; *Heliophobius argenteocinereus*	Czech Republic	Kvicerova & Hypsa, 2013
23	JQ993666	*Eimeria*	*burdai*	Silver mole rat; *Heliophobius argenteocinereus*	Czech Republic	Kvicerova & Hypsa, 2013	JQ993709	*Eimeria*	*burdai*	Mole rat; *Heliophobius argenteocinereus*	Czech Republic	Kvicerova & Hypsa, 2013
24	JQ993649	*Eimeria*	*caviae*	Guinea pig; *Cavia porcellus*	Czech Republic	Kvicerova & Hypsa, 2013	JQ993689	*Eimeria*	*caviae*	Guinea pig; *Cavia porcellus*	Czech Republic	Kvicerova & Hypsa, 2013
25	KT360995	*Eimeria*	*ferrisi*	House mouse; *Mus musculus*	Czech Republi	Hofmannova et al., 2016	KT361028	*Eimeria*	*ferrisi*	Rodent; *Mus musculus*	Czech Republi	Hofmannova et al., 2016
26	KT360977	*Eimeria*	*lancasterensis*	Eastern gray squirrel; *Sciurus carolinensis*	Italy	Hofmannova et al., 2016	KT361005	*Eimeria*	*lancasterensis*	Squirrel; *Sciurus carolinensis*	Italy	Hofmannova et al., 2016
27	KT184353	*Eimeria*	*tamiasciuri*	American red squirrel; *Tamiasciurus hudsonicus*	Canada	Ogedengbe et al., 2016	KT184375	*Eimeria*	*tamiasciuri*	Squirrel; *Tamiasciurus hudsonicus*	Canada	Ogedengbe et al., 2016
28	JQ993659	*Eimeria*	*alorani*	Striped field mouse; *Apodemus agrarius*	Czech Republi	Kvicerova & Hypsa, 2013	JQ993701	*Eimeria*	*alorani*	Rodent; *Apodemus agrarius*	Czech Republi	Kvicerova & Hypsa, 2013
29	KT184350	*Eimeria*	*papillata*	House mouse; *Mus musculus*	USA	Ogedengbe et al., 2016	KT184377	*Eimeria*	*papillata*	Rodent; *Mus musculus*	USA	Ogedengbe et al., 2016
30	JQ993647	*Eimeria*	*cahirinensis*	Eastern spiny mouse; *Acomys dimidiatus*	Czech Republic	Kvicerova & Hypsa, 2013	JQ993687	*Eimeria*	*cahirinensis*	Rodent; *Acomys dimidiatus*	Czech Republic	Kvicerova & Hypsa, 2013
31	JQ993651	*Eimeria*	*nkaka*	Tree pangolin; *Phataginus tricuspis*	Czech Republic	Kvicerova & Hypsa, 2013	JQ993697	*Eimeria*	*nkaka*	Pangolin; *Phataginus tricuspis*	Czech Republic	Kvicerova & Hypsa, 2013
32	EU025113	*Eimeria*	*tenella*	Chicken	Canada	Ogedengbe et al., 2011	EU025109	*Eimeria*	*tenella*	Chicken	Canada	Ogedengbe et al., 2011
33	JN596589	*Eimeria*	*pavonina*	Peafowl	Germany	Hauck & Hafez, 2011	JN596590	*Eimeria*	*pavonina*	Peafowl	Germany	Hauck & Hafez, 2011
34	FJ236377	*Eimeria*	*cf. mivati*	Chicken	USA	Schwarz et al., 2009	FJ236433	*Eimeria*	*cf. mivati*	Chicken	USA	Schwarz et al., 2009
35	KT184351	*Eimeria*	*praecox*	Red junglefowl; *Gallus gallus*	Canada	Ogedengbe et al., 2016	KT184378	*Eimeria*	*praecox*	Red junglefowl; *Gallus gallus*	Canada	Ogedengbe et al., 2016
36	FJ236345	*Eimeria*	*maxima*	Chicken	USA	Schwarz et al., 2009	FJ236387	*Eimeria*	*maxima*	Chicken	USA	Schwarz et al., 2009
37	KU351728	*Eimeria*	*brasiliensis*	Cattle; *Bos taurus*	Turkey	Yildirim et al., 2015	KU351698	*Eimeria*	*brasiliensis*	Cattle; *Bos taurus*	Turkey	Yildirim et al., 2015
38	KU351729	*Eimeria*	*bukidnonensis*	Cattle; *Bos taurus*	Turkey	Yildirim et al., 2015	KU351700	*Eimeria*	*bukidnonensis*	Cattle; *Bos taurus*	Turkey	Yildirim et al., 2015
39	KU052235	*Eimeria*	*auburnensis*	Cattle; *Bos taurus*	Turkey	Yildirim et al., 2015	KU351692	*Eimeria*	*auburnensis*	Cattle; *Bos taurus*	Turkey	Yildirim et al., 2015
40	KU052237	*Eimeria*	*cylindrica*	Cattle; *Bos taurus*	Turkey	Yildirim et al., 2015	KU351687	*Eimeria*	*cylindrica*	Cattle; *Bos taurus*	Turkey	Yildirim et al., 2015
41	KU351730	*Eimeria*	*illinoisensis*	Cattle	Turkey	Yildirim et al., 2015	KU351703	*Eimeria*	*illinoisensis*	Cattle	Turkey	Yildirim et al., 2015
42	KT184336	*Eimeria*	*bovis*	Cattle; *Bos taurus*	Canada	Ogedengbe et al., 2016	KT184372	*Eimeria*	*bovis*	Cattle; *Bos taurus*	Canada	Ogedengbe et al., 2016
43	KT184334	*Eimeria*	*ahsata*	Sheep; *Ovis aries*	Canada	Ogedengbe et al., 2016	KT184373	*Eimeria*	*ahsata*	Sheep; *Ovis aries*	Canada	Ogedengbe et al., 2016
44	HQ173828	*Eimeria*	*coecicola*	Rabbit	Czech Republic	Oliveira et al., 2010	JQ993690	*Eimeria*	*coecicola*	Rabbit; *Oryctolagus cuniculus*	Czech Republi	Kvicerova & Hypsa, 2013
45	KF225636	*Eimeria*	*quokka*	Quokka; *Setonix brachyurus*	Australia	Austen et al., 2014	KF225637	*Eimeria*	*quokka*	Quokka; *Setonix brachyurus*	Australia	Austen et al., 2014
46	KF225639	*Eimeria*	*setonicis*	Quokka; *Setonix brachyurus*	Australia	Austen et al., 2014	KF225638	*Eimeria*	*setonicis*	Quokka; *Setonix brachyurus*	Australia	Austen et al., 2014
47	JQ392575	*Eimeria*	*macropodis*	Wallaby; *Macropus eugenii*	Australia	Hill et al., 2012	JQ392578	*Eimeria*	*macropodis*	Wallaby; *Macropus eugenii*	Australia	Hill et al., 2012
48	FJ829320	*Eimeria*	*trichosuri*	Mountain brushtail possum; *Trichosurus cunninghami*	Australia	Power et al., 2009	JN192136	*Eimeria*	*trichosuri*	Voucher	Canada	Ogedengbe et al., 2015
49	KU180241	*Isospora*	*amphiboluri*	Central bearded dragon; *Pogona vitticeps*	Spain	Megia-Palma et al., 2016	KR108297	*Isospora*	*amphiboluri*	Voucher	Canada	Hafeez & Barta, 2015
50	HG793041	*Eimeria*	*dispersa*	Turkeys and Bobwhite Quail	Czech Republic, Poland and Germany	Vrba & Pakandl, 2014	HG793048	*Eimeria*	*dispersa*	Turkeys and Bobwhite Quail	Czech Republic, Poland and Germany	Vrba & Pakandl, 2014
51	KU140597	*Eimeria*	*purpureicephali*	Rred-Capped Parrot; *Purpureicephalus spurius*	Australia	Yang et al., 2016	KU140598	*Eimeria*	*purpureicephali*	Rred-Capped Parrot; *Purpureicephalus spurius*	Australia	Yang et al., 2016
52	HG793045	*Eimeria*	*innocua*	Turkeys and Bobwhite Quail	Czech Republic, Poland and Germany	Vrba & Pakandl, 2014	HG793049	*Eimeria*	*innocua*	Turkeys and Bobwhite Quail	Czech Republic, Poland and Germany	Vrba & Pakandl, 2014
53	AF111183	*Cyclospora*	*cayetanensis*	Monkeys	Ethiopia	Eberhard et al., 1999	KP658101	*Cyclospora*	*cayetanensis*	Humans	USA	Ogedengbe et al., 2015
54	KJ767187	*Eimeria*	*paludosa*	Dusky moorhen	Australia	Yang et al., 2014	KJ767189	*Eimeria*	*paludosa*	Dusky moorhen	Australia	Yang et al., 2014
55	KR779871	*Choleoeimeria*	*pogonae*	Western bearded dragon; *Pogona minor minor*	Australia	Yang et al., 2015	KR779872	*Choleoeimeria*	*pogonae*	x	Australia	Yang et al., 2015
56		*Lankesterella*	*sp*	Common river frog; *Amietia delalandii*	South Africa	This study	This study	*Lankesterella*	*sp*	Common rivier frog; *Amietia delalandii*	South Africa	This study
57							KT184381	*Lankesterella*	*minima*	Frog; *Lithobates clamitans*	Canada	Ogedengbe et al., 2016
58							KT184382	*Lankesterella*	*minima*	Frog; *Lithobates clamitans*	Canada	Ogedengbe et al., 2016

Appendix E

Table E1: Multiple alignment distance matrix percentage (%) comparison between *Hepatozoon theileri* samples generated in the current study. Alignment was checked and a distances matrix table was created within UGENE.

Code	Species	T3	P5	P1	P2	P3	P6	P4	SPB4	SPB3	SPB1	SPB2	P13	P11	P14	P12	P7	P8	P9	P10	SPB7	SPB5	SPB6	SPB8
T3	AE210412A14 *Hepatozoon theileri*	0	7	4	5	5	5	5	11	11	11	12	4	4	8	9	2	6	3	5	13	12	11	10
P5	AR150429A268 *Hepatozoon theileri*	7	0	3	3	3	3	3	8	9	8	10	6	5	15	15	9	13	9	12	14	11	18	17
P1	AR150429A268 *Hepatozoon theileri*	4	3	0	0	1	1	1	7	7	7	8	2	3	12	12	6	10	6	9	10	9	15	14
P2	AR150504A274 *Hepatozoon theileri*	5	3	0	0	0	0	0	7	8	6	7	3	3	12	13	6	10	7	9	11	9	15	14
P3	AR150318A165 *Hepatozoon theileri*	5	3	1	0	0	1	1	7	8	7	7	3	3	13	13	7	10	7	10	11	9	16	14
P6	AR150428A253 *Hepatozoon theileri*	5	3	1	0	1	0	0	6	7	6	7	3	3	13	13	7	10	7	10	11	10	16	14
P4	AR150428A253 *Hepatozoon theileri*	5	3	1	0	1	0	0	6	7	6	7	3	3	13	13	7	10	7	10	11	10	16	14
SPB4	AL201201C1 *Hepatozoon theileri*	11	8	7	7	7	6	6	0	1	0	2	9	9	18	18	13	16	13	15	8	7	10	9
SPB3	AL201201C1 *Hepatozoon theileri*	11	9	7	8	8	7	7	1	0	2	2	9	8	18	18	13	16	13	15	9	7	10	9
SPB1	AL201005C3 *Hepatozoon theileri*	11	8	7	6	7	6	6	0	2	0	1	8	8	17	18	12	15	12	14	8	7	10	9
SPB2	AL201126A3 *Hepatozoon theileri*	12	10	8	7	7	7	7	2	2	1	0	10	9	18	19	13	16	13	15	9	7	11	10
P13	AR150623A271 *Hepatozoon theileri*	4	6	2	3	3	3	3	9	9	8	10	0	3	12	12	6	10	6	9	11	10	14	13
P11	AR150429A268 *Hepatozoon theileri*	4	5	3	3	3	3	3	9	8	8	9	3	0	12	12	6	10	6	9	10	10	14	13
P14	AR150504A274 *Hepatozoon theileri*	8	15	12	12	13	13	13	18	18	17	18	12	12	0	2	6	2	7	3	20	19	15	10
P12	AR150504A269 *Hepatozoon theileri*	9	15	12	13	13	13	13	18	18	18	19	12	12	2	0	7	3	7	3	20	20	16	11
P7	AR150318A167 *Hepatozoon theileri*	2	9	6	6	7	7	7	13	13	12	13	6	6	6	7	0	4	0	3	14	14	10	8
P8	AR150318A171 *Hepatozoon theileri*	6	13	10	10	10	10	10	16	16	15	16	10	10	2	3	4	0	4	1	17	17	13	8
P9	AR150504A251 *Hepatozoon theileri*	3	9	6	7	7	7	7	13	13	12	13	6	6	7	7	0	4	0	3	14	14	10	8
P10	AR150428A261 *Hepatozoon theileri*	5	12	9	9	10	10	10	15	15	14	15	9	9	3	3	3	1	3	0	17	16	12	7
SPB7	AL210419F1 *Hepatozoon theileri*	13	14	10	11	11	11	11	8	9	8	9	11	10	20	20	14	17	14	17	0	7	10	11
SPB5	AL201201M1 *Hepatozoon theileri*	12	11	9	9	9	10	10	7	7	7	7	10	10	19	20	14	17	14	16	7	0	11	12
SPB6	AL201005C3 *Hepatozoon theileri*	11	18	15	15	16	16	16	10	10	10	11	14	14	15	16	10	13	10	12	10	11	0	6
SPB8	AL201129D1 *Hepatozoon theileri*	10	17	14	14	14	14	14	9	9	9	10	13	13	10	11	8	8	8	7	11	12	6	0

Appendix F

Table F1: Multiple alignment distance matrix nt substitution site comparison between *Hepatozoon theileri* samples generated in the current study. Alignment was checked and a distances matrix table was created within UGENE.

Code	Species	T3	P5	P1	P2	P3	P6	P4	SPB4	SPB3	SPB1	SPB2	P13	P11	P14	P12	P7	P8	P9	P10	SPB7	SPB5	SPB6	SPB8
T3	AE210412A14 *Hepatozoon theileri*	0	17	10	11	12	12	12	26	26	25	27	9	10	19	20	5	14	6	12	29	28	25	23
P5	AR150429A268 *Hepatozoon theileri*	17	0	8	7	8	6	6	18	20	19	22	13	12	34	35	20	29	21	27	31	26	41	38
P1	AR150429A268 *Hepatozoon theileri*	10	8	0	1	2	2	2	16	17	15	18	5	6	27	28	13	22	14	20	24	20	34	31
P2	AR150504A274 *Hepatozoon theileri*	11	7	1	0	1	1	1	15	18	14	17	6	7	28	29	14	23	15	21	25	21	35	32
P3	AR150318A165 *Hepatozoon theileri*	12	8	2	1	0	2	2	16	19	15	17	7	8	29	30	15	24	16	22	26	21	36	33
P6	AR150428A253 *Hepatozoon theileri*	12	6	2	1	2	0	0	14	17	13	16	7	8	29	30	15	24	16	22	26	22	36	33
P4	AR150428A253 *Hepatozoon theileri*	12	6	2	1	2	0	0	14	17	13	16	7	8	29	30	15	24	16	22	26	22	36	33
SPB4	AL201201C1 *Hepatozoon theileri*	26	18	16	15	16	14	14	0	3	1	4	20	20	41	42	29	36	29	34	19	16	24	21
SPB3	AL201201C1 *Hepatozoon theileri*	26	20	17	18	19	17	17	3	0	4	5	21	19	41	42	29	36	29	34	20	17	24	21
SPB1	AL201005C3 *Hepatozoon theileri*	25	19	15	14	15	13	13	1	4	0	3	19	19	40	41	28	35	28	33	18	15	23	20
SPB2	AL201126A3 *Hepatozoon theileri*	27	22	18	17	17	16	16	4	5	3	0	22	20	42	43	30	37	30	35	21	16	25	22
P13	AR150623A271 *Hepatozoon theileri*	9	13	5	6	7	7	7	20	21	19	22	0	8	27	28	13	22	14	20	25	23	32	30
P11	AR150429A268 *Hepatozoon theileri*	10	12	6	7	8	8	8	20	19	19	20	8	0	27	28	13	22	14	20	22	23	32	29
P14	AR150504A274 *Hepatozoon theileri*	19	34	27	28	29	29	29	41	41	40	42	27	27	0	4	14	5	15	7	45	44	35	24
P12	AR150504A269 *Hepatozoon theileri*	20	35	28	29	30	30	30	42	42	41	43	28	28	4	0	15	6	16	8	46	45	36	25
P7	AR150318A167 *Hepatozoon theileri*	5	20	13	14	15	15	15	29	29	28	30	13	13	14	15	0	9	1	7	33	31	23	18
P8	AR150318A171 *Hepatozoon theileri*	14	29	22	23	24	24	24	36	36	35	37	22	22	5	6	9	0	10	2	40	39	30	19
P9	AR150504A251 *Hepatozoon theileri*	6	21	14	15	16	16	16	29	29	28	30	14	14	15	16	1	10	0	8	33	31	23	18
P10	AR150428A261 *Hepatozoon theileri*	12	27	20	21	22	22	22	34	34	33	35	20	20	7	8	7	2	8	0	38	37	28	17
SPB7	AL210419F1 *Hepatozoon theileri*	29	31	24	25	26	26	26	19	20	18	21	25	22	45	46	33	40	33	38	0	17	23	26
SPB5	AL201201M1 *Hepatozoon theileri*	28	26	20	21	21	22	22	16	17	15	16	23	23	44	45	31	39	31	37	17	0	26	27
SPB6	AL201005C3 *Hepatozoon theileri*	25	41	34	35	36	36	36	24	24	23	25	32	32	35	36	23	30	23	28	23	26	0	13
SPB8	AL201129D1 *Hepatozoon theileri*	23	38	31	32	33	33	33	21	21	20	22	30	29	24	25	18	19	18	17	26	27	13	0